The STRIPAK complex and its role in fruiting-body development of the filamentous fungus *Sordaria macrospora*

Dissertation

for the award of the degree

“Doctor rerum naturalium”

of the Georg-August-Universität Göttingen

within the doctoral program *Molecular Biology of Cells*

of the Georg-August University School of Science (GAUSS)

submitted by

Stefan Frey

from Leer (Ostfriesland)

Göttingen, 2015

Thesis Committee

Prof. Stefanie Pöggeler
Department of Genetics of Eukaryotic Microorganisms
Institute of Microbiology and Genetics

Prof. Gerhard Braus
Department of Microbiology and Genetics
Institute of Microbiology and Genetics

Prof. Blanche Schwappach
Department of Molecular Biology
University Medical Center Göttingen

Members of the Examination Board

Referee:
Prof. Stefanie Pöggeler
Department of Genetics of Eukaryotic Microorganisms
Institute of Microbiology and Genetics

2nd Referee:
Prof. Gerhard Braus
Department of Microbiology and Genetics
Institute of Microbiology and Genetics

Further members of the Examination Board

Prof. Blanche Schwappach
Department of Molecular Biology
University Medical Center Göttingen

Prof. Rolf Daniel
Department of Genomic and Applied Microbiology
Institute of Microbiology and Genetics

Prof. Kai Heimel
Department of Microbial Cell Biology
Institute of Microbiology and Genetics

PD Dr. Michael Hoppert
Department of General Microbiology
Institute of Microbiology and Genetics

Date of the oral exam: 05.03.2015

Affirmation

I hereby declare that this thesis was written independently and with no other sources and aids than quoted.

Göttingen, 23.01.2015

Stefan Frey

This doctoral study was performed in the group of Prof. Stefanie Pöggeler in the Department of Genetics of Eukaryotic Microorganisms at Institute of Microbiology and Genetics, Georg-August-University Göttingen.

Some parts of the results section of this doctoral study were peer-reviewed by the journal “Molecular Microbiology” (and are currently under revision) and some results are submitted for publication in the journal “Eukaryotic Cell”.

Stefan Frey, Yasmine Lahmann, Stefanie Pöggeler. Deletion of *Smgpi1* encoding a GPI-anchored protein suppresses sterility of the STRIPAK mutant ΔSmmob3 in the filamentous ascomycete *Sordaria macrospora.* Molecular Microbiology (in revision)

Author contributions to this publication:
Planned experiments: SP, SF, YL
Performed experiments: SF, YL
Analyzed data: SF, SP
Contributed reagents or other essential material: SP
Wrote the paper: SF, SP

Stefan Frey, Stefanie Pöggeler. Germinal Center Kinases SmKIN3 and SmKIN24 are associated with the *Sordaria macrospora* Striatin-interacting phosphatase and kinase (STRIPAK) complex. Eukaryotic Cell (submitted)

Author contributions to this publication:
Planned experiments: SP, SF
Performed experiments: SF
Analyzed data: SF, SP
Contributed reagents or other essential material: SP
Wrote the paper: SF, SP

List of Tables

List of Figures

List of Abbreviations

aa	amino acids
a. dest.	*aqua destillata*
CMS	complete medium with saccharose
co-IP	co-immunoprecipitation
bp	base pair
BMM	biomalt maize medium
BLAST	basic local alignment search tool
cDNA	complementary DNA
d	days
DIC	differential interference contrast
DsRED	encodes red fluorescence protein of Discosoma sp
ER	endoplasmic reticulum
eGFP	enhanced green fluorescence protein of *Aequorea Victoria*
gDNA	genomic DNA
GPI	glycosylphosphatidylinositol
kDa	kilo Dalton
ORF	open-reading frame
PAGE	polyacrylamide gel electrophoresis
PBS	phosphate buffered saline
PCR	polymerase chain reaction
RT-PCR	real-time PCR
SD	selective dropout
ssi	single spore isolate
SWG	Sordaria Westergaards medium
RT	Room temperatur
Y2H	yeast two-hybrid
wt	wild type

Common abbreviations and units of measurement are not enlisted

Summary

The mammalian Striatin-interacting phosphatase and kinase (STRIPAK) complex consist of many proteins, among them Striatin as scaffold, the putative kinase activator monopolar spindle-one-binder 3 (MOB3), serine/threonine phosphatase PP2A subunits A and C, the Striatin-interacting protein (STRIP)1 and STRIP2, sarcolemmal membrane-associated protein (SLMAP) and the germinal center kinases (GCK) MST4, STK24, STK25 and MINK1. In this study, we used the filamentous ascomycete *Sordaria macrospora* as model organism to analyze the role of the STRIPAK complex in fruiting-body development. *S. macrospora* is coprophytic fungus which solely undergoes a sexually lifecycle and does not require a mating partner for sexual reproduction.

In *S. macrospora*, the STRIPAK complex is required for fruiting-body development and hyphal fusion. Hyphal fusion is a process that results in mixed cell contents of involved cells without lysis. In filamentous ascomycetes, hyphal fusion occurs at different stages of vegetative growth and sexual reproduction.

The STRIPAK complex in *S. macrospora* contains homologs to mammalian Striatin (PRO11), MOB3 (SmMOB3), subunits A and C of PP2A (SmPP2AA and C), STRIP1/2 (PRO22) and SLMAP (PRO45). However, fungal STRIPAK-associated kinases have not been characterized to date.

This study is divided into two parts, one comprises the characterization of SmGPI1, a GPI-anchored protein, identified as interaction partner of SmMOB3 in cross-species microarrays, and the other part is about identification of potential STRIPAK-associated kinases. Interaction between STRIPAK-associated SmMOB3 and SmGPI1 was successfully verified by co-Immunoprecipitation (co-IP) and yeast two-hybrid (Y2H) using *S. macrospora* cDNA. Deletion of *Smgpi1* was the next step to investigate its impact on fruiting-body development; in contrast to Δpro11, Δ pro22, ΔSmMOB3 and Δpro45, ΔSmgpi1 underwent hyphal fusion and was fertile, but generated more fruiting bodies, which were smaller but normal in shape compared to wt.

Interestingly deletion of *Smgpi1* in a sterile ΔSmmob3 deletion background restored the phenotypes caused by *Smmob3* deletion. As already mentioned, ΔSmmob3 is sterile and not capable of hyphal fusion. In contrast, the double-deletion strain ΔSmgpi1/ΔSmmob3 is fertile and underwent hyphal fusion. This effect was Smmob3 specific and did not occur in other

STRIPAK-specific double-deletion strains, e.g. ΔSmgpi1/Δpro11, ΔSmgpi1/Δpro22 and ΔSmgpi1/Δpro45. Moreover, fluorescence microscopy and differential centrifugation of SmGPI1 revealed a dual targeting; SmGPI1 localizes at the cell wall and the mitochondria.

Regarding the identification of STRIPAK-associated kinases in *S. macrospora*, two kinases were identified to be homologous to the mammalian STRIPAK-associated kinases MST4, STK24, STK25 and MINK1 by BLASTP search and were named SmKIN3 and SmKIN24. Phylogenetic analysis revealed a conservation of these kinases among ascomycetes. Interaction of SmKIN3 and SmKIN24 with *S. macrospora* Striatin homolog PRO11 was shown via Y2H and for SmKIN3 and PRO11 also by means of co-IP. Fluorescence microscopy of SmKIN3 and SmKIN24 revealed localization to the septa, whereas SmKIN3 localizes at the outer part of the septum and SmKIN24 to the septal pore.

Deletion of *Smkin3* or *Smkin24* to analyze their impact on fruiting-body development showed only ΔSmkin24 to be sterile. However, ΔSmkin3 and ΔSmkin24 were reduced in vegetative growth and exhibited impaired septa formation; whereas ΔSmkin3 displayed greater distances between adjacent septa compared to wt, deletion of *Smkin24* resulted in numerous closely-packed septal bundles of abnormal shape. Although phenotypically distinct, both kinases appear to function independently because the double-knockout strain ΔSmkin3/ΔSmkin24 displayed the combined phenotypes of each single-deletion strain. Moreover, we discovered that protoplasts harboring the ΔSmkin3 deletion background recover faster than protoplasts obtained from wt. Based on the results of this study and findings in *N. crassa* that homologs to SmKIN3 and SmKIN24 are implicated in septation initiation network (SIN) we assume STRIPAK to function aside from sexual development and hyphal fusion, also in regulation of fruiting-body number via SmMOB3-SmGPI1 interaction and suggest a crosstalk between SIN and STRIPAK in *S. macrospora*.

Zusammenfassung

Der STRIPAK (für engl. „Striatin-interacting phosphatase and kinase")-Komplex in Säugetieren umfasst unter anderem die Proteine Striatin als Gerüsteinheit, Phosphatase 2A, Untereinheit A und C, STRIP (für engl „Striatin-interacting protein") 1 und 2, den putativen Kinaseaktivator MOB3 und die GC (für engl. „germinal center") Kinasen MST4, STK24, STK25 und MINK1, sowie SLMAP (für engl. „sarcolemmal membrane-associated protein"). Im Rahmen dieser Arbeit wird *S. macrospora* als Modellorganismus für die Analyse der Funktion des STRIPAK Komplexes auf die Entwicklung von Fruchtkörpern verwendet. *S. macrospora* ist ein koprophiler selbstfertiler Schlauchpilz (Ascomyzet), der lediglich einen sexuellen Lebenszyklus aufweist. Der STRIPAK-Komplex in *S. macrospora* ist beteiligt an verschiedenen Prozessen, darunter die sexuelle Entwicklung und die Hyphenfusion. Die Hyphenfusion beschreibt die Verbindung von zwei Zellen, ohne dabei zu lysieren. In *S. macrospora* wurden bisher Homologe zu den in Säugern identifizierten Proteinen Striatin (PRO11), MOB3 (SmMOB3), PP2AA und C (SmPP2AA und C), STRIP1/2 (PRO22) und SLMAP (PRO45) identifiziert, jedoch wurden bisher noch keine beteiligten Kinasen identifiziert.

Diese Arbeit befasst sich mit zwei Hauptthemen: Der Charakterisierung von SmGPI1, ein GPI-geankertes Protein, welches als Interaktionspartner von SmMOB3 identifiziert wurde und der Identifizierung und Charakterisierung potentieller STRIPAK-Kinasen.

Im Rahmen dieser Arbeit konnte die Interaktion zwischen SmGPI1 und SmMOB3 erfolgreich mittels Y2H und co-IP bestätigt werden. Zur Untersuchung des Einflusses von *Smgpi1* auf die Fruchtkörperentwicklung, wurde das Gen deletiert. Im Unterschied zu Stämmen, die aus der Deletion von Genen, welche für Proteine des STRIPAK-Komplexes codieren, hervorgingen, ist ΔSmgpi1 fertil und fähig zur Hyphenfusion. Im Vergleich zum Wildtyp, sind die Fruchtkörper von ΔSmgpi1 zwar kleiner, aber normal geformt.

Interessanterweise, führt die Deletion von *Smgpi1* in der sterilen Deletionsmutante ΔSmmob3 zu einer Unterdrückung des ΔSmmob3 Phänotyps. Während ΔSmmob3 steril ist und keine Hyphenfusion zeigt, ist ΔSmmob3/ΔSmgpi1 fertil und befähigt zur Hyphenfusion. Dieser Effekt ist spezifisch und tritt nur in der Deletionsmutante ΔSmmob3/ΔSmgpi1 auf.

Des Weiteren wurde durch Fluoreszenzmikroskopie und differenzieller Zentrifugation gezeigt, daß SmGPI1 dual lokalisiert ist: SmGPI1 wurde sowohl an der Zellwand, als auch in den Mitochondrien gefunden.

Bezüglich der Identifikation von STRIPAK-Kinasen, wurden zwei potentielle Homologe zu den in Säugern identifizierten STRIPAK-Kinasen mittels BLASTP-Suche identifiziert, namentlich SmKIN3 und SmKIN24. Die Interaktion von SmKIN3, SmKIN24 und dem *S. macrospora* Striatin-Homolog PRO11 wurde mittels Y2H bestätigt, die Interaktion von SmKIN3 mit PRO11 zusätzlich auch durch co-IP. Fluoreszenzmikroskopie der eGFP markierten Proteine SmKIN3 und SmKIN24 ergab eine Lokalisierung dieser an den Septen. Die Deletion der beiden Gene *Smkin3* und *Smkin24* zeigte, daß lediglich SmKIN24 an der Fruchtkörperentwicklung beteiligt ist, was sich in Sterilität der Deletionsmutante ΔSmkin24 zeigte. Der Stamm ΔSmkin3 war weiterhin fertil. Interessanterweise zeigten beide Stämme einen Defekt in der Entwicklung von Septen und dem vegetativen Wachstum. Während die Abstände zwischen nebeneinanderliegenden Septen in ΔSmkin3 im Verhältnis zum Wildtyp vergrößert waren, führte die Deletion von *Smkin24* zu vielen, dicht gepackten und deformierten Septen. Dennoch scheinen beide Proteine unabhängig zu fungieren, da der Doppel-Knockout ΔSmkin3/ΔSmkin24 die Phänotypen beider Einzelnockouts zeigt. Des Weiteren zeigten Protoplasten, welche den ΔSmkin3 Deletionshintergrund besaßen, einen deutlich erhöhten Regenerationseffekt.

Basierend auf den Ergebnissen dieser Studie kann dem STRIPAK-Komplex in *S. macrospora* neben der sexuellen Entwicklung und der Hyphenfusion auch eine Funktion in der Regulierung der Fruchtkörperanzahl zugewiesen werden. Zusätzlich vermuten wir eine Verbindung zwischen STRIPAK-Komplex und des Netzwerkes, welches die Septierung einleitet (SIN, für engl. „septation initiation network“).

1. Introduction

Organisms underlie many environmental changes and pressures, such as different salt concentrations, changing nutrient conditions, pheromones, oxidative stress or pH values (Maller, 2003, Martindale & Holbrook, 2002). Thus, it is necessary to respond appropriately to the incoming stimuli and to generate respective responses. On molecular level, the response to different stimuli is facilitated by signaling pathways. To date, many signal transduction pathways have been identified, partially connected to each other. Normally, incoming signals are detected by receptors on the cell surface, which modulate the signal and transmit it to the cell lumen. These signals can be enhanced and transduced by many modifications, for example phosphorylation or protein cleavage (Li & Hristova, 2006, Lieber *et al.*, 1993). In general, signal transduction ends in changed translation pattern of genes, needed for the appropriate response to the stimulus (Lalli & Sassone-Corsi, 1994). Dysfunctions in signal transduction and responses to environmental changes can cause severe diseases such as cancer (Wu *et al.*, 2010).

In the recent years, Striatins have been identified to be regulators of various differentiation processes and thus, it might have a key role in these processes (Benoist *et al.*, 2006).

1.1 Striatins in mammals

In mammals, the group of Striatins comprises the three proteins Striatin, SG_2NA and Zinedin (Figure 1). These proteins are highly similar in their protein domain structure and localization. Functional and structural homologs were discovered in many other organisms like *Drosophila melanogaster*, *Schizosaccharomyces pombe*, *Neurospora crassa*, *Saccharomyces cerevisiae* and *Sordaria macrospora* (Bloemendal *et al.*, 2012, Lisa-Santamaria *et al.*, 2012, Pöggeler & Kück, 2004, Simonin *et al.*, 2010, Tanabe *et al.*, 2001). Mammalian Striatins are characterized by a caveolin-binding side, a Ca^{2+}-Calmodulin binding side, a coiled-coil domain and tryptophan-aspartate (WD) repeat (hereafter WD40) repeats (Benoist *et al.*, 2006).

Caveolins are small integral membrane proteins and the main component of the caveolae; cholesterol-rich, sack shaped, invaginated lipid rafts in the plasma membrane of cells (Parton & Simons, 2007). Caveolins interact with many signaling proteins. This is facilitated by an about 20 aa comprising motif at their N-terminus (Li *et al.*, 1996). The consensus sequence of

caveolin-interaction motifs as present in Striatins is ΦXXXXΦXXΦ, where Φ represents an aromatic aa and X represents random aa (Couet *et al.*, 1997, Benoist *et al.*, 2006).

Calmodulin-binding motifs are protein domains necessary for interaction of proteins with Calmodulin. Calcium-modulated protein (Calmodulin), is a calcium-binding messenger protein expressed in all eukaryotic cells. Interaction with its target proteins is modulated by calcium-ion binding and thus, Calmodulin (CaM) converts calcium concentrations into further signals (Chin & Means, 2000, Stevens, 1983). CaM is highly conserved and consists of approximately 148 aa with a molecular weight of 16.7 kDa. It contains four motifs for Ca^{2+}-ion binding. The tertiary structure shows two globular domains representing the N- and C-terminal domain, separated by a flexible linker region (Chin & Means, 2000)

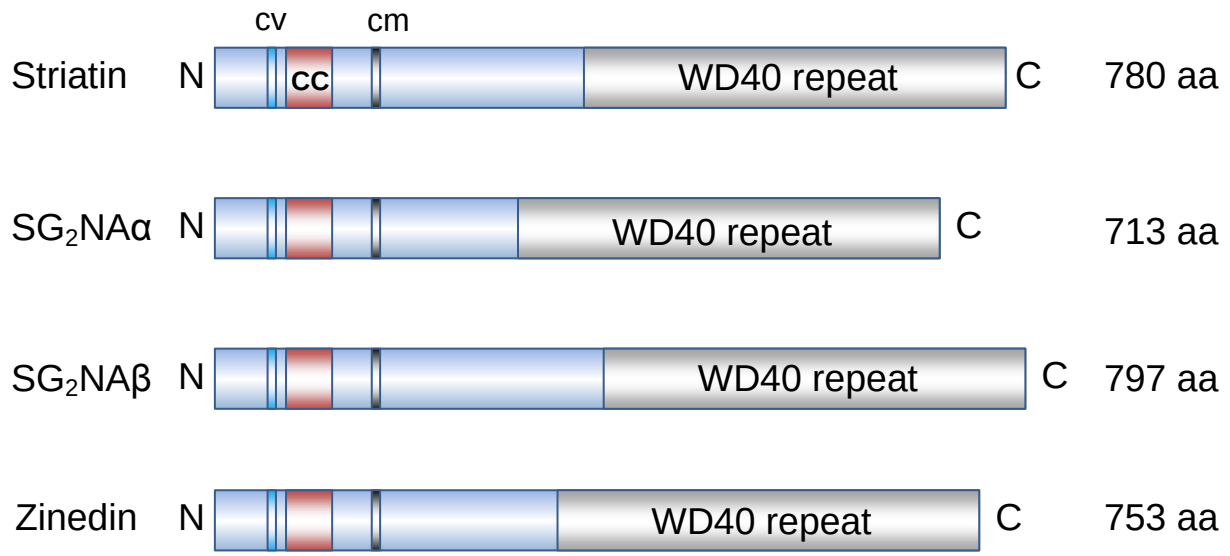

Figure 1. Schematic overview of mammalian Striatins; shown are the structural domains of Striatin, SG_2NA isoform α and β, and Zinedin. cv = caveolin binding domain, cc = coiled-coil domain, cm = Ca^{2+}-calmodulin binding domain, N = N-terminus, C = C-terminus. Domains shown for SG_2NA and Zinedin are predicted and not experimentally proved. Aa in total is given at the end of each protein (according to Hwang & Pallas (2014)).

Coiled-coil domains are motifs of 2-7 alpha helices that are coiled together like rope strands. The common types are dimers and trimers (Liu *et al.*, 2006). Coiled-coil motifs facilitate oligomerization of many proteins (Burkhard *et al.*, 2001). The consensus sequence of coiled-coil motifs is the repeated pattern HxxHCxC, with H = hydrophobic aa and C = charged aa, referred

to as heptad repeat (Mason & Arndt, 2004). For Striatin, oligomerization was shown to be crucial for some interactions with other proteins (Chen *et al.*, 2012, Gaillard *et al.*, 2006).

The WD40 domain is formed by 4 to 16 structurally conserved WD40 repeats (Li & Roberts, 2001, Smith *et al.*, 1999). WD40 repeats consist of 44-60 aa, containing tryptophan-aspartic acid (W-D) dipeptides at the C-terminus and a glycine-histidine pair at 11-24 aa positions from their N-terminus (Neer *et al.*, 1994, van der Voorn & Ploegh, 1992). The WD40 domain forms a propeller-like structure of interlocked beta sheets that serves for protein complex assembly (Hwang & Pallas, 2014, Li & Roberts, 2001).

1.1.1 Striatin

Striatin was first identified in rat brain and named after the striatum, a part of the cerebrum, where it was found most abundantly (Castets *et al.*, 1996). In neural tissues, Striatin was also identified throughout the central and peripheral nervous system but mostly in the striatum and motoneurons. Moreover, Striatin is also expressed in many other tissues, among them fibroblasts, lymphocytes, lung, liver, kidney, skeletal and cardiac muscles (Benoist *et al.*, 2006, Castets *et al.*, 1996, Castets *et al.*, 2000, Moqrich *et al.*, 1998, Moreno *et al.*, 2000). Striatin full-length protein comprises 780 aa and consists of the 4 characteristic domains for interaction; a caveolin-binding motif, a coiled-coil region, a CaM-binding motif and a WD40 repeat domain (Figure 1). Until today only little is known about the function of Striatin-caveolin interaction. Since Striatin was shown to interact with Caveolin-1 (CAV-1), which may act as a scaffolding protein within caveolar membranes, this interaction was hypothesized to facilitate Striatin localization to Caveolin-1 rich domains in dendric spines (Gaillard *et al.*, 2001).

The Ca^{2+}-CaM binding domain of Striatin comprises aa 149-166 and is crucial for Striatin-CaM interaction in a Ca^{2+}-dependent manner. Until today, it is still unknown, how Striatins function in Ca^{2+} signaling. One hypothesis is that Striatin functions as Ca^{2+} sensor that reacts to changing Ca^{2+} concentrations (Benoist *et al.*, 2006). This is among others based on results showing that physiologically relevant calcium concentrations increase presence of cytosolically located Striatin as well as findings, that Striatin distribution in cytosolic, detergent soluble and insoluble fractions of brain tissue depends on calcium presence or absence during lysis (Bartoli *et al.*, 1998, Gaillard *et al.*, 2001). Furthermore, the CaM-binding motif of Striatin appears to function

in protein-protein interaction of Striatin; deletion of its CaM-binding motif enhances interaction of Striatin with germinal center kinases (GCK) mammalian STE20-like protein kinase 4 (MST4) and serine/threonine-protein kinase (STK) 24. By this, Ca^{2+}-CaM binding could regulate MST4 and STK24 binding to Striatin by modifying the subcellular localization of Striatin. However, interaction with other tested proteins was not affected (Gordon *et al.*, 2011).

Additionally, it was shown that Striatin hetero-oligomerizes through its coiled-coil domain with Zinedin, but also homo-oligomerizes (Gaillard *et al.*, 2006). The coiled-coil domain of Striatin comprises aa 64-120, but with the possibility that even parts of the caveolin binding domain belongs to it. Moreover, a trigger sequence necessary for successful coiled-coil interaction is assumed to be located at the N-terminus of Striatin (Gordon *et al.*, 2011).

Striatin contains a WD40 domain composed of 6 or 7 WD40 repeats. It was shown that deletion of this region abolishes interaction of Striatin with other proteins, among them the kinase activator monopolar spindle-one-binder 3 (MOB3)/phocein (Baillat *et al.*, 2001, Moreno *et al.*, 2001).

Striatin is absent from axons but highly concentrated in dendric spines. Based on the Ca^{2+}-CaM binding motif, it is likely regulated by Ca^{2+}-dependent signaling in postsynaptic neurons (Castets *et al.*, 1996).

1.1.2 SG_2NA

SG_2NA was first reported to localize to the nucleus. It is named after its expression levels which have their maximum during the S and the G_2 phase of the cell cycle (Muro *et al.*, 1995). Later it was shown to localize predominantly to the cytosol or membranes. SG_2NA displays the highest expression in cerebellum and cortex where it, similar to Striatin, localizes to somato-dendritic spines with high concentration in dendric spines. However, it is also present in other tissues (Castets *et al.*, 2000, Moreno *et al.*, 2001). As shown in Figure 1, SG_2NA protein domains resemble Striatin. Similarly, it consists of a caveolin-binding domain from aa 71-79, a Ca^{2+}-CaM binding domain from aa 166-183, a coiled-coil domain ranging from aa 77-136 and a WD40 domain of 6 WD40 repeats. SG_2NA was shown bind CaM in a Ca^{2+}-dependent manner. This Striatin variant homo-oligomerizes and hetero-oligomerizes with Zinedin and Striatin by their coiled-coil domains. The coiled-coil domain of SG_2NA was shown to be necessary but not

sufficient to target the protein to dendric spines (Gaillard *et al.*, 2006). Two major isoforms of SG_2NA are known; $SG_2NA\alpha$ with 713 aa and $SG_2NA\beta$ with a length of 797 aa (Figure 1) (Benoist *et al.*, 2006). However, minor isoforms do also exist; $SG_2NA\gamma$ was identified previously in rat brain tissue. It lacks all but one WD40 repeats and localizes to the nucleus. $SG_2NA\gamma$ was shown to organize an estrogen-inducible complex of protein phosphatase 2A (PP2A) and estrogen receptor α (ERα) (Tan *et al.*, 2008). Moreover, SG_2NA exhibits transcriptional activation activity (Zhu *et al.*, 2001). Among Striatins, SG_2NA is the most conserved one (Tanti *et al.*, 2014).

1.1.3 Zinedin

Zinedin was first identified by search for Striatin homologs (Castets *et al.*, 2000). The canonical full-length isoform comprises 753 aa. Similar to Striatin and SG_2NA, Zinedin exhibits the four characteristic domains for protein interaction (Figure 1). Zinedins caveolin-binding domain comprises aa 71-79, its Ca^{2+}-CaM binding domain aa 165-182. Zinedin hetero-oligomerizes with SG_2NA and binds similar to Striatin and SG_2NA CaM in a Ca^{2+}-dependent manner. Zinedin exhibits 7 WD40 repeats ranging from aa 436 to 752. It is most abundantly expressed in the hippocampus and localizes to somato-dendritic spines with high concentration in dendric spines but is also found in various other tissues (Benoist *et al.*, 2008, Gaillard *et al.*, 2006, Gordon *et al.*, 2011). Within the cell, Zinedin localizes cytosolically (Blondeau *et al.*, 2003, Castets *et al.*, 2000).

1.2 Striatin homologs in other eukaryotes

Additionally to the mammalian Striatins, homologs have been identified in other animals and lower eukaryotes, among them the isoforms $SG_2NA\alpha$ and $SG_2NA\alpha$+ from goldfish, *D. melanogaster* "connector of kinase to AP-1" (CKA), *Caenorhabditis elegans* "CKA and Striatin homolog family member" (CASH-1), *S. cerevisiae* "Factor arrest protein 8" (FAR8), *S. pombe* FAR8/CSC3p, *N. crassa* "hyphal anastomosis mutant 3" (HAM-3), *S. macrospora* PRO11 (protoperithecia mutant 11), *Fusarium graminearum* "*Fusarium verticillioides* Striatin ortholog 1" (FSR1) and *Aspergillus nidulans* "*A nidulans* Striatin"

(STRA). All these proteins harbor characteristic domains as described for Striatins (Bloemendal *et al.*, 2012, Chen *et al.*, 2002, Ma *et al.*, 2009, Pöggeler & Kück, 2004, Simonin *et al.*, 2010, Shim *et al.*, 2006).

Deletion of genes encoding for Striatin homologs have a high impact on developmental processes; deletion of *pro11* in *S. macrospora*, *fsr1* in *F. graminearum*, *strA* in *A. nidulans* and *ham-3* in *N. crassa* lead to sterility. Moreover, the deletion strains *S. macrospora* Δpro11 and *N. crassa* Δham-3 and were not capable of hyphal fusion (Bernhards & Pöggeler, 2011, Bloemendal *et al.*, 2012, Shim *et al.*, 2006, Simonin *et al.*, 2010, Wang *et al.*, 2010). Furthermore, decreases deletion of *fsr1* in *F. graminearum* its virulence. Cell fusion, which is also named hyphal fusion in filamentous fungi, occurs in organisms from eukaryotic microbes to multicellular plants and animals and results in mixed cell contents of involved cells without lysis. In filamentous ascomycetes, hyphal fusion occurs at different stages of vegetative growth and sexual reproduction (Rech *et al.*, 2007, Fleißner *et al.*, 2008, Read *et al.*, 2010, Bloemendal *et al.*, 2012). This emphasizes the importance of Striatins (Hwang & Pallas, 2014). Interestingly, sterility of the *S. macrospora* pro11 mutant can be complemented with Striatin cDNA from mouse, showing an evolutionary conservation of Striatins function in signaling (Pöggeler & Kück, 2004). Recent studies revealed that Striatins have evolved from prokaryotic counterparts, but acquired domains exclusive for metazoans. Within this process, SG_2NA might be the earliest evolved Striatin (Tanti *et al.*, 2014).

1.3 Striatin-family complexes

Striatins have been shown to interact with a broad number of proteins, among them Ca^{2+}-CaM, CAV-1 and monopolar spindle-one-binder 3/phocein (MOB3) (Baillat *et al.*, 2001, Castets *et al.*, 2000, Gaillard *et al.*, 2006, Moreno *et al.*, 2001). Moreover, based on their WD40 domain, Striatins are assumed to function as a scaffolding unit for protein interactions (Moreno *et al.*, 2000, Pöggeler & Kück, 2004). Striatin-family members have been shown to interact with the structural (A) and catalytic (C) subunit of PP2A, germinal center kinases (GCK) and other proteins. This led to the name Striatin-interacting phosphatase and kinase (STRIPAK) for protein complexes consisting of Striatins as scaffolding unit, PP2A and kinases (Goudreault *et al.*, 2009, Hyodo *et al.*, 2012). Moreno *et al.* (2001) postulated regarding the PP2A-Striatin interaction that

Striatin functions as novel B''' family of PP2AB-type regulatory subunits by interaction with the PP2A heterodimer. The mammalian STRIPAK complex is a multi-protein complex. Its core components are Striatin as scaffold, PP2A subunit A and C, MOB3, the Striatin-interacting proteins (STRIP)1 and STRIP2 (formerly named Fam40a and Fam40b), cerebral cavernous malformation 3 (CCM3; also called programmed cell death 10, PDCD10) and the mammalian sterile 20-like (MST) kinase, subclass GCK III, MST4, serine/threonine-protein kinase (STK) 24 and STK25 (Goudreault *et al.*, 2009) (Table 1).

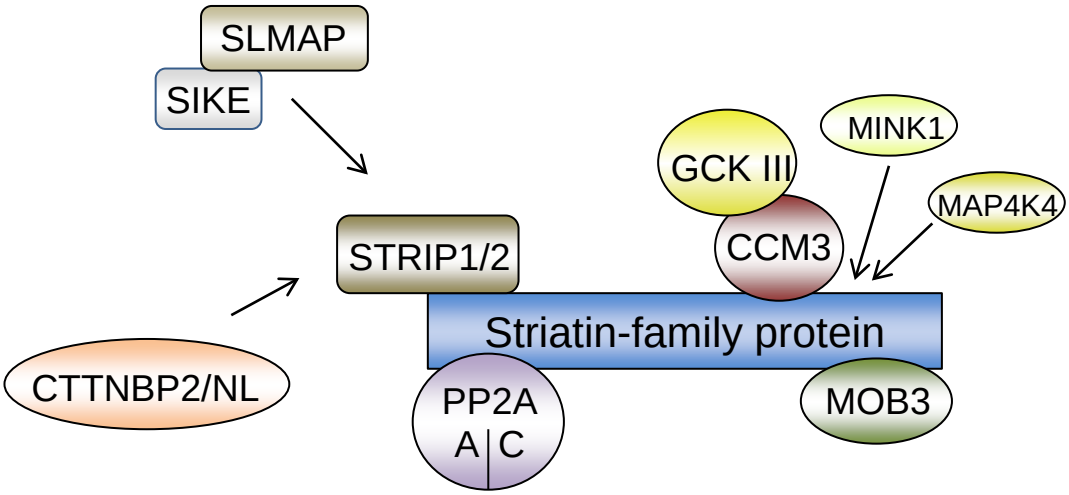

Figure 2. Mammalian STRIPAK complex(es) with its core components and additional proteins. The Striatin-family proteins comprise Striatin, SG_2NA or Zinedin. Core components are the PP2A heterodimer with subunit A and C, MOB3, STRIP1 and STRIP2 as well as kinases of the GC III class, MST4, STK24 and STK25 recruited by CCM3. It is still unknown weather Mishappen-like kinase 1 (MINK1) and Mitogen-activated protein kinase kinase kinase kinase 4 (MAP4K4) are also recruited by CCM3. Some proteins bind mutually exclusive to Striatin-family members (e.g. CTTNBP2/NL, SLMAP and SIKE) resulting in STRIPAK subcomplexes. These interactions are indicated by arrows. The simultaneous interaction of MINK1, MAP4K4 and GCK III has not been proven and thus is assumed to be bind in a mutually exclusive manner. The interaction partners of Striatins are described in the text (according to Hwang & Pallas (2014)).

Table 1. Mammalian STRIPAK components that associate with the complex or subcomplexes

Protein name	Full name/description	Reference
Striatin, SG_2NA, Zinedin	Striatin, putative regulatory subunit B''' of protein phosphatase 2A	(Moreno *et al.*, 2000)
PP2AA, PP2AC	Structural (A) and catalytic (C) subunits of protein phosphatase 2A	(Moreno *et al.* 2000)

MOB3	Monopolar spindle-one-binder 3/phocein	(Baillat *et al.*, 2001, Moreno *et al.*, 2001)
CCM3	Cerebral cavernous malformation 3/ programmed cell death 10	(Goudreault *et al.*, 2009)
MST4	Mammalian sterile 20-like kinase 4, subclass of GC III kinases	
STK24	Serine/threonine-protein kinase 24	
STK25	Serine/threonine-protein kinase 25	
STRIP1/2	Striatin-interacting protein 1 and 2, formerly Fam40a and Fam40b	
SLMAP	Sarcolemmal membrane-associated protein	
CTTNBP2/NL	Cortactin-binding protein 2/cortactin-binding protein 2, N-terminal-like	
SIKE	Suppressor of inhibitor-κB kinase ε	
FGFR1OP2	Fibroblast growth factor receptor 1 oncogene partner 2	
MINK1	Misshapen-like kinase 1	(Hyodo *et al.*, 2012)

As shown in Figure 2, several interaction partners bind mutually exclusive to the Striatin core complex. Goudreault *et al.* (2009) showed that either a cortactin-binding protein 2 family members (CTTNBP2 or CTTNBNL) or sarcolemmal membrane-associated protein (SLMAP) with suppressor of inhibitor-κB kinase ε (SIKE) bind simultaneously to Striatin. This binding behavior results in STRIPAK subcomplexes, which are similar in its core components but differ in its additional interaction partners (Hwang & Pallas, 2014).

Moreover, STRIPAK-like complexes have been identified. These complexes contain at least Striatin as a scaffolding unit and the PP2A subunits PP2AA and PP2AC; however, in most cases, the presence of kinases has not been demonstrated. STRIPAK-like complexes have been identified in mammals (see 1.3.2), *D. melanogaster*, yeast and filamentous ascomycetes. (Frost *et al.*, 2012, Simonin *et al.*, 2010, Xiang *et al.*, 2002, Ma *et al.*, 2009, Chen *et al.*, 2002, Ribeiro *et al.*, 2010, Singh *et al.*, 2011, Hwang & Pallas, 2014, Bloemendal *et al.*, 2012, Dettmann *et al.*, 2013).

The *D. melanogaster* STRIPAK complex contains homologs of Striatin, PP2A, MOB3, STRIP, fibroblast growth factor receptor 1 oncogene partner 2 (FGR10P2)/SIKE and CCM3. Additionally, the GC kinase Hippo (HPO) was identified as part of this complex. HPO is a homolog to mammalian MST1 and MST2, which are not STRIPAK-associated in mammals (Ribeiro *et al.*, 2010). However, STRIPAK-like complexes have also been identified in *D.*

melanogaster, involved in processes, such as activation of mitogen-activated protein kinases in the c-Jun N-terminal kinase (JNK) pathway (Ribeiro *et al.*, 2010, Chen *et al.*, 2002). JNKs are mitogen-activated protein kinase that respond to stress stimuli (Ip & Davis, 1998).

The STRIPAK-like complex in *S. cerevisiae* is named Factor arrest (FAR) complex and consists of proteins which are homologous to Striatin, SLMAP, STRIP and PP2As subunits A and C (Frost *et al.*, 2012, Lisa-Santamaria *et al.*, 2012). *S. cerevisiae* does not encode a MOB3 homolog.

In filamentous fungi, such as *N. crassa* and *S. macrospora*, STRIPAK-like complexes without homologs of mammalian kinases have been identified. These complexes contain proteins homologous to Striatin, PP2AA, PP2AC STRIP, SLMAP and MOB3 (Bloemendal *et al.*, 2012, Dettmann *et al.*, 2013, Nordzieke *et al.*, 2014, Simonin *et al.*, 2010, Xiang *et al.*, 2002).

1.3.1 Function of STRIPAK components

Numerous proteins have been identified to be members of the mammalian STRIPAK complex or to interact with its subunits. Proteins that have been identified as part of the complex or subcomplexes are enlisted in Table 1 and explained in detail in this section.

1.3.1.1 Protein phosphatase 2A

Mammalian PP2A is a herotrimeric serine/threonine phosphatase that contains a 65 kDa scaffolding A subunit, a 36 kDa catalytic C subunit and a regulatory B (separated in B, B', B'' and B''') subunit (Dettmann *et al.*, 2013). Subunit A of PP2A contains 15 tandem repeats of a conserved 39-residue sequence called HEAT (Huntingtin, elongation factor 3 (EF3), PP2A, and the yeast kinase TOR1) that forms rod-like helical structures which function in intracellular transport (Andrade & Bork, 1995). The C subunit is postranslationally methylated or phosphorylated. The methylation of the C subunit alteres binding of the regulatory B subunit but does not affect protein association (Yu *et al.*, 2001). As mentioned before, Striatins appear to function as B''' family of PP2AB-type regulatory subunits. This is deducted from the lack of other regulatory PP2A subunits in the Striatin-PP2A complex and an altered substrate specify of STRIPAK-associated PP2A. To date, 17 regulatory subunits and 2 isoforms of the scaffolding

and the catalytic subunit of PP2A are known (Cho & Xu, 2007, Xu *et al.*, 2006). In general, PP2A functions in various cellular processes e.g. translation and transcription, cell signaling and cell-cycle regulation (Lechward *et al.*, 2001). This variety of functions is mediated by its regulatory B subunits, which guide the phosphatase to its target complex and modulate its activity (Moreno *et al.*, 2000). To date, nearly all Striatin-family complexes contain PP2A subunits A and C, whereas other components are additional. Many of the STRIPAK components are phosphoproteins (Goudreault *et al.*, 2009; Moreno *et al.*, 2001). Moreno *et al.*, (2001) demonstrated that among others Striatin, SG_2NA and MOB3 are highly phosphorylated if PP2A is inactivated. This led to the assumption, that STRIPAK-bound PP2A is the relevant phosphatase. This hypothesis is supported by data of Gordon *et al.* (2011); a point mutation in the *striatin* gene that decreases Striatin-PP2A binding causes hyperphosphorylation of the STRIPAK-associated GCK III STK24 (Goudreault *et al.*, 2009) (1.3.1.4). Additionally, STK25 was shown to be dephosphorylated and partially inactivated by PP2A *in vitro* as well as MST4 showed a gel-shift pattern similar to hyperphosphorylation after PP2A inactivation (Gordon *et al.*, 2011, Pombo *et al.*, 1996).

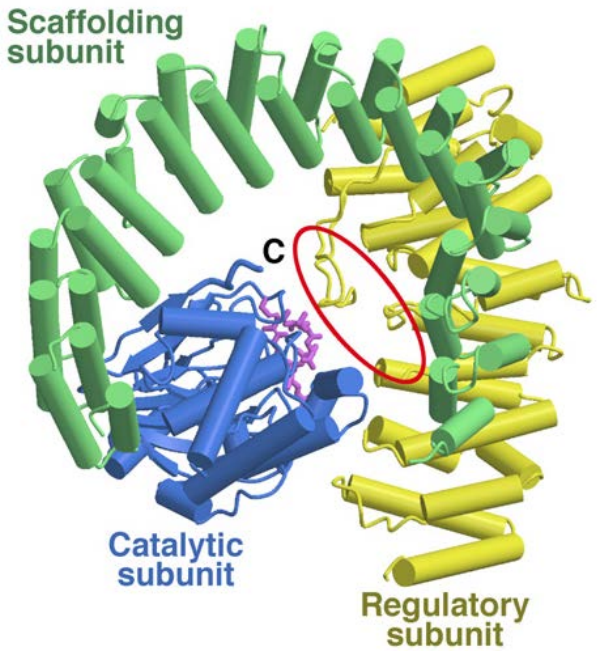

Figure 3. 3D structure of the heterotrimeric PP2A complex. Shown are the scaffolding subunit (green), the regulatory subunit (yellow) and the catalytic subunit (blue). The red circle in the center marks the absence of interactions involving the C-terminus of subunit C, shown are aa 1-294. (according to Cho and Xu (2007).

1.3.1.2 MOB3

One of the first identified interaction partners of Striatins was the 225 aa comprising MOB3 in *Rattus norvegicus* (Baillat *et al.*, 2001). Similar to Striatins, MOB3 localizes primarily to somato-dendritic spines (Baillat *et al.*, 2001, Bailly & Castets, 2007, Trammell *et al.*, 2008). MOB3 belongs to the group of MOB (monopolar spindle one binder) proteins. This protein group is characterized by a Mob domain, which is highly conserved and comprises 180-200 aa of the MOB protein (Baillat *et al.*, 2001, Luca *et al.*, 2001, Ponchon *et al.*, 2004) (Figure 4). Crystal-structure analysis of human MOB1 protein revealed the tertiary setup of Mob domains in general (Stavridi *et al.*, 2003). The conserved Mob domain consists of 9 helices and a hairpin, which form 2 antiparallel beta sheets. The protein forms a globular structure with a core of 4 bundled helices and the hairpin, accompanied by tetrahedrally coordinated zinc atom (Stavridi *et al.*, 2003).

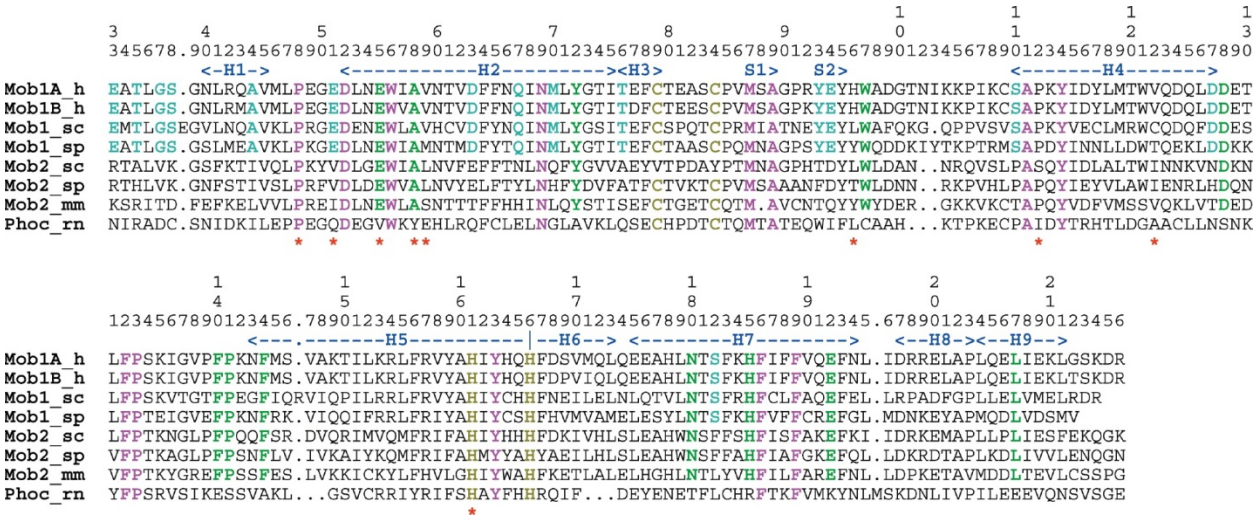

Figure 4. Sequence alignment of human MOB1 with homologs from other species. Aa-sequence alignment of human MOB1A (Mob1A_h, accession Q9H8S9) and MOB1B (Mob2B_h, Q7L9L4) aa 33-216 with *S. cerevisiae* MOB1p (Mob1_sc, E7Q517) aa 132-314, *S. pombe* MOB1p (Mob1_sp, O94360) aa 31-210 and MOB2p (Mob2_sp, O74558) aa 62-243, mouse Mob2 (Mob2_mm, Q8VI63) aa 32-212 and rat phocein (Phoc_rn, Q9QYW3) aa 46-222. Human MOB1 secondary structures are displayed above the aa sequences. Residues conserved in all MOB proteins are colored in magenta, residues conserved in MOB1 and MOB2, but not MOB3 family members are colored green, MOB1-specific residues are shown in blue. The cysteine and histidine residues that surround the zinc atom are shown in gold. The asterisks below the aa sequences indicate the residues targeted by the *S. cerevisiae* MOB1 mutant alleles (modified according to Stavridi *et al.* (2003)).

One function of the Mob domain is to activate NDR (nuclear Dbf2-related) kinases. NDR kinases are essential components of cellular processes, such as cytokinesis, cell proliferation, mitotic exit and apoptosis (Chow *et al.*, 2010). In particular, each MOB protein interacts with NDR kinases through a NDR-kinase specific, conserved N-terminal regulatory domain. This has been shown in yeast, *D. melanogaster* and human cell lines (Jones & Varela-Nieto, 1998). Moreover, MOB proteins are necessary for localization of the kinases NDR1/2 in yeast and "large kinase suppressor kinase 1" (LATS 1) in *D. melanogaster* (Hergovich *et al.*, 2005, Robinson, 1997). According to phylogenetic analysis of Vitulo *et al.* (2007) are MOB proteins divided into the 5 groups MOB1, MOB2, MOB3, MOB4 and MOBp proteins. The fruitfly *D. menalogaster* and the filamentous ascomycete *N. crassa* exhibit genes coding for 4 MOB proteins, the human genome contains genes encoding for 7 MOB proteins (Chow *et al.*, 2010, Maerz *et al.*, 2009, Trammell *et al.*, 2008). Each of them exhibits a gene that encodes a MOB3 protein, whereas a MOB3 homolog is absent in yeast. In contrast to proteins of the other MOB subgroups has MOB3 a versatile function. This is mainly based on its identified interaction partners; aside from Striatins and NDR kinases, MOB3 also interacts with epidermal growth factor receptor substrate 15 (EPS15) and GTPase Dynamin I involved in endocytosis and vesicular trafficking (Baillat *et al.*, 2002). Thus, MOB3 is assumed to has a regulatory function in these processes (Hwang & Pallas, 2014). Additionally was shown, that the MOB3 homolog in *D. melanogaster* is involved in spindle focusing, microtubule organization, neuronal transport and formation of synapses (Schulte *et al.*, 2010, Trammell *et al.*, 2008). Moreover, deletion of *mob3* in the filamentous ascomycetes *S. macrospora* and *N. crassa*, led to sterility and hyphal fusion defects (Bernhards & Pöggeler, 2011, Dettmann *et al.*, 2013, Maerz *et al.*, 2009). The phenotype of Δmob3 in *N. crassa* was independent from NDR-kinases activity (Maerz *et al.*, 2009). Thus, MOB3 has a fundamental role in developmental processes.

1.3.1.3 CCM3

CCM3 (cerebral cavernous malformation 3) also named PDCD10 (programmed cell death 10) was first identified in a premyeloid cell line and was upregulated after induced apoptosis (Bergametti *et al.*, 2005). The name CCM3 is deducted from previous findings that mutations in this gene can cause cerebral cavernous malformations (CCM). CCMs are vascular lesions in the

brain that are characterized by dilated vessels, abnormal in shape. These vessels lack intervening brain parenchyma and thus contain only a monolayer of endothelial cells. The symptoms caused by this malformation vary from headache to stroke (Siegel *et al.*, 2005, Verlaan *et al.*, 2005). The prevalence of these symptoms have been estimated to be 0.1%-0.5% (Otten *et al.*, 1989). Three CCM-related genes have previously been identified, named CCM1, CCM2 and CCM3. All three genes are connected to CCM lesions (Bergametti *et al.*, 2005). The *ccm3* gene encodes 3 isoforms that only differ in their 5' region (Li *et al.*, 2010). CCM3 is an adaptor protein of 25 kDa and functions among others in response to oxidative stress, vascular development, vascular endothelial growth factor signaling (VEGF) and apoptosis (Guclu *et al.*, 2005, He *et al.*, 2010). VEGF is a crucial factor for embryonic circulatory system development (Yla-Herttuala *et al.*, 2007, Fidalgo *et al.*, 2012). CCM3 is optionally acetylated at lysine residue Lys179 and exhibits a C-terminal focal adhesion targeting (FAT)-homology domain for protein-protein interaction (Choudhary *et al.*, 2009, Li *et al.*, 2010). CCM3 interacts with CCM2 and forms a ternary complex with CCM1 (Voss *et al.*, 2007). Moreover, CCM3 interacts with proteins involved in cell adhesion and bound to membranes such as VEGF receptor 2 (He *et al.*, 2010, Li *et al.*, 2010). Furthermore, CCM3 interacts with the mammalian kinases MST4, STK24 and STK25 (Goudreault *et al.*, 2009). MST4, STK24 and STK25 are members of the GC III kinases, a subgroup of sterile-20-like kinases (Pombo *et al.*, 2007) (Figure 5). The interaction between the GC III kinases and CCM3 are important to prevent CCM lesions (Zheng *et al.*, 2010). The GC III kinases function in important cellular processes such as modulation of cell death, proliferation and regulation of the cytoskeleton and Golgi morphology (Dan *et al.*, 2002, Huang *et al.*, 2002, Nogueira *et al.*, 2008, Preisinger *et al.*, 2004). CCM3 is assumed to be important for the shift of GC III kinases from the *cis* Golgi to the STRIPAK complex, because silencing of *ccm3* reduces GCK III binding to the STRIPAK complex and increases their binding to the Golgi matrix protein GM130 (Preisinger *et al.*, 2004). Moreover, CCM3 is essential for MST4 activation after oxidative stress; MST4 phosphorylates ERM proteins (named after their close relation to the paralogs ezrin, radixin and moesin), that crosslink actin filaments with plasma membranes, to protect cells from death. This process is impaired by inactivation of CCM3 (Lankes *et al.*, 1988, Tsukita *et al.*, 1997, Fidalgo *et al.*, 2012). CCM3 was shown to be phosphorylated by STK25 and dephosphorylated by FAS-associated phosphatase FAP-1 *in vitro* (Voss *et al.*, 2007). CCM3 interacts aside of Striatin and the STRIPAK-associated kinases

MST4, STK24 and STK25 also with other proteins of this complex such as MOB3, CTTNBP2NL and STRIP1 (Goudreault *et al.*, 2009) (Figure 2 and Figure 5). CCM3 is part of the mammalian STRIPAK core complex (Kean *et al.*, 2011) .

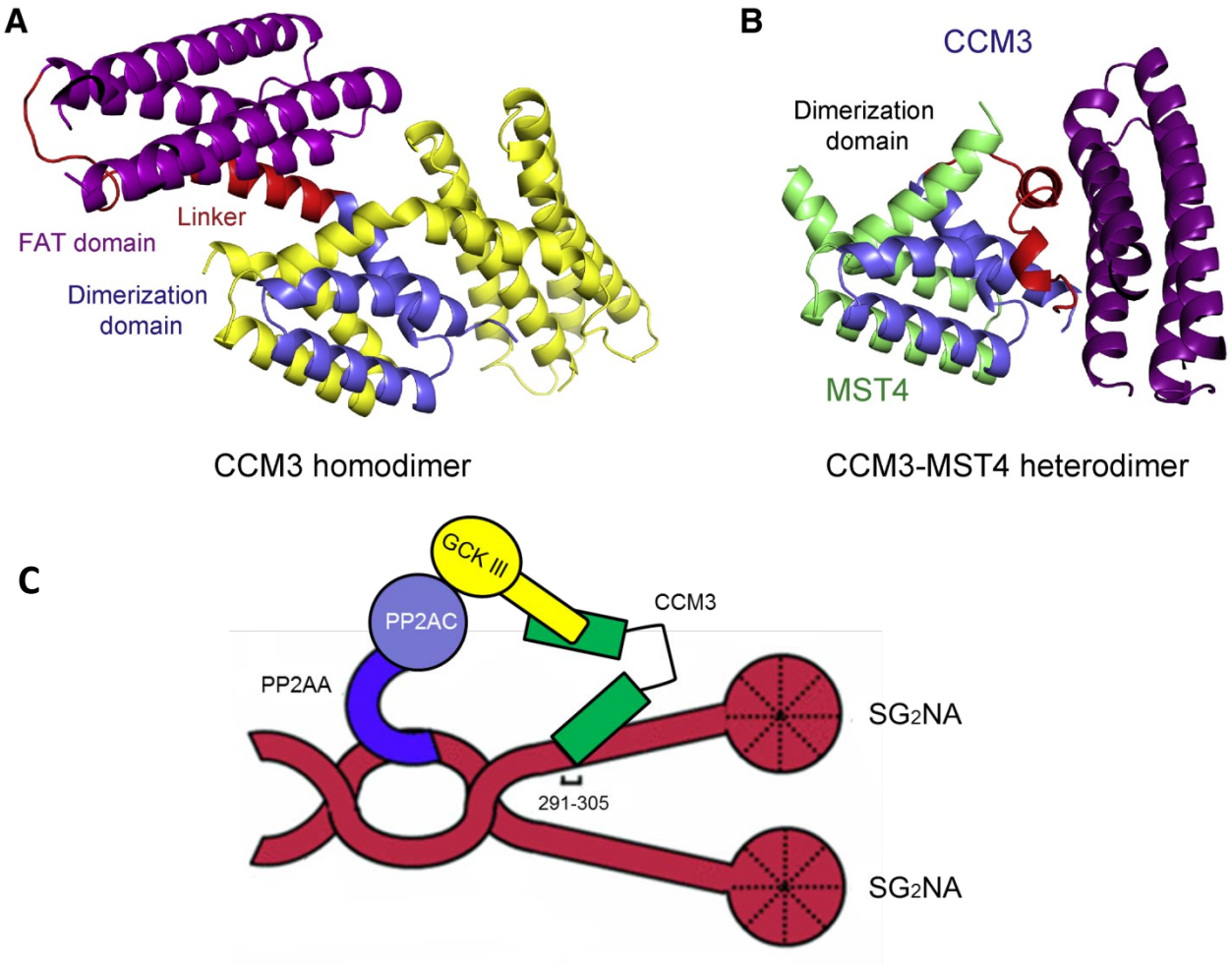

Figure 5. CCM3 functions in MST4 recruitment. (**A**) 3D structure of CCM3 forms a homodimer through its dimerization domain (blue). The FAT domain of CCM3 is shown in purple, the linker (aa 71-97) between these domains folds into a helix and is colored in red. The second CCM3 protein is colored in yellow. (**B**) CCM3 forms a heterodimer with MST4, mediated by their dimerization domains. CCM3s linker region undergoes a conformational change; its helical structure partially changes into a flexible loop in the CCM3-MST4 heterodimer. The dimerization domain of MST4 is shown in light green (according to Zhang *et al.* (2013)). (**C**) GC III kinases are bound to SG_2NA via CCM3. PP2AA and the FAT domain of CCM3/PDCD10 interact with homo-oligomerized SG_2NA. SG_2NA-PP2AA interaction requires the caveolin-binding domain and some of the coiled-coil domain of SG_2NA; CCM3 interacts with SG_2NA at aa 291-305. Although SG_2NA is shown, essentially the same findings apply to Striatin and presumably Zinedin (according to Kean *et al.* (2011)).

1.3.1.4 The GC III kinases MST4, STK24 and STK25

Mammalian GCKs regulate various cellular processes, such as polarization, migration, cell growth, neuronal differentiation, apoptosis and stress response (Sugden *et al.*, 2013, Delpire, 2009). Moreover, fungal GCKs are involved in the regulation of cytokinesis, hyphal growth and differentiation of asexual structures (Boyce & Andrianopoulos, 2011). Based on their structural similarity to the *S. cerevisiae* Sterile-20 protein kinase, GCKs are members of the Ste20-related group of protein kinases. Ste20-like kinases are subclassified into p21-activated kinases (PAK) family and a GCK family depending on the location of their kinase domain (Hanks & Hunter, 1995). The kinase domain of PAKs is located C-terminally to the regulatory domain, whereas the catalytic domain of GCKs is at the N-terminus (Dan *et al.*, 2001). GCKs share a highly conserved catalytic domain and a poorly conserved regulatory C-terminus (Hanks & Hunter, 1995, Dan *et al.*, 2001). The GCK family can be further subdivided into eight families, GCK I to GCK VIII (Dan *et al.*, 2001).

In mammals, the GC III kinases MST4, STK24, STK25 are identified as components of the STRIPAK complex (Kean *et al.*, 2011, Gordon *et al.*, 2011, Goudreault *et al.*, 2009) (Figure 2). CCM3 has recently been shown to act as an adaptor to recruit GC III kinases to the Striatins (Kean *et al.*, 2011, Gordon *et al.*, 2011, Goudreault *et al.*, 2009). The role of CCM3 is to bring GC III kinases in proximity to Striatin-connected phosphatase PP2A (Gordon *et al.*, 2011) (Figure 5) It is thought that the PP2A holoenzyme including Striatin dephosphorylate GCKs and thereby reducing the catalytic activity of GCKs associated with the STRIPAK complex (Gordon *et al.*, 2011). MST4 and STK24 have been shown to possess high basal activity (Qian *et al.*, 2001, Schinkmann & Blenis, 1997) but are also activated by phosphorylation. This process is facilitated by autophosphorylation and/or mitogen activated kinases cascades of a threonine residue at the activation loop (Dan *et al.*, 2002, Huang *et al.*, 2002, Lu *et al.*, 2006), but only little is known about their entire regulation so far. Moreover, deletion of the Ca^{2+}-CaM binding domain of Striatin increases the binding of MST4, STK24 and STK25, whereas binding of MOB3 was unaffected (Gordon *et al.*, 2011).

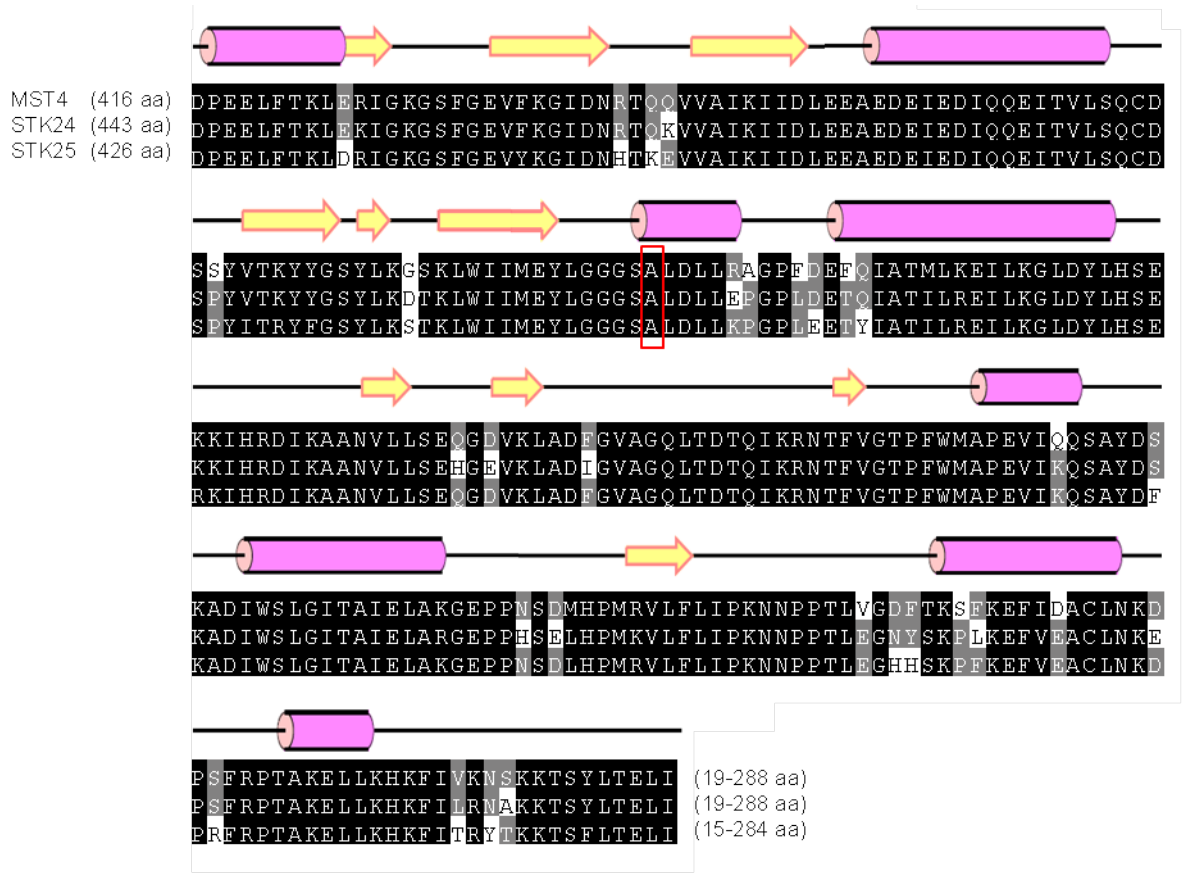

Figure 6. Aa sequence alignment, of mammalian GC III kinases. Shown are MST4 (accession number: Q9P289), MST3/STK24 (Q9Y6E0) and STK25 (O00506). The respective tertiary structure elements are shown under the aa sequence. The pink barrels mark alpha-helices; the yellow arrows represent beta-sheeds. The red box frames the conserved Asp residue that is involved in in ATP coordination (according to Record *et al.* (2010)).

1.3.1.4.1 MST4

The canonical isoform of human serine/threonine-protein kinase comprises 416 aa with a molecular weight of approximately 26.5 kDA. The *mst4* gene is alternatively spliced resulting in 3 isoforms. The kinase domain of the canonical isoform is located at position 24-274, with its active side at aa 144. The ATP binding is mediated by aa 30-38. MST4 is autophosphorylated at Thr178 (Preisinger *et al.*, 2004) (Figure 6). MST4 localizes to the Golgi apparatus and is activated by binding of Golgi matrix protein GM130, possibly as a consequence of autophosphorylation caused by stabilization of dimer formation (Preisinger *et al.*, 2004). Moreover, MST4 is activated by the adaptor molecule MO25 (Hao *et al.*, 2014). MO25 is conserved from yeast to man. In *S. pombe*, MO25 has been shown to play an essential role in

polarized growth and accumulation of F-actin at the cell tip during S and G_2 phases (Mendoza *et al.*, 2005).

Additionally, MST4 is assumed to function in apoptotic pathways because it is cleaved by caspase-3 *in vitro*. MST4 functions with CCM3 in cell growth via modulating the ERK pathway (Lin *et al.*, 2001, Ma *et al.*, 2007) and interacts with Striatin, CCM3, CTTNBP2, SG_2NA, CTTNBP2NL and STRIP1 (Goudreault *et al.*, 2009).

1.3.1.4.2 STK24

Human serine/threonine-protein kinase 24 (STK24) is a protein of approximately 49 kDa. *stk24* is alternatively spliced resulting in 2 isoforms with only slight differences. The canonical form (isoform A) comprises 443 aa in total. The kinase domain is located at position 36-286, the residues responsible for Mg^{2+}-binding are Ala161 and Ala174.

STK24 is activated by phosphorylation either via cAMP-dependend protein kinase A (PKA) at aa 320 or autophosphorylation at aa 190. Solely, isoform B is activated by PKA (Zhou *et al.*, 2000). These residues were verified by mutagenesis (Zhou *et al.*, 2000, Lu *et al.*, 2006, Olsen *et al.*, 2006). STK24 exhibits a nuclear export signal and a bipartite nuclear localization signal (Huang *et al.*, 2002).

Moreover, STK24 is processed by caspases; this results in kinase activation, nuclear translocation of the processed protein and induction of apoptosis (Huang *et al.*, 2002). Similar to MST4, STK24 localizes to the Golgi apparatus where it appears to regulate cell adhesion, protein transport and neuronal migration (Matsuki *et al.*, 2013). Furthermore, STK24 act as a major regulator of axon regeneration (Lorber *et al.*, 2009) and interact with STRIPAK proteins Striatin, SG_2NA and Zinedin, CCM3, MOB3, SLMAP, PP2A, CTTNBP2NL and STRIP1 (Ewing *et al.*, 2007, Goudreault *et al.*, 2009).

1.3.1.4.3 STK25

Human serine/threonine-protein kinase 25 is a protein of 426 aa with a molecular mass of 48 kDa. The kinase is activated by autophosphorylation at Thr178 and ATP binding is mediated by residue 26-34 (Figure 6). Further has been shown that mutagenesis of aa 49 and 159 impairs its kinase activity (Preisinger *et al.*, 2004). Similar to MST4, STK25 is assumed to be activated by

MO25 (Hao *et al.*, 2014). STK25 is activated by oxidative stress and thus, might play a role in response to environmental stress conditions. Similar to MST4 and STK24, STK25 localizes to the Golgi apparatus where it appears to regulate cell adhesion, protein transport and neuronal migration (Matsuki *et al.*, 2013).

1.3.1.5 MINK1

Misshapen-like kinase 1 (MINK1) is a serine/threonine kinase of the class of GC IV kinases. The canonical isoform of human MINK1 comprises 332 aa with a molecular weight of about 150 kDa. 5 isoforms are known, resulting from alternative splicing (Bechtel *et al.*, 2007, Ota *et al.*, 2004). All isoforms were found in brain tissue but with different amounts. However, isoform 1 is most abundant in skeletal muscles, isoform 2 is more abundant in brain tissue and isoform 3 and 4 are ubiquitously expressed (Hu *et al.*, 2004). Mammalian MINK1 functions in fundamental biological processes, such as activation of mitogen-activated protein kinases in the JNK pathway, Ras-mediated p38 MAPK activation, cytoskeletal organization, cell motility and regulation of senescence (Dan *et al.*, 2000, Hu *et al.*, 2004, Kaneko *et al.*, 2011, Nonaka *et al.*, 2008). However, the explicit function of MINK1 is still unknown. Knockdown of MINK1 or Zinedin in HeLa cells resulted in multinucleated cells, caused by abnormal abscission. Moreover, PP2A-mediated dephosphorylation of MINK1 is enhanced by Zinedin *in vitro* (Hyodo *et al.*, 2012). Thus, Zinedin may regulate MINK1 inactivation by PP2A, similar to GC III kinases by Striatin (Gordon *et al.*, 2011, Hwang & Pallas, 2014). Based on gel-shift experiments were hypothesized that this process might be required for proper MINK1 function in abscission. Furthermore, the *D. melanogaster* homolog of MINK1 and the Striatin homolog CKA were shown to function among other biological processes in dorsal closure (Su *et al.*, 2000, Chen *et al.*, 2002).

1.3.1.6 STRIP1/2

Human Striatin-interacting protein 1 (formerly FAM40A) comprises 837 aa with a molecular weight of approximately 96 kDa. The respective gene is alternatively spliced resulting in 4 isoforms (Bechtel *et al.*, 2007, Ota *et al.*, 2004). Its paralog STRIP2 (FAM40B) comprises 834 aa with a molecular weight of about 95 kDa. The *strip2* gene is alternatively spliced and to date,

2 isoforms of STRIP2 are known (Bechtel *et al.*, 2007, Ota *et al.*, 2004). STRIP1/2 are membrane bound and localize to the Golgi, where they are assumed to bridge (in combination with SLMAP) the centrosome and the nuclear envelope (Frost *et al.*, 2012). In mammals, STRIP1 and 2 were shown to interact with STRIPAK components Striatin, CTTNBP2NL and MST4 (Goudreault *et al.*, 2009).

STRIP1/2 have a role in cytoskeletal organization, cell morphology and migration (Bai *et al.*, 2011). Knockdown of *strip1* and *strip2* genes in PC3 prostate cancer cells showed different phenotypes; *strip1* knockdown resulted in changed actin formation and reduced cell spreading, *strip2* knockdown resulted in altered microtubule organization and induced cell elongation. Thus, STRIP1 and 2 might function in targeting STRIPAK complexes to regulate cytoskeletal function and organization (Hwang & Pallas, 2014). Moreover, knockdown of *strip1* in HeLa cells caused increased DNA content and resulted in binuclear cells. Furthermore, these nuclei were dysmorphic and fragmented. These findings indicate that STRIP1/2 function with STRIPAK components in mitotic progression and cytokinesis (Frost *et al.*, 2012).

In *N. crassa*, the STRIP1/2 homolog HAM-2 functions in sexual development and hyphal fusion (Xiang *et al.*, 2002). Deletion or mutation of *ham-2* resulted in decreased growth velocity, shorter aerial hyphae, female sterility, and hyphal fusion defects. Furthermore was hypothesized that functional HAM-2 is needed to produce a yet unknown chemical attractant to attract conidial anastomosis tubes for hyphal fusion (Roca *et al.*, 2005). In *N. crassas* close relative *S. macrospora*, STRIP1/2 homolog PRO22 was shown, aside from sexual development and hyphal fusion, to be necessary for septa formation in protoperithecia (Bloemendal *et al.*, 2010, Rech *et al.*, 2007).

1.3.1.7 SLMAP

The canonical isoform of human sarcolemmal membrane-associated protein comprises 828 aa with a molecular mass of 95 kDa. It contains a transmembrane domain, three coiled-coil domains and a forkhead-associated domain, which is a phosphopeptide recognition domain found in many regulatory proteins (Hofmann & Bucher, 1995). To date, 8 isoforms of SLMAP are known (Wielowieyski *et al.*, 2000, Bechtel *et al.*, 2007, Ota *et al.*, 2004). Isoform 1 and 2 are predominantly found in cardiac slow twitch and smooth muscles (Guzzo *et al.*, 2004,

Wielowieyski *et al.*, 2000). Each SLMAP isoforms contain one or two transmembrane domains, which are crucial for subcellular targeting (Byers *et al.*, 2009). It is not known, which of these isoforms are STRIPAK-associated. However, based on their localization, several SLMAP isoforms have the potential to be STRIPAK-associated (Hwang & Pallas, 2014). Guzzo *et al.* (2004) showed that SLMAP functions in myoblast fusion. Myoblasts are embryonic preliminary skeletal muscles. Differentiation of myoblasts induces expression of a new SLMAP isoform, whereas SLMAP isoform 1 and 3 inhibit myoblast fusion. SLMAP localization is isoform-dependent (Frost *et al.*, 2012, Guzzo *et al.*, 2005). Moreover, a SLMAP isoform is assumed to be involved in glucose uptake (Chen & Ding, 2011). SLMAP localizes primarily to the outer nuclear envelope, some endoplasmatic reticulum structures and to centrosomes (Frost *et al.*, 2012, Guzzo *et al.*, 2005, Guzzo *et al.*, 2004). Further has been speculated, that STRIPAK components, including SLMAP have an important role in proper subcellular localization of mammalian tumor suppressor adenomatous polyposis coli (APC) (Breitman *et al.*, 2008, Tran *et al.*, 2013). SLMAP knockdown in HeLa cells causes slightly increased cellular DNA content and increased the amount of pericentrin foci in cells during interphase (Frost *et al.*, 2012). Pericentrin is a component of the centrosome that serves as a multifunctional scaffold (Delaval & Doxsey, 2010). Thus, SLMAP might function in coordination of mitotic progression and cytokinesis.
Moreover, yeast SLMAP homolog FAR9 is required for secretion of pheromone factor α and has been shown to function in proper sorting of proteins to the vacuole (Bonangelino *et al.*, 2002). SLMAP has been shown to interact with Striatin, SG_2NA, subunit A of PP2A, MST4, STK25 SIKE, STRIP1/2 and FGFR1OP2 (Goudreault *et al.*, 2009).

1.3.1.8 CTTNBP2/NL

Human cortactin-binding protein 2 exists in two natural variants (Cheung *et al.*, 2001). CTTNBP2 consists of 1663 aa with a molecular weight of 181 kDa. It contains a coiled-coil domain for oligomerization and 6 ankyrin repeats. These domains are common for protein-protein interaction in nature (Mosavi *et al.*, 2004). CTTNBP2 N-terminal-like (CTTNBP2NL**)** consists of 639 aa with a molecular weight of about 70 kDa and contains a coiled-coil domain. CTTNBP2/NL are cortactin-binding proteins. Cortactin, named after cortical actin-binding protein, is a monomeric, cytoplasmatically localized protein that promotes polymerization and

rearrangement of the actin cytoskeleton (Cosen-Binker & Kapus, 2006). CTTNBP2 and CTTNBP2NL target cortactin to different populations of actinfibers; CTTNBP2 co-localizes with cortactin at the cell cortex, whereas CTTNBP2NL localizes to cortactin at stress fibers, with higher affinity than CTTNBP2 does (Chen *et al.*, 2012). In contrast to CTTNBP2NL, CTTNBP2 is highly expressed in brain tissues where it regulates dendric spine density and targeting of Striatin and Zinedin to dendric spines (Chen *et al.*, 2012). Furthermore was shown, that overexpression of cortactin but not of CTTNBP2NL or mutated CTTNBP2 impaired in cortactin binding, rescues the CTTNBP2 knockdown phenotype and thus, both proteins might have different functions (Chen *et al.*, 2012, Chen & Hsueh, 2012). It is further assumed that CTTNBP2 and CTTNBP2NL might guide the STRIPAK complexes to different subcellular compartments. Moreover was shown, that N-Methyl-D-aspartate (NMDA) receptor-based synaptic signaling alters the localization of Striatin and Zinedin to dendric spines but not of CTTNBP2. NMDA is an aa derivate that binds to NMDA receptors where it mimics results of glutamate binding. NMDA receptors are ion channels, that facilitate flow of small amounts of Ca^{2+} ions into the cell (Dingledine *et al.*, 1999).

Treatment with NMDA resulted in decreased amounts of Striatin and Zinedin complexed with CTTNBP2, but did not affect CTTNBP2 concentrations in total (Chen *et al.*, 2012). Activation of NMDA receptors leads to an increase of calcium concentrations in the cell. Hwang & Pallas (2014) hypothesized on these data, that this might also cause increased CaM-Ca^{2+} Striatin binding. CTTNBP2 and CaM-Ca^{2+} share the N-terminus of Striatins for interaction and thus, CaM-Ca^{2+} might reduce CTTNBP2 binding to Striatin. CTTNBP2 and CTTNBP2NL associate with the APC-deubiquitinating enzyme Trabid (Tran *et al.*, 2013). In addition, Striatins have been shown to be necessary for proper subcellular localization of APC (Breitman *et al.*, 2008, Tran *et al.*, 2013). Thus, STRIPAK might regulate APC localization and function together with Trabid (Hwang & Pallas, 2014). CTTNBP2NL interacts with kinase MAP4K4 (Herzog *et al.*, 2012). MAP4K4 is a negative regulator of myoblast differentiation and fusion (Wang *et al.*, 2013). SG_2NA and Zinedin were also shown to interact with MAP4K4. Thus, CTTBNBP2NL was speculated to regulate MAP4K4 function in complex with Striatins (Hwang & Pallas, 2014). Furthermore, CTTNBP2/NL were shown to interact with each other, Striatin, MOB3, MST4, STK24, STRIP1 and PP2A subunit A and C (Goudreault *et al.*, 2009).

1.3.1.9 SIKE

The canonical isoform of human SIKE comprises 207 aa with a molecular weight of approximately 24 kDa. To date, 2 slightly different isoforms are known, both contain 2 coiled-coil domains for oligomerization. SIKE is named after suppressor of IKKε, IKKε stands for inhibitor-κB kinase ε (Huang *et al.*, 2005). IKKε and TANK-binding kinase 1 (TBK1) are kinases that phosphorylates interferon regulatory factor 3 (IRF-3), which is important for systemic responses to viral infections. SIKE binds to the IKK-related kinases, IKKε and TBK1, and inhibits their ability to interact with the adaptor proteins TRIF and interferon regulatory factor 3 (IRF-3), and the sensor protein retinoic acid-inducible gene 1 (RIG-1). TRIF is a signaling component that acts upstream of IKKε and TBK1 in toll-like receptor 3 (TLR3)-mediated signaling (Huang *et al.*, 2005).

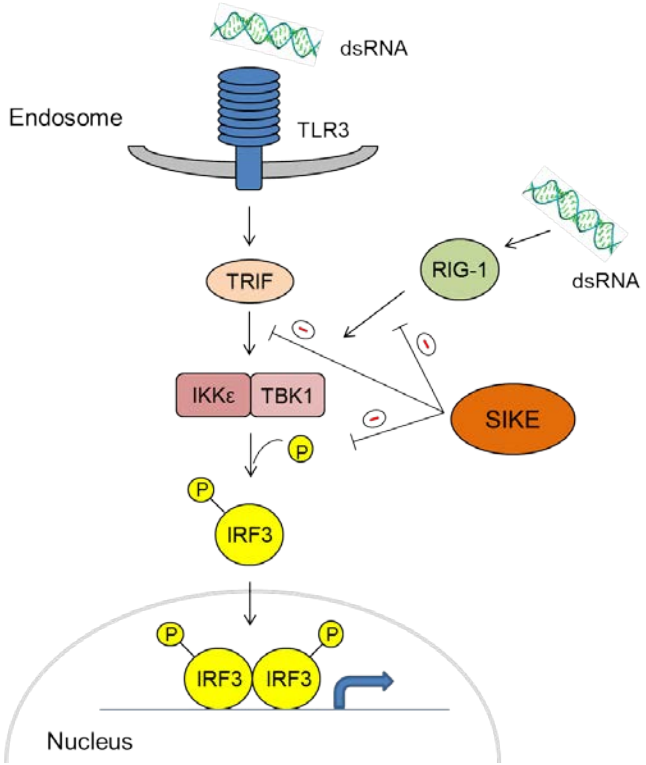

Figure 7. Function of SIKE in IKKε and TBK1-mediated innate immune response. TLR3 is activated by double-stranded RNA (dsRNA), which is generated during virus replication. This leads to interaction between TRIF and the kinases IKKε and TBK1, which phosphorylate IRF3. Phosphorylated IRF3 translocates into the nucleus, where it activates as dimer a special set of promotors. SIKE inhibits interaction between TRIF and IRF3 with IKKε and TBK1; moreover it inhibits interaction between RIG-1 and both kinases. RIG-1 functions in intracellular dsRNA recognition and activates similar to TRIF, IKKε and TBK1 (according to Cardenas (2010) and Ariumi (2014)).

RIG-1 functions as recognition receptor for virus detection (Pichlmair *et al.*, 2006). Activation of TLR3 significantly reduces interaction between SIKE and TBK1 interaction (Huang *et al.*, 2005). It is not known, if interaction of SIKE with Striatin works independently to inhibition of IKKε and TBK1. SIKE is present in various tissues, among them brain, colon, heart, lung and kidney (Huang *et al.*, 2005).

1.3.1.10 FGFR1OP2

The canonical isoform of human fibroblast growth factor receptor 1 oncogene partner 2 (FGFR1OP2) comprises 253 aa with a molecular mass of 29.5 kDa and contains 2 coiled-coil domains. To date, 3 isoforms are known, resulting from alternative splicing (Bechtel *et al.*, 2007, Ota *et al.*, 2004). FGFR1OP2 is a paralog of SIKE and was first identified in gingiva wound healing (Sukotjo *et al.*, 2002). FGFR1OP2 is induced in wounded oral fibroblasts (Sukotjo *et al.*, 2002). Further was shown, that FGFR1OP2 generally contributes to the ability of wound healing in fibroblasts and is important for fibroblast-cell migration (Lin *et al.*, 2010). FGFR1OP2 is not induced in skin wounding but was shown to contribute, if endogenously expressed, to this process (Lin *et al.*, 2010). To date, it is not known, if the STRIPAK complex functions in this process. SIKE and FGFR1OP2 are likely mutually exclusive STRIPAK members (Hwang & Pallas, 2014).

1.3.2 STRIPAK in signaling

The STRIPAK complex functions in various processes among them apoptosis, cell-cycle control, signaling, Golgi assembly and vesicular trafficking, cell migration and polarity, cardiac function as well as neural and vascular development (Hwang & Pallas, 2014). The STRIPAK core complex consists of several proteins, which function in many signaling pathway (see 1.3.1) and interact with proteins, that in turn, functions in further pathways. Based on broad range interaction studies of the recent years, a complex model has developed (Hwang & Pallas, 2014). Figure 8 sums up STRIPAK functions in signaling, as partially discussed under 1.3.1. Additional pathways are described in the text.

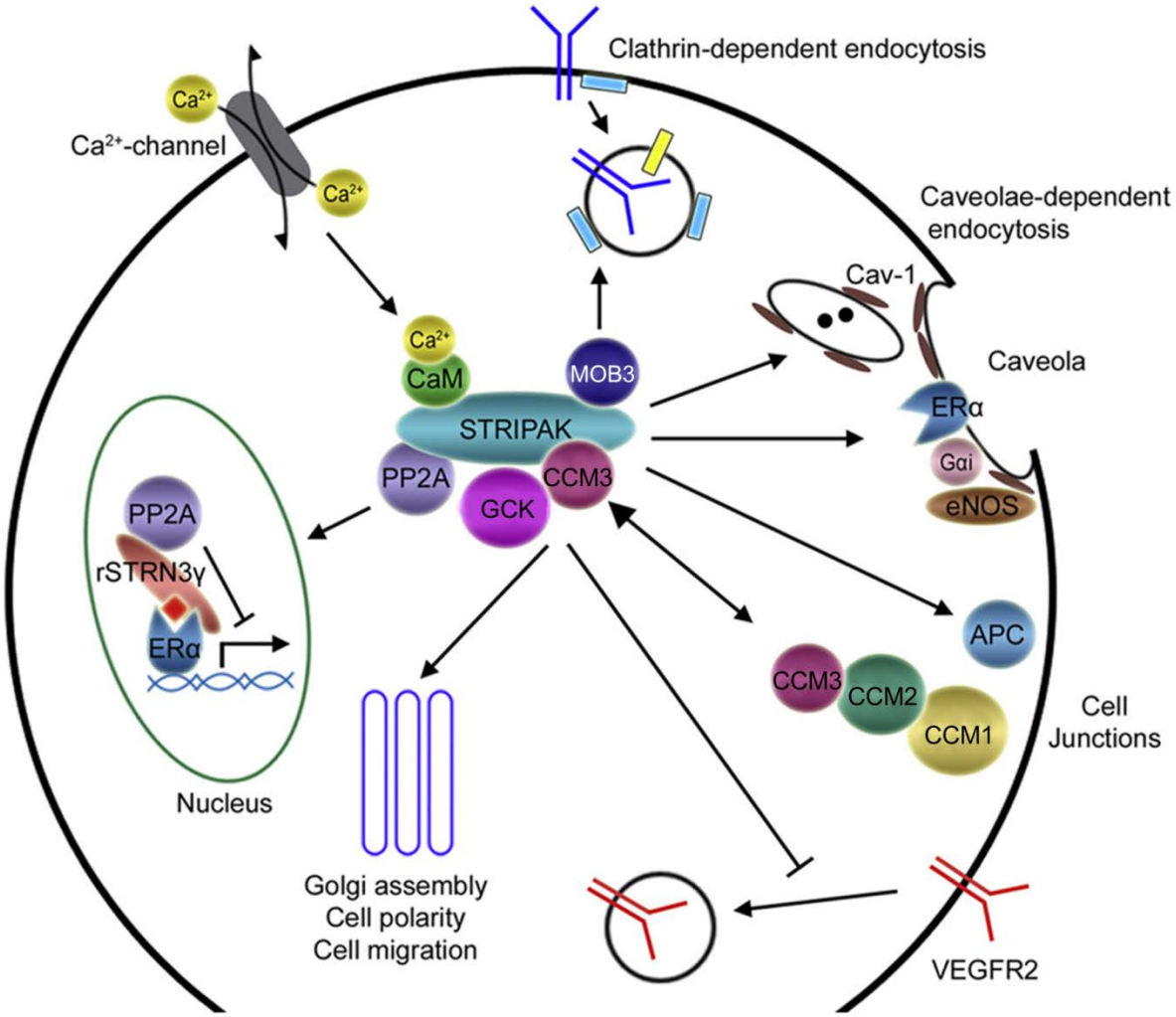

Figure 8. Schematic overview about the STRIPAK core complex in signaling. Shown is the core complex in the center and the signaling pathways it functions in indicated with arrows. The pathways are described in the following text or have been described above (according to Hwang and Pallas (2014)).

The STRIPAK-associated protein MOB3 was shown to interact with components of the clathrin-dependent endocytosis, such as epidermal growth factor receptor substrate 15 (EPS15), nucleoside-diphosphate kinase (NDPK) and Dynamin I. MOB3 was shown to co-localize with Dynamin I in neurons (Baillat *et al.*, 2002). Generally, NDPK, EPS15, and Dynamin I function in membrane dynamics and thus, in endocytosis. EPS15 is an adaptor protein that has a role in ligand-induced receptor endocytosis of receptor-tyrosine kinases (Fazioli *et al.*, 1993). Further was shown, that EPS15 interacts with Dynamin I physically and genetically (Baillat *et al.*, 2002, Salcini *et al.*, 2001). Dynamin I is a GTPase that functions in secession of clathrin-coated

vesicles from the plasma membrane during endocytosis (Hwang & Pallas, 2014). NDPK also physically interacts with Dynamin I (Baillat *et al.*, 2002). Based on these findings and further research in *D. melanogaster*, NDPK is assumed to function in endocytosis by generating GTP for Dynamin I (Krishnan *et al.*, 2001). Thus, the STRIPAK complex is hypothesized to be involved in endocytosis via MOB3 interactions. This assumption is further supported by findings in *D. melanogaster*, where the MOB3 homolog has a role in axonal transport, microtubule organization, neurite growth and branching and synapse assembly (Schulte *et al.*, 2010, Sepp *et al.*, 2008). Furthermore, the STRIPAK complex is also suggested to function in caveolae-dependent endocytosis. This has already been described in section 1.1.1.

Moreover, the STRIPAK complex is implicated in regulating and targeting estrogen receptor α (ERα) to membranes. This is based identification of a STRIPAK-like complex containing ERα, the heterotrimeric guanine nucleotide binding protein subunit Gαi and endothelial nitric oxide synthetase (eNOS). Estrogens mediate cellular functions via receptor signaling (O'Lone *et al.*, 2004). Genomic, ERα-mediated signaling takes place at the nucleus, where ERα functions in transcription. Nongenomic signaling of estrogens is facilitated by caveolae-associated ERα and in endothelial cells including enzymes such as eNOS for rapid activation (Chambliss *et al.*, 2000, Raz *et al.*, 2008).

The STRIPAK complex serves as scaffolding unit for PP2A and ERα in nongenomic and genomic estrogen-mediated ERα signaling (Tan *et al.*, 2008). In rat was shown, that a SG_2NA splice variant localizes to the nucleus (see also 1.1.2). This isoform forms an STRIPAK-like complex containing PP2A and ERα and is induced by estrogens. This complex regulates ERα activity by PP2A-dependent dephosphorylation (Tan *et al.*, 2008). However, a STRIPAK complex involved in nongenomic ERα signaling is facilitated by direct Striatin-ERα interaction. Lu *et al.* (2004) showed that aa 1-203 of Striatin and aa 183-253 of ERα are sufficient for Striatin-ERα complex formation and aa 176-253 of Striatin are needed for estrogen-induced nongenomic eNOS activation.

Additionally, the STRIPAK complex is involved in APC-mediated organization of tight junctions via SIKE and CTTNBP2NL as described previously under 1.3.1.9 and 1.3.1.8. Tight junctions are small ribbons of membrane proteins especially found in epithelial cells, which function mainly as diffusion barrier (Bauer *et al.*, 2014). Moreover, observation in many CCM lesions led to the hypothesis, that CCM1, CCM2 and CCM3 are important for stability or

assembly of cell-junctions of endothelial cells (Burkhardt *et al.*, 2010, Clatterbuck *et al.*, 2001, Schneider *et al.*, 2011). Mammalian Striatin and SG_2NA have been identified as interaction partners of GAIP-interacting protein, C terminus (GIPC) (Varsano *et al.*, 2006). The GTPase activating protein GAIP functions in vascular endothelial growth factor receptors 2 (VEGFR2) signaling, endocytosis and trafficking (Varsano *et al.*, 2006). VEGFR2 in turn, is necessary for formation of the circulatory system (Holmes *et al.*, 2007). Thus, the STRIPAK complex is assumed to function similar to MOB3-EPS15 interaction, in endocytosis of cell surface receptors (Hwang & Pallas, 2014). The signaling pathways including GC III kinases and Ca^{2+} have already been mentioned in section 1.1 and 1.3.1.4.

The STRIPAK complex was shown to modulate signaling in the cell lumen in many ways, depending on the incoming signal, such as changed Ca^{2+} concentrations (Figure 8). However, incoming signals from environmental changes are first detected by receptors, which are localized at the exterior of the cell. Thus, cellular mechanisms are required that mediate signal transduction from the recognized signal at the cell exterior to the cell lumen. This process could be mediated by glycosylphosphatidylinositol (GPI)-anchored proteins, a group of proteins that are attached to the outer leaflet of the cell by a glycolipid anchor (Kinoshita, 2014). To function in this process, the GPI-anchor act as an intermediary for communication between cell exterior and internal signaling (Robinson, 1997, Jones & Varela-Nieto, 1998). Using antibody cross-linking, some GPI-anchored proteins have been shown to effect activating or inhibitory signals, such as phosphorylation or Ca^{2+} influx (Robinson, 1997, Jones & Varela-Nieto, 1998). Even though the GPI-anchored protein might not pass the cell membrane completely, it transduces incoming signals by interaction with other transmembrane proteins, such as, integrins or protein kinases (Simons & Toomre, 2000).

1.4 GPI-anchoring

Eisenhaber *et al.* (2001) previously calculated that 0.5-1% of the total number of proteins encoded in the eukaryotic genome are GPI-anchored. Further is known that 10-20% of eukaryotic membrane proteins are attached to the cell surface by GPI-anchoring (Orlean & Menon, 2007). These proteins are various in function such as enzymatic reactions, signal transduction, bacterial infection and cell to cell interaction (Ilangumaran *et al.*, 2000). Further has been shown that metabolites of GPI-anchored proteins serves as second messenger in

hormonal pathways (Young & Moss, 2000) or mediate protein and glycoprotein endocytosis and turnover (Guo, 2013). GPI-anchors are complex glycolipids posttranslationally linked to a certain aa at the C-terminus of a group of specifically structured proteins (Eisenhaber *et al.*, 1999) (Figure 9).

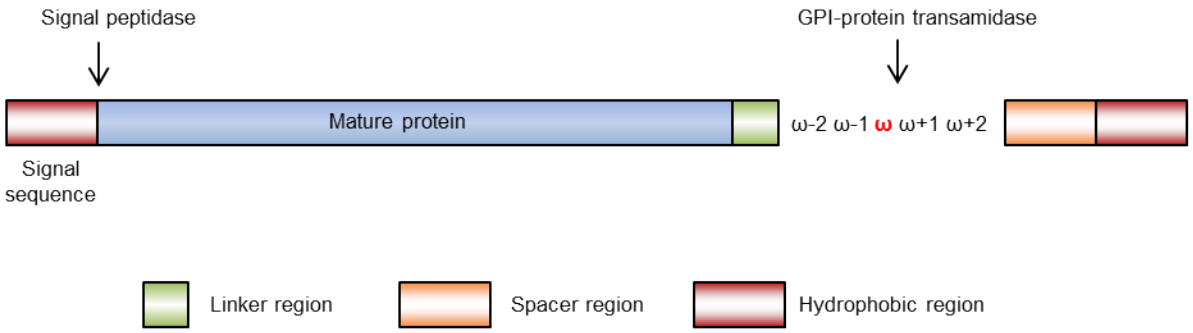

Figure 9. Schematic model of GPI-anchored protein precursors. GPI-anchored proteins are synthesized as precursors and consists of two characteristic domains, an N-terminal signal sequence and a region for GPI-anchor attachment. The signal sequence consists of hydrophobic aa and is removed by cleavage. The region for GPI-anchor attachment consists of a linker region, the ω-residue, followed by a polar spacer and a hydrophobic region to the C-terminal end. The ω-residue is the aa, where the GPI-anchor, a glycolipid for membrane anchoring, is attached to. GPI-anchor attachment requires transamidase cleavage of the precursor between position ω and ω+1. The residues ω+1 and ω+2 are crucial but unknown in function. ω-1 and ω-2 are assumed to function in cell-wall anchoring. The Linker region separates the mature protein from the GPI-anchor (modified according to Mayor and Riezman (2004)).

The precursor of a GPI-anchored protein consists of two characteristic domains; an N-terminal signal sequence and a C-terminally located region for GPI-anchor attachment (Mayor & Riezman, 2004) (Figure 9). The signal sequence commonly comprises 5-30 aa (Blobel & Dobberstein, 1975) and serves for the transport to the ER (Rapoport, 2007). In the ER the protein precursor is processed (Orlean & Menon, 2007) and the synthesis as well as the covalent attachment of the glycolipid anchor to the target proteins takes place (Pittet & Conzelmann, 2007). The glycolipid is attached to a special residue within the sequence of the protein precursor, named ω-residue. Prior to the attachment, the ω-residue is exposed by transamidase cleavage (Eisenhaber *et al.*, 1999). According to present-day research, the region for GPI-anchor attachment comprises approximately aa ω-10 up to the C-terminal end of the protein precursor (Pierleoni *et al.*, 2008). As already mentioned, the ω-residue is exposed by cleavage. It has been shown that aa ω-1 to ω+2 are part of the transamidase cleavage side (Eisenhaber *et al.*, 1998,

Paladino *et al.*, 2008). Efficient cleavage depends also on the polar spacer region and the hydrophobic tail. The spacer region encompasses the aa from position ω+3 to ω+9 and consists of polar residues (Pierleoni *et al.*, 2008), the hydrophobic tail comprises aa ω+10 to the C-terminal end, represented by hydrophobic aa (Mayor & Riezman, 2004). According to Galian *et al.* (2012) the hydrophobic tail was described to be "less hydrophobic than type II transmembrane anchors and more hydrophobic than the most hydrophobic segments found in secreted proteins". After successful cleavage and glycolipid attachment to the proteins ω-residue, the aa ω-12 to ω-1 are assumed to serve as linker between the GPI-anchor and the protein and are characterized by a low amount of secondary structure (Pierleoni *et al.*, 2008). The region for GPI-anchor attachment might also influence the destination of the protein; aa ω-1 and ω-2 were previously shown to be necessary for optional cell-wall attachment in yeast (Frieman & Cormack, 2003) and *Aspergillus fumigatus* (Ouyang *et al.*, 2013). Various structures of GPI-anchors have been identified (Thomas *et al.*, 1990, Paulick & Bertozzi, 2008, Guo, 2013) sharing the core structure of 3 mannose residues, ethanolamine, glucosamine and phosphoinositol bound to fatty acids (Paulick & Bertozzi, 2008) (Figure 10).

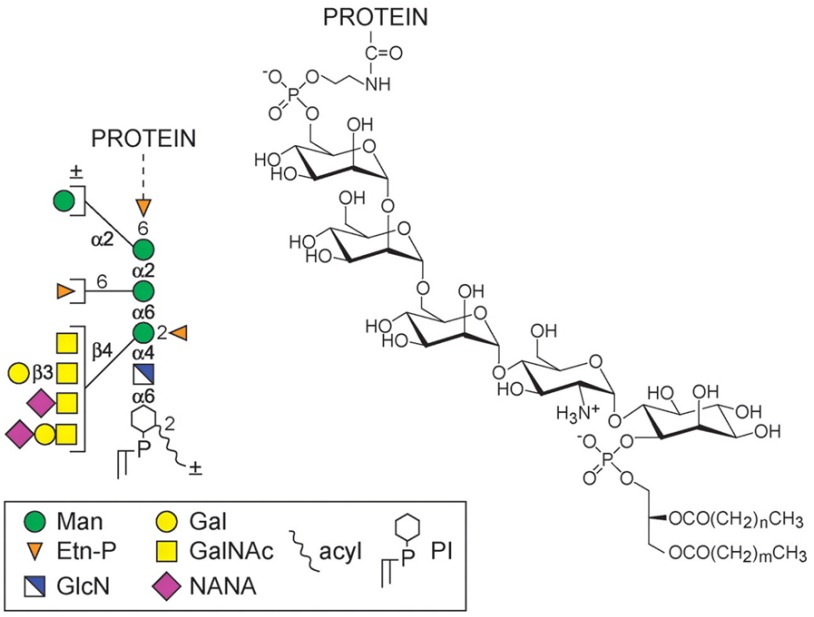

Figure 10. Structure of yeast and mammalian GPI-anchors. GPI-anchors in chemical detail are shown on the right, the schematic model is shown on the left. GPI encompasses a core of 3 mannose residues, glucosamine (GlcN), and Phosphatidylinositol (PI). The mannose residues are named Man. Man-1 is the residue linked to glucosamin (GlcN). The third mannose residue is modified with an ethanolamine phosphate (Etn-P). GalNAc = N-acetylglucosamin, NANA = N-acetylneuraminic acid (according to Orlean & Menon (2007)).

1.5 *Sordaria macrospora*: A model for fruiting-body development

The haploid filamentous ascomycete *S. macropsora* is an established model organism to study multicellular fruiting-body development (Teichert *et al.*, 2014). Under natural conditions, *S. macrospora* grows on herbivore dung (Esser, 1992). It is self-fertile (homothallic) and lacks an asexual life cycle, meaning it solely undergoes a sexual life cycle without need for a mating partner (Pöggeler *et al.*, 1997, Lord & Read, 2011). Thus, mutations can be directly tested on their influence on fruiting-body formation.

Its 39.8 Mb comprising genome is entirely sequenced, allowing easy identification of orthologs known from other organisms (Kück *et al.*, 2009, Nowrousian *et al.*, 2010). Further advantages are its haploidy and its largely-sized ascospores, which allow classical genetic experiments and the isolation of homokaryotic mutants after mutagenesis. The formation of multicellular fruiting bodies is an essential step in sexual reproduction of filamentous fungi and involves highly controlled cellular differentiation programs (Pöggeler *et al.*, 2006). After the ascospores germinate, the fungus grows as two-dimensional mycelium. At day 3 of development the sexual life cycle starts with formation of ascogonia, representing female gametangia. At day 4, these hyphal coils develop into pre-fruiting bodies, called protoperithecia. Karyogamy, meiosis, and postmeiotic mitosis occur in mature fruiting bodies (perithecia) resulting in asci with 8 linearly ordered ascospores. These spores are released from the perithecia by increased turgor pressure at day 7 as shown in Figure 11 (Engh *et al.*, 2010, Lord & Read, 2011).

Several PRO proteins essential for fruiting-body formation were identified in a forward genetic screen (Bloemendal *et al.*, 2010, Dirschnabel *et al.*, 2014, Engh *et al.*, 2007, Masloff *et al.*, 1999, Nowrousian *et al.*, 2007, Nowrousian *et al.*, 2012, Pöggeler & Kück, 2004). Pro mutants, including pro11, are characterized by a life-cycle arrest at the stage of protoperithecia formation. The *S. macrospora pro11* gene encodes a homolog to mammalian Striatin (Pöggeler & Kück, 2004). Striatin proteins are scaffolding units of the recently identified supramolecular STRIPAK complex (Goudreault *et al.*, 2009) (1.3). In filamentous ascomycetes, several of the yet identified homologs of mammalian STRIPAK components have been identified and are essential for fruiting-body development and cell fusion (Bloemendal *et al.*, 2010, Maerz *et al.*, 2009, Pöggeler & Kück, 2004, Shim *et al.*, 2006, Simonin *et al.*, 2010, Xiang *et al.*, 2002)

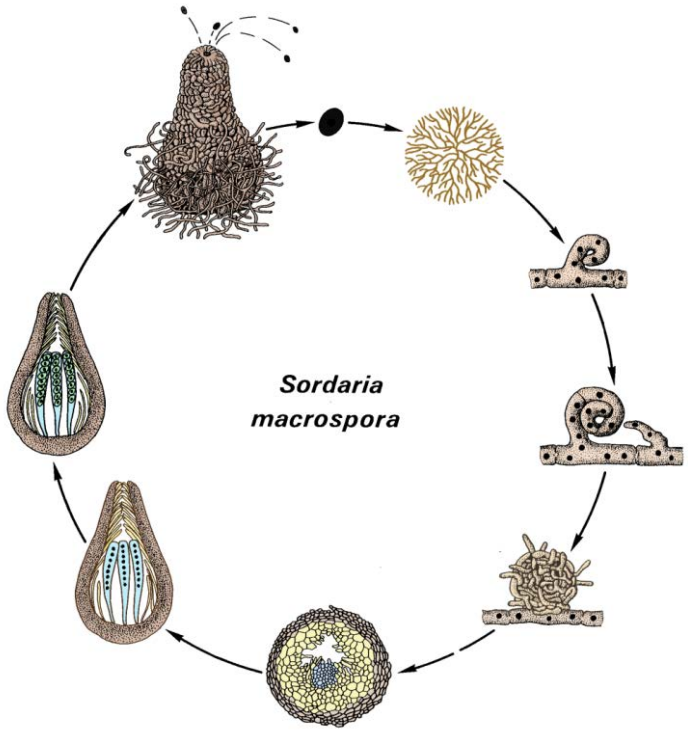

Figure 11. Schematic model of the *S. macrospora* life cycle. The life cycle starts with ascospore germination which further develops to a two-dimensional mycelium. At day 3 of development the sexual life cycle starts with formation of ascogonia. These hyphal coils develop into pre-fruiting bodies, called protoperithecia at day 4. The mature fruiting body, named perithecium contains asci with 8 linearly ordered ascospores, resulting from karyogamy, meiosis, and postmeiotic mitosis. Under laboratory conditions, the life cycle is completed after 7 day (according to Kück *et al.* (2009)).

1.6 Aim of this study

The central aim of this thesis was to get more insight in the role of the STRIPAK complex in the filamentous ascomycete *S. macrospora*. This comprised the characterization of *Smgpi1*, gene coding for a GPI-anchored protein which was first identified as interaction partner of SmMOB3, and the identification of potential STRIPAK-associated kinases. The potential kinases should be identified by a BLAST search against the *S. macrospora* genome using the respective mammalian kinases MST4, STK24, STK25 and MINK1 as query. Subsequently, the potential homologs should be tested for interaction with Striatin homolog PRO11. Moreover, the genes *Smgpi1,* and these encoding for the putative homologs of STRIPAK-associated kinases should be replaced by an *hph* resistance cassette to investigate their impact on sexual development and vegetative growth. The respective strains are supposed to be complemented with full-length genes and in case of ΔSmgpi1, also with truncated gene versions encoding proteins comprising or lacking the signal sequence for ER targeting and the region for GPI-anchor attachment. Moreover, localization studies with fluorescence marker eGFP should be used to identify their cellular localizations. Localization of SmGPI1 should be performed with several constructs, similar to the complementation analysis but tagged with eGFP. Furthermore, generation of double-knockout strains are supposed to be generated including deletion of *Smgpi1* in combination with other genes coding for STRIPAK-associated proteins PRO11 (Striatin homolog), PRO22 (STRIP1/1 homolog, SmMOB3 and PRO45 (SLMAP homolog).

2. Material and Methods

2.1 Strains

Table 2 contains the strains used and generated for this study, ordered by organism.

Table 2. Strains generated and used for this study

Name	Genotype	Source
	Escherichia coli	
Mach1	*ΔrecA139 endA1 tonA Φ80*(*lacZ*)*Δ*M15 *ΔlacX74 hsdR(rK-mK+)*, recipient strain for vector amplification	Invitrogen, Germany
	Saccharomyces cerevisiae	
PJ69-4A	*MATa trp1-901 leu2-3_112 ura3-52 his3_200 ga14Δ ga18OΔ LYS2::GALl-HIS3 GAL2-ADE2 met2::GAL7-lacZ*	James *et al*.,1996
Y187	*MATα; ura3-52; his3-200; ade2-101; trp1-901; leu2-3, 112; gal4Δ; metΔ; gal80Δ; MEL1; URA3::GAL1*$_{UAS}$*-GAL1*$_{TATA}$*-lacZ*	Clontech, Mountain View, USA
AH109	*MATa; trp1-901; leu2-3, 112; ura3-52; his3-200; ade2-101; gal4Δ; gal80Δ; LYS2::GAL1*$_{UAS}$*-GAL1*$_{TATA}$*-HIS3; GAL2*$_{UAS}$*-GAL2*$_{TATA}$*-ADE2; URA3::MEL1*$_{UAS}$*-MEL1*$_{TATA}$ *-lacZ; MEL1*	Clontech, Mountain View, USA
Y187 + pBD-SmGPI1 aa 1-253	*MATα; ura3-52; his3-200; ade2-101; trp1-901; leu2-3,112; gal4Δ; metΔ; gal80Δ;MEL1;URA3::GAL1*$_{UAS}$*-GAL1*$_{TATA}$*-lacZ;* GAL4-binding domain N-terminally fused SmGPI1 from *Smgpi1* cDNA encoding aa 1-253 under control of *adh* promoter	this study
Y187 + pBD-SmGPI1 aa 28-227	*MATα; ura3-52; his3-200; ade2-101; trp1-901; leu2-3,112; gal4Δ; metΔ; gal80Δ;MEL1;URA3::GAL1*$_{UAS}$*-GAL1*$_{TATA}$*-lacZ;* GAL4-binding domain N-terminally fused SmGPI1 from *Smgpi1* cDNA encoding aa 28-227 under control of *adh* promoter	this study
Y187 + pBD-SmGPI1 aa 1-100	*MATα; ura3-52; his3-200; ade2-101; trp1-901; leu2-3,112; gal4Δ; metΔ; gal80Δ;MEL1;URA3::GAL1*$_{UAS}$*-GAL1*$_{TATA}$*-lacZ;* GAL4-binding domain N-terminally	this study

	fused SmGPI1 from *Smgpi1* cDNA encoding aa 1-100 under control of *adh* promoter	
Y187 + pBD-SmGPI1 aa 101-253	*MATα; ura3-52; his3-200; ade2-101; trp1-901; leu2-3,112; gal4Δ; metΔ; gal80Δ;MEL1;URA3::GAL1*$_{UAS}$*-GAL1*$_{TATA}$*-lacZ;* GAL4-binding domain N-terminally fused SmGPI1 from *Smgpi1* cDNA encoding aa 101-253 under control of *adh* promoter	this study
AH109 + pAD-SmMOB3	*MATa; trp1-901; leu2-3, 112; ura3-52; his3-200; ade2 -101; gal4Δ; gal80Δ; LYS2::GAL1*$_{UAS}$*-GAL1*$_{TATA}$*-HIS3; GAL2*$_{UAS}$*-GAL2*$_{TATA}$*-ADE2; URA3::MEL1*$_{UAS}$ *-MEL1*$_{TATA}$*-lacZ; MEL1;* GAL4-activation domain N-terminally fused to SmMOB3 from *Smmob3* cDNA coding for SmMOB3 full-length under control of *adh* promoter	this study
AH109 + pAD-SmMOB3 aa 1-144	*MATa; trp1-901; leu2-3, 112; ura3-52; his3-200; ade2-101; gal4Δ; gal80Δ; LYS2::GAL1*$_{UAS}$*-GAL1*$_{TATA}$*-HIS3; GAL2*$_{UAS}$*-GAL2*$_{TATA}$*-ADE2; URA3::MEL1*$_{UAS}$*-MEL1*$_{TATA}$*-lacZ; MEL1;* GAL4-activation domain N-terminally fused to SmMOB3 from *Smmob3* cDNA coding for SmMOB3 aa 1-144 under control of *adh* promoter	this study
AH109 + pAD11 aa 282-845	*MATa; trp1-901; leu2-3, 112; ura3-52; his3-200; ade2-101; gal4Δ; gal80Δ; LYS2::GAL1*$_{UAS}$*-GAL1*$_{TATA}$*-HIS3; GAL2*$_{UAS}$*-GAL2*$_{TATA}$*-ADE2; URA3::MEL1*$_{UAS}$*-MEL1*$_{TATA}$*-lacZ; MEL1;* GAL4-activation domain N-terminally fused to PRO11 from *pro11* cDNA encoding aa 282-845 under control of *adh* promoter	this study
AH109 + pAD11FL	*MATa; trp1-901; leu2-3, 112; ura3-52; his3-200; ade2-101; gal4Δ; gal80Δ; LYS2::GAL1*$_{UAS}$*-GAL1*$_{TATA}$*-HIS3; GAL2*$_{UAS}$*-GAL2*$_{TATA}$*-ADE2; URA3::MEL1*$_{UAS}$*-MEL1*$_{TATA}$*-lacZ; MEL1;* GAL4-activation domain N-terminally fused to PRO11 from *pro11* full-length cDNA under control of *adh* promoter	this study
Y187 + pBD-SmKIN3	*MATα; trp1-901; leu2-3, 112; ura3-52; his3-200; ade2-101; gal4Δ; gal80Δ; LYS2::GAL1*$_{UAS}$*-GAL1*$_{TATA}$*-HIS3; GAL2*$_{UAS}$*-GAL2*$_{TATA}$*-ADE2; URA3::MEL1*$_{UAS}$*-MEL1*$_{TATA}$*-lacZ; MEL1;* GAL4-binding domain N-terminally fused to SmKIN3 from *Smkin3* full-length cDNA under control of *adh* promoter	this study

Y187 + pBD-SmKIN24	*MATα; trp1-901; leu2-3, 112; ura3-52; his3-200; ade2-101; gal4Δ; gal80Δ; LYS2::GAL1*$_{UAS}$*-GAL1*$_{TATA}$*-HIS3; GAL2*$_{UAS}$*-GAL2*$_{TATA}$*-ADE2; URA3::MEL1*$_{UAS}$*-MEL1*$_{TATA}$*-lacZ; MEL1;* GAL4 activation domain N-terminally fused toSmKIN24 from *Smkin24* full-length cDNA under control of *adh* promoter	this study
	Sordaria macrospora	
S48977	wild type	U. Kück, Bochum[a]
S66001	Δ*ku70::nat*^{R}; fertile	Pöggeler & Kück, 2006
S23442	mutation in *fus1-1* gene; brownish ascospores	Nowrousian *et. al*., 2012
S67813	mutation in gene *r*; pink ascospores	U. Kück, Bochum[a]
ΔSmkin3	Δ*Smkin3::hyg*^{R}, ssi, fertile	this study
ΔSmkin3/R2	Δ*Smkin3::hyg*^{R}, pink ascospores, ssi, fertile	this study
ΔSmKIN3::pRS-SmKIN3+	Δ*Smkin3::hyg*^{R}, pRS-SmKIN3+^{ect}, ssi, fertile	this study
ΔSmkin3::pDS-SmKIN3ngfp	Δ*Smkin3::hyg*^{R}, pDS-SmKIN3ngfp^{ect}, ssi, fertile	this study
ΔSmkin24	Δ*Smkin24::hyg*^{R}, ssi, sterile	this study
ΔSmkin24/R2	Δ*Smkin24::hyg*^{R}, pink ascospores, ssi, sterile	this study
ΔSmkin24::pRS-SmKIN24+	Δ*Smkin24::hyg*^{R}, pRS-SmKIN24+^{ect}, ssi, fertile	this study
ΔSmkin24::pDS-SmKIN24ngfp	Δ*Smkin24::hyg*^{R}, pDS-SmKIN24ngfp^{ect}, ssi, fertile	this study
ΔSmkin3/ΔSmkin24	Δ*Smkin3::hyg*^{R}, Δ*Smkin24::hyg*^{R}, ssi, sterile	this study
S48977::pHA11	nat^{R}, pHA11^{ect}, ssi, fertile	this study
S67813::pFLAG-SmKIN3	pink ascospores, hyg^{R}, pFLAG-SmKIN3^{ect}, ssi, fertile	this study
S48977::pFLAG-SmKIN3, S48977::pHA11	pFLAG-SmKIN3^{ect}, pHA11^{ect}, nat^{R}, hyg^{R}, ssi, fertile	this study
ΔSmgpi1	Δ*Smgpi1::hyg*^{R}, ssi, fertile	Bernhards 2010
ΔSmgpi1/r2	Δ*Smgpi1::hyg*^{R}, pink ascospores, ssi, fertile	this study
ΔSmmob3	Δ*Smmob3::hyg*^{R}, ssi, sterile	Bernhards & Pöggeler, 2011
ΔSmmob3/r2	Δ*Smmob3::hyg*^{R}, pink ascospores, ssi, sterile	this study
ΔSmgpi1/ΔSmmob3	Δ*Smgpi1::hyg*^{R}, Δ*Smmob3::hyg*^{R}, ssi, fertile	this study

ΔSmgpi1/ΔSmmob3/r2	Δ*Smgpi1::hyg*^{R}, Δ*Smmob3::hyg*^{R}, pink ascospores, ssi, fertile	this study
ΔSm3978	Δ*Sm3978::hyg*^{R}, ssi, fertile	this study
ΔSmmob3/ΔSm3978	Δ*Smmob3::hyg*^{R}, Δ*Sm3978::hyg*^{R}, ssi, sterile	this study
Δpro11	Δ*pro11::hyg*^{R}, ssi, sterile	Bernhards & Pöggeler, 2011
ΔSmgpi1/Δpro11	Δ*Smgpi1::hyg*^{R}, Δ*pro11::hyg*^{R}, ssi, sterile	this study
Δpro22	Δ*pro22::hyg*^{R}, ssi, sterile	Bloemendal *et al*., 2012
ΔSmgpi1/Δpro22	Δ*Smgpi1::hyg*^{R}, Δ*pro22::hyg*^{R}, ssi, sterile	this study
Δpro45	Δ*pro45::hyg*^{R}, ssi, sterile	U. Kück, Bochum[a]
ΔSmgpi1/Δpro45	Δ*Smgpi1::hyg*^{R}, Δ*pro45::hyg*^{R}, ssi, sterile	this study
ΔSmgpi1:: pRS-SmGPI1-egfp aa 1-492	Δ*Smgpi1::hyg*^{R}, pRS-SmGPI1-egfp aa 1-492^{ect}, *nat*^{R}, ssi, fertile	this study
ΔSmgpi1::pRS-SmGPI1-egfp aa 28-492	Δ*Smgpi1::hyg*^{R}, pRS-SmGPI1-egfp aa 28-492^{ect}, *nat*^{R}, ssi, fertile	this study
ΔSmgpi1::pRS-SmGPI1-egfp aa 1-466	Δ*Smgpi1::hyg*^{R}, pRS-SmGPI1-egfp aa 1-466^{ect}, *nat*^{R}, ssi, fertile	this study
ΔSmgpi1::pRS-SmGPI1-egfp aa 28-466	Δ*Smgpi1::hyg*^{R}, pRS-SmGPI1-egfp aa 28-466^{ect}, *nat*^{R}, ssi, fertile	this study
ΔSmgpi1::pRS-SmGPI1-egfp aa 1-27	Δ*Smgpi1::hyg*^{R}, pRS-SmGPI1-egfp aa 1-27^{ect}, *nat*^{R}, ssi, fertile	this study
ΔSmgpi1::pRS-SmGPI1-egfp aa 1-27-KDEL	Δ*Smgpi1::hyg*^{R}, pRS-SmGPI1-egfp aa 1-27-KDEL^{ect}, *nat*^{R}, ssi, fertile	this study
ΔSmgpi1::pRS-SmGPI1 aa 1-253	Δ*Smgpi1::hyg*^{R}, pRS-SmGPI1 aa 1-253^{ect}, *nat*^{R}, ssi, fertile	this study
ΔSmgpi1::pRS-SmGPI1 aa 28-253	Δ*Smgpi1::hyg*^{R}, pRS-SmGPI1 aa 28-253^{ect}, *nat*^{R}, ssi, fertile	this study
ΔSmgpi1::pRS-SmGPI1 aa 1-227	Δ*Smgpi1::hyg*^{R}, pRS-SmGPI1 aa 1-227^{ect}, *nat*^{R}, ssi, fertile	this study
ΔSmgpi1::pRS-SmGPI1 aa 28-227	Δ*Smgpi1::hyg*^{R}, pRS-SmGPI1 aa 28-227^{ect}, *nat*^{R}, ssi, fertile	this study
S48977::p1783	S48977, p1783^{ect}, *hyg*^{R}, ssi, fertile	Voigt & Pöggeler, 2013
S48977::pMOB3-FLAG S48977::pRS-SmGPI1-egfp aa 1-492	S48977, pMOB3-FLAG^{ect}, pRS-SmGPI1-egfp aa 1-492^{ect}, *hyg*^{R}, *nat*^{R}, ssi, fertile	this study
S48977::pMOB3-FLAG	S48977, pMOB3-FLAG^{ect}, *hyg*^{R}, ssi	this study
S48977::pRS-SmGPI1-egfp aa 1-492	S48977, pRS-SmGPI1-egfp aa 1-492^{ect}, *nat*^{R}, ssi, fertile	this study
S48977::p1783-1 S48977 ::pFLAG Mob3	S48977, p1783-1^{ect}, pFLAG Mob3, *hyg*^{R}, ssi	this study
S48977::pFLAGN1 S48977::pRS-SmGPI1-	S48977, pFLAGN1, *hyg*^{R}, pRS-SmGPI1-egfp aa 1-492^{ect},	this study

egfp aa 1-492	*nat*^{R}, ssi, fertile	
ΔSmgpi1/ΔSmmob3:: pRS-SmGPI1 aa 1-253	ΔSmgpi1::*hyg*^{R}, ΔSmmob3::*hyg*^{R}, pRS-SmGPI1 aa 1-253^{ect}, *nat*^{R}, ssi, sterile	this study
ΔSmgpi1/ΔSmmob3:: pRS-SmGPI1 aa 28-253	ΔSmgpi1::*hyg*^{R}, ΔSmmob3::hyg^{R}, pRS-SmGPI1 aa 28-253^{ect}, *nat*^{R}, ssi, sterile	this study
ΔSmgpi1/ΔSmmob3:: pRS-SmGPI1 aa 1-227	ΔSmgpi1::*hyg*^{R}, ΔSmmob3::*hyg*^{R}, pRS-SmGPI1 aa 1-227^{ect}, *nat*^{R}, ssi, sterile	this study
ΔSmgpi1/ΔSmmob3:: pRS-SmGPI1 aa 28-227	ΔSmgpi1::*hyg*^{R}, ΔSmmob3::*hyg*^{R}, pRS-SmGPI1 aa 28-227^{ect}, *nat*^{R}, ssi, sterile	this study
ΔSmgpi1/ΔSmmob3:: pRS-SmGPI1 aa 1-253	ΔSmgpi1::*hyg*^{R}, ΔSmmob3::*hyg*^{R}, pRS-SmGPI1 aa 1-253^{ect}, *nat*^{R}, ssi, sterile	this study
ΔSmgpi1/ΔSmmob3:: pMobFL	ΔSmgpi1::*hyg*^{R}, ΔSmmob3::*hyg*^{R}, pMobFL^{ect}, *nat*^{R}, ssi, fertile	this study
Δpro11/ΔSmkin3	Δ*pro11::hyg*^{R}, Δ*Smkin3::hyg*^{R}, ssi, sterile	this study
Δpro11/ΔSmkin24	Δ*pro11::hyg*^{R}, Δ*Smkin24::hyg*^{R}, ssi, sterile	this study

ect = ectopically integrated, FL = full-length, nat = nourseothricin-cassette, *hph* = hygromycin-cassette, pt = primary transformant, ssi = single spore isolate, *hyg*^{R} = hygromycin resistant, *nat*^{R} = nourseothricin resistant, *amp*^{R} = ampicillin resistant, *kan*^{R}= kanamycine resistant [a] Institute of Biochemistry, University of Stuttgart, Germany.

2.2 Plasmids

Table 3 contains the plasmids used and generated for this study with the respective features.

Table 3. Plasmids generated and used for this study

Plasmid	Feature	Source
pDS23-egfp	*egfp* under control of *gpd* promoter and *trpC* terminator, *ura3*, *nat*-cassette	Teichert *et al*., 2012
pRSnat	*ura*3, *nat* cassette, amp^{R}	Klix *et al*., 2010
pRShyg	*ura3*, *hph* cassette, amp^{R}	Bloemendal et. al 2012
pFLAGN1	*his-3::ccg-1(p)::3xFLAG*	Kawabata & Inoue, 2007
pHAN1	*his-3::ccg-1(p)::HA*	Kawabata & Inoue, 2007
pGBKT7	*trp1*, *GAL4-BD*, *kan*^{R}	Clonetech
pGADT7	*leu2*, *GAL4-AD*, *amp*^{R}	Clonetech
p1783-1	*egfp* under control of *gpd* promoter and *trpC* terminator, *hph*-cassette	Pöggeler *et. al*, 2003
pRS-Smkin3+	*Smkin3* bp -1038 to 3811 in pRSnat	this study
pDS-Smkin3ngfp	*Smkin3* bp 1 to 2755 in pDS23, *egfp* is fused upstream to *Smkin3*	this study
pRS-Smkin3cgfp	*Smkin3* bp 1 to 2755 in pRSnat, *egfp* is fused downstream to *Smkin3*	this study
pRS-Smkin24+	*Smkin24* bp -1036 to 4023 in pRSnat	this study
pDS-Smkin24ngfp	*Smkin24* bp 1 to 2947 in pDS23,	this study

	egfp is fused upstream to *Smkin24*	
pRS-Smkin24cgfp	*Smkin24* bp 1 to 2947 in pRSnat, *egfp* is fused downstream to *Smkin24*	this study
pRS-KoSmkin3	1038 bp of the upstream region and 1016 bp of the downstream region of *Smkin3* interrupted by the *hph*-cassette in pRSnat	this study
pRS-KoSmkin24	1036 bp of the upstream region and 756 bp of the downstream region of *Smkin24* interrupted by the *hph*-cassette in pRSnat	this study
pKOSm3978	988 bp of the downstream region and 962 bp of the upstream region of *Sm3978* interrupted by the *hph*-cassette in pRSnat	this study
pRS-SmGPI1_pre	*Smgpi1* bp -986 to 903 fused to *egfp*, followed by *Smgpi1* bp 904 to 980 under control of *trpC* terminator in pRSnat	this study
pRS-SmGPI1-egfp aa 1-492	*Smgpi1* bp -986 to 869 fused to *egfp*, followed by *Smgpi1* bp 870 to 980 under control of *trpC* terminator in pRSnat	this study
pRS-SmGPI1-egfp aa 28-492	*Smgpi1* bp -986 to +3 fused to *Smgpi1* bp 82 to 901 fused to *egfp*, followed by *Smgpi1* bp 902 to 980 under control of *trpC* terminator in pRSnat	this study
pRS-SmGPI1-egfp aa 1-466	*Smgpi1* bp -986 to 901 fused to *egfp*, followed by *Smgpi1* bp 902 to 980 under control of *trpC* terminator in pRSnat	this study
pRS-SmGPI1-egfp aa 28-466	*Smgpi1* bp -986 to 901 fused to *egfp*, under control of *trpC* terminator in pRSnat	this study
pDS23-SmGPI1ngfp	*Smgpi1* full-length in pDS23, *egfp* is fused upstream to *Smgpi1*	this study
pRS-SmGPI1-egfp aa 1-27	*Smgpi1* bp 1 to81 fused to *egfp*, under control of *gpd* promotor and *trpC* terminator in pRSnat	this study
pRS-SmGPI1-egfp aa 1-27-KDEL	*Smgpi1* bp 1 to 81 fused to *egfp*, followed by a short sequence encoding the ER retention signal KDEL under control of *gpd* promotor and *trpC* terminator in pRSnat	this study
pRS-SmGPI1 aa 1-253	*Smgpi1* bp -986 to1535 in pRSnat	this study
pRS-SmGPI1 aa 28-253	*Smgpi1* bp -986 to 1 fused to *Smgpi1* bp 82 to 1535 in pRSnat	this study
pRS-SmGPI1 aa 1-227	*Smgpi1* bp -986 to 681 fused to *Smgpi1* bp 981 to 1535 in pRSnat	this study
pRS-SmGPI1 aa 28-227	*Smgpi1* bp -986 to 1 fused to *Smgpi1* bp 82 to 961 fused to *Smgpi1* bp 981 to 1535 in pRSnat	this study
pMOBFlag	3xFLAG fused to *Smmob3* under	Bloemendal *et al*., 2012

	control of *ccg1* promotor in pRShyg	
pMOBFL	Full-length *Smmob3* in pRSnat	Bernhards & Pöggeler, 2011
pBD-SmGPI1 aa 1-253	*Smgpi1* cDNA bp 1 to 762 fused to GAL4-BD in pGBKT7	this study
pBD-SmGPI1 aa 28-227	*Smgpi1* cDNA bp 82 to 762 fused to GAL4-BD in pGBKT7	this study
pBD-SmGPI1 aa 1-100	*Smgpi1* cDNA bp 1 to 300 fused to GAL4-BD in pGBKT7	this study
pBD-SmGPI1 aa 101-253	*Smgpi1* cDNA bp 301 to 762 fused to GAL4-BD in pGBKT7	this study
pBD-SmKIN3	SmKIN3 cDNA bp 1-2463 fused to GAL4-BD in pGBKT7	this study
pBD-SmKIN24	SmKIN24 cDNA bp 1-2616 fused to GAL4-BD in pGBKT7	this study
pBD11 aa 282-845	*pro11* cDNA bp 843 to 2538 fused to GAL4 BD in pGBKT7	this study
pAD-SmMOB3 aa 1-144	*Smmob3* cDNA bp 1 to 432 fused to GAL4-AD in pGADT7	this study
pAD-SmMOB3	*Smmob3* cDNA bp 1 to 1992 fused to GAL4-AD in pGADT7	this study
pAD11FL	*pro11 full-length* cDNA fused to GAL4-AD in pGADT7	this study

gpd promoter, glycerin aldehyde 3-phosphate dehydrogenase promoter; *trpC* terminator, anthranilate synthase terminator from *A. nidulans*; amp^R, ampicillin resistance; kan^R, kanamycin resistance; *hph*, hygromycin B phosphotransferase; nat, nourseothricin N-acetyl transferase

2.3 Primers

Table 4 contains the oligonucleotides used for amplification, verification or RT-PCR for this study. Primer sequences are stated in 5'-3' direction, restriction restriction recognition sequences are shown in italics.

Table 4. Primers used for this study

Name	Sequence (5'-3')	Binding position
Localization, overexpression or multiple usage		
Smkin3_5F	GACTGCCCCGGCGCGGCAGC	*Smkin3* bp -929 to -910
Smkin3_3R	CAACGTAGGTATGTACGTAG	*Smkin3* bp 3641 to 3660
Smkin24_F	ATGGCCGACCGCGAATATGA	*Smkin24* bp 1 to 20
Smkin24_R	TCATGTTCCTTGTTTCATTC	*Smkin24* bp 2928 to 2947
Smkin3_F	ATGGCCGACGAAGGAGTCGC	*Smkin3* bp 1 to 20
Smkin3_R	CTAAGATCCGGCAACAGCCC	*Smkin3* bp 2736 to 2755
3int 1-3_R	TGCTTAATGACCTCGGGAGCCA	*Smkin3* bp 822 to 841
24int 1-3_R	TGCTTAATGACCTCGGGAGCCA	*Smkin24* bp 540 to 563
24int 4_F	CCTTCGATGCTCTATCACCAGC	*Smkin24* bp 1801 to 1822
24int 4_R	CCAGCTTATACACCAACTTGCGTATC	*Smkin24* bp 2436 to 2458
Smkin3ngfp_F	TCACTCTCGGCATGGACGAGCTGTACAAGATGGCCGAC GAAGGAGTCGC	*Smkin3* bp 1 to 20, overhang to *egfp*

Smkin3ngfp_R	GTTTGATGATTTCAGTAACGTTAAGTGGATCATCTGTTCACCTTCTCTT	*Smkin3* bp 2736 to 2755, overhang to *trpC* terminator
Smkin24ngfp_F	TCACTCTCGGCATGGACGAGCTGTACAAGATGGCCGACCGCGAATATGA	*Smkin24* bp 1 to 20, overhang to *egfp*
Smkin24ngfp_R	GTTTGATGATTTCAGTAACGTTAAGTGGATCATGTTCCTTGTTTCATTC	*Smkin24* bp 2928 to 2947, overhang to *trpC* terminator
kin3_pBD_inf_F	AGGAGGACCTGCATATGGCCGACGAAGGAGTCGC	*Smkin3* bp 1 to 20, overhang to pGBKT7
kin3_pBD_inf_R	GGATCCCCGGGAATTCTCATCTGTTCACCTTCTCTT	*Smkin3* bp 2736 to 2755, overhang to pGBKT7
kin24_pBD_inf_F	AGGAGGACCTGCATATGGCCGACCGCGAATATGA	*Smkin24* bp 1 to 20, overhang to pGADT7
kin24_pBD_inf_R	GGATCCCCGGGAATTCTCATGTTCCTTGTTTCATTCCC	*Smkin24* bp 2928 to 2947, overhang to pGADT7
kin3_FLAG_F	ATTACAAGGATGACGATGACAAGGGTTCAATGGCCGACGAAGGAGTCGC	*Smkin3* bp 1 to 20, overhang to FLAG
TtrpC_F	TCCACTTAACGTTACTGAAAT	*trpC* terminator bp 1 to 21
pRS426GFPrev	GCGGATAACAATTTCACACAGGAAACAGCTCGAGTGGAGATGTGGAGTG	*trpC* terminator bp 749 to 768, overhang to pRS426
pRSccg1	GTAACGCCAGGGTTTTCCCAGTCACGACGTAGAAGGAGCAGTCCA	*ccg1* promotor bp 1 to 21, overhang to pRS426
Gpi1_5_inf_F2	CGGGCCCCCCCTCGAGGGTCTCTGCTGCGAACCTTT	*Smgpi1* bp -967 to -948, overhang to pRS426
pRS4269375-4F	GTAACGCCAGGGTTTTCCCAGTCACGACGAGGTACAAGTAGTCGGCGTG	*Smgpi1* bp -1123 to 1103, overhang to pRS426
5utr-GPI1oh-R	GGGAATGCGACTGCTGATTATCATGACGGCAAATCTGTATTGCT	*Smgpi1* bp -20 to -1, overhang to *Smgpi1* ORF
SmGPI1core5'oh_F	CACCTTCCAAGCAATACAGATTTGCCGTCATGCAACAACCGTTCCTGCCCG	*Smgpi1* bp 82 to101, contains an additional start codon, overhang to *Smgpi1* promotor
GFP_r_TtrpCoh_R	GTTTGATGATTTCAGTAACGTTAAGTGGATTACTTGTACAGCTCGTCCAT	*egfp* bp 694 to 713 (lacks a stop codon), overhang to *trpC* terminator
Omega-gfp_inf_F	GACGAGCTGTACAAGAGCGGCTTCTACTTTGGCA	*egfp* bp 1 to 20, overhang to *Smgpi1* 870 to 888
Core-gfp_inf_R2	GCCCTTGCTCACCATAGGCGCACCCGTGCCAAAGT	*Smgpi1* bp 879 to 899, overhang to *egfp*
Gpi1_5_R2	GACGGCAAATCTGTATTGCT	*Smgpi1* bp -20 to -1
GFP_F	ATGGTGAGCAAGGGCGAGGAGC	*egfp* bp 1 to 22
GFP_R	CTTGTACAGCTCGTCCATGCCGAGAGTG	*egfp* bp 717 to 689
TtrpCKDEL-F	TGGACGAGCTGTACAAGGACGAGCTCTAAGATCCACTTAACGTTAC	*trpC* terminator bp 749 to 768, contains bases encoding for ER retention signal KDEL
GFP9375ss-R	GTGAACAGCTCCTCGCCCTTGCTCACCATAGCGTGGACGGACAAGACCA	*Smgpi1* bp 62 to 81, overhang to *egfp*

9375_o_R	TTGATGATTTCAGTAACGTTAAGTGGATCTCAGAGAAG ACCTGACACCG	*Smgpi1* bp 961 to 980, overhang to *trpC* terminator
Knockout and verification		
Smkin24_1k_5F	GTAACGCCAGGGTTTTCCCAGTCACGACGCAGTGAGCT AAGTGCTAACC	*Smkin24* bp -1019 to -1038, overhang to pRS426
Smkin24_5F	GACATGCCTGCCCCACAAAT	*Smkin24* bp -1053 to -1072
Smkin24_5R	GTAACGCCAGGGTTTTCCCAGTCACGACGCGATTAAGG AGGCTGGCCTG	*Smkin24* bp -20 to -1, overhang to *hph*
Smkin24_3F	GAGTAGATGCCGACCGGGAACCAGTTAACTAGTTAGAG GACTTGCATAT	*Smkin24* bp 2945 to 2964, overhang to *hph*
Smkin24_1k_3R	GCGGATAACAATTTCACACAGGAAACAGCGACAGTGTA AGGGTACCTAC	*Smkin24* bp 4004 to 4023, overhang to pRS426
Smkin24_2k_3R	ACTTTGATGGAAGGCTTGGTG	*Smkin24* bp 4924 to 4945
Smkin3_1k_5F	GTAACGCCAGGGTTTTCCCAGTCACGACGCGACTCGAC AGGCATGCGAA	*Smkin3* bp -1038 to -1019, overhang to pRS426
Smkin3_5R	CAAAAAATGCTCCTTCAATATCAGTTAACCTTTTGGTTA CAGAAGGGTG	*Smkin3* bp -20 to -1, overhang to *hph*
Smkin3_3F	GAGTAGATGCCGACCGGGAACCAGTTAACTAGTGAGGT GATGAATGGTG	*Smkin3* bp 2756 to 2775, overhang to *hph*
Smkin3_1k_3R	GCGGATAACAATTTCACACAGGAAACAGCATCGCTTCA TGACTCCCCGG	*Smkin3* bp 3792 to 3811, overhang to pRS426
Smkin3_2k_3R	CTTTTCCCTTTTCTTCAACCA	*Smkin3* bp 4736 to 4755
Hph_F	GTTAACTGATATTGAAGGAGCATTTTTTGG	*hph bp 1 to 29*
Hph_R	GTTAACTGGTTCCCGGTCGGCATCTACTC	*hph bp 1414 to 1386*
TC1	CACCGCCTGGACGACTAAACC	*hph* bp 273 to 292
H3	GTACTCGCCGATAGTGGAAAC	*hph* bp 955-974
Smgpi1_3R	GCGGATAACAATTTCACACAGGAAACAGCTTCGTTGTC AGTCTAGATGG	*Smgpi1* bp 1516 to 1535, overhang to pRS426
Smgpi1_5F	GTAACGCCAGGGTTTTCCCAGTCACGACGGGTCTCTGCT GCGAACCTTT	*Smgpi1*bp -986 to -967, overhang to pRS426
Pho1-14F	CCCCGACATATCGAATCCAGC	*Smmob3* bp -225 to -205
Pho1-2R	CCCCTAATGATGCCTCTACGC	*Smmob3* 2166 to 2146
11-21	AAGCGCGCTTGCCAGTCGCTGC	*pro11* bp -783 to -762
11-Kor	ACGATCAGCCTCGGAAAGACCGC	*pro11* bp 3564 to 3586
Pro22_ver_F	GAAGTTCGGTGGGCGATGCC	*pro22* bp -801 to 820
Pro22_ver_R	CAAGAAGGGTCGAGATAAAG	*pro22* bp 4154 to 4184
Pro45_ver_F	GGACCAAAGCAACGGAACGT	*pro45* bp -1092 to -1111
Pro45_ver_R	ATACAAACCCGCTGTCGTGA	*pro45* bp 3534 to 3553
3978_5F	TGGCGCGGCAAGCTGCGAGCGTAACGCCAGGGTTTTCC CAGTCACGACG	*Sm3978* bp -962 to -943, overhang to pRS426
3978_5R	CAAAAAATGCTCCTTCAATATCAGTTAACATCGGAAGG CGGCAGAAA	*Sm3978* bp -20 to -1, overhang to *hph*
3978_3F	GAGTAGATGCCGACCGGGAACCAGTTAACAGGCCTGAT GCCTAGTCTTT	*Sm3978* bp 4213 to 4232, overhang to *hph*
3978_3R	GCGGATAACAATTTCACACAGGAAACAGCCAAAGAGG GAGAGGAGGTCG	*Sm3978* bp 5201 to 5220, overhang to pRS426

3978_5F2	CCAAGGCCGCAAGGCGGGCA	*Sm3978* bp -1143 to -1103
3978_3R2	TCGAGGGGTGCCTGGGGTCG	*Sm3978* bp 5305 to 5324
Yeast two-hybrid		
Sm9375_Y2H_ges_F	*CATATG*GATAATCAGCAGTCGCA	*Smgpi1* bp 1 to 20, *Nde*I recognition sequence
Sm9375_Y2H_ges_R	*GAATTC*TCAGAGAAGACCTGACACCG	*Smgpi1* bp 961 to 980, *Eco*RI recognition sequence
Sm9375_Y2H_5'_2R	*GAATTC*TCAGCCGGTGCAGACGGCAT	*Smgpi1* cDNA bp 283 to 303, *Nde*I recognition sequence
Sm9375_Y2H_3'_F	*CATATG*AATGCCGTCTGCACCGGCAC	*Smgpi1* cDNA bp 304 to 323, *Nde*I recognition sequence
Sm9375_Y2H_oSigseq_F	*CATATG*CAACAACCGTTCCTGCCCGT	*Smgpi1* bp 82 to 101, *Nde*I recognition sequence
Sm9375_Y2H_oSigseq_2R	*GAATTC*TCAAGGCGCACCCGTGCCAA	*Smgpi1* cDNA bp 665 to 684, *Eco*RI recognition sequence
Mob3_Y2H_F	*CATATG*TCGCTTCCTCTAAGC	*Smmob3* bp 1 to19, *Nde*I recognition sequence
Mob3_Y2H_R	*GAATTC*CTAGTCCACCTTTGGGGCCT	*Smmob3* bp 2078 to 2061, *Eco*RI recognition sequence
Mob3_as1-144_R	*GAATTC*GCA GGG CGG CTC ATC AAA CA	*Smmob3* bp 499 to 518, *Eco*RI recognition sequence
Pro11_Y2H_F	*CATATG*GGCACCAACGGCGTTCA	*pro11* bp 1 to 20, *Nde*I recognition sequence
Pro11_Y2H_R	*GAATTC*TCACCTCGCATACACCTTGACC	*pro11* bp 2696 to 2716, recognition sequence
Pro11_WD40_Y2H_R	*CATATG*GGACAACAGCTACACGATATTC	*pro11* bp 968 to 986, *Nde*I recognition sequence
Southern hybridization		
Pho1-3F	AGCACAGCGAACACAAGAGG	*Smmob3* bp 2748 to 2762
Pho1-3R	AGCCTAGTCCACCTTTGGGGCCT	*Smmob3* bp 2748 to 2762
9375_Sprobe_F	CCGGTCTCGCGGGCACCAAC	*Smgpi1* bp -432 to -413
Kin3_probe_F	GGTGATGAATGGTGAAGAGA	*Smkin3* bp 2761 to 2780
Kin3_probe_R	GTGATGAGAAAAGCGTGAATAG	*Smkin3* bp 448 to 467
Kin24_probe_F	GTTAAAGGGGGACACCGGGG	*Smkin24* bp 2976 to 2996
Kin24_probe_R	GACAAGAGGACAGTAGGTACACG	*Smkin24* bp 559 to 536

2.4 Chemicals and Materials

Acetic acid (Roth GmbH, 3738.2), acrylamide (Rotiphorese® Gel 40 37,5:1) (Roth GmbH, 3029.1), adenine (Sigma-Aldrich, 01830-50G), AEBSF (4-(2-aminoethyl)benzen-sulfonylfluorid) (AppliChem, A1421,0001), agar-agar (Roth GmbH, 5210.2), agar-agar SERVA high gel-strength (SERVA, 11396.03), agarose (Biozym Scientific GmbH, 840004), ammonium chloride (VWR International, BDH0208-500G), ammonium sulfate (AppliChem, A1032,1000), ampicillin (Sigma-Aldrich, A9518-25G), arginine (AppliChem, A3709,0250), ammonium persulfate (APS) (Roth GmbH, 9592.3), aprotinin (AppliChem, A232,0025), bacto-yeast-extract (Oxoid LTD., LP0021), ß-glycerophosphat (AppliChem, A2253,0100), benzamidine (AppliChem, A1380,0005), bio malt maize extract (Brau-Partner Kling, 115), biotin (Sigma-Aldrich, B4501-1G), bismaleimidohexane (Thermo Scientific, 22330), boric acid (Roth GmbH, 6943.1), bromophenol blue (AppliChem, A3640,0005), caffeine anhydrous (Roth GmbH, N815.3), calcium chloride (Roth GmBH, CN92.1), calcium chloride dihydrate (Roth GmbH, 5239.1), chloroform (Merck Millipore, 1024451000), citric acid monohydrate (Roth GmbH, 3958.1), copper (II) sulfate 5-hydrate (Roth GmbH, P024.1), Corning® Spin-X® UF concentrators (Corning, 431489), coomassie brilliant blue G-250 (Roth GmbH, 9598.1), coomassie brilliant blue R-250 (Roth GmbH, 3862.1) CSM-Ade-His-Leu-Trp-Ura (MP Biomedicals, 4550-122), DAPI (4'-6-diamidino-2-phenylindole) (AppliChem, A1001,0010), deoxycholic acid sodium (Roth GmbH, D6750), desoxynucleotid triphosphate (dNTPs) (Thermo Scientific, R0191), Difco™ skim milk (BD Biosciences, 232100), Difco™ Yeast Nitrogen Base w/o amino acids and ammonium sulfate (BD Biosciences, 233520), dimethylformamide (Roth GmbH, T921.1), di-sodium hydrogen phosphate (Merck-Millipore, 1065855000), DMSO (dimethyl sulfoxide) (Merck Millipore, 1029310500), DTT (1,4-dithiothreitol) (AppliChem, A1101,0025), EDTA (ethylenediamine tetraaceticacid disodium salt dihydrate) (Roth GmbH, 8043.2), electroporation cuvettes (VWR International, 732-1137), ethanol (VWR International, 20821.321), ethidium bromide (Sigma-Aldrich, 46065), Flat Optical 8-Cap Strip 0.2 ml (Biozym, 712100), FM 4-64 (Invitrogen, F34653), formaldehyde (Roth GmbH, 4979.2), formamide (Sigma-Aldrich, 47670), formic acid (Merck Millipore, 1002641000), Gene Ruler DNA Ladder Mix (Thermo Scientific, SM0331, GeneScreen Hybridization Transfer Membrane (PerkinElmer Lifesciences, NEF988001PK), GfpTrap_A (Chromotek, gta-20), glass beads Ø 0.25-0.5 mm (Roth GmbH, A553.1), glass beads Ø 2.85-3.45 mm (Roth GmbH, A557.1),

glucose (AppliChem, A3617,1000), glycine (Roth GmbH, 0079.1), glycerine (VWR International, 24388.295), HEPES (4-(2-hydroxyethyl)-1-piperazineethanesulfonicacid) (Roth GmbH, 9105.4), histidine (Merck Millipore, 1.04351.0025), hydrochloric acid (Roth GmbH, 4625.2), hydrogen peroxide 30% (H_2O_2) (Merck Millipore, 8.22287.2500), hygromycin B (Merck-Millipore, 400051-10MU), IPTG (isopropyl-β-D-galactopyranoside) (Roth GmbH, 2316.3), iron (II) chloride (Roth GmbH, 231-753-5), iron(II) sulfate heptahydrate (Sigma-Aldrich, 31236), imidazole (Roth GmbH, X998.1), isopropanol (AppliChem, A0900,2500GL), kanamycin sulfate (Sigma-Aldrich, 60615), leucine (AppliChem, A1426,0100), leupeptin (N-acetyl-L-leucyl-L-leucyl-L-argininal) (AppliChem, A2183,0025), lithium acetate (Roth GmbH, 5447.1), maize flour (Mühle Levers, Bochum, Germany), magnesium chloride hexahydrate (Merck Millipore, 1.05833.1000), magnesium sulfate heptahydrate (Roth GmbH, P027.2), manganese (II) chloride tetrahydrate (Roth GmbH, T881.1), manganese (II) sulfate monohydrate (Roth GmbH, 4487.1), menadione sodium bisulfite (Sigma-Aldrich, M5750), methanol (VWR International, 20864.320), n-dodecyl-ß-D-maltoside (AppliChem, A0819,0500), MitoTracker® Red FM (life technologies) M22425, MOPS (3-(N-Morpholino)-propane sulfonic acid) (AppliChem, A2947,0500), Nitrocellulose Transfer Membrane Protran® BA (Whatman, 10401196), Nonident® P40 (AppliChem A2239,0025), nourseothricin (WernerBioAgents, 5004000), PEG 6000 (Sigma-Aldrich, 81255), pepstatin A (AppliChem, 2205,0025), phenol (AppliChem, A1153,0500), phosphoric acid (Roth GmbH, 6366.1), PMFS (phenylmethylsulfonylfluoride) (Sigma-Aldrich, P-7626), potassium acetate (Merck Millipore, 1.04820.1000), potassium chloride (AppliChem, A3582,1000), potassium dihydrogen phosphate (Merck Millipore, 1.04873.1000), potassium hydroxide (Roth GmbH, 6751.1), potassium nitrate (Merck Millipore, 1.05063.1000), potassium nitrite (Sigma-Aldrich, 31443), RNA Loading Dye (2x) (Thermo Scientific, R0641), Rotiphorese Gel 40 (Roth GmbH, 3030.2), SDS (sodium dodecyl sulfate) (Roth GmbH, 4360.2), sepharose A (GE Healthcare, 17-0780-01), sodium acetate (Roth GmbH, 6773.2), sodium chloride (AppliChem, A3597,1000), sodium dihydrogen phosphate monohydrate (Merck Millipore, 1.06346.1000), sodium fluoride (AppliChem, A0401,0100), sodium hydroxide (VWR International, 28244.295), sodium molybdate-dihydrate (Sigma-Aldrich, 31439), sodium orthovanadate (AppliChem, 2196,0005), sorbitol (Roth GmbH, 6213.1), β-mercaptoethanol (Roth GmbH, 4227.1), sterile filter 0.45/0.2 µm (Sarstedt, 83.1826/83.1826.001), sucrose (AppliChem, A4734,1000), TEMED (N,N,N',N'-

tetramethylethylenediamine) (Roth GmbH, 2367.3), theophylline (Sigma-Aldrich, T1633), thiourea (Roth GmbH, HN37.1), Tris (Tris-hydroxymethyl-aminomethane) (Roth GmbH, AE15.2), Tris/HCl (Roth GmbH, 9090.3), Triton X-114 (Sigma-Aldrich, X114), Trizol (Invitrogen,15596026), tryptone/peptone (Roth GmbH, 8952,2), tryptophan (MP Biomedicals, 4061-012), Tween 20® (AppliChem, A4974,0100), uracil (MP Biomedicals, 4061-212), urea (Roth GmbH, 2317.3), Whatman Paper B002 580x600 mm (Schleicher & Schuell, 88-3852), X-Gal (5-bromo-4-chloro-3-indolyl-beta-D-galacto-pyranoside) (Thermo Scientific, R0404), X-ray films (Fujifilm, 4741019236), xylene Cyanol (AppliChem, A4976,0005), yeast extract (Roth GmbH, 2904.1), zinc chloride (Sigma-Aldrich, 14424), zinc sulfate heptahydrate (Roth GmbH, K301.1)

2.5 Enzymes

Calf Intestine Alkaline Phosphatase (CIAP) (Thermo Scientific, EF0341), DNase I (Thermo Scientific, EN0521), natuzym (Schliessmann, 5090), HotstarTaq MasterMix (Qiagen, 203443), lysozyme (SERVA, 28262.03), Moltaq (Molzym GmbH and Co, P-010-1000), Phospholipase C (Invitrogen, P6466), Pfu polymerase (Promega GmbH, M7741), Phusion® Hot Start High-Fidelity DNAPolymerase (New England Biolabs, M0530S), restriction endonucleases (Thermo Scientific), RNase A (AppliChem, A2760,0100), T4 DNA ligase (Thermo Scientific, EL0011)

2.6 Kits

CloneJET PCR Cloning Kit (Thermo Scientific, K1231), High Prime DNA Labelling and Detection Starter Kit II (Roche, 1585614), HiSpeed Plasmid Midi Kit (Qiagen, 12643), In-Fusion® HD Cloning Kit (Clontech, 639648), Protein Deglycosylation Mix (NEB, P6039S), Qiagen PCR Cloning Kit (Qiagen, 231124), QIAprep Spin Miniprep Kit (Qiagen, 27106), QIAquick Gel Extraction Kit (Qiagen, 28704), QIAquick PCR Purification Kit (Qiagen, 28104), Substrat HRP Immobilon Western (Merck Millipore WBKLS0500), Transcriptor High Fidelity cDNA Synthesis Kit (Roche, 05091284001)

2.7 Media and Solutions

2.7.1 Solutions

2.7.1.1 Amino-acid stock solutions

Adenine: 0.02% (w/v) adenine in H_2O

Histidine: 1% (w/v) histidine in H_2O

Leucine: 1% (w/v) leucine in H_2O

Tryptophan: 0.02% (w/v) tryptophan in H_2O

Uracil: 0.02% (w/v) uracil in H_2O

Trace-element stock solution:
5% (w/v) citric acid ($C_6H_8O_7$ monohydrate), 5% (w/v) $ZnSO_4$ heptahydrate, 1% (w/v) $Fe(NH_4)_2(SO_4)_2$ hexahydrate, 0.25% (w/v) $CuSO_4$ pentahydrate, 0.05% (w/v) $MnSO_4$ monohydrate, 0.05% (w/v) H_3BO_3, 0.05% (w/v) Na_2MoO_4 dihydrate

Biotin stock solution: 0.01% (w/v) biotin, 50% (v/v) ethanol

2.7.1.2 Transformation

S. cerevisiae

Lithium Acetate (10x): 1 M lithium acetate, pH 7.5

TE(D) (10x): 10 mM Tris/HCl, 1 mM EDTA, pH 7.2

DTT: 1M DTT in H_2O

Sorbitol: 1M sorbitol in H_2O

S. macrospora

Protoplast buffer (PPB): 45 mM KH_2PO_4, 13 mM Na_2HPO_4, 0.6 M KCl, pH 6.0

Transformation buffer (TPS): 1 M sorbitol, 80 mM $CaCl_2$, pH 7.4

2.7.1.3 Solutions regarding DNA

Plasmid isolation (Birnboim & Doly, 1979)

B&D I:	50 mM glucose, 25 mM Tris/HCl, 10 mM EDTA, 0.2% lysozyme
B&D II:	0.4 M NaOH, 2% (w/v) SDS
B&D III:	3 M potassium acetate, 1.8 M formic acid

Southern Blot

Buffer I:	0.25 M HCl
Buffer II:	0.5 M NaOH, 1.5 M NaCl
Buffer III:	1.5 M NaCl, 0.5 M Tris
Washing buffer I:	2 M urea, 0.1% SDS, 50 mM NaH_2PO_4 x H_2O pH 7, 150 mM NaCl, 1mM $MgCl_2$, 0.2% blocking reagent
Washing buffer II (20x):	1 M Tris pH 10, 2 M NaCl, 1 mM $MgCl_2$
DNA-loading dye (6x):	0.25% (w/v) xylene cyanol FF, 0.25% (w/v) bromophenol blue, 40% (w/v) sucrose
dNTP mix:	10 mM dATP, dCTP, dGTP, dTTP separately solved in a. dest.
EtBr solution:	10 mg/ml ethidium bromide in H_2O
MOPS buffer (10x):	0.2 M MOPS pH 7.0, 50 mM sodium acetate, 10 mM EDTA
TBE (10x):	1 M Tris/HCl, 1 M boric acid, 20 mM EDTA, pH 8.3
S.macrospora lysis buffer:	100 mM NaCl, 10 mM Tris/HCl, 1 mM EDTA, 2% SDS, pH 8.0
Yeast lysis buffer:	100 mM NaCl, 2% (v/v) Triton X-100, 1% (w/v) SDS, 10 mM Tris (pH 8.0), 1 mM EDTA

2.7.1.4 Protein regarding solutions

Coomassie:	0.02% (w/v) coomassie brilliant blue R250, 0.02% (w/v) coomassie brilliant blue G250, 42.5% (v/v) ethanol 0.5% (v/v) methanol 10% (v/v) acetic acid
Destaining solution:	45% (v/v) ethanol, 10% (v/v) acetic acid

Loading dye (5x):	125 mM Tris/HCl pH 6.8, 50% (v/v) glycerine, 2% (w/v) SDS, 0.01% (w/v) bromophenol blue, 0.01% (w/v) β-mercaptoethanol
Lysis buffer:	20 mM imidazole, 300 mM NaCl, 50 mM NaH_2PO_4
PBS (10x):	1.4 M NaCl, 27 mM KCl, 101 mM Na_2HPO_4, 17.6 mM KH_2PO_4, pH 7.4
TAP buffer:	100 mM Tris, 200-300 mM NaCl, 2 mM EDTA, 10% glycerol, 0,1-0,5% (v/v) Nonident® P40, 2 mM DTT, 1 mM PMSF
TBE (10x):	1 M Tris/HCl, 1 M boric acid, 20 mM EDTA, pH 8.3
Transfer buffer:	192 mM glycine, 25 mM Tris, 20% (v/v) methanol
SDS-PAGE-running buffer:	1.5% (w/v) Tris pH 8.3, 9.4% (w/v) glycine, 20% (w/v) SDS

2.7.2 Media

E. coli

LB: 1% (w/v) tryptone/peptone, 0.5% NaCl, pH 7.2; 0.5% yeast extract, 1.5% (w/v) agar-agar for solid medium; optional ampicillin (100 µg/ml) or kanamycin (60 µg/ml) for selection.

SOB: 2% (w/v) tryptone, 0.5% (w/v) yeast extract, 10 mM $MgCl_2$, 10 mM $MgSO_4$, 10 mM NaCl, 2.5 mM KCl, pH 7.5.

TB: 1.86% (w/v) KCl, 0.66% (w/v) $MnCl_2$ tetrahydrate, 0.3% (w/v) HEPES, 0.22% (w/v) $CaCl_2$ dihydrate, pH 6.7.

S. cerevisiae

YEPD: 2% (w/v) tryptone, 2% (w/v) glucose, 1% (w/v) yeast extract, pH 5.8; 1.5% (w/v) agar-agar SERVA for solid medium.

YEPDA: YEPD + 0.003% (w/v) adenine, pH 6.5; 1.5% (w/v) agar-agar SERVA for solid medium.

SD: 0.17% (w/v) Difco™ Yeast Nitrogen Base w/o amino acids and ammonium sulfate, 2% (w/v) glucose, 0.064% (w/v) CSM-Ade-His-Leu-Trp-Ura (0.002% (w/v) L-methionine, 0.005% (w/v) L-arginine hydrochloride, L-isoleucine, L-lysine hydrochloride, L-phenylalanine, L-

tryptophan, L-tyrosine, uracil, each 0.008% (w/v) L-aspartic acid, 0.01% (w/v) L-leucine and L-threonine, 0.014% (w/v) L-valine), pH 5.8; 1.5% (w/v) Agar-Agar SERVA for solid medium. Selection of transformants is facilitated by exclusion of respective amino acid(s).

S. macrospora

BMM: 0.8% bio malt maize extract and maize flour (25 g/l), pH 6.5; 1.5% (w/v) agar-agar for solid medium; optional: addition of hygromycin B (110 U/ml) and/or nourseothricin dihydrogen sulfate (50 µg/ml) for selection.

BMM + sodium acetate: BMM + 0.5% (w/v) sodium acetate (sporulation induction).

CMS: 1% (w/v) glucose, 0.2% (w/v) tryptone/peptone, 0.2% (w/v) yeast extract, 0.15% (w/v) KH_2PO_4, 0.05% (w/v) KCl, 0.05% (w/v) $MgSO_4$ heptahydrate, 0.37% (w/v) NH_4Cl, 10.8% (w/v) sucrose, 0.01% (v/v) trace element-stock solution (10 mg/l $ZnSO_4$, 10 mg/l $Fe(II)Cl_2$, 10 mg/l $MnCl_2$), pH 6.5; 1.5% (w/v) agar-agar for solid medium.

MM + starch: 0.1% (w/v) soluble starch, 1.8 mM KH_2PO_4, 1.7 mM K_2HPO_4 trihydrate, 8.3 mM urea, 1 mM $MgSO_4$ heptahydrate, 0.01% (v/v) trace element-stock solution, 5 mM biotin, pH 6.6-6.8; 1.5% (w/v) SERVA-agar for solid medium.

SWG: 1x Westergaard´s (0.1% (w/v) KNO_3, 0.1% (w/v) KH_2PO_4, 0.05% (w/v) $MgSO_4$ heptahydrate, 0.01% (w/v) NaCl, 0.01% (w/v) $CaCl_2$, 0.01% (v/v) trace element-stock solution [5% (w/v) citric acid ($C_6H_8O_7$ monohydrate) 5% (w/v) $ZnSO_4$ heptahydrate, 1% (w/v) $Fe(NH_4)_2(SO_4)_2$ hexahydrate, 0.25% (w/v) $CuSO_4$ pentahydrate, 0.05% (w/v) $MnSO_4$ monohydrate, 0.05% (w/v) H_3BO_3, 0.05% (w/v) Na_2MoO_4 dihydrate] 0.1% (v/v) chloroform), 2% (w/v) glucose, 0.1% (w/v) arginine, 0.1% (v/v) biotin-stock solution (0.01% in 50% ethanol), pH 6.5; 1.5% (w/v) agar-agar for solid medium; addition of hygromycin B (110 U/ml) or nourseothricin dihydrogen sulfate (50 µg/ml) for selection.

2.8 Strains and culture conditions

All strains used in this study are enlisted in Table 2.

E. coli Mach1 strain was used for amplification of generated plasmids. The respective strains were grown in liquid LB medium at 37°C and 200 rpm, supplemented with antibiotics depending on the amplified plasmid.

S. cerevisiae strains were inoculated in liquid or on solid YEPD(A) or SD minimal medium supplemented with appropriate aa for selection. Strains were incubated at 30°C. Cultures in liquid medium were shaken at 150 rpm (Amberg *et al.*, 2005).

S. macrospora was grown on BMM, complete medium containing 10.8% saccharose (CMS) and fruiting-body development inducing SWG medium at 27°C. For DNA extraction, transformation or protein extraction, *S. macrospora* strains were grown in liquid medium containing petri dishes (Nowrousian & Cebula, 2005).

Basic methods have been conducted according to Sambrook *et al.* (2001) and were not separately described.

2.8.1 Preparation and transformation procedures

E. coli

For preparation of chemo-competent *E. coli* cells, strain Mach1 was grown in liquid SOB medium at 20-30 rpm to an OD_{600} of 0.6. Subsequently, cells were incubated on ice for 10 min and harvested by centrifugation at 2500 g at 4°C. The cell pellet was resuspended in TB and incubated for additional 10 min on ice, followed by a centrifugation step at 2500 g for 10 min at 4°C. Afterwards the cell pellet was resuspended in TB and DMSO, incubated for 10 min on ice, aliquoted in 150 µl samples and frozen in liquid nitrogen. Cells were stored at -80°C. Transformation was done according to Sambrook *et al.* (2001). For transformation, cells were thawed at RT, mixed with plasmid DNA and incubated on ice for 20 min, followed by an incubation for 1 min at 42°C and subsequently again for 10 min on ice. Then, liquid LB was added to the cells and the samples were incubated for 20-40 min at 37°C at 200 rpm. Finally, the cells were transferred to LB medium supplemented with respective antibiotics.

S. cerevisiae

For preparation of electro-competent *S. cerevisiae* cells, yeast strains were grown to an OD_{600} of 1.0-1.2 in YPD medium, centrifuged for 5 min at 8000 g and resuspended in a LiAc/TE(D)/H_2O solution in the ratio 1:1:8. This step was followed by incubation at 30°C on a shaker with 100 rpm. After 45 min, DDT was added, and the incubation was prolonged for additional 10 min. Cells were harvested by centrifugation, washed once with H_2O and once with 1M sorbitol. After final uptake in 1 M sorbitol, transformation was carried out by electroporation using an Eppendorf Electroporator 2510 (Eppendorf) with 1.5 kV. Samples were mixed as followed: 40 µl of competent cells and the respective DNA fragments were added to an electroporation cuvette, shocked and resuspended in 600 µl sorbitol and plated on solid SD medium lacking the respective aa for selection (Becker & Lundblad, 2001).

S. macrospora

Protoplastation of *S. macrospora* strains was achieved according to Pöggeler *et al.* (1997). Cultures of *S. macrospora* were grown for 3-4 days in petri dishes as described above. Strains were harvested, transferred to PPB containing 20 mg/ml natuzym and incubated for 3 hours at 27°C and 125 rpm. Protoplasts were isolated using a frit (ROBU glass, pore size 1) into a 50 ml tube. Protoplasts were washed twice with 10 and 5 ml PPB by centrifugation at 4.400 rpm for 5.5 min. Protoplasts were resuspended in 100 µl TPS. For each transformation sample, 100 µl protoplasts were added to 20 µg DNA and incubated on ice for 10 min. A PEG6000 solution (25% [w/v] PEG6000 in PPB) was added to the transformation samples and gently mixed by inverting the reaction tube. After 20 min incubation at RT, the protoplast suspension was spread on solid CSM medium and incubated for 24 h at 27°C. Regenerated protoplasts were covered with hygromycin or nourseothricin supplemented top-agar (4.7% [w/v] NaCl and 0.8% [w/v] SERVA-agar) for selection. The final concentration of antibiotics was 50 µg/ml nourseothricin dihydrogen sulfate or/and 110 U/ml hygromycin B.

2.8.2 DNA methods

2.8.2.1 Plasmid isolation from *E. coli* and *S. cerevisiae*

E. coli

Plasmids were isolated using either the QIAprep Spin Miniprep Kit, the HiSpeed Plasmid Midi Kit or the plasmid extraction protocol according to Birnboim and Doly (Birnboim & Doly, 1979). Plasmid extraction kits were used according to the manufacturer's protocol. Plasmid extraction protocol according to Birnboim & Doly (1979) was applied to 50 ml LB *E. coli* cultures. Cells were grown over night at 37°C at 200 rpm and harvested by centrifugation at 4000 g for 15 min. The cell pellet was resuspended in 2 ml B&D I solution containing 10 µg freshly added RNase and incubated at RT for 5 min. Afterwards 2 ml B&D II solution were added and the sapmle mixed by vortexing and incubated for 5 min at RT. After addition of 2 ml B&D III solution, the sample was mixed by inverting the tube and centrifuged for 15 min at max rpm. The supernatant was transferred to a new tube and mixed with 7.5 ml isopropanol and incubated for 20 min at -20°C for DNA precipitation. The precipitated DNA was collected by centrifugation and washed with 5 ml of 70% ethanol. The residual ethanol was removed and the pellet was air dried. The DNA pellet was resuspended in 1-2 ml a. dest depending on its concentration.

S. cerevisiae

Plasmids were isolated using either the QIAprep Spin Miniprep Kit or the Smash and Grab protocol according to Hoffman and Winston (1987). Plasmid extraction kits were used according to the manufacturer's protocol with minor changes. Additionally 0.3 g of glass beads (Ø 0.25-0.5 mm) were added to the P1 buffer in the tube to disrupted cell walls mechanically by vortexing. The Smash and Grab protocol was applied to yeast cultures grown <16 h in 5-20 ml liquid medium and harvested by centrifugation for 3 min at 8000-12000 g. The cell pellet was resuspended in 0.5-1 ml H_2O and centrifuged again at 12000 g for 2 min. The supernatant was discarded and the cell pellet resuspended in residual liquid through vortexing. 200 µl lysis buffer, 200 µl phenol/chloroform solution and 0.3 g of glass beads (Ø 0.25-0.5 mm) were added and the sample was vortexed in a thermomixer (Eppendorf) for 8 min at 1,400 rpm at 4°C. The content was centrifuged for 15 min at 12000 g. Subsequently, 250 µl of the upper, aqueous layer were

transferred in a fresh reaction tube. DNA was precipitated with isopropanol to remove residual phenol.

2.8.2.2 Isolation of RNA and genomic DNA from *S. macrospora*

RNA isolation: RNA isolation was done according to Elleuche and Pöggeler (2009) with minor changes. The mycilium was harvested, dried and grounded in liquid nitrogen. About 1 g of powdered mycelium was mixed with 1 ml Trizol and centrifuged for 10 min at 13000 rpm and 4°C. The supernatant was transferred to a new tube and mixed with 200 µl chloroform. After centrifugation, the chloroform-generated upper phase was transferred to a new tube mixed with the same amount of isopropanol and after 10 min of incubation at RT centrifuged for 10 min at 13000 rpm and 4°C. The obtained pellet was dried under an outlet and resuspended in 120 µl RNA free H_2O. Finally, the sample was incubated for 30 min at 1000 rpm and 60°C in a thermomixer (Eppendorf).

DNA extraction: gDNA isolation was done using phenol/chloroform extraction according to Lecellier and Silar (1994). The mycelium was harvested, transferred to a 2.0 ml reaction tube and frozen at -80°C for 30 min. The frozen pellet was taken up in 600 µl *S. macrospora* lysis buffer. 8-10 glass beads (Ø 2.85-34.45 mm) were added to the tube to (finally) mechanically disrupt the cell wall in a TissueLyser (Eppendorf) for 5 min at 30 Hz. The sample was mixed with 500 µl phenol, briefly vortexed and centrifuged at 13000 rpm for 10 min. The upper (aqueous) phase was transferred to another 2.0 ml reaction tube and mixed with 1 ml phenol/chloroform by vortexing. After another centrifugation step, the aqueous layer was transferred to a new 2.0 ml reaction tube and mixed with 1 ml chloroform followed by centrifugation. Again, the aqueous layer was transferred into a 1.5 ml reaction tube. The DNA was precipitated by adding isopropanol and incubation for 15 min at RT. After a final centrifugation step, the DNA pellet was dried under an outlet and resuspended in an appropriate amount of H_2O.

2.8.2.3 PCR

Amplification of *S. macrospora* cDNA and gDNA as well as verification of strains via PCR or colony PCR on *E. coli* or *S. cerevisiae* plasmid DNA was achieved with HotStarTaq Master Mix Kit (Qiagen), Molzyme MolTaq polymerase (Molzym GmbH & Co. KG), Pfu polymerase

(Promega GmbH) or Phusion High-Fidelity DNA polymerase (New England Biolabs). All polymerases were used according to the manufacturer's protocol.

2.8.2.4 Purification of amplified DNA

Gel extraction

DNA extraction from agarose gels was done using the QIAquick Gel Extraction Kit (Qiagen) according to the manufacture's protocol.

Micro-dialysis membranes

Dialysis of nucleic acids after PCR amplification was conducted to get rid of salts present in reaction buffers. Nucleic acids were pipetted on membranes (Millipore, 0.02 µm pore size) floating on a. dest. in a petri dish and incubated for 10 min at RT. The desalted DNA was removed from the membranes via pipetting and used for further experiments.

.

2.8.2.5 cDNA synthesis

To ensure that the template RNA contained no remaining gDNA, it was treated with DNaseI according to the manufacturer's protocol. Reverse transcription reaction was done with Transcriptor High Fidelity cDNA Synthesis kit according to the manufacturer's recommendations. 2 µg of RNA were conducted as template for reverse transcriptase reaction. Each reaction was made twice, once with and once without reverse transcriptase. The sample without template served after RNase treatment as control for final exclusion of gDNA remnants by PCR.

2.8.2.6 Hydrolysis of nucleic acids.

DNA for southern blot analysis, ligation after gel extraction or plasmid verification was done by hydrolysis with restriction enzymes according to the manufacturer's protocol. The sample size depended on further use or experimental setup (generally ranging from 5-75 µl).

2.8.2.7 Ligation of DNA fragments

Fragments were ligated into the respective vectors using either QIAGEN PCR Cloning Kit (Qiagen), T4 ligase (Thermo Scientific) or In-Fusion® HD Cloning Kit (Clontech). QIAGEN

PCR Cloning Kit and Clontech In-Fusion® HD Cloning Kit were used according to the manufacture's recommendations.

T4 ligase reactions were set up as follows: 1 µl T4 ligase, 2 µl 10x ligation buffer, 1-2 µl vector DNA and 15-16 µl dialyzed PCR fragment. The sample was incubated at 30 or 37°C for 30 min or overnight at 16°C. Before ligation with T4 ligase, the hydrolyzed vectors were dephosphorylated with calf intestine alkaline phosphatase (CIAP, Thermo Scientific). The general setup contained 2.5 µl 10x CIAP buffer, 1 µl CIAP and 21.5 µl vector DNA, with incubation at 37°C for 10 min followed by 10 min at 75°C to inactivate the enzyme.

.

2.8.2.8 Separation of nucleic acids by gel electrophoresis

DNA

DNA fragments contained after PCR or digestion were mixed with 6x loading dye and separated in 0.8-1% agarose gels (1% [w/v] agarose in 1x TBE buffer) in a gel electrophoresis chamber at a voltage of 50-135 V. 0.5x TBE buffer was used as electrophoresis buffer. The gel, containing the separated DNA was incubation in a 1 µg/ml ethidium bromide solution for 10-20 min and visualized under UV light.

RNA

RNA fragments were separated in agarose gels containing 1.2% 1x MOPS and 5% formaldehyde at 80-100 V in a gel electrophoresis chamber. Prior, the respective RNA was mixed in a ratio 1:1 with 2x RNA loading dye already containing ethidium bromide and incubated for 10 min at 65°C. 1x MOPS was used as electrophoresis buffer. Similar to DNA, RNA was visualized under UV light, Gene Ruler DNA Ladder Mix served as marker.

2.8.2.9 Southern blotting

Total gDNA of the respective strains for Southern blotting was isolated as described above. Depending on the final concentrations, about 25 µl of the obtained gDNA was hydrolyzed and separated by gel electrophoresis. The gel was washed in buffer I (0.25 M HCl) for 10 min, in buffer II (0.5 M NaOH) for 25 min and finally in buffer III (1.5 M NaCl, 0.5 Tris, pH 7.4) for 30 min. The DNA was transferred to a GeneScreen Hybridization Transfer Membrane (PerkinElmer) by capillary blotting technique and cross-linked to the membrane via exposure to

UV light for 5 min. DNA-DNA hybridization and detection reaction were done with High Prime DNA Labeling and Detection Starter Kit II (Roche) according to the manufacturer's protocol. After adding the detection agent to the membrane, the X-ray films were exposed for a minimum of 30 min to a maximum of 6 hours.

2.8.3 Protein methods

2.8.3.1 *S. macrospora protein* extraction

S. macrospora strains were grown in liquid BMM or SWG medium at 27°C for 3-6 days, optional with additives hygromycin B (80 U/ml) and/or nourseothricin dihydrogen sulfate (35 µg/ml). The mycelium was harvested, dried and grounded in liquid nitrogen. 560 µl protein buffer were added to 1 g pulverized mycelium. The samples were centrifuged for 15 min at 8000-12000 g (depending on the sample size), the supernatant was transferred into a new tube, mixed with an appropriate amount of loading dye and heated up for 5-10 min at 95°C (Laemmli, 1970). For analysis of protein secretion, liquid medium was filtered with filter papers (Sartorius FT-3-303-185, 3 hw) and proteins were concentrated using Spin-X UF concentrator (Corning, Germany).

2.8.3.2 Protein concentration measurement

Protein concentrations were measured by a Bradford assay (Bradford 1976). Prior to adding loading dye to the protein extracts, 10 µl of the extraction was mixed with 990 µl of Bradford reagent and incubated for 5 min at RT. The concentration was measured at 595 nm with a Libra S12 (biochrom, UK) spectrophotometer in 1 ml cuvettes.

2.8.3.3 Immuno Blotting

For detection of proteins *S. macrospora* protein extracts were separated in 10-15% SDS-PAGE and transferred onto a PVDF or nitrocellulose membrane by Western blot (Bloemendal *et al.*, 2012, Laemmli, 1970, Towbin *et al.*, 1979). For immunodetection monoclonal mouse anti-eGFP antibody (Santa Cruz Biotechnology, sc-9996, 1:4000), anti-FLAG (Sigma-Aldrich, F3165, 1:12000), anti-HA (Sigma-Aldrich, H9658, 1:3000) or monoclonal anti-Actin antibody (Novus Biochemicals, NB100-74340, 1:2000) combined with a secondary HRP-linked goat anti-mouse antibody (Dianova, 115-035-003, 1:10000) were used (except for eGFP-antibody, this one is

already labeled). Signals were detected by the Immobilon Western Kit (Millipore, WBKLS0500). Membranes were stripped in a solution of 0.2% Ponceau S dissolved in 3% TCA for 1h at RT and washed with 5% skim milk containing PBS or TBS.

2.8.3.4 Yeast Two-Hybrid studies

Two hybrid analysis in *S. cerevisiae* was conducted by using Matchmaker two-hybrid system 3 (Clontech). For protein interaction studies in *S. cerevisiae*, strain MATα Y187 was transformed with plasmids pBD-SmGPI1 aa 1-253, pBD-SmGPI1 aa 28-227, pBD-SmGPI1 aa 1-100, pBD-SmGPI1 aa 101-253 and pBD11 aa 282-845, pBD-SmKIN3 or pBD-SmKIN24. To generate pBD-SmGPI1 aa 1-253, *Smgpi1* was amplified from cDNA with primer Sm9375_Y2H_ges_f and Sm9375_Y2H_ges_r, subcloned in vector pJET (Thermo Scientific K1232), hydrolyzed with *Nde*I and *Eco*RI and ligated into vector pGBKT7. Similarly, plasmid pBD-SmGPI1 aa 28-227 was generated by using primers Sm9375_Y2H_oSigseq_f and Sm9375_Y2H_oSigseq_2r. Plasmids pBD-SmGPI1 aa 1-100 and pBD-SmGPI1 aa 101-253 were constructed by using primer Sm9375_Y2H_ges_f and Sm9375_Y2H_5'_2r or Sm9375_Y2H_3'_f and Sm9375_Y2H_ges_r, respectively. pGBKT7 constructs were transformed into yeast strain Y187. pBD-SmKIN3 or pBD-SmKIN24 were generated by using In-Fusion HD Cloning Kit (Clontech). *Smkin3* was amplified from cDNA with primers kin3_pBD_inf_F and kin3_pBD_inf_R, *Smkin24* was amplified from cDNA with primers kin24_pBD_inf_F and kin24_pBD_inf_R and inserted into vector pGBKT7. Yeast strain MATa AH109 was transformed with pAD-SmMOB3, pAD-SmMOB3 aa 1-144 or pAD11FL. For construction of plasmid pAD-SmMOB3, *Smmob3* was amplified from cDNA using primer Mob3_Y2H_f and Mob3_Y2H_R. Plasmid pAD-SmMOB3 aa 1-144 was generated by ligation of *Smmob3* cDNA amplified with primers Mob3_Y2H_f and Mob3_as1-144_r into pGADT7. pAD11FL was constructed by ligation of *pro11* full-length cDNA amplified with primers Pro11_Y2H_F and Pro11_Y2H_R into pGADT7. The respective Y187 and AH109 strains were mated as described previously (Bendixen *et al.*, 1994) and selected on solid SD medium lacking leucine (leu) and tryptophan (trp). Positive colonies from SD medium without leu and trp were used for drop plate assays. A serial dilution of cells was spread on SD agar plates without leu, trp and adenine (ade). To prove whether the respective genes in vector pGBKT7 were expressed properly, a test based

on RanBPM was used (Tucker *et al.*, 2009). Each construct was additionally checked for self-activation as described by Jacobsen *et al.* (2002).

2.8.3.5 Co-IP

Co-Immunoprecitation was conducted as described previously by Bloemendal *et al.* (2012) with minor changes. Interaction studies of SmKIN3 and PRO11 were done with additional use of thiol cross-linking reagent bismaleimidohexane BHM (Thermo Scientific, 22330) solved in DMSO at a concentration of 20 mM. The cross-linker was used in a final concentration of 0.2 mM. The reaction was stopped after incubation for 2 h at 4°C by adding DTT in a final concentration of 25 mM as recommended in the manufacturers protocol.

2.8.3.6 Differential centrifugation

Pulverized mycelium was mixed with extraction buffer and centrifuged at 3000 g for 3 min. The obtained crude extract was centrifuged for additional 15 min at 8000 g. The remaining pellet was used as sample containing cell detritus, including the cell wall. An aliquot of the supernatant of this sample served as crude extract. The remaining supernatant was centrifuged for 1 h at 4000 g followed by an ultracentrifugation step for 1.5 h at 90000 g. The supernatant containing the cytosol obtained by ultracentrifugation as well as the pellet containing membranes were both used as sample for distribution analysis.

2.8.4 Crossbreeding of *S. macrospora*

The respective *S. macrospora* strains were crossed, usually with a spore-color mutant, by inoculating them directly towards each other on a petri dish with solid SWG medium. The plates were incubated for 10-12 days at 27 °C until the crossing front was formed in the middle of the petri dish. This crossing front represents the genetic assembly of the crossed strains and thus, contained the recombinant crossing perithecia. In case of using spore-color mutant, these contained spores with 2 colors in a typical pattern based on segregation (Esser, 1992). To obtain single spore isolates crossing perithecia were broken on preparation agar (5% agar-agar in H_2O). The spores were separated and spread on solid BMM sodium acetate medium optionally supplemented with hygromycin B (110 U/ml) or nourseothricin dihydrogen sulfate (50 µg/ml) for selection.

2.8.5 Generation of *S. macrospora* single-knockout strains

For generation of the ΔSmkin3, ΔSmkin24 and ΔSm3978 single-deletion strains, 5' flanking regions and 3' flanking regions of the respective genes were fused to the *hph* hygromycin resistance cassette and integrated into plasmid backbone pRSnat (Klix *et al.*, 2010) by homologous recombination in the yeast strain PJ69-4A (Colot *et al.*, 2006). 5' regions of *Smkin3, Smkin24* and *Sm3978* were amplified with primer combinations Smkin3_1k_5F x Smkin3_5R, Smkin24_1k_5F x Smkin24_5R and 3978_5F x 3978_5R. The 3' flanking regions of *Smkin3, Smkin24* and *Sm3978* were amplified with primer pairs Smkin3_3F x Smkin3_1k_3R, Smkin24_3F x Smkin24_1k_3R or Sm3978_3F x Sm3978_3R. Each amplified flanking region had an overhang to *hph* amplified with primers hph_F x hph_R from plasmid pCB1003 (Carroll *et al.*, 1994). This resulted in deletion constructs consisting of the *hph* resistance cassette surrounded by the 5' and the 3' flanking region of the gene of interest. After homologous recombination in yeast, the plasmids were isolated and the deletion constructs were amplified from the respective plasmids, purified and transformed into *S. macrospora* strain Δku70 (Pöggeler & Kück, 2006). The Δku70 background (nourseothricin resistance) was eliminated by crossing primary transformants to spore-color mutant r2 (Teichert *et al.*, 2014). Hygromycin resistant, nourseothricin sensitive single-spore isolates were selected. The constructed single deletion strains were verified by PCR and Southern blot. For PCR verification, gDNA was isolated and presence of the deletion cassette at the correct gene locus was ensured by amplification with primers binding upstream of the 5' region or downstream of the 3' region and within the *hph* resistance cassette. Thus, primers binding outside of the flanking regions used for the deletion cassette and within the *hph* gene verified that the gene of interest was disrupted by the *hph* gene. Any deletion cassette was amplified in total with primers binding outside the flanking regions or each flanking region in particular. The complementary primers for flanking-region amplification bound within the *hph* cassette. The amplicons obtained from the knockout strains were compared to amplicons with the same primer combinations from wt. Insertion of multiple deletion constructs at various locations was excluded by southern blot.

2.8.6 Generation of *S. macrospora* double-knockout strains

Double-deletion strains were obtained by crossing the respective single-deletion strains as described above. Usually, at least one of the single deletion strains used for crossing was previously crossed with a spore-color mutant to identify crossing perithecia easily. After crossing perithecia were broken, entire asci were separated and all 8 included spores were spread on solid BMM sodium acetate medium. After germination, the isolated single spore isolates were verified by PCR as described for single-knockout strains and via southern blot.

2.8.7 Generation of *S. macrospora* complementation strains

To verify whether observed phenotypes were based on the respective gene deletion, each deleted gene was inserted ectopically in the genome of the respective single- or double-knockout strain by transformation. The complementation constructs were generated by using the forward 5' flanking region and the reverse 3' flanking region primer for PCR on wt gDNA. This resulted in amplicons, equal in flanking regions to the deletion constructs but also containing the ORF of the deleted genes. Similar to gene deletion, integration of the complementation constructs was verified by PCR. The obtained, genetically complemented strains were subsequently phenotypically analyzed for phenotypic complementation. By this, phenotypes could be dedicated to gene deletions. Additionally, eGFP-constructs were checked for complementation and thus to be functional.

2.8.8 Analytic procedures

2.8.8.1 Light and fluorescence microscopy investigations

To localize SmGPI1 and to verify the predicted signal sequence and the region for GPI-anchor attachment, several eGFP constructs were generated. Plasmid pRS-SmGPI1-eGFP aa 1-492 represents the eGFP-tagged full-length construct of SmGPI1. To generate pRS-SmGPI1-eGFP aa 1-492, the sequence encompassing bp -967 to 869 was amplified using primer Gpi1_5_inf_F2 and Core-gfp_inf_R2. In the next step, *egfp* was amplified with GFP_f and GFP_r from plasmid p1783-1 (Pöggeler *et al.*, 2003) and the region for GPI-anchor attachment encompassing bp 870-980 using primer pair Omega-gfp_inf_F and 9375_o_r. Finally, the *trpC* terminator of *A. nidulans* was amplified from plasmid p1783-1 using primer TrpC_F and pRS426GFPrev. All

fragments were ligated using In-Fusion HD Cloning Kit into pRSnat in the same order, as listed. This resulted in plasmid pRS-SmGPI1-eGFP aa 1-492 encoding for an eGFP-tagged version of SmGPI1 consisting of aa 1-217 of SmGPI1 fused to eGFP, fused to the region for GPI-anchor attachment from ω-10 to the C-terminal end of SmGPI1 under control of the native promoter and the *trpC* terminator. For construction of pRS-SmGPI1-eGFP aa 1-466 *Smgpi1* was amplified with primer Gpi1_5_inf_F2 and Core-gfp_inf_R2, *egfp*. The native promoter and the *trpC* terminator were amplified as described above. These fragments were ligated into pRSnat resulting in a plasmid encoding SmGPI1 aa 1-227 fused to eGFP under control of its native promoter and the *trpC* terminator. Plasmid pRS-SmGPI1-eGFP aa 28-492 encodes eGFP-tagged SmGPI1 without the signal sequence at position aa 1-27 and was generated by amplifying the promoter of *Smgpi1* separately with primer pair Gpi1_5_inf_F2 and 5utr-GPI1oh-r. Fragments consisting of bp 82-900 of the *Smgpi1* ORF, *egfp*, the putative omega region and the *trpC* terminator were amplified from pRS-SmGPI1_pre aa 1-492 using Omega-gfp_inf_F and pRS426GFPrev. Plasmid pRS-SmGPI1-eGFP aa 28-466 lacking N-terminal and C-terminal processing sites was generated by ligation of amplified fragments from pRS-SmGPI1-eGFP aa 28-492 with primer pair Gpi1_5_inf_F2 and Core-gfp_inf_R2 to the *trpC* terminator amplified from pRS-SmGPI1-eGFP aa 1-466 with primer GFP_F and pRS426GFPrev. To localize SmKIN3 and SmKIN24 in *S. macrospora*, N-terminally eGFP tagged constructs were generated and traced in the respective deletion strain. Plasmids coding for SmKIN3-eGFP and SmKIN24-eGFP were constructed by amplifying the full length genes *Smkin3* or *Smkin24* and inserting them into *Not*I digested pDS23-egfp vector (Teichert *et al.*, 2012) via homologous recombination in yeast. For light and fluorescence microscopic analysis, *S. macrospora* strains were inoculated on solid BMM medium slightly overlapping to a piece of cellophane at 27°C for 1 or 2 days or were grown on BMM covered glass slides. For microscopy, the cellophane sheet with the mycelium was transferred to a glass slide. Glass slides with cellophane or BMM were covered with water and a cover slip for microscopic analysis. For the visualization of hyphae or sexually developed structures, an AxioImager M1 microscope (Zeiss, distributed by Visitron Systems GmbH) combined with a Photometrics CoolSNAP$_{2\ HQ}$ camera (Roper Scientific, Photometrics) was used. The obtained pictures were processed with Metamorph (version 6.3.1; Universal Imaging) and GIMP 2.8.2. (GNU Image Manipulation Program, The GIMP Development Team) as well as Illustrator CS2 (Adobe). To display eGFP, DsRED or DAPI fluorescence chroma filter

set 49002, 49005 and 49000 were used, respectively. DAPI staining was conducted by adding 20-50 µl DAPI (AppliChem, A1001,0010), dissolved in fixing solution (3.7% formaldehyde, 0.2% Triton X-100, 50 mM phosphate buffer pH 7.0, 1 M K_2HPO_4, 1 M KH_2PO_4, diluted 1:1 with H_2O) directly on the mycelium. Staining with FM 4-64 (Invitrogen, F34653) was performed by adding 20-50 µl of a FM 4-64 (1 µg/ml a. dest.) solution similar to DAPI staining. MitoTracker Red (Life Technologies, M22425) was used in a concentration of 25 nM diluted in DMSO according to the guidelines of the manufacturer. Calcofluor white staining was conducted by adding 40 µl calcofluor white (Sigma-Aldrich, 18909), freshly diluted 1:1 with 10% KOH solution and directly applied on the mycelium.

2.8.8.2 Sequence analysis and oligonucleotide synthesis

Primers used in this study were purchased at MWG Biotech AG and are listed in Tab 3. DNA sequencing was done by the G2L-sequencing service of the "Göttinger Genom Labor" (Georg-August-University Göttingen). Molecular weights, isoelectric points of proteins and domain predictions were done with programs from the ExPASy Proteomics Server (http://www.expasy.org). Protein sequence alignments were performed using the ClustalX2 program as described by Larkin *et al.* (2007) and visualized using GeneDoc (Nicholas *et al.*, 1997). Protein and nucleotide sequences were obtained from the public databases at NCBI (http://www.ncbi.nlm.nih.gov/entrez/) or by BLAST searches of the complete sequenced genomes at the Broad Institute (http://www.broad.mit.edu/annotation/fungi/fgi/).

2.8.8.3 Phylogenetic analysis

Multiple protein sequence alignments were performed using the ClustalX2 program (Larkin *et al.*, 2007). Phylogenetic analysis were made with programs from package PHYLIP version 3.6 (http://evolution.genetics.washington.edu/phylip.html). Distance matrices were calculated using the program PRODIST and afterwards used for constructing phylogenetic trees with the neighbor-joining (NJ) program NEIGHBOR. To evaluate the statistical significance a bootstrap analysis with 1000 iterations of bootstrap samplings and reconstruction of trees was performed. A majority rule consensus tree was subsequently generated with the program CONSENSE, viewed using the program TreeView 1.6.6 (Page, 1996) and saved for graphical representation using Adobe Illustrator.

2.8.9 Measures of safety

Genetic engineering experiments of security level 1 have been conducted according to the guide lines of the genetic engineering law (GenTG) stated on 16.12.1993 (recently altered by Art. 42 Abs. 1 G on 09.12. 2010).

3. Results

3.1 The GPI-anchored protein SmGPI1

3.1.1 A two-hybrid screen identified a GPI-anchored protein as an interaction partner of STRIPAK SmMOB3

S. macrospora is more closely related to *N. crassa* than any other previously sequenced filamentous fungus, with 90% nucleic acid identity in coding regions of orthologous genes (Nowrousian, 2010, Nowrousian *et al.*, 2004). Previously, cross-species microarrays with *S. macrospora* cDNA hybridized on *N. crassa* microarrays have been performed successfully (Nowrousian *et al.*, 2005, Pöggeler *et al.*, 2006). To identify new interaction partners of the STRIPAK protein SmMOB3, we performed cross-species yeast two-hybrid (Y2H) screens with a Matchmaker Two-Hybrid System 3 (Clontech) and an *N. crassa* cDNA library (S. Seiler, pers. comm). Using *Smmob3* cDNA as bait, the *N. crassa* NCU09375 protein was identified as an interaction partner of SmMOB3. A BLASTP search of the *S. macrospora* proteome identified SMAC_12074 as NCU09375 homolog. The ORF of *SMAC_12074* (F7W197) is 980 bp with two introns of 96 and 122 bp at positions 285-380 and 677-798, respectively. Intron splicing was verified by cDNA sequencing (data not shown). The calculated molecular mass of the 253 aa protein SMAC_12074 is 26 kDA with an isoelectric point of 5. *In silico* analysis using SignalP (Petersen *et al.*, 2011) revealed a signal sequence at aa 1-27. In addition, a region for posttranslational modification with a GPI-anchor was identified using big-PI Predictor (Eisenhaber *et al.*, 1998, Eisenhaber *et al.*, 1999, Eisenhaber *et al.*, 2000, Sunyaev *et al.*, 1999). The GPI-anchor is linked to a C-terminal residue after a proteolytic cleavage at the ω-residue. In SMAC_12074, the ω-residue is predicted to be Asn228. The surrounding region of the predicted ω-residue has the general features of GPI-anchored proteins such as an upstream linker region, characterized by a low amount of predicted secondary structures, small side-chain residues at positions ω-1 to ω+2, a spacer region between positions ω+3 and ω+9; and a hydrophobic tail from ω+10 to the C-terminus (Pierleoni *et al.*, 2008) (Figure 12). Thus, *SMAC_12074* appeared to encode a pre-protein posttranslationally cleaved at the N-terminal and C-terminal regions and modified by attachment of a C-terminal GPI-anchor.

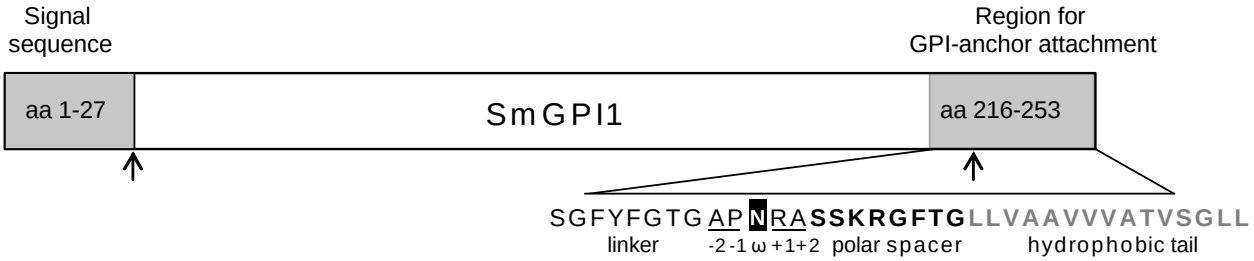

Figure 12. Schematic illustration of the SmGPI1 precursor. N-terminally located grey colored signal sequence was predicted by SignalP (Bendtsen *et al.*, 2004, Emanuelsson *et al.*, 2007). C-terminally grey colored region for GPI-anchor attachment was predicted by big-PI-Predictor (Eisenhaber *et al.*, 1998, Eisenhaber *et al.*, 1999, Eisenhaber *et al.*, 2000, Sunyaev *et al.*, 1999). Putative processing sides are indicated by arrows. The black boxed omega residue is predicted to be aa 228. This aa is exposed for GPI-anchor attachment by a GPI transamidase (Mayor & Riezman, 2004).

Based on these findings, *SMAC_12074* was named *Smgpi1* to indicate that it encodes the first described GPI-anchored protein in *S. macrospora*. Sequence alignment of SmGPI1 with 7 putative homologs from other fungi revealed conservation of this protein among filamentous ascomycetes (Figure 13A).

All identified proteins were predicted to have a signal sequence and a region for GPI-anchor attachment. Based on aa sequences, *N. crassa* NCU09375 shared the highest level of identity to SmGPI1 (91%), followed by *Podospora anserina* with (49%), *Magnaporthe oryzae* and *Chaetomium globosum* (45%) (Figure 13B).

A

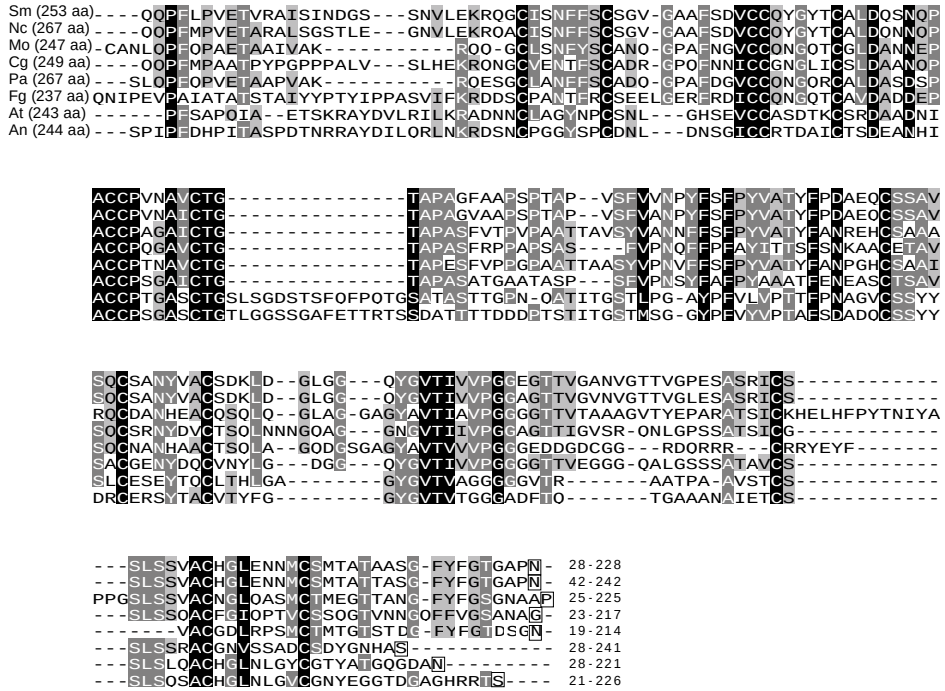

B

	Sm	Nc	Pa	Cg	Mo	Fg	At	An
Sm	100%							
Nc	91%	100%						
Pa	49%	49%	100%					
Cg	45%	45%	44%	100%				
Mo	45%	43%	58%	39%	100%			
Fg	42%	42%	33%	41%	32%	100%		
At	26%	26%	25%	26%	24%	27%	100%	
An	26%	26%	22%	24%	21%	23%	50%	100%

Figure 13. Multiple sequence alignment and aa identity of SmGPI1 with putatively homologue proteins from other Ascomycota. (**A**) Alignment was made using ClustalX2 (Larkin *et al.*, 2007). Sm, *Sordaria macrospora*, F7W197; Nc, *Neurospora crassa*, Q7SCN6; Mo, *Magnaporthe oryzae*, G4MNK5; Cg, *Chaetomium globosum*, Q2HAL9; Pa, *Podospora anserina*, B2AM33; Fg, *Fusarium graminearum* I1RCP4; At, *Aspergillus terreus*, Q0CT61; An, *Aspergillus nidulans*, Q5B70. Total numbers of aa are given in brackets. For alignment only aa sequences downstream of the putative signal sequence up to the omega site were used. (**B**) Identity of the aligned aa sequences in pair-wise comparison.

3.1.2 SmGPI1 interacts physically with SmMOB3

Using the Y2H system we confirmed that SmGPI1 physically interacted with SmMOB3 in *S. cerevisiae* (Figure 14). Full-length and truncated *Smgpi1* cDNAs were cloned into the GAL4 DNA-binding domain of the Y2H vector pGBKT7. Plasmid pAD-SmMOB3 encoding *Smmob3* full-length protein, and its derivative pAD-SmMOB3 aa 1-144 encoding for the N-terminally truncated version, were used as prey vectors. Plasmids were transformed into yeast strains MATa Y187 (pGBKT7 constructs) or MATα AH109 (pGADT7 constructs). The pGBKT7-SmGPI1 bait-constructs were checked for transactivation activity by mating Y187 transformants with yeast strain AH109 carrying the empty pGADT7 plasmid (data not shown). A strain carrying both empty plasmids served as negative control. Interaction of PRO11 and SmMOB3 served as positive control (Bloemendal *et al.*, 2012). Expression of GAL4 fusion proteins from pGBKT7-SmGPI1 plasmids was also checked by mating Y187 transformants with AH109 carrying pAD-RanBPM (Tucker *et al.*, 2009) (data not shown).

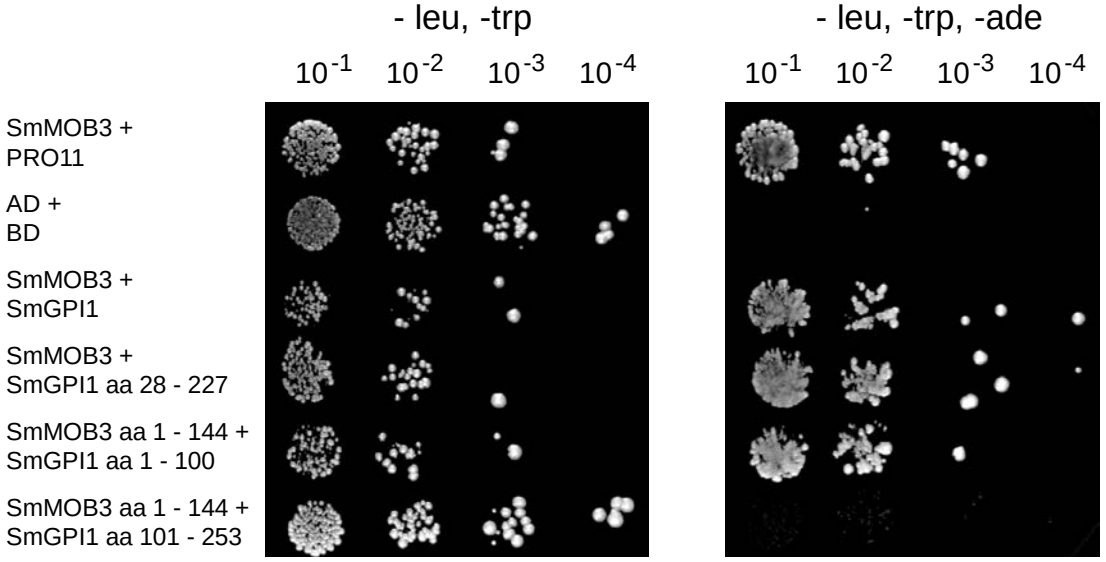

Figure 14. Yeast two-hybrid analysis of the interaction of SmGPI1 and SmMOB3. Serial dilutions of diploid yeast strains obtained after mating spread on SD medium lacking tryptophan (trp) and leucine (leu) or trp, leu and adenine (ade) to verify the interaction of both proteins. Full-length and truncated versions of SmGPI1 and SmMOB3 were tested. BD = DNA-binding domain of GAL4, AD = activation domain of GAL4. GAL4 binding domain was fused to SmGPI1, GAL4 activating domain to SmMOB3. Reverse application of activation and binding domain was not possible due to transactivation of SmMOB3. Yeast transformants carrying pAD-SmMOB3 (SmMOB3) and pBD11 aa 282-845 (PRO11) served as positive control (Bernhards and Pöggeler, 2011). As negative control a diploid strain carrying empty vectors pGADT7 (AD) and pGBKT7 (BD) was used.

Y2H results demonstrated interaction between SmGPI1 and SmMOB3 (Figure 14). Neither the signal sequence nor the region for GPI-anchor attachment was necessary for SmGPI1/SmMOB3 interaction. The N-terminal regions of SmGPI1 (aa 28-100) and SmMOB3 (aa 1-144) mediated interaction (Figure 14). To verify physical interaction of SmMOB3 and SmGPI1 *in vivo*, we performed co-Immunoprecipitation (co-IP) studies in *S. macrospora*. We expressed functional, N-terminally tagged FLAG-SmMOB3 (Bloemendal *et al.*, 2012) and an eGFP-tagged full-length SmGPI1 in *S. macrospora*. As SmGPI1 was predicted to be posttranslationally cleaved at the N-terminus and C-terminus, we fused eGFP upstream of the linker of the GPI attachment region between aa position 217 and 218 (SmGPI1-eGFP aa 1-492) (Figure 12). Tagged versions of the proteins were separately expressed and co-expressed in *S. macrospora* wt transformants. Co-IP confirmed the physical interaction of SmGPI1-eGFP aa 1-492 and full length FLAG-SmMOB3 (Figure 15).

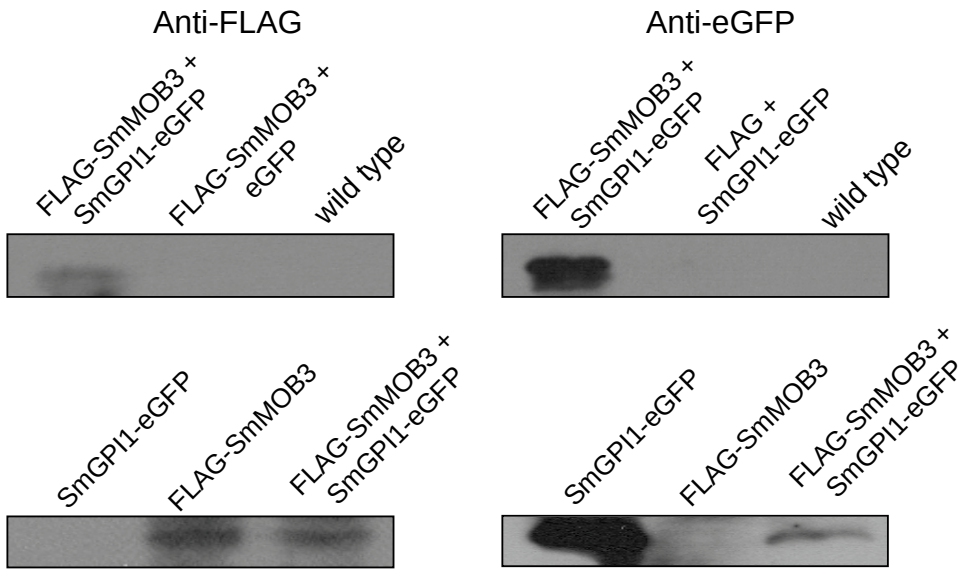

Figure 15. Co-Immunoprecipitation of SmGPI1 and SmMOB3 with anti-FLAG and anti-eGFP antibodies combined with Western blot analysis. Separately expressed constructs and SmGPI1 co-expressed with FLAG or SmMOB3 co-expressed with eGFP served as control. Shown are SmMOB3-FLAG, fished with SmGPI1-eGFP and *vice versa*.

3.1.3 SmGPI1 binds to the cell wall and is partially secreted

SmGPI1 was predicted to have a signal sequence and a region for GPI-anchor attachment (Figure 12). To verify this prediction, plasmids encoding SmGPI1-eGFP aa 1-492 and SmGPI1-eGFP aa 1-466, lacking the GPI-anchor attachment region (Figure 16A) were transformed into a *S. macrospora* wt strain. Crude extracts were fractionated by differential centrifugation and analyzed by Western blot (Figure 16B).

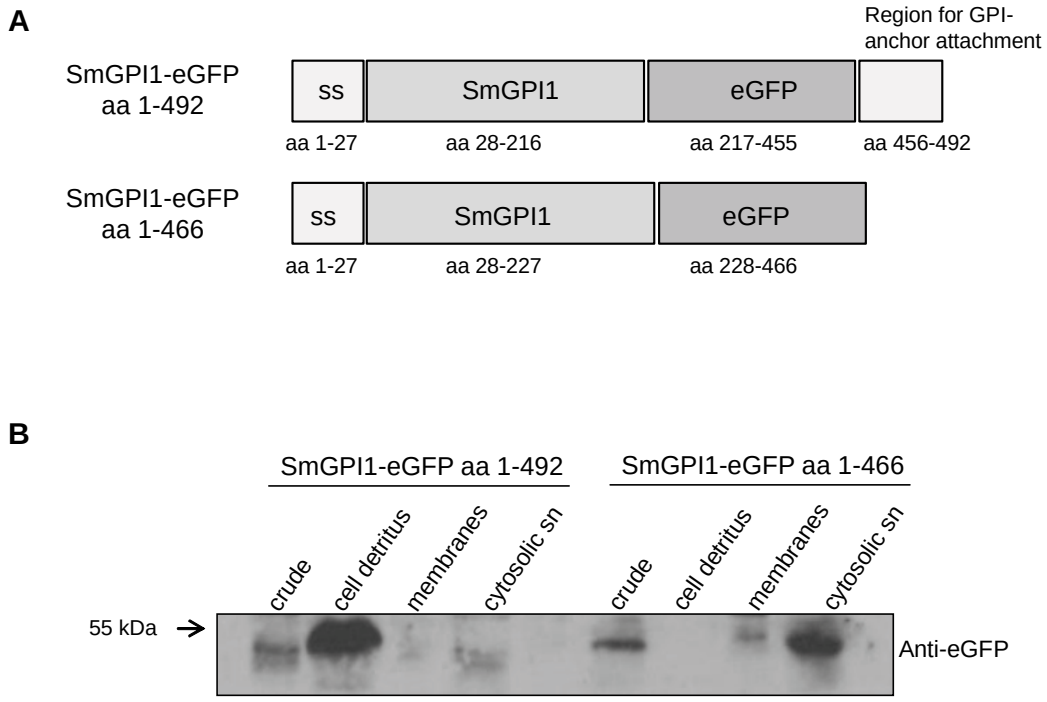

Figure 16. Western blot analysis of SmGPI1 after differential centrifugation of cellular components. (**A**) Schematic overview of SmGPI1 versions used in this analysis. SmGPI1-eGFP aa 1-492 consists of SmGPI1 aa 1-216 fused to eGFP followed by the region for GPI-anchor attachment ω-10 to ω+25 of SmGPI1. The ω-residue is predicted to be aa 228 when eGFP is introduced between position 217 and 218 it changes to aa position 466. SmGPI1-eGFP aa 1-466 lacks the C-terminal region for GPI-anchor attachment (ω-ω+25). (**B**) Western blot using eGFP antibody. SmGPI1-eGFP aa 1-492 is predominantly found in the cell detritus containing remnants of the cell wall. SmGPI1 aa 1-466 is mainly present in the cytosolic supernatant (sn) after ultracentrifugation. Samples were separated on 15% SDS-PAGE, blotted on nitrocellulose membranes and probed with anti-eGFP antibody.

SmGPI1-eGFP aa 1-492 appeared predominantly in the fractions containing remnants of the cell wall (cell detritus), whereas SmGPI1-eGFP aa 1-466 was mainly present in the cytosolic

supernatant but not in the fraction containing the cell detritus (Figure 16B). Thus, SmGPI1 seemed to be mainly localized to the cell wall.

Three further SmGPI1-eGFP versions were used to analyze the functionality of the predicted signal sequence (Figure 17A). SmGPI1-eGFP aa 28-492 lacked the signal sequence for secretion. The signal sequence of SmGPI1 was fused to eGFP in SmGPI1-eGFP aa 1-27. The version SmGPI1-eGFP aa 1-27-KDEL carried the C-terminal ER retention signal Lys-Asp-Glu-Leu (Pelham, 1990).

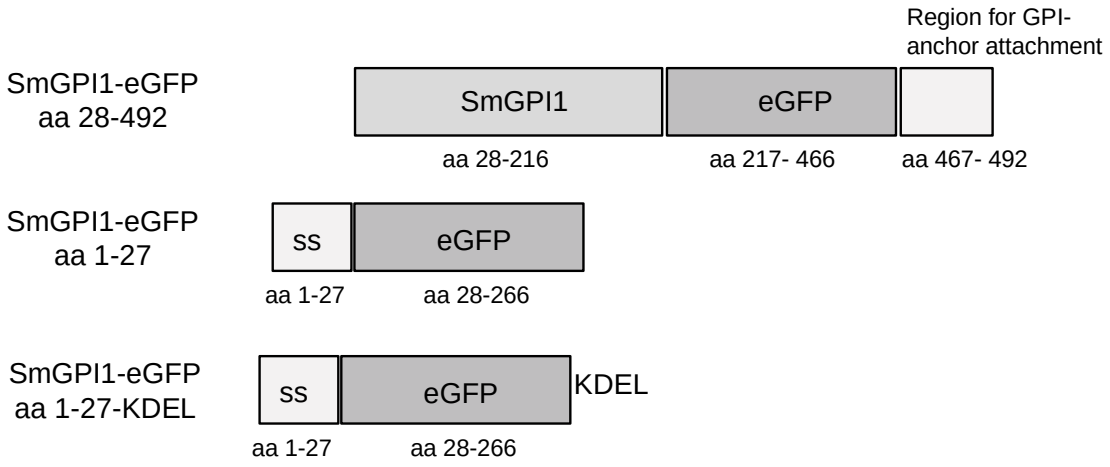

Figure 17. Schematic overview of SmGPI1 versions used for Western blot (see also Figure 16). SmGPI1-eGFP aa 28-492 consists of SmGPI1 aa 28-216 fused to eGFP followed by the region for GPI-anchor attachment ω-10 to ω+25 of SmGPI1. SmGPI1-eGFP aa 1-27 consists of aa 1-27 of SmGPI1 fused to eGFP. SmGPI1-eGFP aa 1-27-KDEL carries additionally the ER retention signal KDEL.

Protein extracts from mycelium ground in liquid nitrogen and cell-free supernatants from strains expressing genes encoding SmGPI1-eGFP aa 1-492, SmGPI1-eGFP aa 28-492 and SmGPI1-eGFP aa 1-466 were analyzed by Western blot (Figure 18B). SmGPI1-eGFP aa 28-492 was seen only in the mycelium sample, whereas SmGPI1-eGFP aa 1-492 and SmGPI1-eGFP aa 1-466 were also detected in cell-free supernatant. Two signals were observed in the liquid medium of transformants expressing full-length SmGPI1-eGFP aa 1-492. The faster migrating signal was the size of free eGFP (27 kDa) and was probably a degradation product of the full-length SmGPI1-eGFP aa 1-492 fusion protein that appeared as a protein of 52 kDa (Figure 18B). To ensure cell-free supernatants we used anti-actin antibody as control.

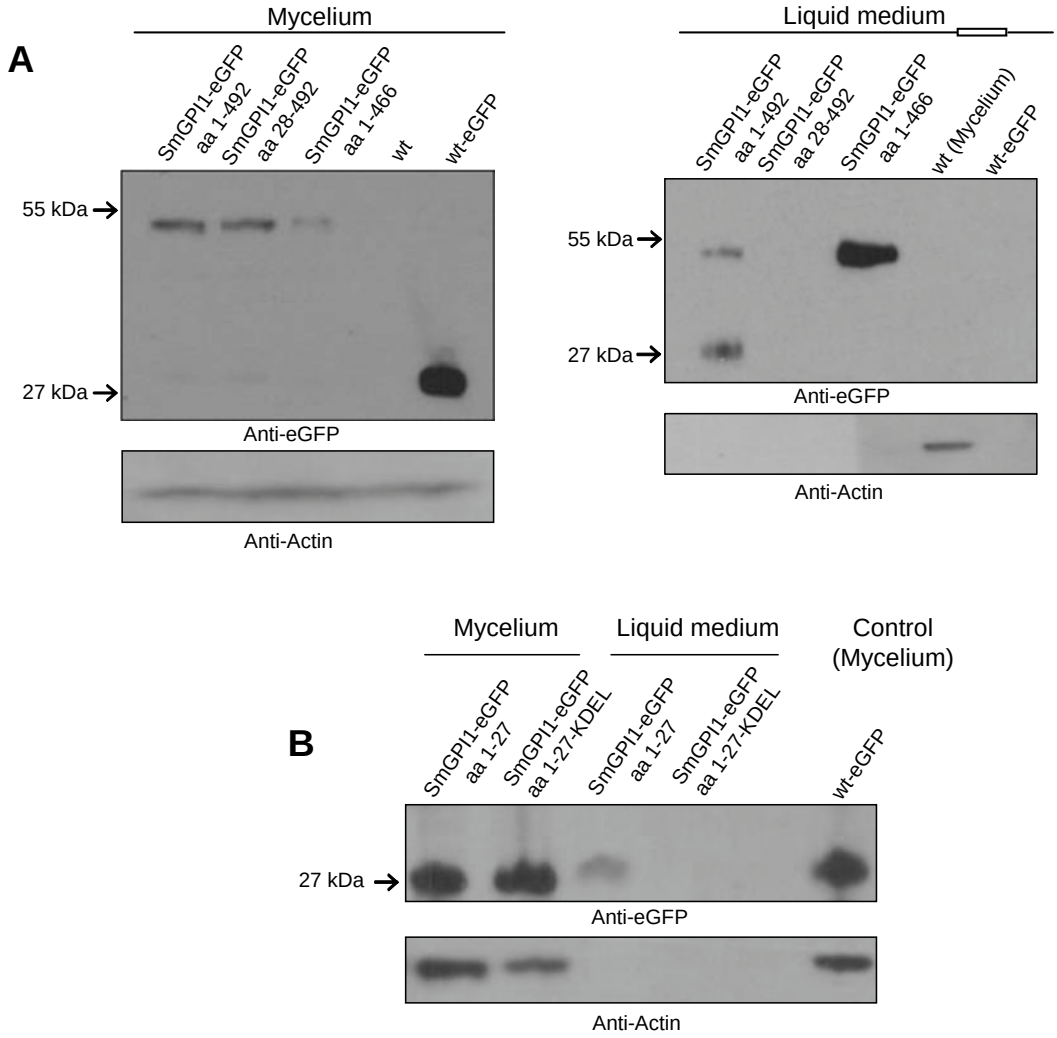

Figure 18. Western blot analysis of SmGPI1 aa 1-492 and aa 28-492 using cell-free supernatants and crude extracts of the mycelium. (**A**) Total cellular (mycelium) and total secreted (liquid medium) proteins were separated by SDS-PAGE and visualized by Western blotting using an anti-eGFP antibody. For the Western blot of the mycelial crude extracts the protein extract of the wt was used as a negative control and wt expressing *egfp* as a positive control. Actin served as loading control and was visualized anti-actin antibody was used. In addition, anti-actin antibody was used to verify that no cellular proteins are present in the liquid medium. Total protein extract of the wt served as a positive control for anti-Actin antibody. (**B**) Western blot analysis of the functionality of SmGPI1 signal sequence. SmGPI1 aa 1-27 was fused to eGFP optionally tagged with ER-retention signal KDEL and visualized by anti-eGFP antibody. Actin was used as a loading control and visualized by an anti-Actin antibody.

To further investigate the functionality of the predicted signal sequence, the coding sequence of the first 27 aa of SmGPI1 was fused to *egfp* (SmGPI1-eGFP aa 1-27). As a control, the construct was C-terminally tagged with the ER retention signal KDEL (SmGPI1-eGFP aa 1-27-KDEL). Western blot showed that only eGFP N-terminally tagged with the signal sequence and lacking

the ER retention signal was detected in cell-free supernatants. After tagging this construct with an ER retention signal it no longer appeared in the cell-free supernatant (Figure 18C). Thus, the signal sequence of SmGPI1 was sufficient to mediate eGFP secretion.

3.1.4 SmGPI1 localizes to the cell wall and mitochondria

Fluorescence microscopy was performed to determine the localization of SmGPI1 *in vivo*. Strains expressing genes coding for SmGPI1-eGFP aa 1-492, SmGPI1-eGFP aa 28-492, SmGPI1-eGFP aa 1-466 and SmGPI1-eGFP aa 28-466 were analyzed (Figure 16 and Figure 17). SmGPI1-eGFP aa 1-492 was detected at the cell wall and intracellular structures resembling mitochondria. For verification, hyphae were co-stained with the membrane dye FM 4-64 or MitoTracker Red (Figure 19). SmGPI1-eGFP aa 1-492 co-localized with the membrane dye FM 4-64 and MitoTracker Red. MitoTracker Red co-staining was displayed by focusing into the intracellular lumen. In contrast to the localization of the full-length protein, the N-terminally truncated SmGPI1-eGFP aa 28-492 and SmGPI1-eGFP aa 28-466 were diffusely distributed within the cytosol and did not co-localize with FM 4-64 or MitoTracker Red. However, SmGPI1-eGFP aa 1-466, containing the putative N-terminal secretion signal, localized to mitochondria but not to the cell wall.

Localization of SmGPI-eGFP did not change in ΔSmmob3. The protein localized to the plasma membrane and mitochondria. Similarly, the distribution of SmMOB3-eGFP to the nuclear envelope and cytoplasm did not change in ΔSmgpi1, as shown in Figure 20.

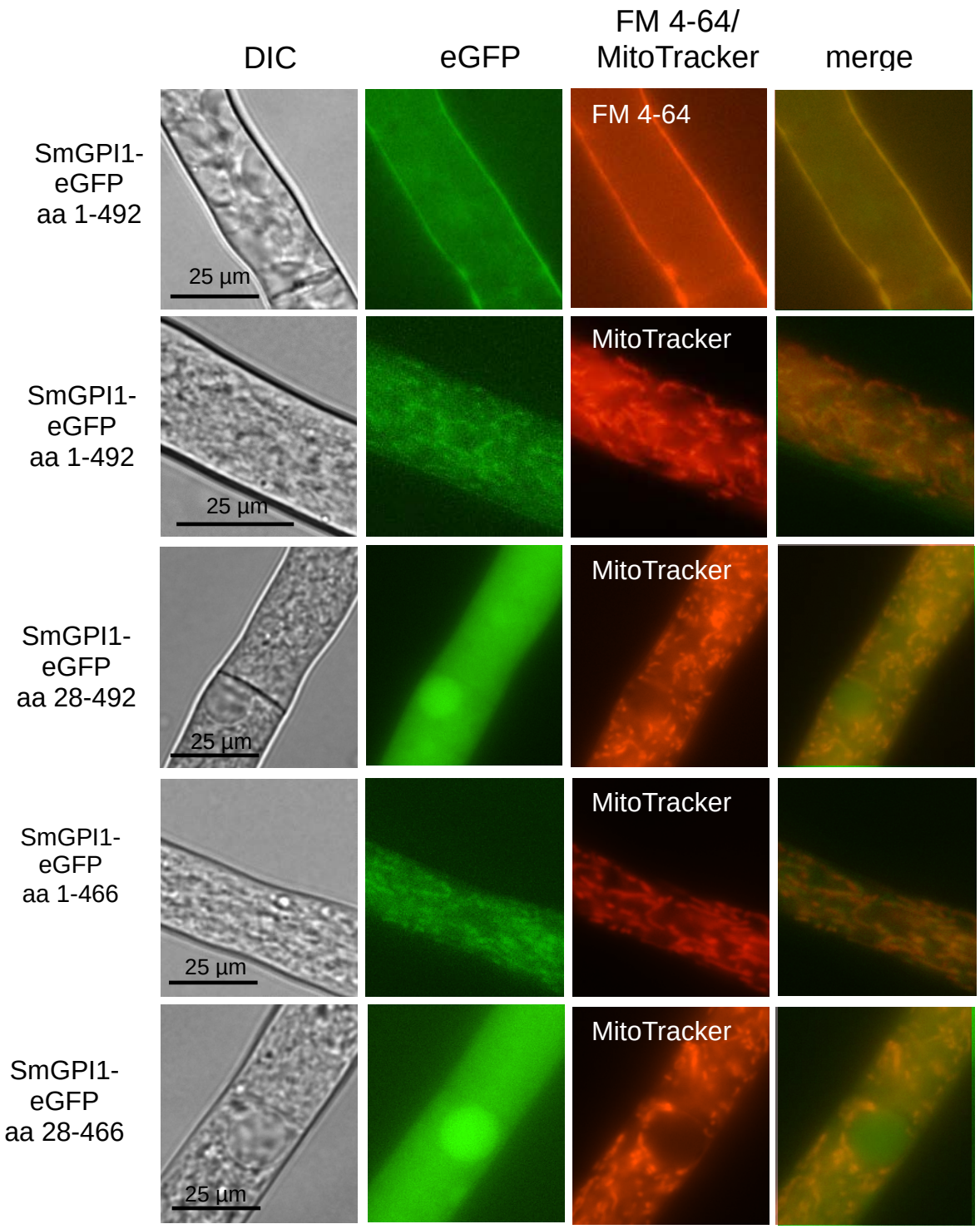

Figure 19. Localization of SmGPI1-eGFP. Deletion of the omega side aborts localization to the cell wall but maintained localization to mitochondria. Deletion of the signal sequence results in cytosolic localization. For visualization was focused either to the cell wall or to the cytoplasm.

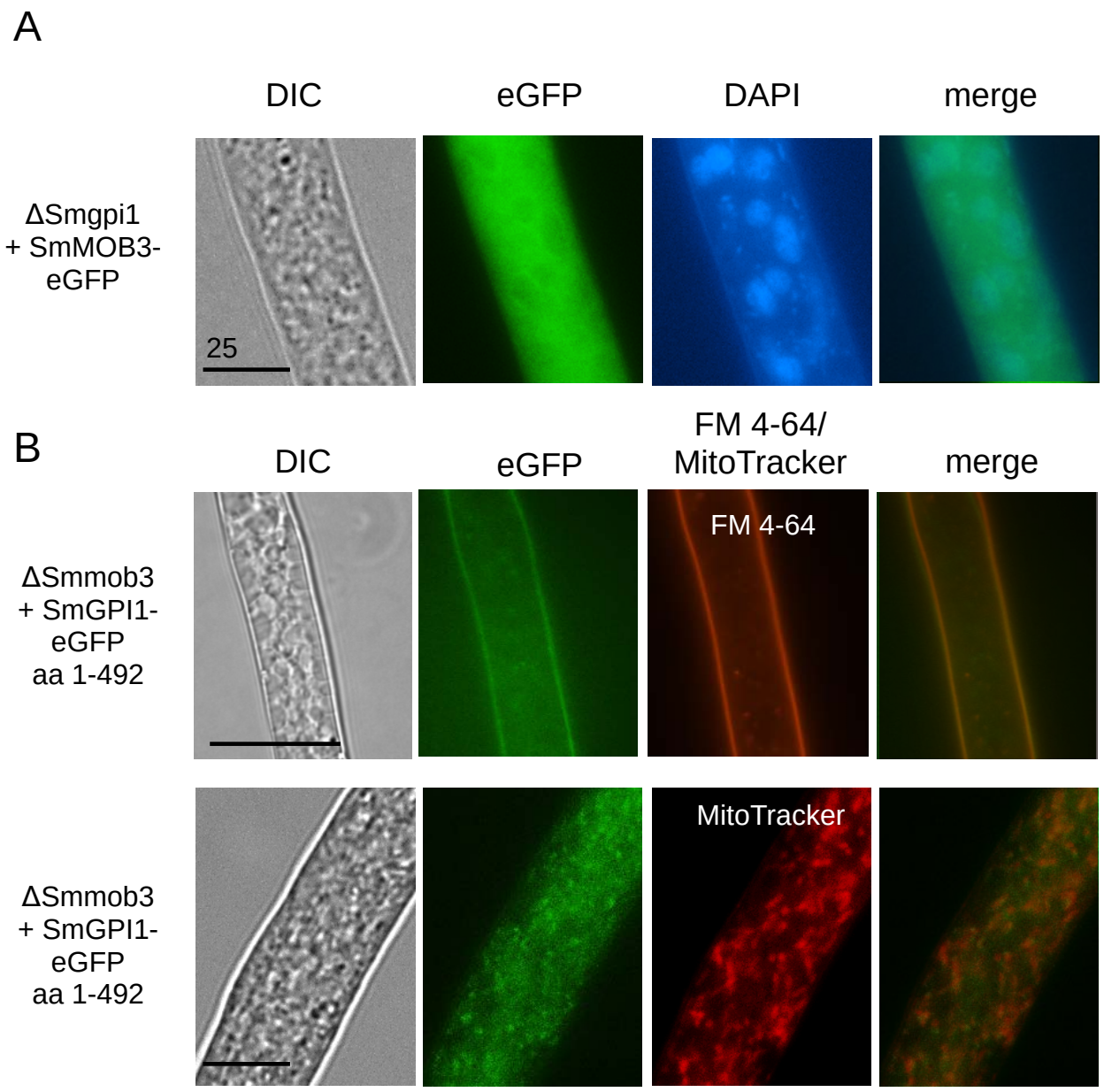

Figure 20. Localization of SmMOB3 in ΔSmgpi1 and SmGPI1 in ΔSmmob3. (**A**) SmMOB3 localizes to the nuclear envelope in ΔSmgpi1. (**B**) SmGPI1 localizes to the cell membrane and mitochondria in ΔSmmob3. For visualization of cell membranes cells were stained with FM 4-64, mitochondria were stained with MitoTracker Red as described in material and methods. DAPI was used for nuclei staining. Scale bar as indicated.

3.1.5 Deletion of *Smgpi1* restores fertility and hyphal fusion of sterile ΔSmmob3

Previous studies of the *S. macrospora* STRIPAK complex including SmMOB3 revealed that it is intracellularly localized (Bernhards & Pöggeler, 2011, Bloemendal *et al.*, 2012). To analyze the interplay of the intracellular protein SmMOB3 and the GPI-anchored protein SmGPI1 in more detail, a single ΔSmgpi1 mutant and a double ΔSmgpi1/ΔSmmob3 mutant were generated. *Smgpi1* was replaced with a hygromycin-resistance cassette via homologous recombination in a Δku70 strain (Pöggeler & Kück, 2006) (Figure 21).

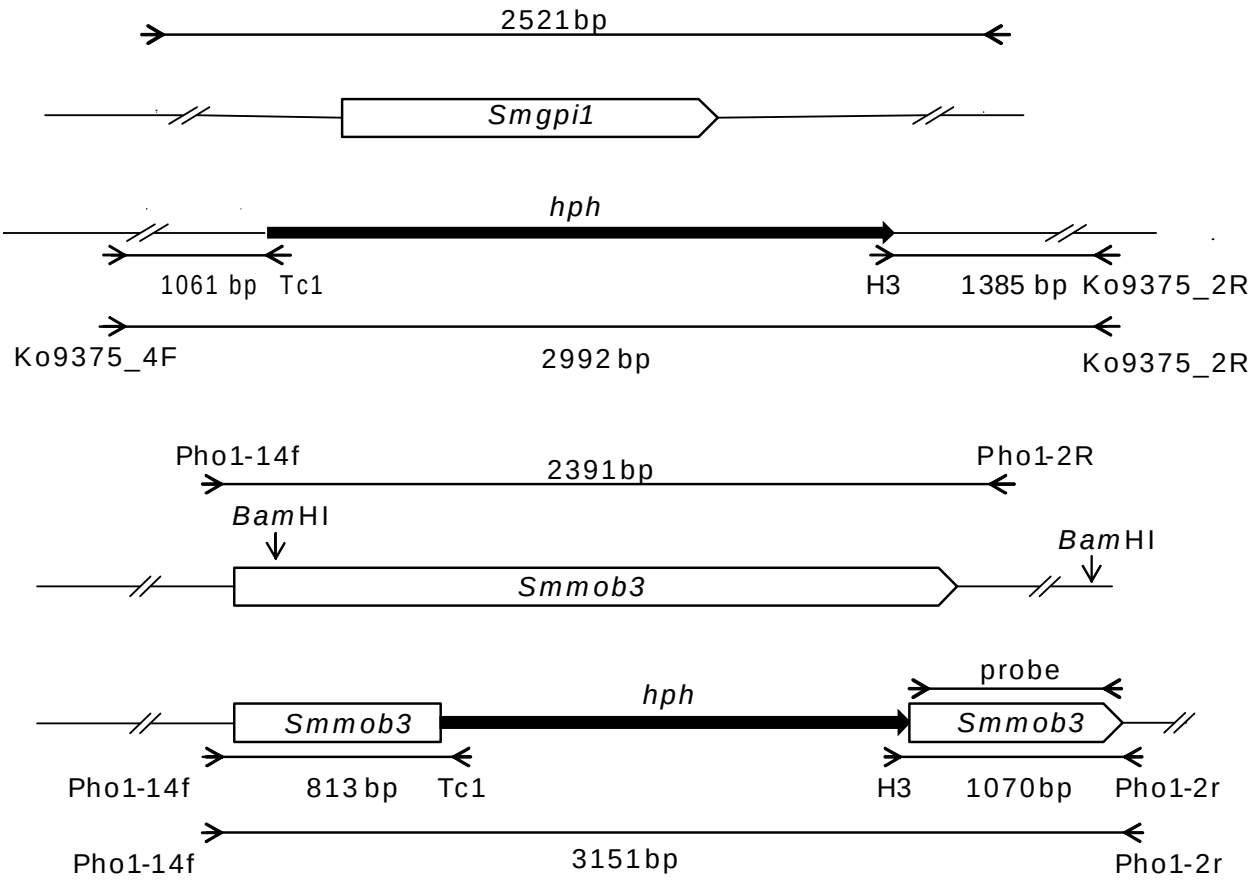

Figure 21. Generation of a ΔSmgpi1/ΔSmmob3 double-deletion strain. Schematic illustration of the *Smgpi1* and *Smmob3* locus before and after homologous integration of the deletion cassette. Primers used for the verification of the respective gene deletion are shown by arrows. Sizes of PCR fragments as well as for the probe used for *Smmob3* Southern hybridization are given.

The homokaryotic Δku70/ΔSmgpi1 mutant was crossed to the spore-color mutant fus1-1 (Nowrousian *et al.*, 2012) to eliminate the *ku70* deletion background. Gene deletion was verified

by PCR and Southern blot hybridization (Figure 22). Subsequently, ΔSmgpi1 was phenotypically analyzed with regard to sexual development. ΔSmgpi1 was fertile and completed the life cycle within 7 days (Figure 23). Similar to wt, first ascogonia were visible after 3 days, developing to non-pigmented protoperithecia at day 4 and pigmented protoperithecia at day 5. Two days later, mature fruiting bodies containing ascospores were formed.

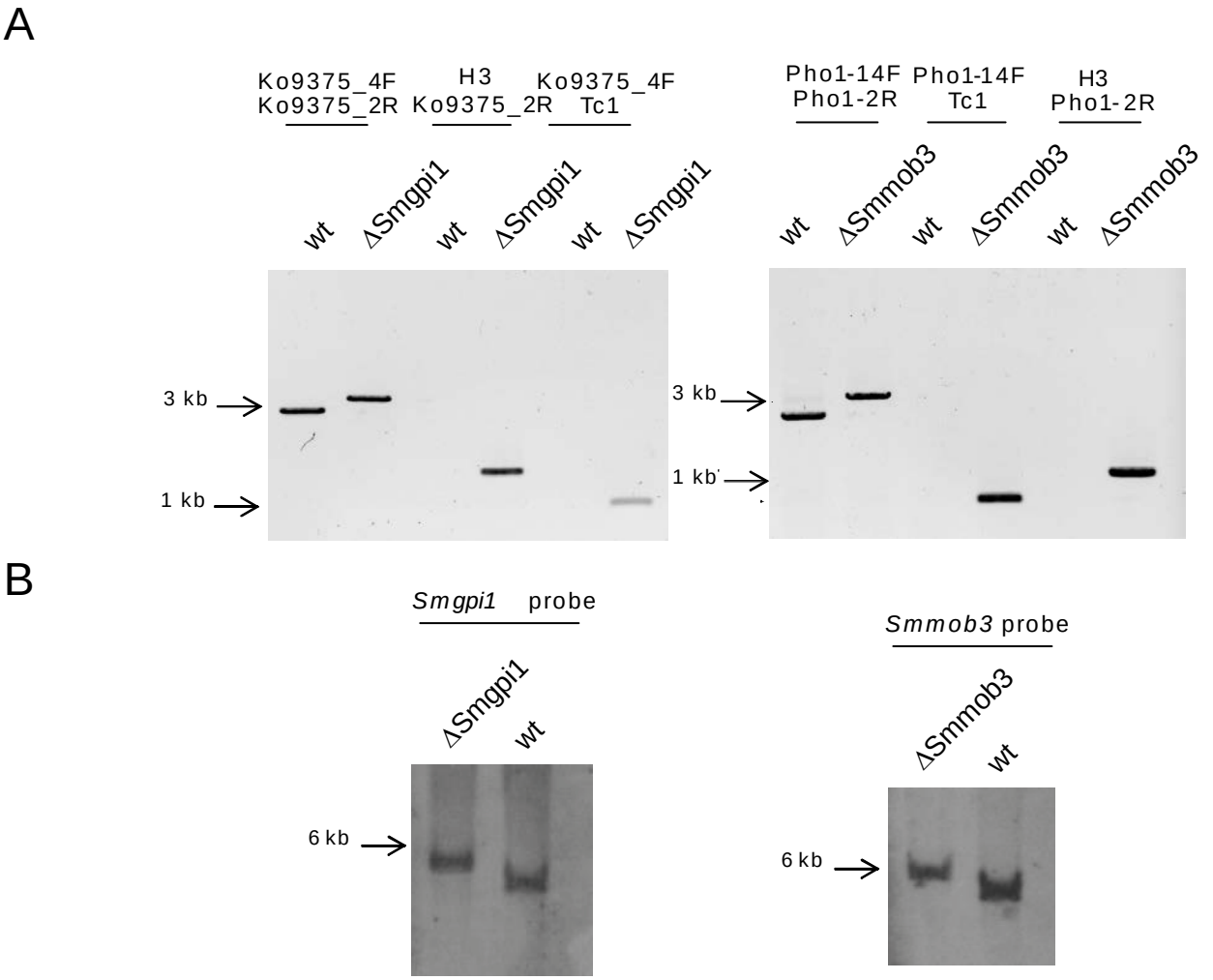

Figure 22. Verification of ΔSmgpi1/ΔSmmob3 via PCR and Southern blot. (A) Verification of the deletion using PCR. Shown are the calculated fragment sizes for wt and the gene deletions. (B) Southern hybridization (Sambrook & Russell, 2001) for *Smmob3* confirmed the successful integration of the deletion cassette via gene-specific probe.

In other organisms, genes coding for GPI-anchored proteins are sensitive to cell membrane and cell wall stress inducing agents (Sestak *et al.*, 2004, Vaknin *et al.*, 2014). To test stress

conditions on *Smgpi1*, we performed growth tests on supplemented solid media. The ΔSmgpi1 strain showed no sensitivity to cell wall stress agents calcofluor white and caffeine or to the cell wall degrading enzymes polygalacturonase or arabanase as present in Natuzym (data not shown). In addition, ΔSmgpi1 was as sensitive as wt to different types of stresses induced by NaCl, KCl, sorbitol, menadione, SDS, H_2O_2 or low and high pH (data not shown). Growth velocity was tested in race tubes with fructification medium over 10 days. The average growth of ΔSmgpi1 was 29 ± 4 mm/day which is similar to wt growth (29 ± 5 mm/day) (Table 5).

Table 5. Average growth value of ΔSmgpi1, complemented ΔSmgpi1 (Smgpi1+), ΔSmmob3 and the double knockout ΔSmgpi1/ΔSmmob3 in mm/day, measured over 10 days on SWG medium.

Strain	Growth velocity (mm/day)
wild type	29,5 ± 5
ΔSmgpi1	29,4 ± 4
ΔSmgpi1+	30,7 ± 6
ΔSmmob3	8 ± 3
ΔSmgpi1/ΔSmmob3	25,5 ± 5

The double deletion strain ΔSmgpi1/ΔSmmob3 was constructed by crossing the single-deletion strains ΔSmgpi1 and ΔSmmob3 (Bernhards & Pöggeler, 2011) (Figure 23). In *S. macrospora* and *N. crassa*, MOB3 is required for hyphal fusion and fruiting-body development (Bernhards & Pöggeler, 2011, Fu *et al.*, 2011, Maerz *et al.*, 2009). Deletion of *Smgpi1* in the sterile ΔSmmob3 deletion background restored fertility (Figure 23). In contrast to the single-deletion strain ΔSmmob3, ΔSmgpi1/ΔSmmob3 completed the life cycle but after a prolonged time of 13 days. Thus, the double-deletion mutant was fertile, but had delayed sexual development (Figure 23). Transformation of ΔSmgpi1/ΔSmmob3 with the *Smgpi1* wt gene resulted in sterility (Figure 24); therefore, fertility of the double-deletion mutant was caused by deletion of *Smgpi1* in the sterile ΔSmmob3 background.

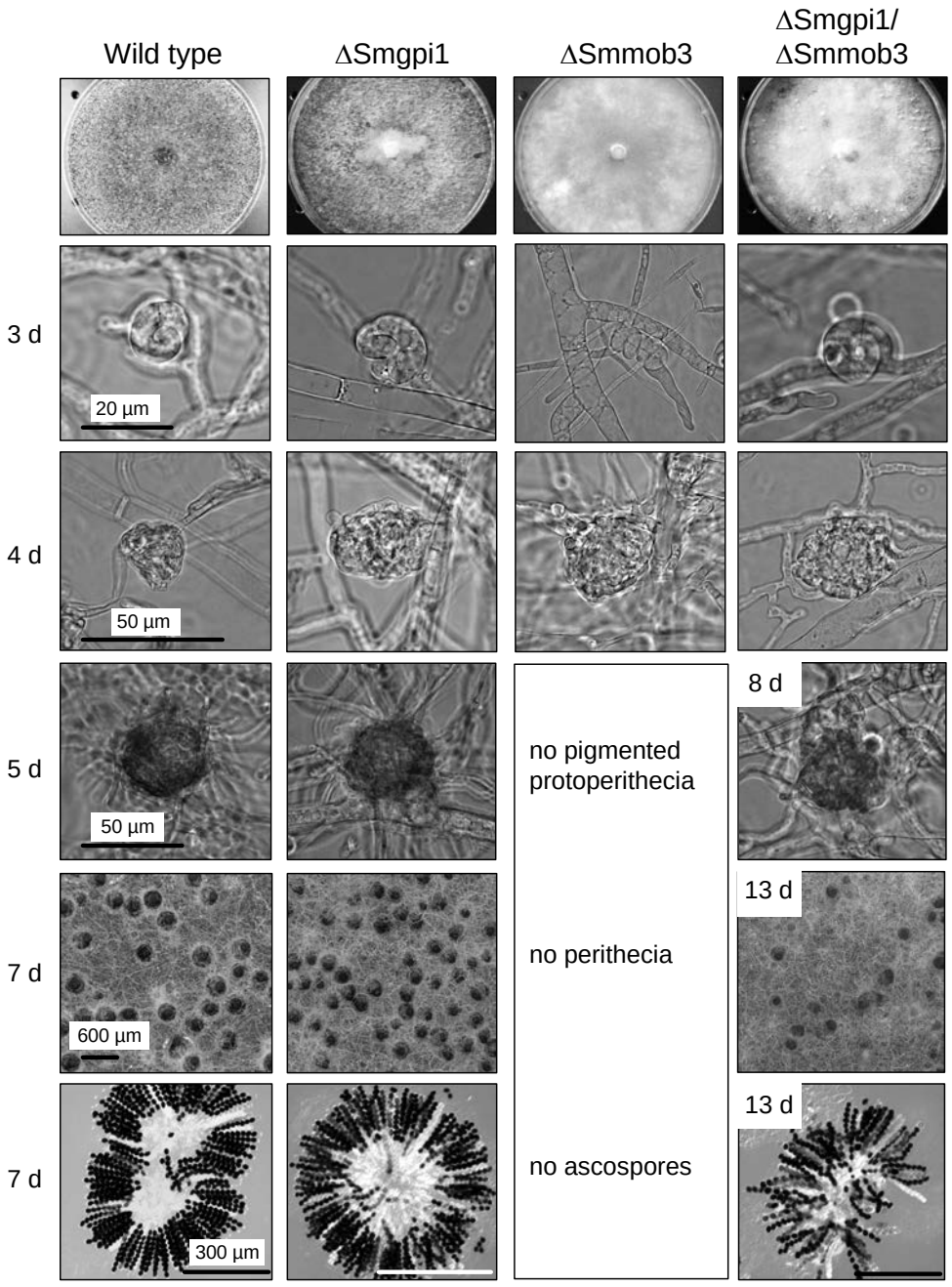

Figure 23. Sexual development of ΔSmgpi1, ΔSmmob3 and ΔSmgpi1/ΔSmmob3. Shown are the respective deletion strains compared to wt. The wt strain generates ascogonia after 3 days, which develop to protoperithecia at day 5 and within 7 days to mature perithecia containing the ascospores. ΔSmgpi1 completes the life cycle within 7 days, whereas ΔSmmob3 develops only protoperithecia. Fruiting-body development in the ΔSmgpi1/ΔSmmob3 mutant is delayed. Strains were inoculated on solid SWG medium.

To ensure that the observed genetic interaction between *Smmob3* and *Smgpi1* is specific, additional double-deletion mutants lacking genes encoding other STRIPAK components such as Δpro11 (Bernhards & Pöggeler, 2011, Bloemendal *et al.*, 2012), Δpro22 (Bloemendal *et al.*, 2012) or Δpro45 (Nordzieke *et al.*, 2014) and ΔSmgpi1 (Figure 25, Figure 26 and Figure 27) were generated by crosses.

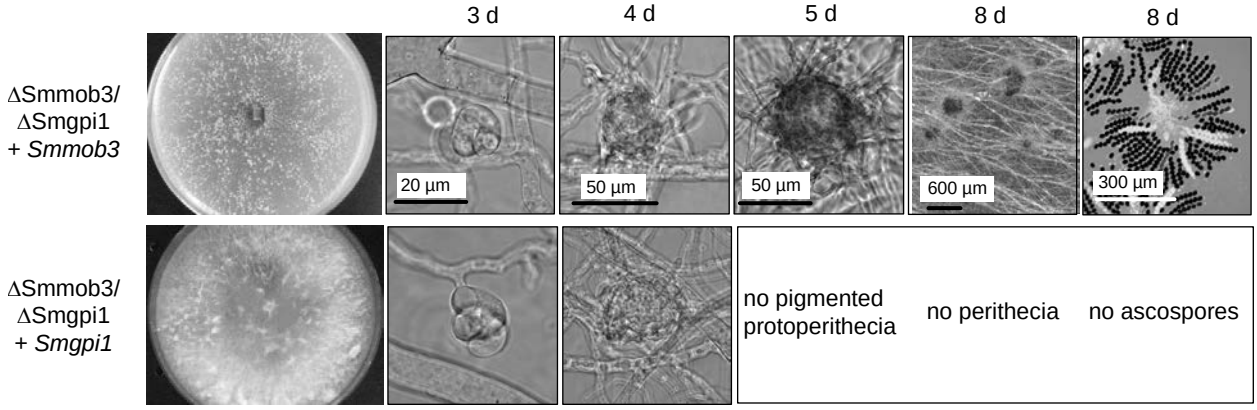

Figure 24. Phenotypic analysis of ΔSmgpi1/ΔSmmob3 complemented with full-length *Smgpi1* or *Smmob3* using microscopy. ΔSmgpi1/ΔSmmob3 + *Smmob3* completes the life cycle within 8 days whereas ΔSmgpi1/ΔSmmob3 + *Smgpi1* only develops protoperithecia. *Smgpi1* and *Smmob3* were under control of their native promotor and terminator. Both complemented double-deletion strains are phenotypically identical to the respective single-deletion strain.

Similar to deletion of *Smmob3*, mutation or deletion of *pro11* or *pro22* led to sterility of *S. macrospora* (Bernhards & Pöggeler, 2011, Bloemendal *et al.*, 2012, Bloemendal *et al.*, 2010, Pöggeler & Kück, 2004). The double-deletion mutants ΔSmgpi1/Δpro11 (Figure 25), ΔSmgpi1/Δpro22 (Figure 26) or ΔSmgpi1/Δpro45 (Figure 27) did not reverse the sterile phenotype as ΔSmgpi1/ΔSmmob3. Furthermore, a double-deletion ΔSMAC_03978/ΔSmmob3 strain, lacking *Smmob3* and *SMAC_03978*, an unrelated gene encoding a hypothetical GPI-anchored protein, was generated. Deletion of the unrelated gene did not suppress the sterile phenotype of ΔSmmob3 (Figure 28). Thus, suppression of ΔSmmob3 by deletion of *Smgpi1* is a specific effect and suggested genetic interaction.

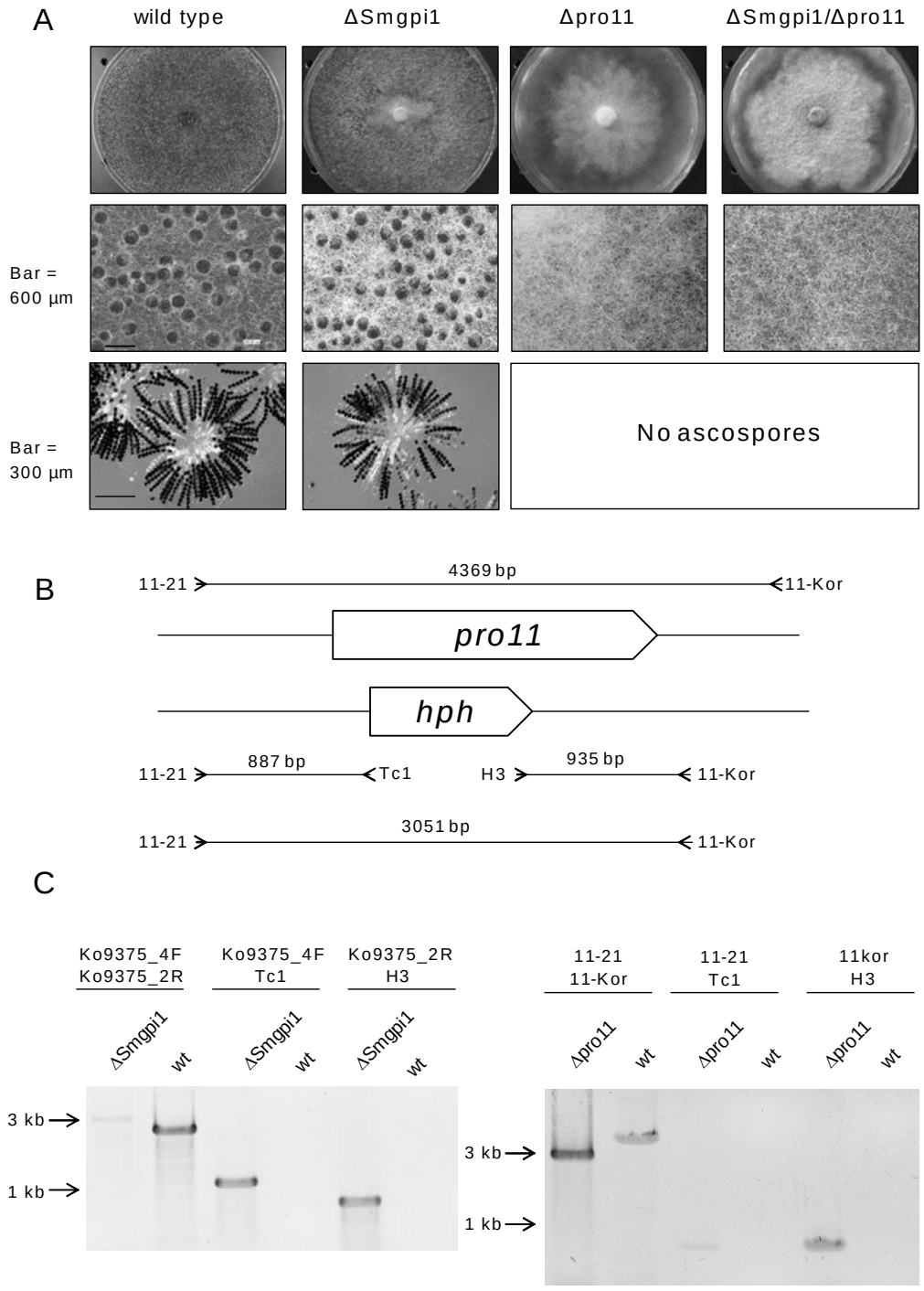

Figure 25. Generation of a ΔSmgpi1/Δpro11 double-deletion strain. (**A**) Phenotype of ΔSmgpi1/Δpro11, respective single-knockout strains and wt with focus on fruiting-body development. (**B**) Schematic illustration of the *pro11* locus (Pöggeler and Kück, 2004) before and after homologous integration of the deletion cassette. Primers used for verification of the deletion strain are shown by arrows. PCR-fragment sizes are given. (**C**) Verification of gene deletions in the ΔSmgpi1/Δpro11 using PCR. Shown are the calculated fragment sizes for wt and the respective gene deletion. Strains were obtained by crossing single-deletion strains ΔSmgpi1/r2 and Δpro11.

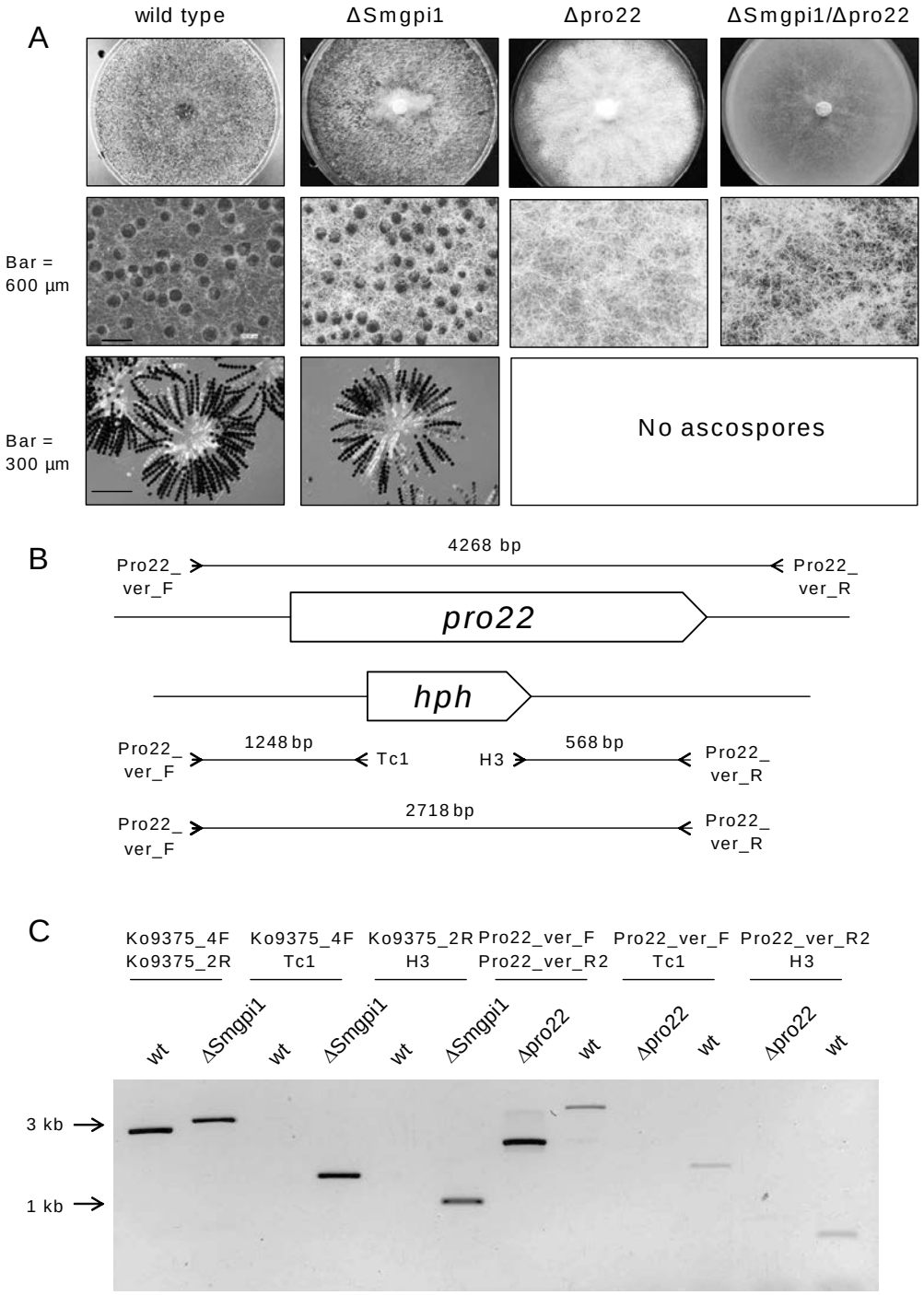

Figure 26. Generation of a ΔSmgpi1/Δpro22 double-deletion strain. (**A**) Phenotype of ΔSmgpi1/Δpro22, respective single-knockout strains and wt with focus on fruiting-body development. (**B**) Schematic illustration of the *pro22* (Bloemendal *et al.*, 2010) locus before and after homologous integration of the deletion cassette. Primers used for verification of the deletion strain are shown by arrows. PCR fragment sizes are given. (**C**) Verification of gene deletions in ΔSmgpi1/Δpro22 using PCR. Shown are the calculated fragment sizes for wt and the respective gene deletion. Strains were obtained by crossing the respective single-deletion strains ΔSmgpi1/r2 and Δpro22.

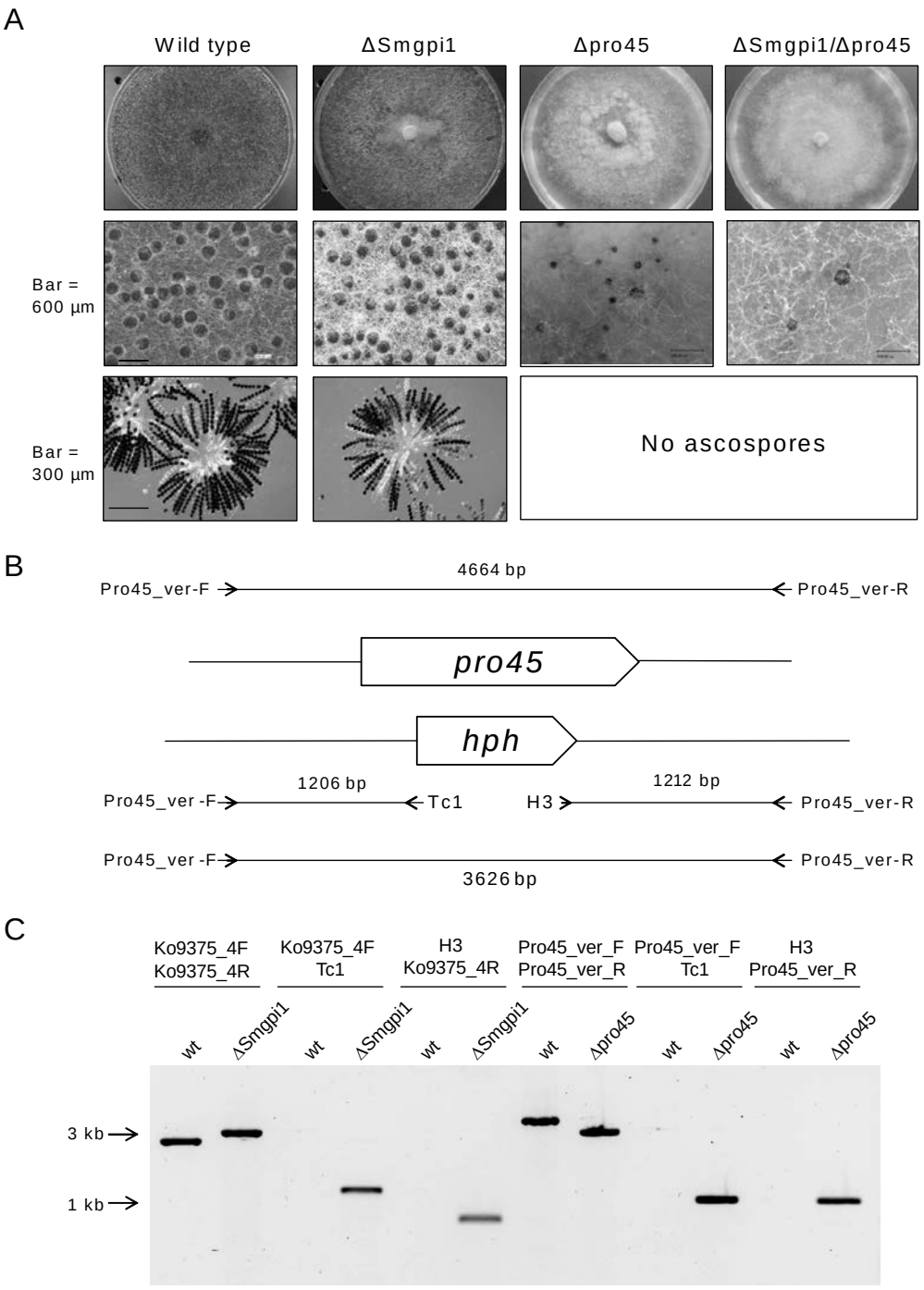

Figure 27. Generation of a ΔSmgpi1/Δpro45 double-deletion strain. (**A**) Phenotype of ΔSmgpi1/Δpro45, respective single-knockout strains and wt with focus on fruiting-body development. (**B**) Schematic illustration of the *pro45* locus (Nordzieke *et al.*, 2014) before and after homologous integration of the deletion cassette. Primers used for verification of the deletion strain are shown by arrows. PCR fragment sizes are given. (**C**) Verification of gene deletions in ΔSmgpi1/Δpro45 using PCR. Shown are the calculated fragment sizes for wt and the respective gene deletion. Strains were obtained by crossing the respective single-deletion strains ΔSmgpi1/r2 and Δpro45.

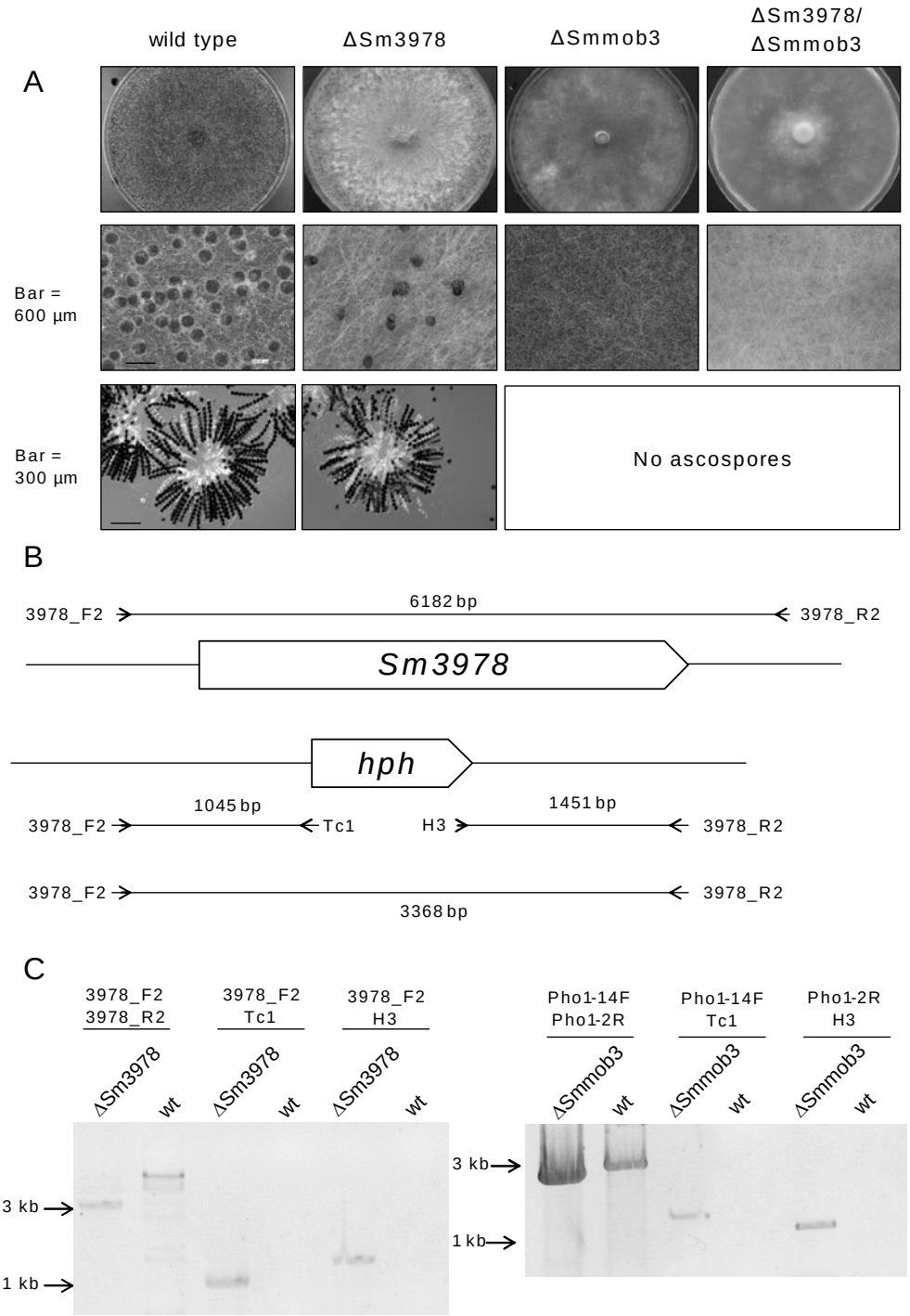

Figure 28. Generation of a ΔSm3978/ΔSmmob3 double-deletion strain. (**A**) Fruiting body and ascospores development of ΔSm3978/ΔSmmob3, respective single-knockout strains and wt. (**B**) Schematic illustration of the *Sm3978* locus before and after homologous integration of the deletion cassette. Primers used for verification of the deletion strain are shown by arrows. Sizes of PCR fragments are given. (**C**) Verification of *Sm3978* deletion using PCR. Shown are the calculated fragment sizes for wt and the respective gene deletion. Strains were obtained by crossing single deletion strains ΔSm3978 and ΔSmmob3/r2.

Previously, Maerz *et al.* (2009) demonstrated in *N. crassa* that MOB3 is essential for hyphal fusion under vegetative growth conditions. Similarly, disruption of *Smmob3* impairs hyphal fusion in *S. macrospora* (Bernhards & Pöggeler, 2011). These findings raised the question whether the double mutant ΔSmgpi1/ΔSmmob3 underwent hyphal fusion. Hyphal fusion was investigated under two conditions. First, vegetative hyphae of wt, ΔSmgpi1, ΔSmmob3 and ΔSmgpi1/ΔSmmob3 were microscopically observed (Figure 29A). Vegetative hyphae of wt and ΔSmgpi1 were capable of hyphal fusion. Hyphal fusion events were detected two days after inoculation.

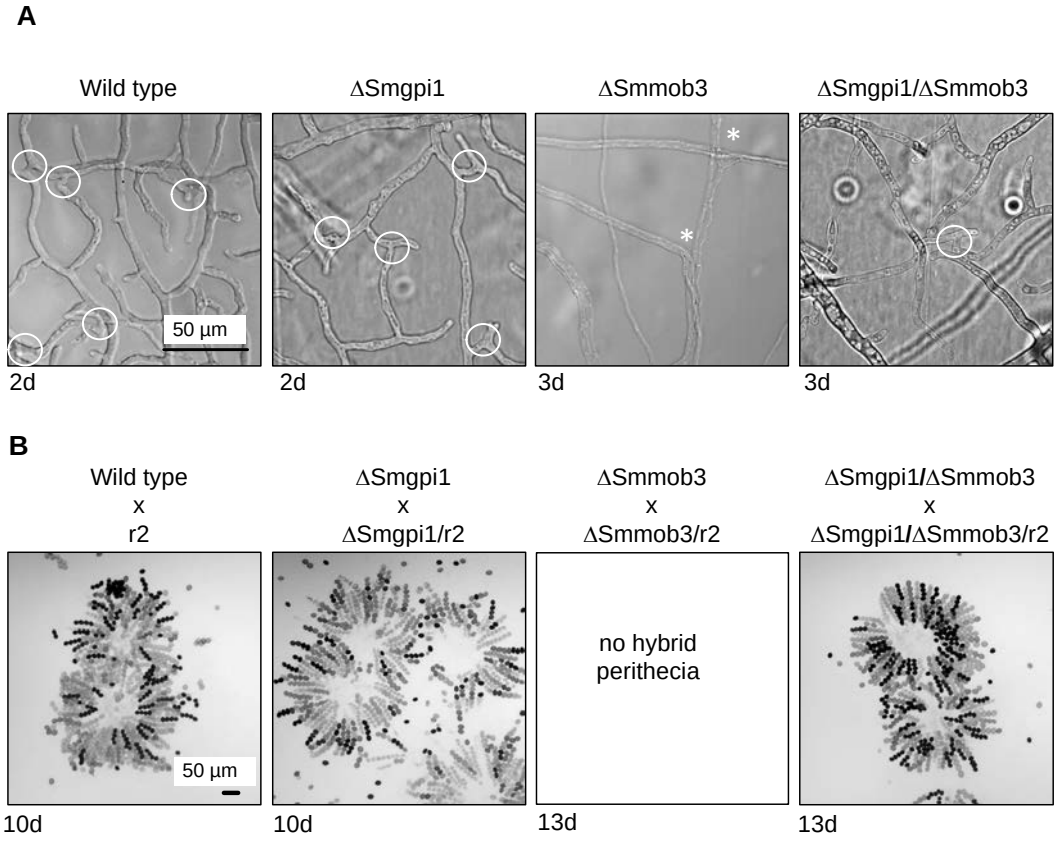

Figure 29. Deletion of *Smgpi1* in a sterile ΔSmmob3 background restores hyphal fusion. (**A**) Microscopic investigation of hyphal fusion in wt, ΔSmgpi1, ΔSmmob3 and ΔSmgpi1/ΔSmmob3. Hyphal fusion events are marked with circles; hyphal contacts without fusion are indicated by asterisks. Pictures were taken at subperiphal regions 10 mm from the growth front. Hyphal fusion was investigated 2-3 days past inoculation. ΔSmgpi1/ΔSmmob3 is delayed in hyphal fusion. First fusion was visible after 3 days. (**B**) Wt, ΔSmgpi1, ΔSmmob3 and ΔSmgpi1/ΔSmmob3 were crossed to r2 spore-color mutants with the same deletion background. Crossing perithecia were isolated after 10 days and 13 days past inoculation, respectively. ΔSmmob3 did not develop fruiting bodies at all. Crossing perithecia of wt, ΔSmgpi1, ΔSmmob3 and ΔSmgpi1/ΔSmmob3 contain spores allocated in typical 4:4 pattern of successful crossing events of red and black spored strains.

As described previously, ΔSmmob3 was impaired in hyphal fusion (Bernhards & Pöggeler, 2011). Even after 10 dpi, no hyphal fusion was visible. The mutant ΔSmgpi1/ΔSmmob3 rarely formed hyphal fusions and did so after a prolonged time of three days. After this time hyphal fusion events were not detectable under the microscope because of extensive aerial hyphae formation. Therefore, recovery of the hyphal fusions in ΔSmgpi1/ΔSmmob3 was verified by crosses with spore-color mutants. *S. macrospora* is a self-fertile fungus that produces perithecia without crossing. Thus, the distinction between self-fertile and hybrid perithecia is difficult. To circumvent this problem, we crossed the spore-color mutant r2 with the mutant strains ΔSmgpi1, ΔSmmob3 and ΔSmgpi1/ΔSmmob3 for red-spored strains ΔSmgpi1/r2, ΔSmmob3/r2 and ΔSmgpi1/ΔSmmob3/r2. The mutant r2 produces red ascospores because of a mutation in a pigment biosynthesis gene (Teichert *et al.*, 2014). Successful hyphal fusion events resulted in black-spored and red-spored asci of hybrid perithecia in the contact zone. The r2 strain, ΔSmgpi1/r2, ΔSmmob3/r2 and ΔSmgpi1/ΔSmmob3/r2 were self-crossed with respective black-spored strains (Figure 29). Similar to crosses wt x r2 and ΔSmgpi1 x ΔSmgpi1/r2, selfing of ΔSmgpi1/ΔSmmob3 x ΔSmgpi1/ΔSmmob3/r2 resulted in hybrid perithecia with typical 4:4 segregation of black and red spores. No hybrid perithecia were formed after selfing of sterile ΔSmmob3 strains (Figure 29).

The vegetative growth defect of ΔSmmob3 was also suppressed in the double-deletion strain ΔSmgpi1/ΔSmmob3. In contrast to the drastically impaired growth of ΔSmmob3 (8 ± 3 mm/d) the growth of ΔSmgpi1/ΔSmmob3 was similar to wt (25 ± 5 mm/d) (data not shown).

3.1.6 ΔSmgpi1 forms more fruiting bodies that are small but normally shaped

To analyze the function of *Smgpi1* and the reason for its suppression of ΔSmmob3, the ΔSmgpi1 phenotype was studied in detail. Counts of fruiting bodies revealed that ΔSmgpi1 produced 152% ± 6.3 fruiting bodies per cm^2 compared to the wt strain, the double-deletion mutant ΔSmgpi1/ΔSmmob3 formed only half of the number of perithecia (55% ± 5.9) compared to the wt (Figure 30).

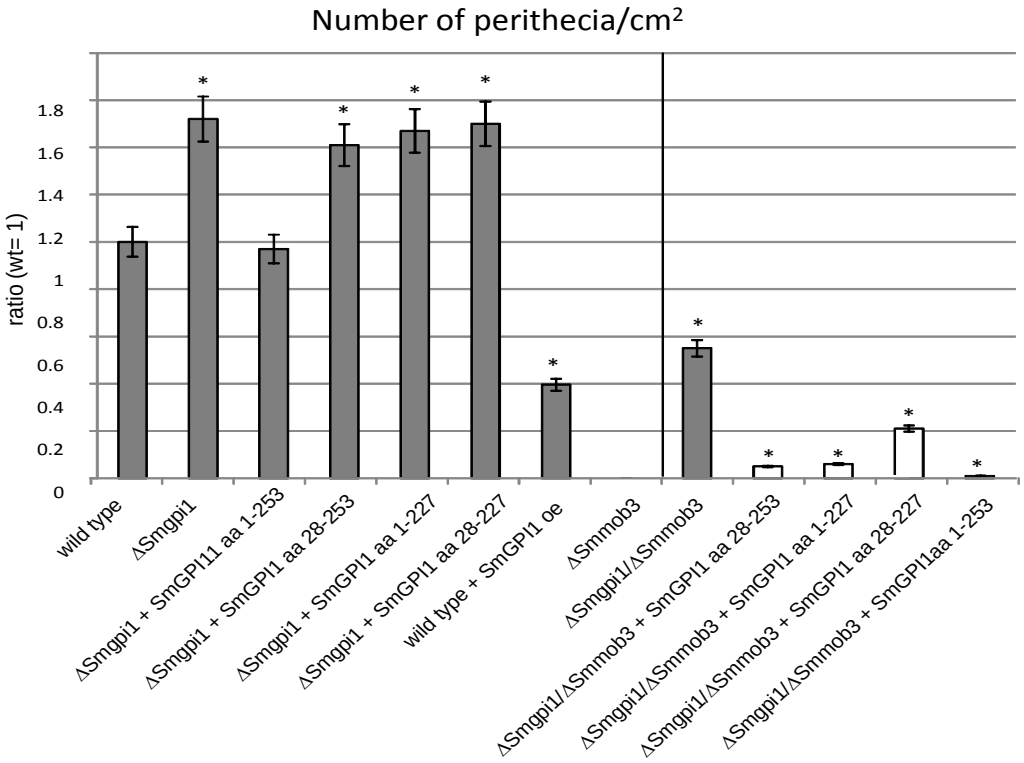

Figure 30. Number of fruiting bodies produced by ΔSmgpi1, ΔSmmob3 and ΔSmgpi1/ΔSmmob3 and complemented strains compared to wt. Wt and ΔSmgpi1 were grown for 8 days at 27 °C on solid SWG medium, ΔSmgpi1/ΔSmmob3 for 14 days, respectively. Data for the respective strains was obtained by counting the number of perithecia produced on an area of 5 cm^2 at the edge of the plate. Bars represent the mean value calculated from 10 strains (n=10) for each data set. Ratio of each strain compared to the wt (wt was set 1). Error bars (SD) are given as indicated. Grey bars indicate fertile perithecia containing ascospores; white bars represent sterile perithecia without ascospores. Asterisks indicate significance according to Student's t-test. Thus, values of grey colored bars were compared to wt number of perithecia; white colored bars significance was calculated compared to ΔSmgpi1/ΔSmmob3. P-value < 0.0003.

The increased number of perithecia returned to wt levels when ΔSmgpi1 was complemented by full-length construct SmGPI1 aa 1-253 but not by versions lacking the N-terminal signal sequence (SmGPI1 aa 28-253), the C-terminal processing region for GPI-attachment (SmGPI1 aa 1-227) or both regions (SmGPI1 aa 28-227) (Figure 30). Overexpression of *Smgpi1* in wt decreased the total number of produced perithecia per cm^2 to 51% ± 3.5 compared to wt (Figure 30). To determine whether localization of SmGPI1 plays a role to suppresses ΔSmmob3 sterility, *Smgpi1* variants encoding SmGPI1 aa 1-253, SmGPI1 aa 28-253, SmGPI1 aa 1-227 or SmGPI1 aa 28-227 were transformed into ΔSmgpi1/ΔSmmob3 (Figure 30). All ΔSmgpi1/ΔSmmob3 transformants produced a small number of immature perithecia; however, even after prolonged

incubation, these never contained asci or ascospores. No fruiting bodies were produced from strain ΔSmgpi1/ΔSmmob3 transformed with *Smgpi1* full-length. The higher number of fruiting bodies produced by ΔSmgpi1 led us to inspect the size and shape of the fruiting bodies in detail. Similar to the wt, ΔSmgpi1 produced pear-shaped fruiting bodies; however, they were smaller (Figure 31A). ΔSmgpi1 perithecia contained a similar number of asci and ascospores compared to wt (Figure 31B). The decreased size of ΔSmgpi1 fruiting bodies was complemented by full-length *Smgpi1* (SmGPI1 aa 1-253), with or without *egfp* fusion (SmGPI1-eGFP aa 1-492).

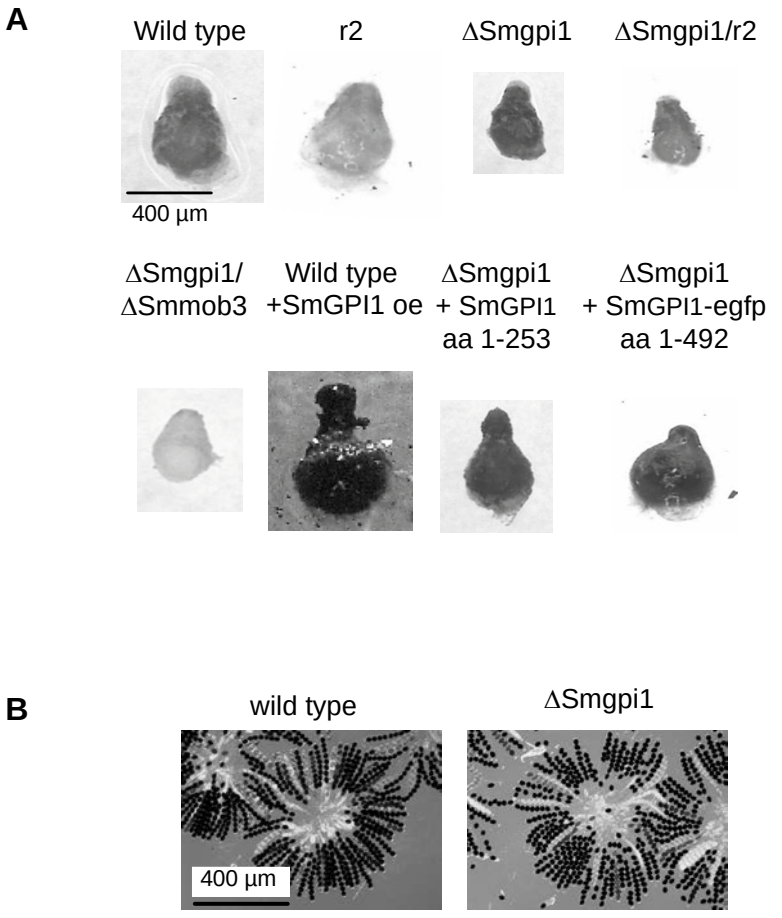

Figure 31. Deletion of *Smgpi1* results in smaller mature fruiting bodies. (**A**) Microscopic analysis of fruiting-body size of wt, ΔSmgpi1, ΔSmgpi1 complemented with the full length *Smgpi1* (SmGPI1 aa 1-253) or *Smgpi1-egfp* (SmGPI1 aa 1-492), ΔSmgpi1/ΔSmmob3 and wt expressing an additional copy of *Smgpi1*. Fruiting bodies were isolated at day 8 after inoculation. Complementation of the gene deletion restores normal size of fruiting bodies. (**B**) Ascus rosette from wt perithecium compared to perithecium of ΔSmgpi1. Both strains produce an equal number of asci and ascospores.

Truncated versions of *Smgpi1* (SmGPI1 aa 28-253, 1-227 and 28-227) did not restore fruiting-body size (data not shown). Quantitative analysis revealed a different distribution of fruiting-body diameters in the deletion mutant ΔSmgpi1 (Figure 32). Compared to wt, ΔSmgpi1 developed more mature fruiting bodies with a diameter of 0.2-0.3 mm and fewer with a diameter of > 0.4 mm. This effect was complemented by full-length *Smgpi1*. Overexpression of *Smgpi1* in wt slightly increased perithecia diameter (Figure 32). Fruiting bodies in the double-deletion strain ΔSmgpi1/ΔSmmob3 were slightly smaller than in ΔSmgpi1 (Figure 31).

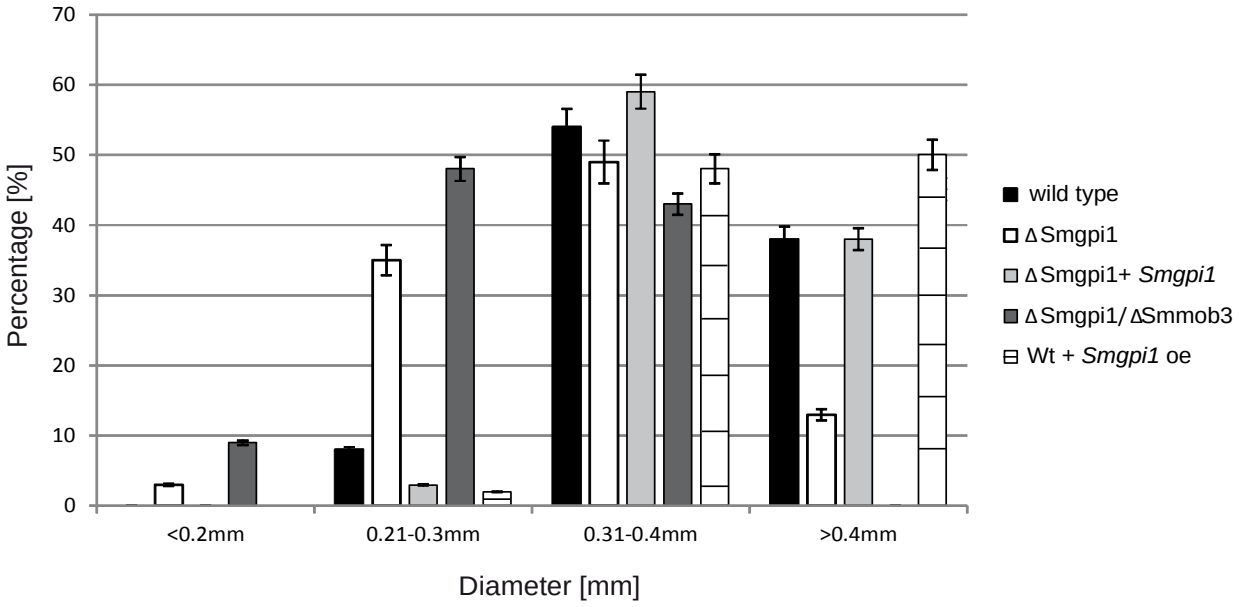

Figure 32. Quantitative evaluation of perithecia size (diameter) from wt, ΔSmgpi1 and ΔSmgpi1 expressing the full length *Smgpi1* (SmGPI1 aa 1-253), ΔSmgpi1/ΔSmmob3 and wt expressing an additional copy of *Smgpi1*. Bars represent the mean value calculated from data obtained from 100 measured fruiting bodies of three biological replicates, respectively. Error bars (SD) are given as indicated (n=100). Scale bar as indicated.

3.2 The GCKs SmKIN3 and SmKIN24

3.2.1 *S. macrospora* encodes two kinases similar to the mammalian STRIPAK-associated kinases STK24, STK25, MST4 and MINK1.

In mammals three members of the GCK III subfamily of the Ste20 kinases (STK24, STK25, and MST4); and one member of the GCK IV family (Mishappen-like kinase 1, MINK1) are associated with the STRIPAK complex (Goudreault *et al.*, 2009, Hyodo *et al.*, 2012). To date, no STRIPAK-associated kinases have been identified in filamentous fungi so far.

Therefore, we performed a BLASTP search using mammalian kinases STK24, STK25, MST4 and MINK1 as query against the *S. macrospora* proteome (http://blast.be-md.ncbi.nlm.nih.gov/(Nowrousian, 2010)) to identify putative *S. macrospora* homologs of the mammalian kinases. This search revealed the putative germinal center kinases SMAC_01456 (F7VQV9) and SMAC_04490 (F7VYS5) to be orthologous to the mammalian GCKs (Table 6).

Table 6. BLASTP search of the human STRIPAK associated GC kinases against the *S. macrospora* proteom

Type	***Human*** (accession number)	***S. macrospora*** best hit (e-value)
GCK III	MST3, STK24 (Q9Y6E0.1)	SMAC_01456 ($5e^{-136}$) SMAC_04490 ($9e^{-126}$)
GCK III	MST4,MASK (Q9P289.2)	SMAC_01456 ($4e^{-136}$) SMAC_04490 ($6e^{-125}$)
GCK III	STK25, SOK1, YSK1 (O00506.1)	SMAC_01456 ($3e^{-134}$) SMAC_04490 ($4e^{-123}$)
GCK IV	MINK1 (NP_722549.2)	SMAC_01456 ($8e^{-75}$) SMAC_04490 ($2e^{-69}$)

The open reading frame (ORF) of *SMAC_04490* comprises 2758 bp and contains three putative introns: 96 bp at position 53-148, 117 bp at position 217-333 and 82 bp at position 502-583 (Figure 34). The calculated molecular weight (MW) of the encoded 820 aa protein is 91.4 kDa with an isoelectric point (pI) of 9.47. It showed a high sequence identity to the serine/threonine-protein kinase 3 of *Neurospora crassa* (locus tag NCU04096, gene symbol *prk-9*) (Figure 33) and was therefore named SmKIN3.

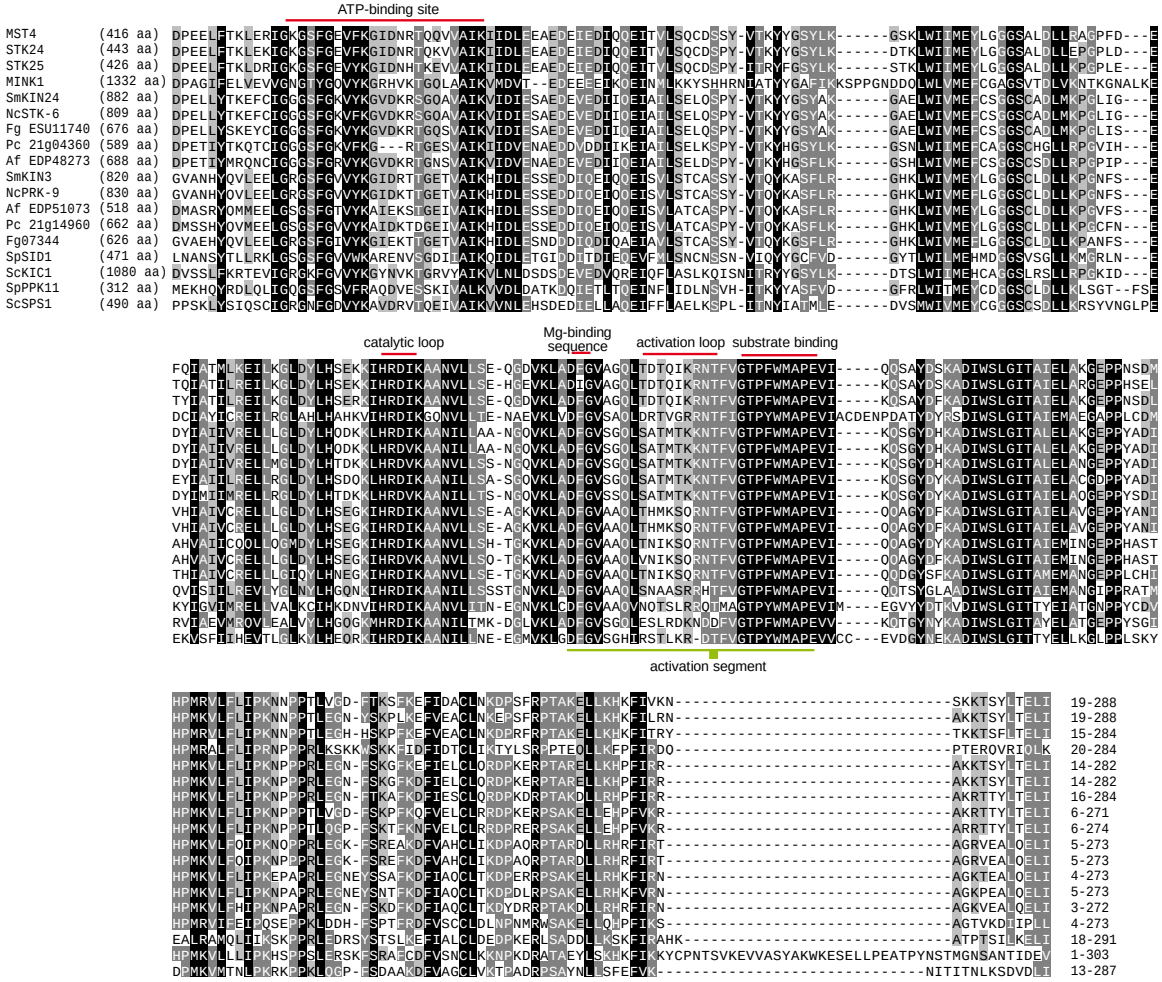

Figure 33. Multiple sequence alignment and aa identity of mammalian kinases identified as STRIPAK members with putative homologues from Ascomycota. Protein sequences were aligned with ClustalX2 (Larkin *et al.*, 2007) and visualized with GeneDoc (Nicholas *et al.*, 1997). MST4, mammalian STE20-like protein kinase 4 (Accession number: Q9P289); STK24, mammalian STE20-like protein kinase 3 (Q9Y6E0); STK25, mammalian serine/threonine-protein kinase 25 (O00506); MINK1, mammalian misshapen-like kinase 1 (Q8N4C8); SmKIN24, putative serine/threonine-protein kinase 24 from *S. macrospora* (F7VQV9), NcSTK-6, serine/threonine-protein kinase 24 from *N. crassa* (V5IQF9); Fg ESU11740, serine/threonine-protein kinase 24 from *F. graminearum* (I1RNY7); Pc21g04360, putative STE20-like protein kinase from *P. chrysogenum* (B6HMA9); Af EDP48273, putative STE20-like kinase from *A. fumigatus* (BA78_1793), SmKIN3, putative serine/threonine-protein-kinase 3 from *S macrospora* (F7VYS5); NcPRK-9, serine/threonine-protein-kinase 3 from *N. crassa* (V5INC1); Af EDP51073, putative Ste20-like kinase from *A. fumigatus* (B0Y2A3); Pc21g14960, putative serine/threonine-protein kinase from *P. crysogenum*; (B6HJ11); Fg07344, putative serine/threonine-protein kinase from *F. graminearum* (A0A016PPL3); SpSID1, serine/threonine-protein kinase from *Schizosaccharomyces pombe*, (O14305); ScKIC1, serine/threonine-protein kinase from *S. cerevisiae*, (P38692); SpPPK11, serine/threonine-protein kinase from *S. pombe*, (O14047); ScSPS1, sporulation-specific protein 1 from *S. cerevisiae* (P08458). Total numbers of aa are given in brackets. Regions of the aligned N-terminal domain of the protein sequences are indicated in brackets at the end of the alignment.

ATP-binding side, catalytic loop, Mg-binding sequence, activation loop and region for substrate binding are marked with red lines. The entire activation segment is underlined in green. Filled box indicate the threonine residue (Thr190 in in MST4, Thr182 in STK24, and Thr174 in STK25), phosphorylated during activation. Total numbers of aa are given in brackets at the beginning of the alignment. Aligned N-terminal domains of the protein sequences are given at the end of the alignment.

Two variants have been reported for *N. crassa* NCU04096 protein: a long version resulting from a transcript after splicing of three introns, and a short version derived from a transcript retaining intron 3 and following initiation of translation at a down-stream ATG codon (http://www.broadinstitute.org/annotation/genome/neurospora/). The position of all three introns is conserved in *Smkin3* and *prk-9*, but we identified splicing of all three introns in *Smkin3* using RT-PCR and cDNA sequencing, and splicing of intron 3 did not appear to be optional (Figure 34). In addition, the position of the down-stream start codon is conserved in *Smkin3*. Initiation of translation from this ATG codon would lead to an N-terminally truncated SmKIN3 version of 663 aa with an MW of 74.3 kDa. The second ORF (*SMAC_01456)* encoding a putative homolog of mammalian GC III and GC IV kinases, encompasses 2947 bp and is predicted to be disrupted by four introns: 107 bp at position 77-183, 76 bp at position 215-290, 51 bp at position 608-658 and 64 bp at position 2413-2476. The calculated MW of the encoded protein of 882 aa is 98.3 kDa with an isoelectric point (pI) of 7.70.The closest homolog of this protein was serine/threonine-protein kinase 24 of *N. crassa* (locus tag NCU00772, gene symbol *stk-6* alias *mst-1*). The *S. macrospora* protein was therefore designated SmKIN24.

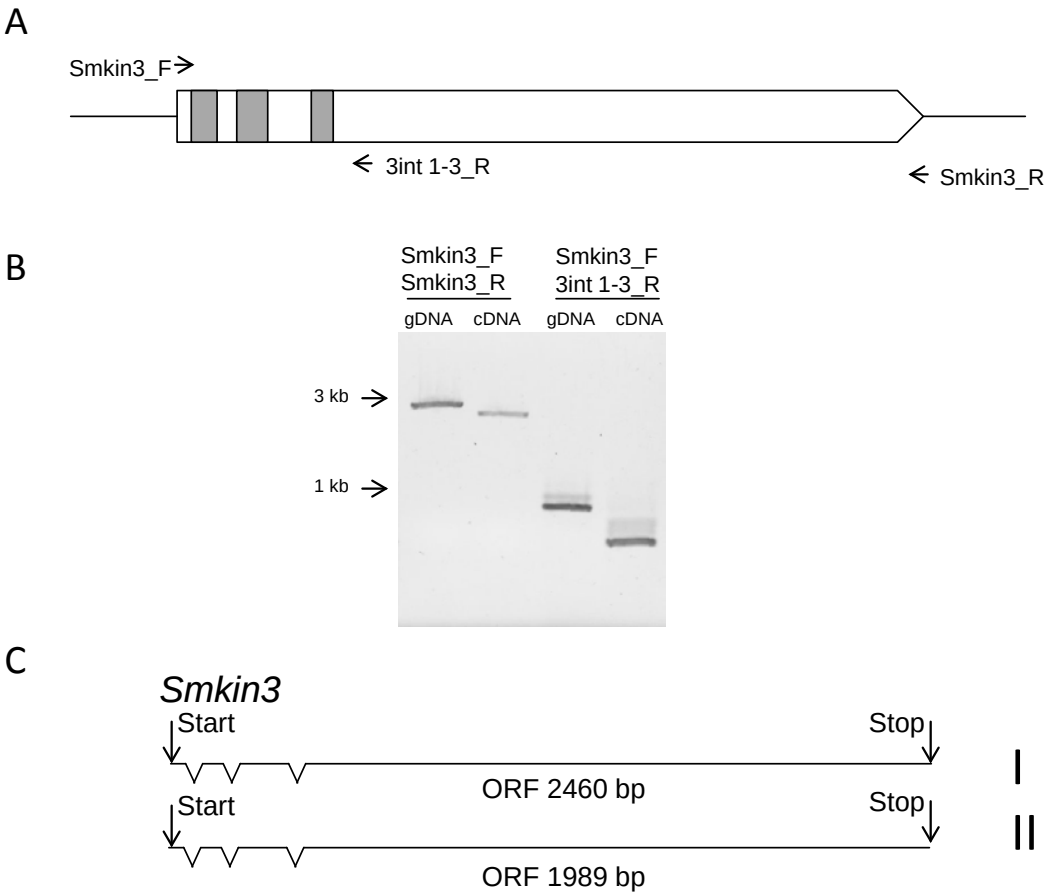

Figure 34. RT-PCR analysis of *Smkin3*. (**A**) Schematic illustration of *Smkin3*. Introns are indicated as grey boxes, positions of primers used for analysis of intron splicing are indicated by arrows. (**B**) Results of the RT-PCR analysis. Shown are the obtained amplicons for respective primer pairs from cDNA and gDNA. (**C**) Schematic illustration of *Smkin3* transcripts.

Similarly to *NCU04096*, two gene products have been identified for *NCU00772*: a long version resulting from splicing of three introns at same positions as the first three introns of *Smkin24*, and a short version resulting from skipping of intron 1 and translation initiation at a down-stream ATG start codon. This downstream start codon is conserved in *Smkin24*. RT-PCR and cDNA sequencing of *Smkin24* revealed that, like *NCU0772*, splicing of the first intron was optional. Additionally, sequencing of full length RT-PCR products showed optional splicing of intron 4, which is not present in *NCU0772* (Figure 35).

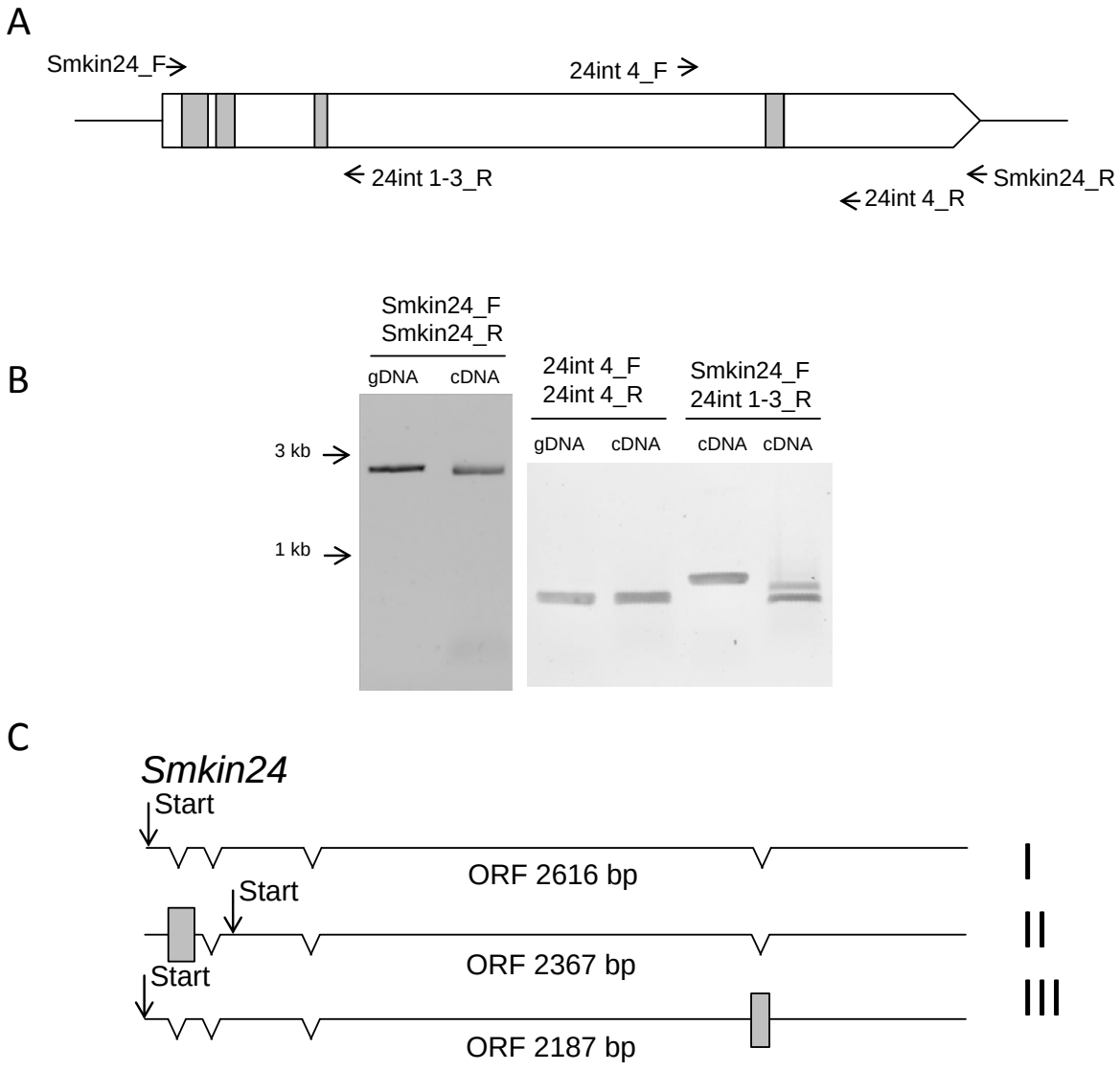

Figure 35. RT-PCR analysis of *Smkin24*. (A) Schematic illustration of *Smkin24*. Introns are indicated as grey boxes, positions of primers used for analysis of intron splicing are indicated by arrows. (B) Results of the RT-PCR analysis. Shown are the obtained amplicons for respective primer pairs from cDNA and gDNA. (C) Schematic illustration of *Smkin24* transcripts identified by cDNA sequencing.

Thus, in addition to the full-length protein two further variants are encoded by *Smkin24*. Skipping the splicing of intron 1 and initiation of translation at the downstream ATG codon would result in a 789 aa protein with a MW of 88 kDa, whereas skipping intron 4 splicing would lead to a C-terminal truncated version of 729 aa with a MW of 82 kDa (Figure 36).

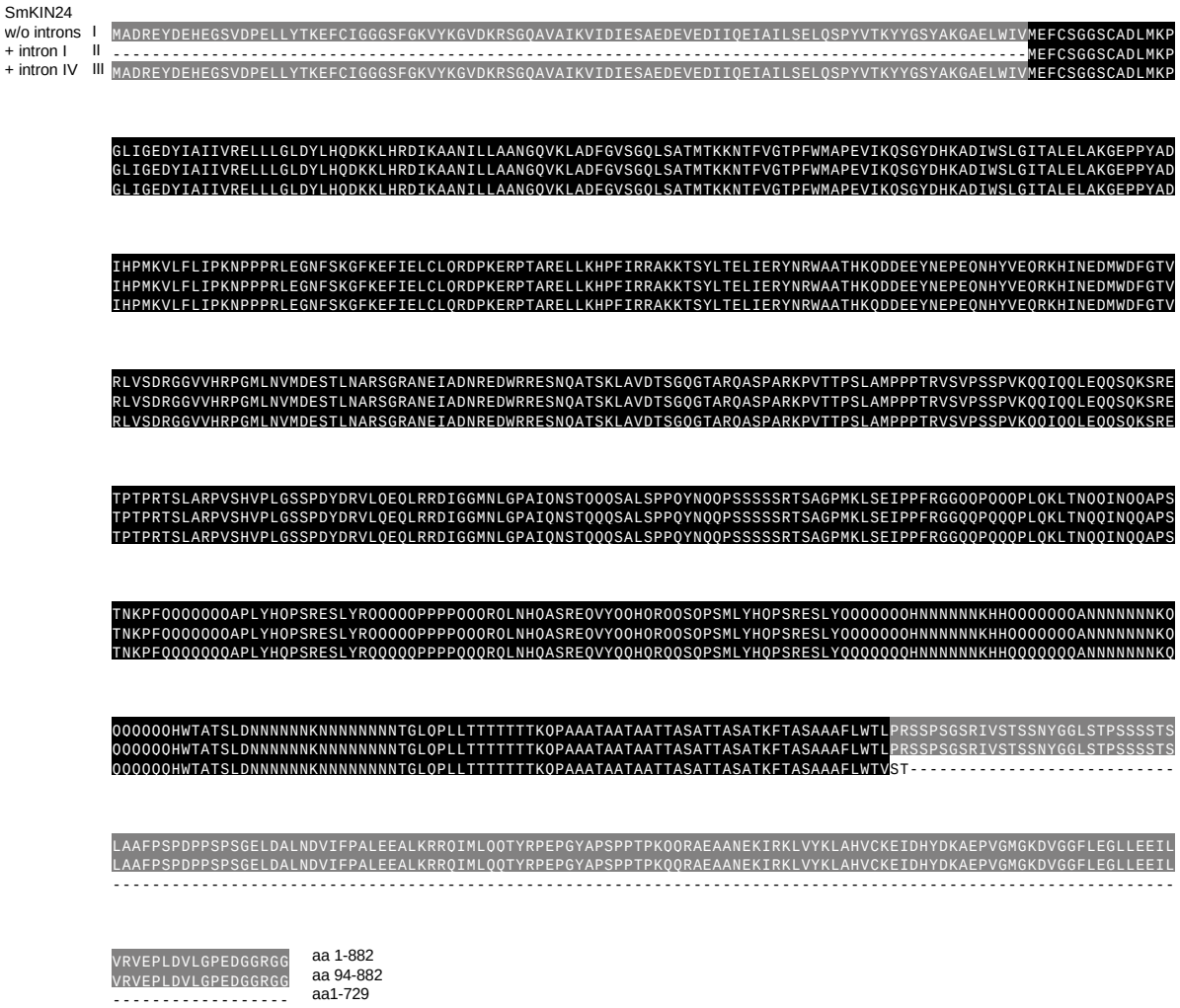

Figure 36. Alignment of aa sequences encoded by alternatively spliced *Smkin24* transcripts. *Smkin24* without introns results in a protein of 882 aa and thus representing the largest protein. Expression of *Smkin24* with remaining intron I but removed intron II-IV results in a protein comprising aa 94-882 of the protein derived from *Smkin24* without introns. *Smkin24* with spliced intron I-III but remaining intron IV results in a protein comprising aa 1-729. The numbers I-III at the beginning of the aa acid sequences for each Isoform refers to Figure 35.

In mammalian GC III and IV kinases the regulatory domain lies C-terminal to the catalytic domain and is heterogeneous in sequence (Record *et al.*, 2010). A search for conserved domains at CCD http://www.ncbi.nlm.nih.gov/Structure/cdd/wrpsb.cgi (Marchler-Bauer *et al.*, 2011) revealed that both SmKIN3 and SmKIN24 exhibit a typical STKc MST3-like catalytic domain of mammalian Ste20-like kinase 3 serine/threonine-protein kinases (accession cd06609, E-value SmKIN3 =1.13e^{-177}, E-value SmKIN24 =0.0) at the N-terminal part of the protein. As shown in

Figure 33, SmKIN3 and SmKIN24 possess a conserved ATP-binding site [GXGX(F)GX$_{16}$K], a catalytic loop sequence [HRDIK], a Mg^{2+}-coordinating sequence [DFG], a substrate binding motif [GTPFWMAPE] and a critical threonine residue, phosphorylated during activation, at the end of the activation loop (Sugden *et al.*, 2013, Delpire, 2009). Based on an aa alignment of the N-terminal catalytic domain, *S. macrospora* SmKIN3 and SmKIN24 share a high level of sequence identity with the N-terminus of MST4 (67%/67%), STK24 (68%/68%), STK25 (67%/68%) and MINK1 (46%/46%). However, the C-terminally located regulatory domains are structurally different to GCKs from other filamentous ascomycetes, as well as *S. cerevisiae* and *S. pombe* (less than 20%) (Figure 37).

	MST4	STK24	STK25	MINK1	SmKIN24	NcSTK-6	FgESU11740	Pc21g04360	AfEDP48273	SmKIN3	NcPRK-9	AfEDP51073	Pc21g14960	Fg07344	SpSID1	ScKIC1	SpPPK1	ScSPS1
MST4	100%	88%	86%	46%	67%	67%	66%	66%	65%	64%	64%	62%	62%	62%	52%	49%	44%	45%
STK24		100%	88%	45%	68%	68%	67%	67%	66%	64%	64%	63%	63%	62%	51%	50%	45%	46%
STK25			100%	45%	68%	67%	66%	67%	66%	65%	65%	63%	63%	63%	52%	50%	45%	48%
MINK1				100%	47%	46%	47%	42%	46%	44%	45%	43%	43%	44%	41%	42%	33%	37%
SmKIN24					100%	98%	91%	79%	81%	62%	63%	60%	61%	61%	50%	51%	46%	47%
NcSTK-6						100%	92%	79%	81%	62%	63%	60%	61%	61%	50%	50%	47%	47%
Fg ESU11740							100%	78%	82%	63%	65%	62%	62%	63%	50%	49%	46%	47%
Pc21g04360								100%	84%	60%	61%	59%	59%	58%	52%	48%	44%	47%
Af EDP48273									100%	60%	62%	58%	81%	58%	51%	48%	45%	49%
SmKIN3										100%	98%	79%	81%	84%	55%	46%	46%	48%
NcPRK-9											100%	80%	57%	85%	56%	45%	46%	47%
Af EDP51073												100%	80%	80%	55%	45%	43%	46%
Pc21g14960													100%	80%	55%	45%	43%	47%
Fg07344														100%	55%	45%	42%	45%
SpSID1															100%	40%	43%	42%
ScKIC1																100%	35%	42%
SpPPK11																	100%	44%
ScSPS1																		100%

Figure 37. Identity of aligned aa sequences of mammalian kinases identified as STRIPAK members with putative homologues from Ascomycota in pair-wise comparison.

Phylogenetic analysis revealed that SmKIN3 and SmKIN24 were strictly separated and cluster together with putative homologs from other filamentous ascomycetes (Figure 38).

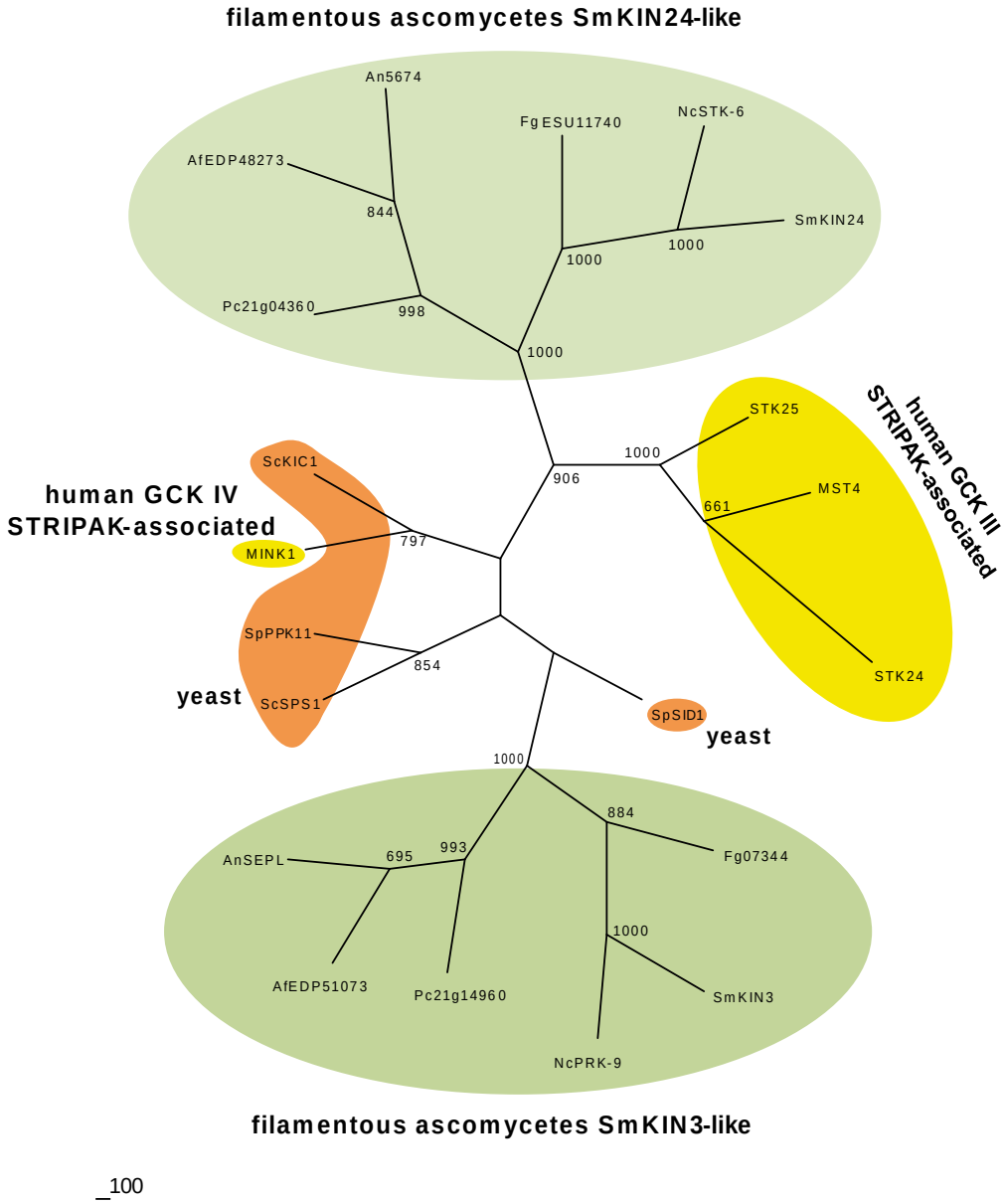

Figure 38. Unrooted neighbor-joining tree of human GCKs MST4, STK24, STK25, MINK1 and their orthologs in ascomycetes. Orthologs were identified by BLAST search using the listed human GCKs as template. Catalytic domains proteins were aligned with ClustalX2 (Larkin *et al.*, 2007). The phylogenetic tree was made with programs included in PHYLIP 3.695 (Felsenstein, 2013). The human GCKs are displayed in yellow, the orthologs from the yeasts *S. cerevisiae* and *S. pombe* in orange. KIN3-like kinases and KIN24-like kinases from filamentous ascomycetes are shown in light green. The respective accession numbers of the proteins are given in Figure 33 except of the *Aspergillus nidulans* kinases AnSEPL (C8V5Z7) and An56574 (Q5B1A6).. The tree is divided into four branches, comprising the human GCKs MST4, STK24, and STK25, the KIN24-like group of filamentous ascomycetes, the KIN3-like group of filamentous ascomycetes, and MINK1 with SPS1 and KIC1 from *S. cerevisiae* as well as *S. pombe* PPK11 from. SID1 from *S. pombe* is separately positioned, near the SmKIN3-like group. The numbers at the nodes indicate bootstrap support.

Mammalian GC III kinases contain putative nuclear export signals (NES) and bipartite nuclear localization sequences (NLS) (Lee *et al.*, 2004). A putative NES at aa position 493-509 was predicted for SmKIN3 by NetNES1.1 (la Cour *et al.*, 2004) and a bipartite NLS by the program cNLS (Kosugi *et al.*, 2009) for SmKIN3 at position 463-490 (score 4.1) and SmKIN24 at position 783-817 (score 3.8).

3.2.2 SmKIN3 interacts physically with PRO11

Striatin is the scaffold of mammalian STRIPAK complex kinases MST4, STK24, STK25 and MINK1 (Hyodo *et al.*, 2012, Goudreault *et al.*, 2009). PRO11 was previously shown to be the *S. macrospora* homolog of mammalian Striatin (Pöggeler & Kück, 2004). The sequence similarity between SmKIN3 and SmKIN24 and the mammalian GC III and GC IV kinases (Figure 36) led us to inspect whether both *S. macrospora* kinases can interact with PRO11 in a Y2H system. Full-length cDNAs of *Smkin3* and *Smkin24* were cloned into the Y2H vector pGBKT7 that contains the GAL4 DNA-binding domain. Plasmid pAD11FL encoding full-length PRO11 served as prey vector. Plasmids were transformed into yeast strains Y187 (pGBKT7 constructs) or AH109 (pGADT7 constructs). Strains carrying pBD-SmKIN3 and pBD-SmKin24 plasmids were checked for transactivation activity by mating with yeast strain AH109 containing pGADT7. A strain carrying pGBKT7 and pGADT7 was used as negative control. Expression of GAL4 fusion proteins from pBD-SmKIN3 and pBD-SmKIN24 was checked by interaction with the yeast protein RanBPM (Tucker *et al.*, 2009). Previously, we showed that the Mob domain protein SmMOB3, the mammalian phocein homologue, is a strong interaction partner of PRO11 (Bloemendal *et al.*, 2012, Bernhards & Pöggeler, 2011). We therefore tested the interaction of both kinases with SmMOB3. Using the Y2H system we confirmed that both SmKIN3 and SmKIN24 could physically interact with PRO11 but not with SmMOB3 (Figure 39).

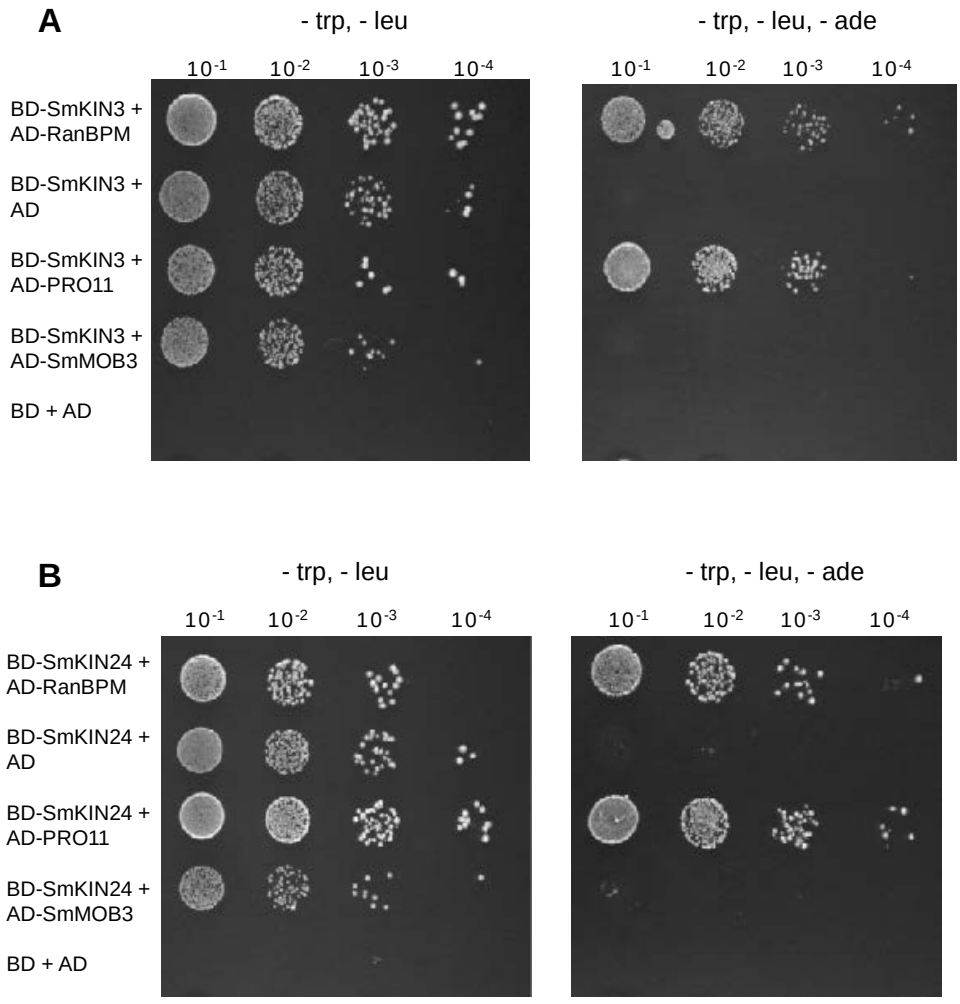

Figure 39. SmKIN3 and SmKIN24 interact physically with PRO11. Yeast two-hybrid analysis of interaction between SmKIN3 and PRO11 (**A**) as well as SmKIN24 and PRO11(**B**). For Y2H analysis, serial dilutions of diploids obtained after mating spread on medium lacking tryptophan (trp) and leucine (leu) or trp, leu and adenine (ade). BD = DNA-binding domain of GAL4, AD = activation domain of GAL4. GAL4 binding domain was fused to SmKIN3 (BD-SmKIN3) or SmKIN24 (BD-SmKIN24), GAL4 activation domain was fused to PRO11 full-length (AD-PRO11). A diploid strain carrying empty pGADT7 (AD) and pGBKT7 (BD) served as negative control. Expression of the GAL4-BD fusion protein from pBD-SmKIN3 (BD-SmKIN3) and pBD-SmKIN24 (BD-SmKIN24) plasmids were checked by mating Y187 transformants with AH109 carrying pAD-RanBPM (AD-RanBPM) (Tucker *et al.*, 2009)

To test whether PRO11 and GCKs SmKIN3 and SmKIN24 could interact *in vivo*, we performed co-IP studies in *S. macrospora*. We expressed N-terminally FLAG-tagged SmKIN3 as well as SmKIN24 and HA-tagged PRO11 (Bloemendal *et al.*, 2012) in *S. macrospora*. We were not able to express FLAG-tagged SmKIN24 in *S. macrospora* in amounts suitable for co-IP, under

control of either the native or *ccg1* promoter. All obtained viable transformants expressed *Smkin24* in low amounts (data not shown). We therefore concluded that SmKIN24 is highly instable. However, tagged SmKIN3 and PRO11 could be expressed separately and co-expressed in wt *S. macrospora*. Pull-down experiments without adding a cross-linker did not result in precipitation of PRO11 (data not shown). Since protein kinases often interact weakly and transiently their substrate, we performed sulfhydryl cross-linking with bismaleimidohexane BHM which confirmed the physical interaction of full length SmKIN3 and PRO11 (Figure 40).

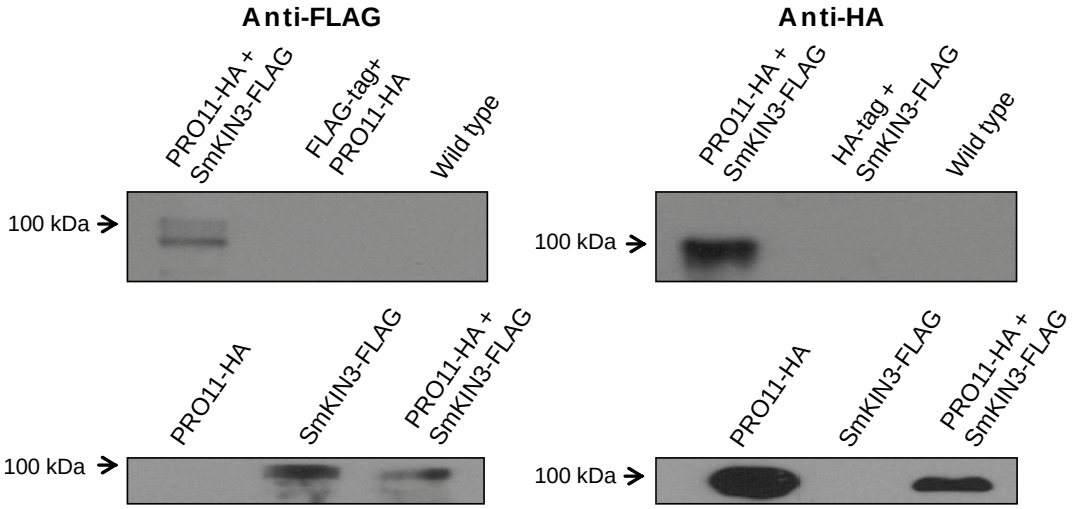

Figure 40. Co-IP of SmKIN3-FLAG and PRO11-HA. The Western-blot was performed with anti-FLAG and anti-HA antibody, respectively. Protein extract of the wt, separately expressed constructs and co-expression of each construct with complementary empty vectors served as controls.

3.2.3 Deletion of *Smkin3* or *Smkin24* impairs vegetative growth but only ΔSmkin24 is sterile

In order to investigate the functional role of *Smkin3* and *Smkin24*, we generated single and double deletion strains ΔSmkin3, ΔSmkin24 and ΔSmkin3/ΔSmkin24 (Figure 41). The respective genes were replaced by homologous recombination in the *S. macrospora* Δku70 (Pöggeler & Kück, 2006) strain (Figure 41A). The Δku70 background was removed afterwards by crossing the homokaryotic deletion strains with *S. macrospora* spore-color mutant r2 (Teichert *et al.*, 2014) and the obtained single-spore isolates were verified by PCR (Figure 41B) and Southern blotting (Figure 41C).

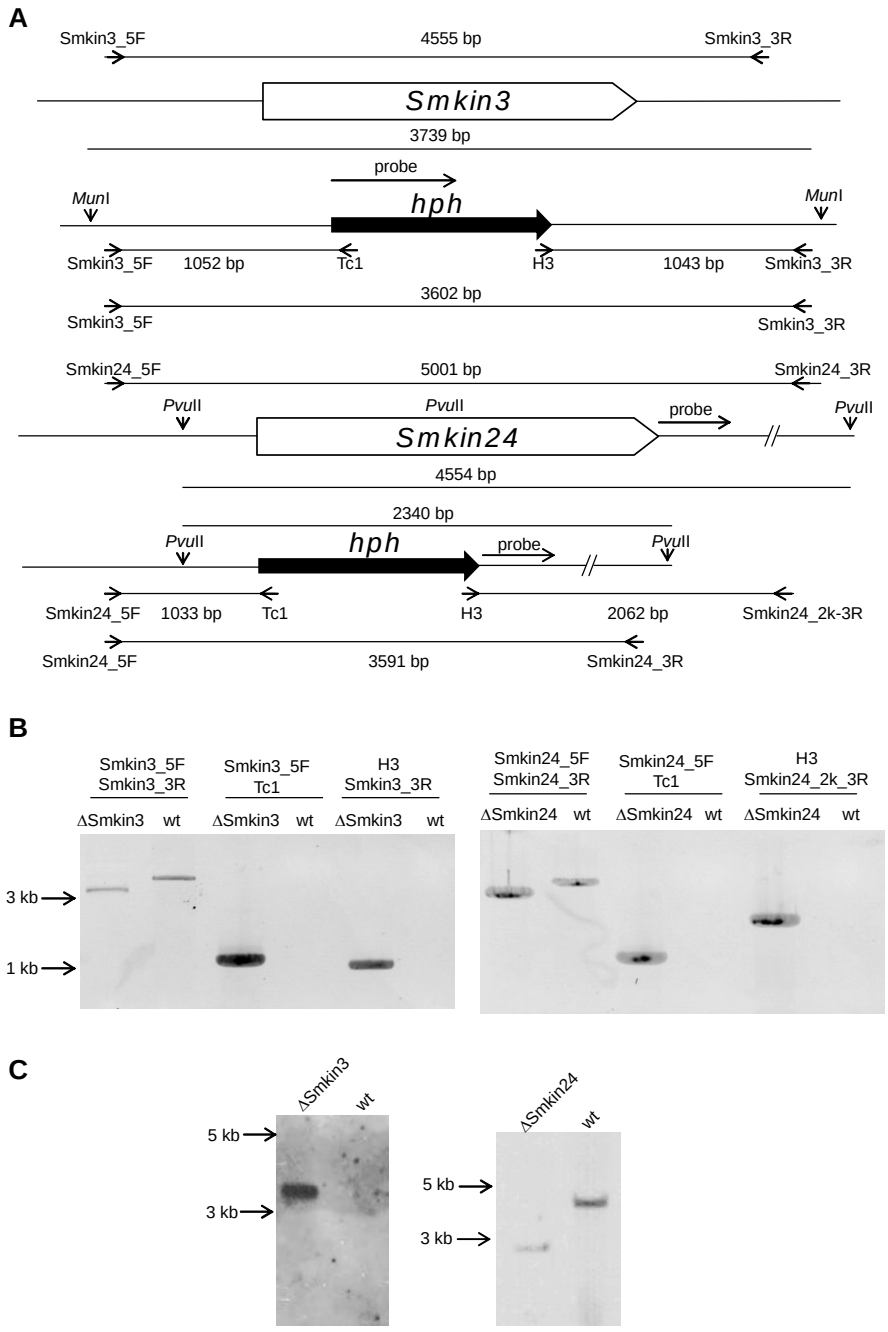

Figure 41. Generation of ΔSmkin3 and ΔSmkin24 deletion strains. (**A**) Schematic illustration of the *Smkin3* and *Smkin24* loci before and after homologous integration of the respective deletion cassette. Primers used for verification of the deletion strains are indicated by arrows. Sizes of PCR fragments and probes used for Southern hybridization are given. (**B**) Verification of the respective deletion using PCR. Sizes of amplicons and positions of the primers as indicated in (A). (**C**) Integration of the deletion cassette was verified by Southern hybridization (Sambrook *et al*., 2001). Positions of the respective probes are indicated in (A). ΔSmkin3 (left) was verified using a hygromycin specific probe that only binds within the deletion cassette. ΔSmkin24 (right) was verified using a probe binding at the 3' region of *Smkin24*. In this case, the successful integration is represented by a band shift.

Microscopic analysis of the knockout strains revealed that only ΔSmkin3 was fertile and able to generate fruiting bodies with ascospores within 7 days (Figure 42).

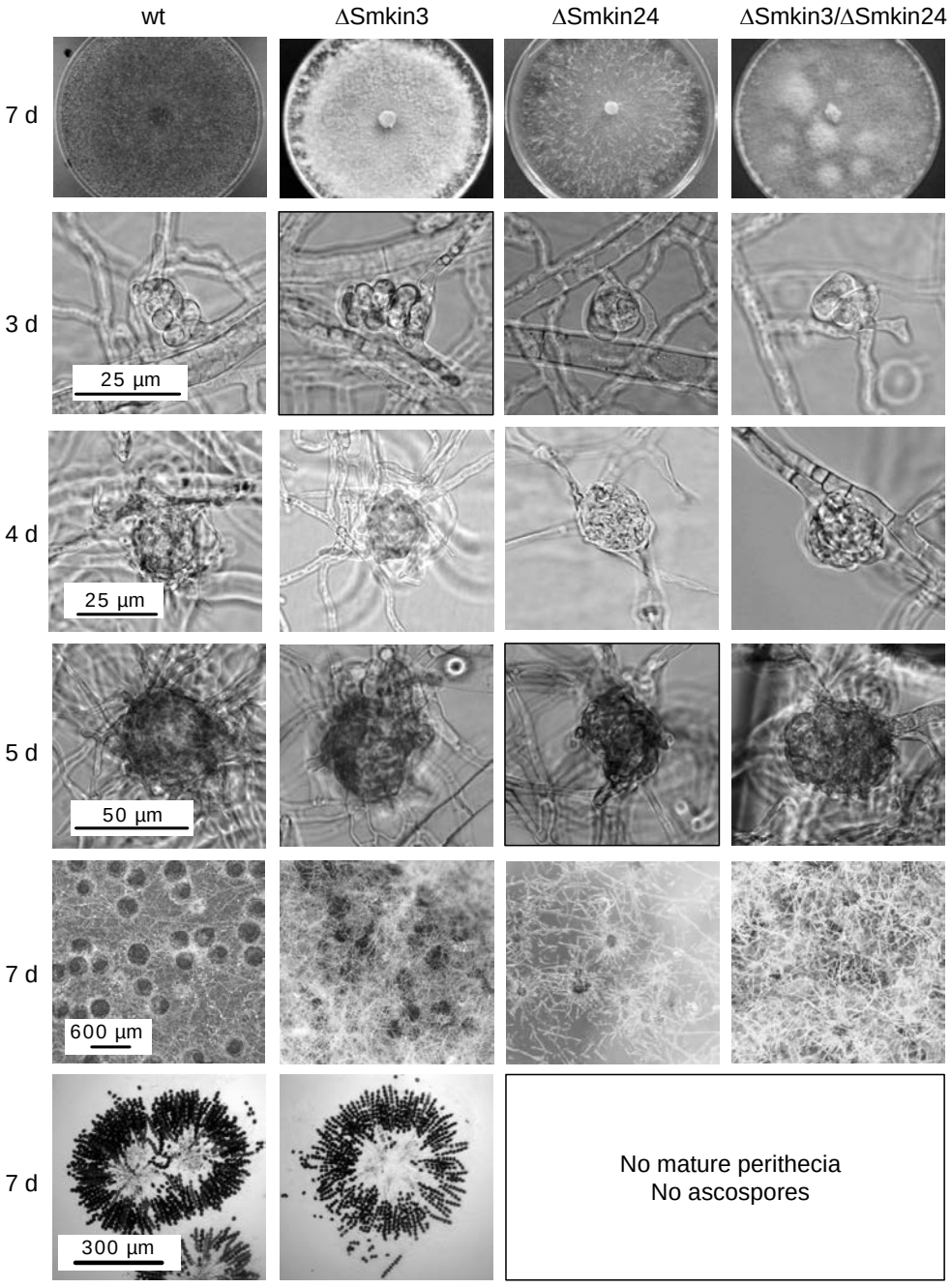

Figure 42. Macroscopic and microscopic analysis of the sexual development of wt, ΔSmkin3, ΔSmkin24 and ΔSmkin3/ΔSmkin24. The wt strain produces ascogonia after 3 days which develop to unpigmented protoperithecia at day 4 and pigmented protoperithecia at day 5. After 7 days mature perithecia with asci and ascospores are formed. Like the wt, ΔSmkin3 completes the lifecycle within 7 days and produces germinable ascospores. Development of ΔSmkin24 and the double-deletion strain ΔSmkin3/ΔSmkin24 is arrested at the stage of late protoperithecia formation. Scale bars as indicated.

The deletion strain ΔSmkin24 was halted during late protoperithecia maturation and thus failed to develop mature fruiting bodies (Figure 42). Additionally, ΔSmkin3 produced more aerial hyphae on solid SWG fructification medium compared to wt (Figure 42).

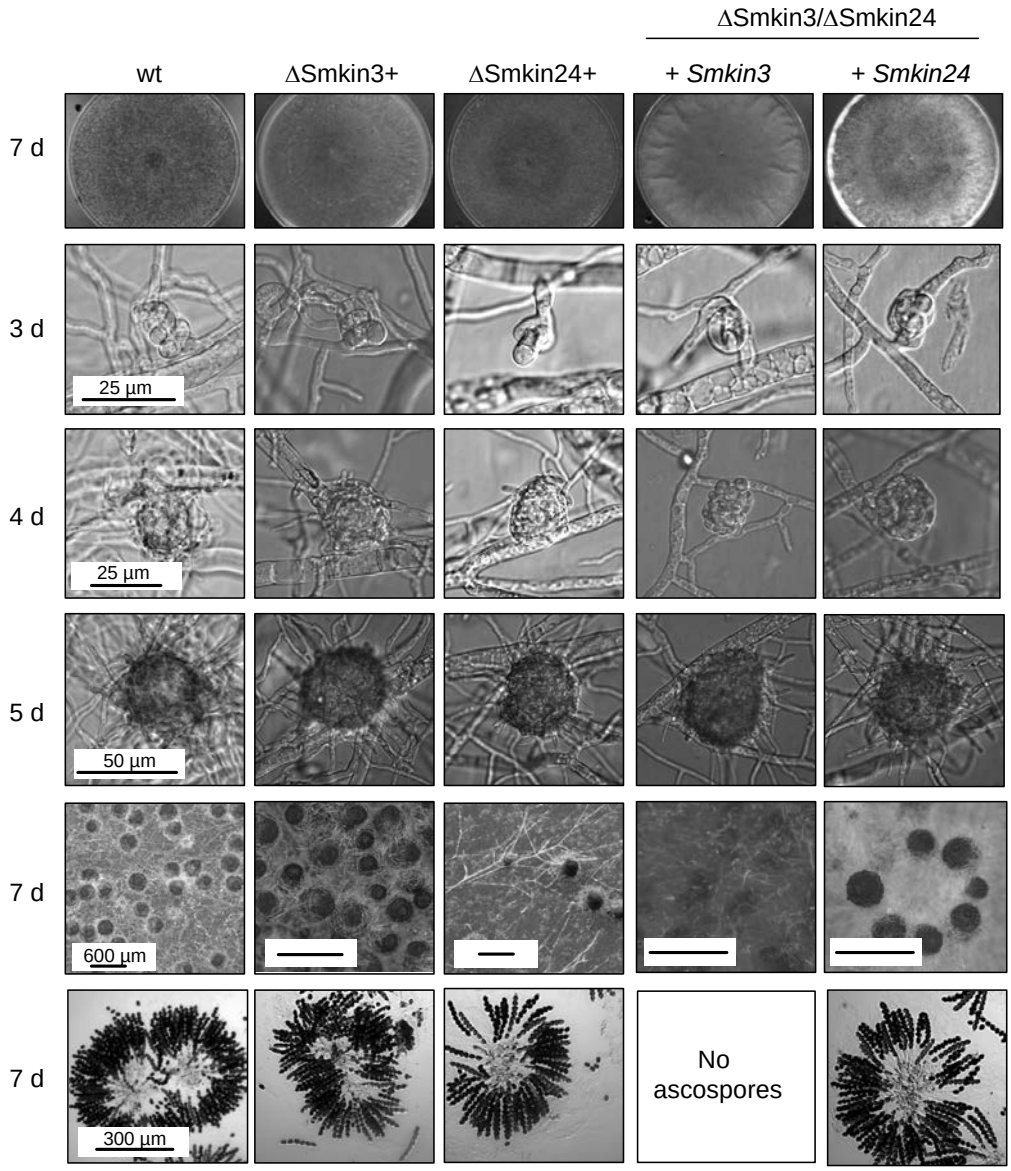

Figure 43. Macroscopic and microscopic analysis of the sexual development of wt, complemented ΔSmkin3 (ΔSmkin3+), complemented ΔSmkin24 (ΔSmkin24+) and partially complemented ΔSmkin3/ΔSmkin24. The wt strain produces ascogonia after 3 days which develop to unpigmented protoperithecia at day 4 and pigmented protoperithecia at day 5. After 7 days mature perithecia with asci and ascospores are formed. Similar to the wt ΔSmkin3+ and ΔSmkin24+ and ΔSmkin3/ΔSmkin24 + *Smkin24* completed the lifecycle within 7 days and produced mature ascospores. Development of ΔSmkin3/ΔSmkin24 + *Smkin3* is arrested at stage of late protoperithecia formation, similar to ΔSmkin24. Scale bars as indicated.

The double-deletion strain was generated by crossing the single deletion strains, and ΔSmkin3/ΔSmkin24 exhibited a phenotype that was a combination of the phenotypes of both single deletion strains (sterility and increased aerial hyphae on solid SWG medium). Each of the described phenotypes could be complemented by inserting a copy of the deleted gene ectopically as shown in Figure 43.

Sterility of STRIPAK mutants pro11, pro22 and ΔSmmob3 is accompanied by defects in hyphal fusion (Bernhards & Pöggeler, 2011, Bloemendal *et al.*, 2012). However, in contrast with these previously characterized mutants, fusion of vegetative hyphae was not affected in ΔSmkin3 and ΔSmkin24 (Figure 44). Furthermore, deletion of *Smkin3* and *Smkin24* impaired vegetative growth of *S. macrospora*: Growth velocity experiments revealed that ΔSmkin3 (1.70 ± 0.24 cm/d), ΔSmkin24 (1.82 ± 0.41 cm/d) and ΔSmkin3/ΔSmkin24 (1.54 ± 0.28 cm/d) grew more slowly than wt (3.09 ± 0.37 cm/d) (Figure 44).

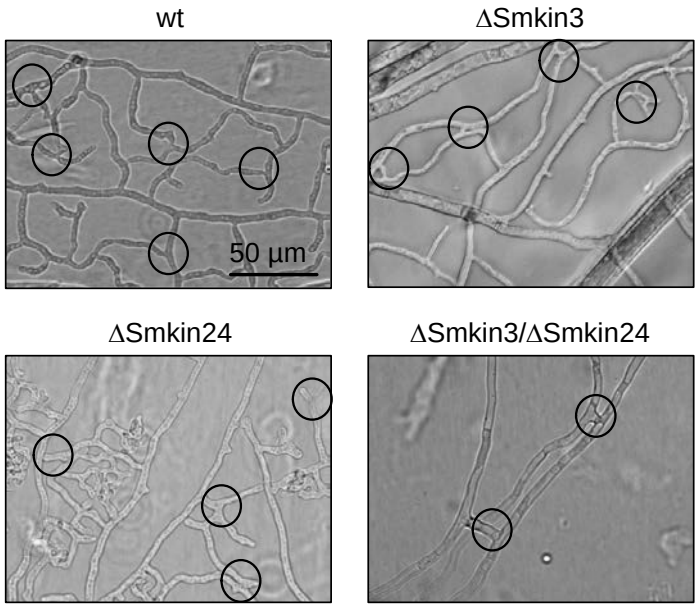

Figure 44. Microscopic investigation of hyphal fusion in wt, ΔSmkin3, ΔSmkin24 and ΔSmkin3/ΔSmkin24. ΔSmkin3, ΔSmkin24 and ΔSmkin3/ΔSmkin24 are capable of hyphal fusion. Hyphal fusion events are highlighted with circles. Pictures of hyphal fusion events were taken at subperiphal regions 10 mm behind the growth front. Hyphal-fusion was investigated 2-3 days past inoculation.

Furthermore, the deletion of *Smkin3* and *Smkin24* impairs vegetative growth of *S. macrospora*. Measuring growth velocity in race tubes over ten days revealed that ΔSmkin3 (1.70 ± 0.24 cm/d), ΔSmkin24 (1.82 ± 0.41 cm/d) and ΔSmkin3/ΔSmkin24 (1.54 ± 0.28 cm/d) display a reduced growth velocity than wt (3.09 ± 0.37 cm/d).

3.2.4 SmKIN3 and SmKIN24 localize to septa and influence septum formation

In order to determine the localization of SmKIN3 and SmKIN24 *in vivo*, fluorescence microscopy was performed. Genes coding N-terminally eGFP-tagged full-length SmKIN3 or SmKIN24 were expressed in the respective *S. macrospora* deletion strains, which show that both kinases were localized at the septa (Figure 45). However SmKIN3 was localized mainly at the outer part of the septum, whereas SmKIN24 was localized at the middle (Figure 45) and this was verified by co-staining with calcofluor white (Figure 45).

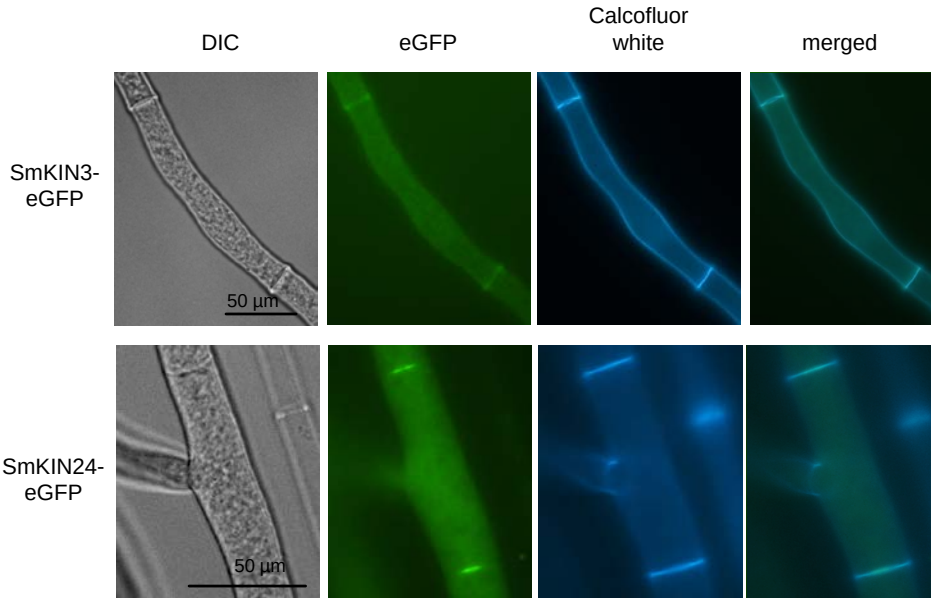

Figure 45. Localization of SmKIN3-eGFP and SmKIN24-eGFP in *S. macrospora*. SmKIN3-eGFP and SmKIN24-eGFP localize to septa. For visualization of cell walls and septa, hyphae were co-stained with calcofluor white. Scale bars as indicated.

These findings lead us to quantify septum formation in the ΔSmkin3, ΔSmkin24 and ΔSmkin3/ΔSmkin24 strains by staining with calcofluor white after 18 or 32 h of growth (Figure 46).

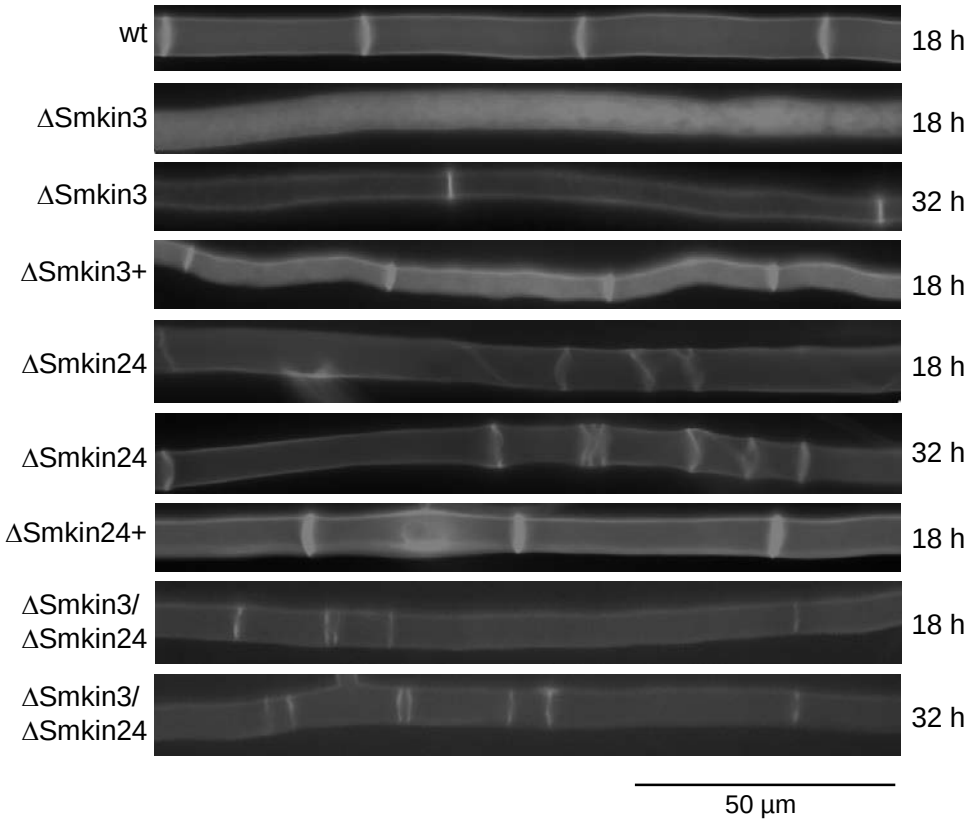

Figure 46. Analysis of septal development in wt, ΔSmkin3, ΔSmkin24 and ΔSmkin3/ΔSmkin24 and complemented mutants. Distribution of septa was investigated under the microscope after 18 h and 32 h past inoculation. Septa were stained with calcofluor white.

Furthermore, we quantified the distances between adjacent septa in wt and deletion mutants after 24 h of growth (Figure 47). Septa were distributed in a uniform manner in wt with hyphal compartment length between 31-70 µm (Figure 47). In contrast ΔSmkin3 exhibited larger distances between adjacent septa (>71 µm), although this effect begun to revert after 24 h of growth (Figure 46). Strikingly, ΔSmkin24 developed numerous closely-packed septal bundles of abnormal shape, with much smaller hyphal compartments of 0-30 µm (Figure 47). ΔSmkin3 produced about half the total number of septa within a distance of 18 mm than wt, while ΔSmkin24 produced 20% more than wt after 24 h of growth. With respect to septation, the double deletion mutant ΔSmkin3/ΔSmkin24 displayed a similar phenotype to the ΔSmkin24 single deletion strain. Ectopic integration of the respective wt gene into deletion mutants restored septal formation to wt level (Figure 46 and Figure 47).

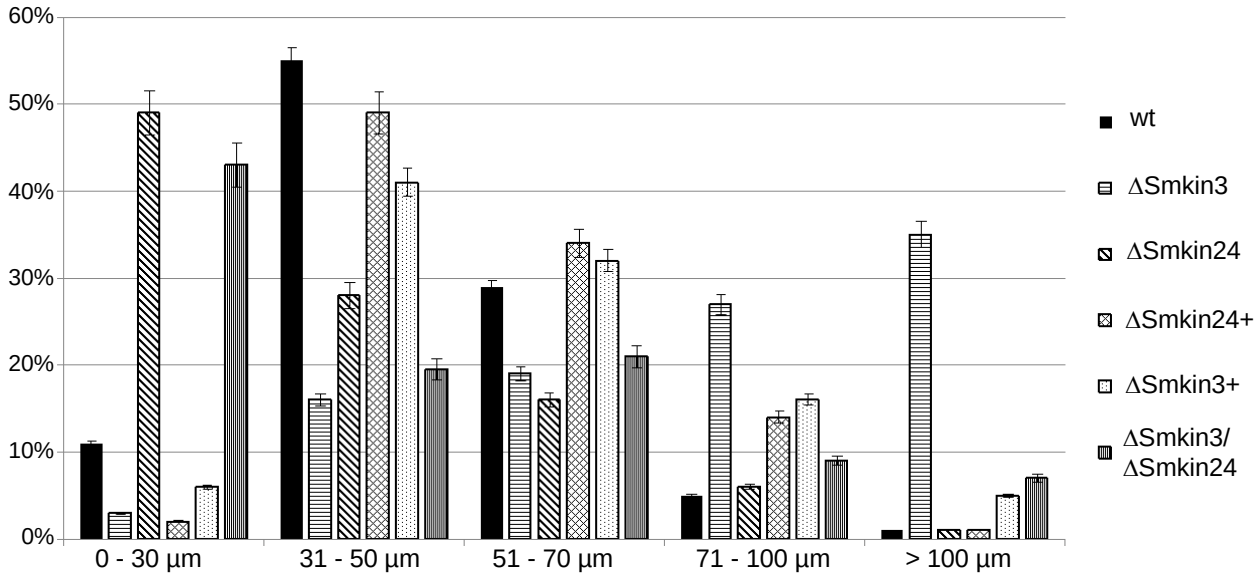

Figure 47. Quantitative analysis of septal development in wt, ΔSmkin3, ΔSmkin24 and ΔSmkin3/ΔSmkin24 and complemented mutants. For quantification, distances between adjacent septa were measured over a distance of 18 mm per strain 24 h past inoculation. The total distance of 18 mm was divided into 30 segments of 600 µm. Measurements were binned into five different compartment lengths: 0-30 µm, 31-50 µm, 51-70, 71-100 mm, and more than 100 µm. The number of analysed compartments was normalized to 100%. Error bars (SD) are given as indicated (n=30). ΔSmkin3+, ΔSmkin24+ complemented mutants carrying an ectopic copy of the respective wt gene.

3.2.5 ΔSmkin3 protoplasts recover significantly faster than wt protoplasts

We observed an increased growth rate in ΔSmkin3 protoplasts compared to wt, therefore we isolated protoplasts from wt, ΔSmkin3, ΔSmkin24 and ΔSmkin3/ΔSmkin24 strains using a previously described protocol (Nowrousian *et al.*, 1999, Pöggeler *et al.*, 1997) and adjusted the protoplast concentration to 4 x 10^4 protoplasts/ml. The protoplasts were spread on solid complete medium with 10.8% saccharose (CMS) (Nowrousian *et al.*, 1999) and microscopically and macroscopically analyzed after 24, 4 and 72 h of growth (Figure 48). After 24 h, wt protoplasts developed a slightly branched mycelium expanded further after 48 h (Figure 48). Mycelia were only faintly visible without magnification on agar plates after 72 h. Regeneration of protoplasts from ΔSmkin24 resembled those of wt. In contrast, protoplasts from ΔSmkin3 and ΔSmkin3/ΔSmkin24 recovered markedly faster within the first days than wt and mycelia generated by ΔSmkin3 protoplasts were much denser and clearly visible with the naked eye after 72h. Increased aerial hyphae were also present with ΔSmkin3 and this effect was complemented

by ectopically integrated wt copy of *Smkin3* in the ΔSmkin3 mutant (Figure 48). The accelerated growth rate of ΔSmkin3 vegetative mycelium disappeared after five days.

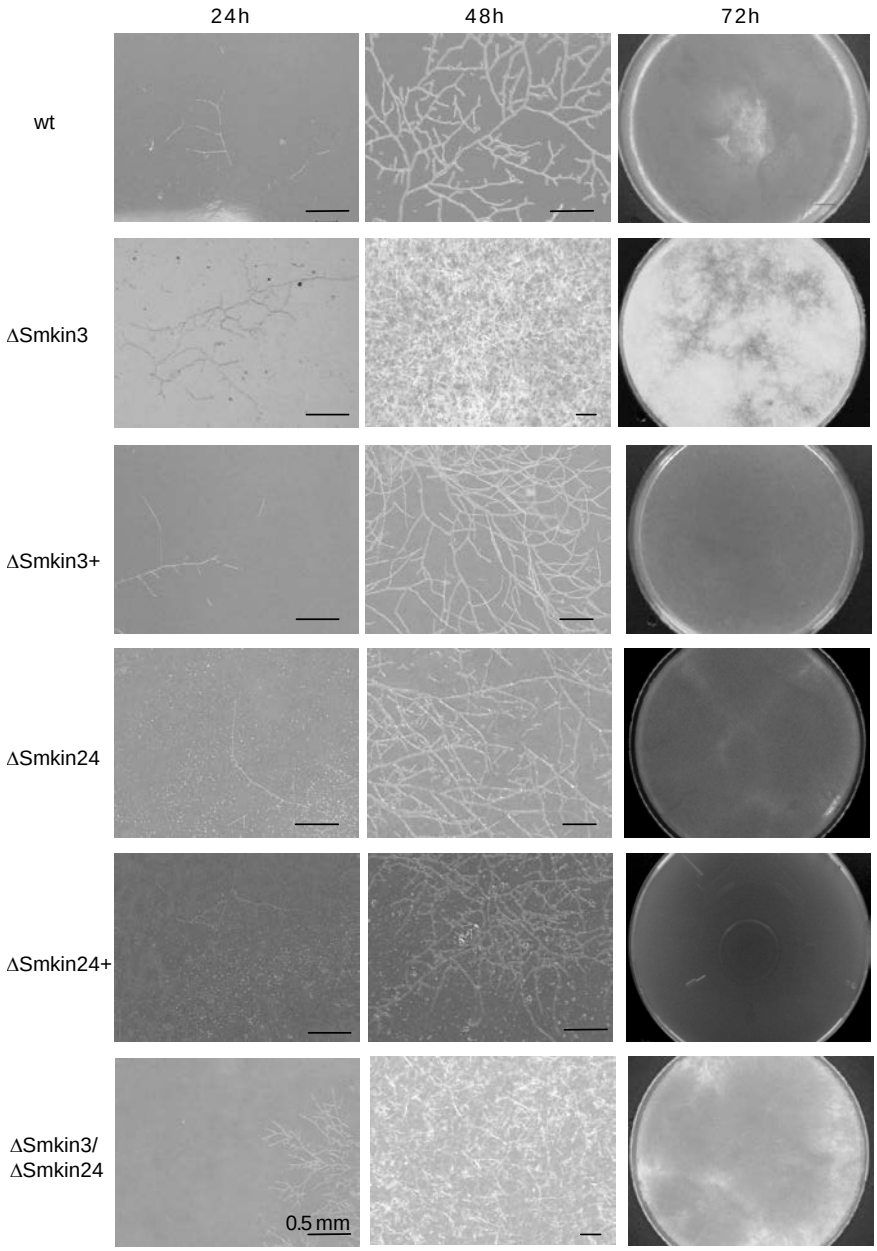

Figure 48. Investigation of protoplast recovery and vegetative growth of ΔSmkin3, ΔSmkin24 and ΔSmkin3/ΔSmkin24. Protoplasts of the respective strains were obtained as described by Nowrousian *et al.* (1999) and spread on solid CMS agar plates. Microscopic pictures were taken after 24 h, 48 h past inoculation, pictures of agar plates 72 h past inoculation. Compared to wt, protoplasts obtained from ΔSmkin3 and ΔSmkin3/ΔSmkin24 recovered and grew faster within the first 2-3 days. Recovery and vegetative growth of protoplasts obtained from ΔSmkin24 is equal to wt ΔSmkin3+, ΔSmkin24+ complemented mutants carrying an ectopic copy of the respective wt gene. Scale bars as indicated.

4. Discussion

In animals and fungi, STRIPAK and STRIPAK-like complexes are implicated in various cellular processes such as signaling, cell-cycle control, apoptosis, vesicular trafficking, Golgi assembly, cell polarity, cell migration and fusion, neural development and cardiac function (Hwang & Pallas, 2014). In the filamentous ascomycete *S. macrospora*, the STRIPAK-like complex contains the Striatin homolog PRO11, the STRIP1/2 homolog PRO22, the SLMAP homolog PRO45, the phocein homolog SmMOB3 and structural and catalytic subunits of the protein phosphatase PP2A. Components of the STRIPAK complex are required for *S. macrospora* sexual differentiation and cell fusion (Bernhards & Pöggeler, 2011, Bloemendal *et al.*, 2012, Bloemendal *et al.*, 2010, Pöggeler & Kück, 2004, Nordzieke *et al.*, 2014).

4.1 The GPI-anchored protein SmGPI1

4.1.1 SmGPI1 is a GPI-anchored protein

SmGPI1 was first discovered in a Y2H screen using SmMOB3 as bait. *In silico* analysis of SmGPI1 using SignalP (Petersen *et al.*, 2011) and big-PI Predictor (Eisenhaber *et al.*, 1998, Eisenhaber *et al.*, 1999, Eisenhaber *et al.*, 2000, Sunyaev *et al.*, 1999) revealed a putative signal sequence and a region for GPI-anchor attachment (Figure 12). Posttranslational attachment of the GPI-glycolipid at the C-terminus of proteins generally results in anchoring to the plasma membrane outer leaflet (Fujita & Kinoshita, 2012, Singh *et al.*, 2011). The signal sequence is necessary, because synthesis and attachment of the GPI-anchor occur in the ER. Many proteins have been shown to contain a signal sequence for ER translocation, which generally consists of 5-30 aa at the N-terminus of proteins (Rapoport, 2007, Blobel & Dobberstein, 1975). Signal sequences tend to form a single alpha-helix (Rapoport, 2007). Further *in silico* analysis with Quick_2D (Biegert *et al.*, 2006) predicted a single alpha-helix for SmGPI1s putative signal sequence. Moreover, the putative signal sequence of SmGPI1 has been shown to be sufficient to transport eGFP to the ER and in case of an added ER-retention signal, to remain there. Thus, the signal sequence is functional (Figure 18). In contrast to proteins with other destinations after ER translocation, GPI-anchored proteins have a structured region for GPI-anchor attachment.

Analysis of various GPI-anchored proteins revealed that the region for GPI-anchor attachment generally share identical features; it consists of an ω-residue for GPI-anchor attachment, a polar spacer region between ω+3 to ω+9 and a hydrophobic tail from ω+10 to the C-terminal end of the protein (Caro *et al.*, 1997, De Groot *et al.*, 2003, Mayor & Riezman, 2004, Pierleoni *et al.*, 2008). The presence of small side chain residues at position ω+1, ω+2 and ω+3 is assumed to be necessary for transamidase cleavage (Pierleoni *et al.*, 2008). The ω-residue of SmGPI1 is predicted to be aa 228, aa ω+1 is arginine, ω+2 is alanine and ω+3 is serine; alanine and serine are small side-chain aa. However, aa ω+1 is arginine, which is a large aa. The polar spacer of SmGPI1 at position ω+3 to ω+10 has the aa sequence SSKRGFTG and thus, contains indeed with serine, threonine and glycine 50% polar aa. Regarding the fact that two polar aa particularly enclose the polar region it is likely, that residue ω+10 is also part of the polar spacer. Residues ω+11 to ω+25 represent with the sequence LLVAAVVVATVSGLL the hydrophobic tail. This aa sequence contains with leucine, valine and alanine about 87% hydrophobic aa (Figure 12). It was shown, that deletion of the region for GPI-anchor attachment of SmGPI1 impaired localization to the cell wall or membrane of the cell (Figure 16). Moreover, inspection of SmGPI1s aa sequence showed a sequence pattern similar to previously identified CFEM (common in several fungal extracellular membrane proteins) domains. These domains are primarily found in fungal GPI-anchored proteins bound to cell walls. CFEM domains are approximately 60 aa long and contain 8 spaced cysteine residues usually near the N-terminus of the respective protein (Vaknin *et al.*, 2014, Kulkarni *et al.*, 2003). SmGPI1 exhibits 14 cysteine residues, which are conserved among SmGPI1-orthologs in ascomycetes (Figure 13). Thus, it is likely, that these residues have a function similar to these of the CFEM domains. In addition, each predicted ortholog has a putative signal sequence and a putative region for GPI-anchor attachment, but these differ in their sequence. SmGPI1 is not homologous to the recently described *N. crassa* GPI-anchored protein HAM-7, which is involved in fruiting-body formation and hyphal fusion (Fu *et al.*, 2011, Maddi *et al.*, 2012).

4.1.2 SmGPI1 is a dual targeted protein

GPI-anchored proteins normally localize to the outer leaflet of the plasma membrane (Fujita & Kinoshita, 2012, Singh *et al.*, 2011). In *S. cerevisiae*, the region ω-1 to ω-5 can support membrane localization (Caro *et al.*, 1997, Frieman & Cormack, 2003, Hamada *et al.*, 1999,

Stefanova *et al.*, 1991). Moreover, GPI-anchored proteins in ascomycetes can also be covalently bound to the cell wall (Gilbert *et al.*, 2012). The switch between localization to the membrane or cell wall depends among other factors, on the presence or absence of dibasic residues at position ω-1 or ω-2 (Stefanova *et al.*, 1991, Ouyang *et al.*, 2013). Absence of dibasic residues at position ω-1 and ω-2 support localization of the anchored protein to the cell wall (Stefanova *et al.*, 1991, Ouyang *et al.*, 2013). Fluorescence microscopy and Western blot analysis of eGFP-tagged SmGPI1, however, showed localization at the plasma membrane or cell wall, a fluorescence pattern similar to mitochondrial localization and partial secretion (Figure 16, Figure 18 and Figure 19).

A high content of serine and threonine residues in GPI-anchored proteins was shown to support cell-wall attachment of GPI-anchored proteins, approximately 70% of *S. cerevisiae* cell-wall bound GPI-anchored proteins contain more than 30% serine/threonine residues (Frieman & Cormack, 2004).

Sequence analysis of SmGPI1 revealed a serine/threonine content of 20% in total, compared to the average in proteins of 7.6% for serine and 6% for threonine (Bruice, 2004), the serine content of SmGPI1 (12.7%) but not the threonine (7.2%) is significantly increased. These results indicate that the final destination of GPI-anchored proteins is mediated by several factors. For example, De Sampaio *et al.* (1999) showed for the glucanosyltransferase GAS1p in *S. cerevisiae* localization to the cell wall, although it contains a dibasic residue at position ω-1 and ω-2. SmGPI1-eGFP localizes to structures, resembling the plasma membrane or the cell wall (Figure 19). Moreover, after differential centrifugation, SmGPI1 was mainly found in the cell detritus, but in case of deletion of the predicted region for GPI-anchor attachment, it appears mainly in the cytosol (Figure 16). The cell detritus contained remnants after early centrifugation, such as parts of the cell wall. Thus, the region containing the ω-residue might be crucial for localization of SmGPI1 to the outer leaflet of the plasma membrane. This data is also supported by eGFP localization of SmGPI1 without the GPI-anchor attachment region (Figure 19), which was no longer present at the cell wall or membrane (Figure 19). These findings are consistent with many studies, made with other organisms. Ouyang *et al.* (2013) showed recently that only the signal sequence and the region for GPI-anchor attachment comprising ω-10 to the C-terminal end of cell-wall protein Mp1p, glucanosyltransferase Gel1 and Ecm33, which function in maintaining fungal cell-wall integrity and virulence, are sufficient for proper localization to the cell

membrane or the cell wall. In their experiments, they fused the respective signal sequences and omega regions to eGFP and thus, mediated eGFP localization to the cell wall and membrane. In contrast to De Sampaio *et al.* (1999), Ouyang *et al.* (2013) showed that mutation of the residues ω-1 and ω-2 can alter the protein localization. *Cryptococcus neoformans* chitin deacetylase 2 is an enzyme that converts chitin to chitosan and is an established virulence factor for *C. neoformans* infection. Gilbert *et al.* (2012) showed that the protein is bound to membranes and non-covalently associated to cell walls. Interestingly, cell wall association was independent from its GPI-anchor.

SmGPI1 full-length protein also appears in the cell-free medium (Figure 18). Deletion of its omega region not only impairs cell-wall localization, but slightly decreases secretion of the protein. Secretion of GPI-anchored proteins in general is well documented (Low, 1989, Mayor & Riezman, 2004, Paulick & Bertozzi, 2008). Djordjevic *et al.* (2005) showed that *C. neoformans* virulence factor phospholipase B1 localizes (Plb1) to the cell wall, membrane structures and was also detectable in the cell-free medium. Furthermore, that this localization pattern was GPI-anchor dependent. Similar to SmGPI1, deletion of the GPI-anchor led to an increased secretion of the protein. Moreover, SmGPI1 was shown to localize to structures resembling mitochondria (Figure 19). This was confirmed by co-staining with MitoTracker Red and likely caused the signal detected for the membrane fraction after differential centrifugation (Figure 16). In eukaryotes, dual targeting of a single proteins to more than one subcellular compartment is well documented (Raza, 2011, Ben-Menachem *et al.*, 2011, Dinur-Mills *et al.*, 2008, Yogev *et al.*, 2011). These examples include GPI-anchored proteins such as *S. cerevisiae* β-1,3-glucanosyltransferase GAS1, which plays as a GPI-anchored cell-wall protein a role in the formation and maintenance of the cell wall and when targeted to the nucleus, in regulation of transcriptional gene silencing and rDNA stability. When targeted to the cell wall, GAS1 elongates and arranges 1,3-glucan side chains, which are linked to glucan, chitin and proteins, and in sum, form the main layer of cell walls. The sub population of GAS1 detected in the nucleus interacts with the histone deacetylase SIR2 and increases rDNA silencing in a SIR2-dependent manner (Koch & Pillus, 2009, Bauer *et al.*, 2014). Pfeiffer *et al.* (2013) demonstrated that ER signal peptides of the GPI-anchored prion-like Shadoo, the neuropeptide hormone somatostatin, and the amyloid precursor protein mediate alternative targeting to mitochondria. This effect is mediated by structural features within the nascent chain; the signal sequences of

each protein promotes proper ER import of the nascent chain containing alpha-helical domains, but unstructured polypeptides are targeted to mitochondria. Increased transport to mitochondria causes unproductive transport to the ER lumen, and *vice versa*. By this, they presented a novel mechanism of dual targeting of proteins to the ER or mitochondria, facilitated by structural features in the nascent chain.

In silico analysis using GlobPlot2 (Linding *et al.*, 2003) revealed extended intrinsic disorder regions within SmGPI1 (Figure 49). The signal sequence of SmGPI1 seemed to be necessary for mitochondrial localization because N-terminally eGFP-tagged SmGPI1 (data not shown) and SmGPI1 with its first 27 aa deleted led to a diffuse localization to the cytosol. In contrast, removal of the C-terminal GPI-signal sequence slightly increased mitochondrial localization (Figure 19).

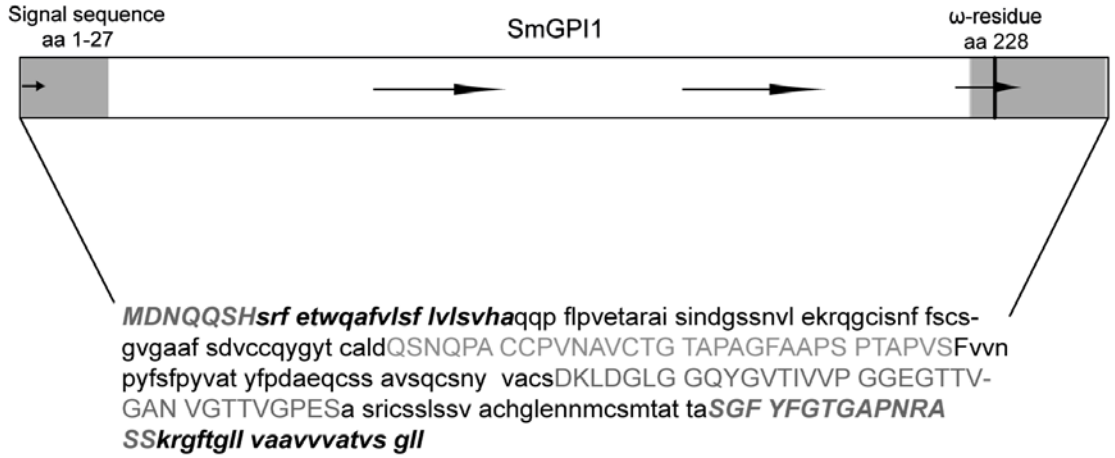

Figure 49. SmGPI1 exhibits regions of disorder. Shown is the protein precursor aa 1-253. The omega residue is marked in black. Grey boxes and italic letters in the aa sequence below represent N-terminal and C-terminal signal sequences. Arrows and grey capital letters in the aa sequence below represent disorder regions predicted by GlobPlot2 (Linding *et al.*, 2003).

Similarly, Pfeiffer *et al*. (2013) showed that loss of the C-terminal GPI-signal sequence interferes with efficient ER import and increased mitochondrial import of mammalian GPI-anchored prion proteins. In this study was shown, that the C-terminal alpha-helical structure of Shadoo, which lies within the region for GPI-anchor attachment, can mediate ER import of the intrinsically disordered protein. *In silico* analysis with Quick_2D (Biegert *et al.*, 2006) predicted for SmGPI1

a single alpha-helical structure at the C-terminus. However, deletion of the C-terminal signal sequence of SmGPI1 did not completely impaired secretion but changed localization to the cell wall as shown by differential centrifugation and fluorescence microscopy (Figure 16 and Figure 19). The summarized mechanism of dual targeting of SmGPI1 in *S. macrospora* is shown in Figure 50.

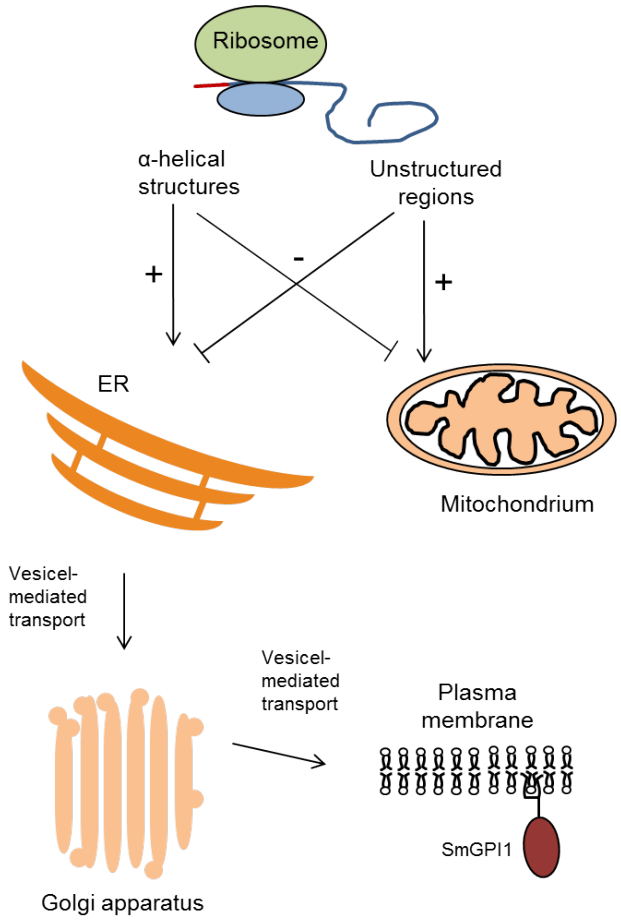

Figure 50. Dual targeting of SmGPI1 in *S. macrospora.* Features within the nascent chain determine the destination of SmGPI1, which is targeted to the cell wall and the mitochondria. Alpha-helical regions within the nascent chain facilitate transport to the ER and inhibit targeting to the mitochondria. Unstructured regions within the nascent chain regulate this process *vice versa*. For localization to the cell wall, the protein precursor is processed in the ER and transported via vesicles to the final destination. Based on the model presented by Pfeiffer *et al.* (2013).

4.1.3 STRIPAK protein SmMOB3 interacts physically with SmGPI1

The GPI-anchored protein SmGPI1 was first identified as an interaction partner of SmMOB3 in a Y2H screen using a *N. crassa* cDNA library (Bernhards, 2010). This interaction was verified using *S. macrospora* cDNA and in a Y2H as well as by means of co-IP (Figure 14 and Figure 15), defined as a 144 aa N-terminal region of SmMOB3 and a 100 aa N-terminal region of SmGPI1. This region of SmMOB3 has recently shown to physically interact with the WD domain of Striatin homolog PRO11 in *S. macrospora* (Bloemendal *et al.*, 2012). Since SmMOB3 was shown not to homodimerizes, it was suggested that the predicted alpha-helix of SmMOB3 mediates the SmMOB3-PRO11 interaction (Bernhards, 2010). Regarding that MOB3 interacts with several proteins via its N-terminus, it is possible that interaction between SmMOB3 and PRO11 might alter SmMOB3-SmGPI1 binding and *vice versa*. This could be further investigated by co-IP analysis of SmMOB3-PRO11 interaction in strains with ΔSmgpi1 background compared to strains with wt background. Or, more appropriate, measuring binding kinetics of PRO11-SmMOB3 interaction *in vitro* before and after adding SmGPI1. Moreover, it would be interesting to analyze if these proteins exist in a tertiary complex, to gain a better understanding about the function of SmGPI1-SmMOB3 interaction.

As mentioned above, the final destination of fungal GPI-anchored proteins is the plasma membrane or the cell wall (Ouyang *et al.*, 2013), but fungal MOB3/phocein homologs do not contain transmembrane domains (Maerz *et al.*, 2009, Bernhards & Pöggeler, 2011). Therefore, localization of SmGPI1 and SmMOB3 suggested that physical interaction of the proteins is prevented by their presence in different cell compartments. However, *N. crassa* MOB3 localizes at the nuclear envelope. This process requires HAM-2 (PRO22 homolog) and HAM-3 (PRO11 homolog) for membrane localization (Dettmann *et al.*, 2013). Similarly, in *S. macrospora*, eGFP-tagged SmMOB3 was detected at the nuclear envelope and in diffuse cytosolic patches (Figure 20).

Nordzieke *et al.* (2014) recently demonstrated that PRO45, a homolog of the mammalian STRIPAK core component SLMAP, interacts with PRO11 and SmMOB3 in *S. macrospora*. Moreover, PRO45 localizes at the mitochondria, showing that STRIPAK proteins in *S. macrospora* are mitochondria-associated (Nordzieke *et al.*, 2014).

Mammalian SG_2NA was detected in multiple cellular compartments including the plasma membrane, ER and mitochondria. SG_2NA was shown to recruit protein kinase B (Akt) and the

antioxidant protein DJ-1 into mitochondria and membranes (Tanti & Goswami, 2014). Since SmMOB3 is a strong interaction partner of the *S. macrospora* Striatin homolog PRO11 (Bernhards & Pöggeler, 2011, Bloemendal *et al.*, 2012), one hypothesis is that PRO11 might mediate also SmMOB3 translocation to the mitochondria, where SmGPI1 was also shown to localize (Figure 19).

Under these conditions, portions of SmGPI1 and SmMOB3 share a common sub-cellular localization that allows direct physical interaction. This hypothesis could be further proved by isolation of mitochondria in strains, expressing tagged versions of SmGPI1 and SmMOB3 combined with Western blot analysis.

4.1.4 SmGPI1 is a positive regulator of fruiting-body number

In filamentous fungi, the development of multicellular fruiting bodies requires highly conserved differentiation processes and is essential for sexual reproduction (Pöggeler & Kück, 2006). Various proteins function directly or indirectly in this process to determine the structure of the multicellular tissue of the fruiting bodies (Lord & Read, 2011). In *S. macrospora*, deletion or mutation of genes encoding STRIPAK-associated proteins such as PRO11, PRO22, PRO45 or SmMOB3 cause sterility and thus, have a high impact on fruiting-body development (Bernhards & Pöggeler, 2011, Bloemendal *et al.*, 2012, Bloemendal *et al.*, 2010, Nordzieke *et al.*, 2014, Pöggeler & Kück, 2004). Interestingly, all these mutants are capable of forming protoperithecia, suggesting that the main regulation of fruiting-body formation occurs after day three of development. In contrast, deletion of *Smgpi1* did not lead to sterility, but increased the number of fruiting bodies although they were slightly reduced in size (Figure 30, Figure 31 and Figure 32). The deletion mutant completed the life cycle similar to wt after 7 days (Kück *et al.* 2009). This result suggested that SmGPI1 functions as a negative regulator of perithecia number and likely also as a positive regulator of perithecia size. Thus, SmGPI1 functions in this process but is not crucial for fertility and proper fruiting-body development. These results are confirmed by findings, that *Smgpi1* overexpression decreased the number of perithecia per cm^2 but these were slightly larger (Figure 32). Schindler & Nowrousian (2014) previously reported about the *S. macrospora* polyketide synthase gene *pks4*. Deletion of the respective gene causes a developmental arrest at the stage of protoperethecia formation, but overexpression resulted in mount-like fruiting bodies, which kept growing even after 14 days, whereas perithecia growth in

wt stops after 7 days. These mount-like fruiting bodies did not contain an increased number of ascospores, which is consistent with findings for ΔSmgpi1. Although, the perithecia of ΔSmgpi1 were slightly smaller in this mutant, they contained equal numbers of spores compared to wt (Figure 31). In *S. macrospora*, energy and nutrients required to form multicellular fruiting bodies are at least partially supplied by the mycelium (Nowrousian *et al.*, 1999, Voigt & Pöggeler, 2013). The increased number of fruiting bodies of deletion mutant ΔSmgpi1 probably exhausted the mycelium and resulted in smaller perithecia. And referring to *Smgpi1* overexpression that fewer fruiting bodies were supplied with more nutrients and grew slightly larger. Finally, based on these data a model for fruiting-body development in *S. macrospora* could be hypothesized. An initial input or signal leads to development of first sexual structures. After this step, a major checkpoint is reached, involving several gene products directly or indirectly by their function in signaling pathways. Afterwards, protoperithecia develop further to mature fruiting bodies. During the process of ripening, tissue-size control is mediated by proteins like PKS4 and SmGPI1. Moreover, only full-length version of the *Smgpi1* could rescue perithecia number and size phenotypes, demonstrating that N-terminal and C-terminal signal sequences, and thus proper localization is required for SmGPI1 function in this process (Figure 30, Figure 31 and Figure 32).

4.1.5 *Smgpi1* deletion partially bypasses vegetative growth, hyphal fusion and fruiting-body development defects in ΔSmmob3

Deletion of *Smmob3* leads to sterility, reduced vegetative growth and defects in hyphal fusion in the filamentous ascomycete *S. macrospora* (Bernhards & Pöggeler, 2011). This is consistent with other phenotypes of STRIPAK-deletion strains, such as Δpro11, Δpro22 and Δpro45 (Bloemendal *et al.*, 2010, Bloemendal *et al.*, 2012, Nordzieke *et al.*, 2014). In contrast to this, deletion of *Smgpi1* does neither affect vegetative growth and hyphal fusion nor sexual development. (Figure 23). Interestingly, deletion of *Smgpi1* in a sterile ΔSmmob3 deletion background partially reverted the defects in vegetative growth, hyphal fusion and fertility and thus acted as an intergenic suppressor of *Smmob3* deletion. However, deletion of *Smgpi1* does not restore fertility of *S. macrospora* STRIPAK mutants Δpro11, Δpro22 and Δpro45 (Figure 25, Figure 26 and Figure 27). The gene *pro11* encodes the central STRIPAK component Striatin;

pro22 encodes the STRIP1/2 homolog, whereas PRO45 is homologous to STRIPAK component SLMAP. In *N. crassa*, PRO11 and PRO22 are essential for assembly and function of the STRIPAK complex at the nuclear envelope. MOB3 and HAM-4/PRO45 are only peripheral subunits of the complex (Dettmann *et al.*, 2013). Thus, genetic interaction between *Smgpi1* and *Smmob3* is specific since even the deletion phenotype of a second peripheral subunit of the STRIPAK complex could not be bypassed by *Smgpi1* deletion.

Thus, the impact of *pro11* and *pro22* deletion on developmental processes in *S. macrospora* occurs in many ways compared to SmMOB3. The summarized findings offer for SmMOB3-SmGPI1 interplay the model that SmMOB3 amplifies an incoming signal and SmGPI1 negatively regulates the SmMOB3-dependent signal required for fruiting-body development (Figure 51). The signal is probably derived from the cell wall, the plasma membrane or mitochondria and is transmitted to the STRIPAK complex, which modulates it further. Direct interaction between intracellularly localized SmGPI1 and SmMOB3 might modulate the signal or SmGPI1 in the plasma membrane or cell wall compartment might interact with undefined transmembrane proteins that transduce the signal. Referred to the different phenotypes of ΔSmgpi1 and ΔSmmob3 single- and double-deletion strains, we assume the following scheme: in the ΔSmgpi1 mutant, the incoming signal is amplified, resulting in an increased number of fruiting bodies. In ΔSmmob3, the signal negatively regulated by SmGPI1 is too weak to activate the SmMOB3-depleted STRIPAK complex. In the double-deletion mutant, the amplified signal is sufficient to activate the SmMOB3-depleted STRIPAK complex and fruiting-bodies develop although fewer than in the wt, caused by absence of the negative regulator SmGPI1 (Figure 51). Similar to the above mentioned regulation, SmGPI1 might not only negatively regulate fruiting-body formation, but also hyphal fusion and vegetative growth. Thus, it seems that SmMOB3 and SmGPI1 are regulators of developmental processes in *S. macrospora.* To further elucidate this, we have to increase our knowledge about the genetic interplay of signaling pathways, which in sum, might function as major regulators of fundamental processes. The interesting question that remains is, why does deletion of *Smgpi1* in a sterile ΔSmmob3 background reclaim aside of fruiting-body development, also hyphal fusion and vegetative growth? The model outlined in Figure 51 explains only the bypassed sterility. This is based on data, that SmGPI1 functions in regulation of perithecia size and probably also in their number. However, ΔSmgpi1 does not grow faster than wt or tend to form more hyphal fusions. For these processes, the outlined model

seems not to be appropriate. One reason might be that proteins not involved in fruiting-body development function in this processes and down regulate hyphal fusion and vegetative growth to a level as present in wt.

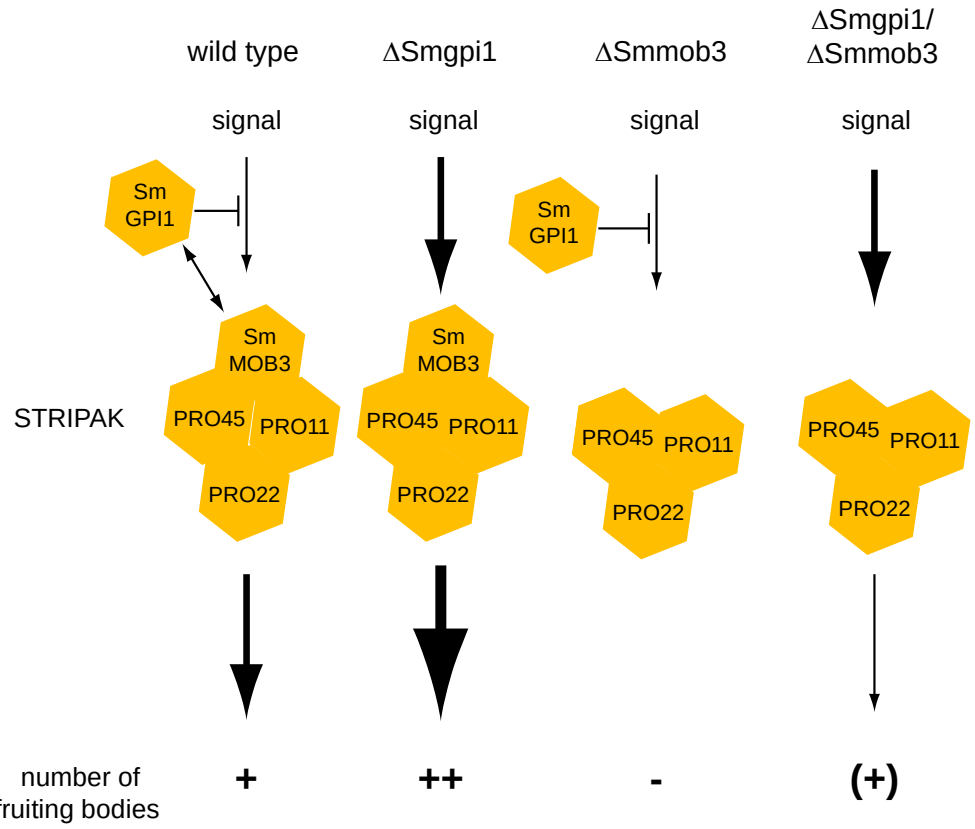

Figure 51. Schematic model of the genetic interplay between SmGPI1 and SmMOB3 and the STRIPAK complex in wt, single and double mutants. Double arrow indicates a direct physical interaction between SmGPI1 and SmMOB3. The thickness of arrows reflects the strength of the transmitted signal. Plus and minus symbols indicate the number of formed fruiting bodies

4.2 The GCKs SmKIN3 and SmKIN24

In mammals, the GCKs III MST4, STK24, STK25 and the GCK IV MINK1 are identified as components of the STRIPAK complex, but presence of STRIPAK-associated kinases has not yet been shown in filamentous fungi (1.3.1.4). To identify STRIPAK kinases in *S. macrospora* we performed a BLASTP search with the mammalian STRIPAK kinases MST4, STK24, STK25 and MINK1 against the *S. macrospora* genome. This identified SmKIN3 and SmKIN24 as putative homologs of mammalian STRIPAK-associated kinases.

4.2.1 Are SmKIN3 and SmKIN24 STRIPAK-associated kinases?

The N-terminal part of the mammalian STRIPAK kinases is conserved among ascomycetes (Figure 33). GCKs have their enzymatic active region at the N-terminus, whereas the kinase domain of PAKs is located C-terminally (Dan *et al.*, 2002, Delpire, 2009). Moreover, the phylogenetic allocation of MST4, STK24, STK25 and MINK1 with their orthologs in ascomycetes revealed two groups (SmKIN3-like and SmKIN24-like) of putative STRIPAK-associated GCKs in filamentous fungi (Figure 38). Thus, it seems that presence of these two GC kinases is conserved among ascomycetes. Interestingly, all identified putative homologs in yeast share the highest similarity with MINK1 except SID1 from *S. pombe*, which functions in the septation initiation network (SIN). The SIN is a signal transduction network required for proper coordination of mitosis and cytokinesis (Krapp & Simanis, 2008). *S. pombe* SID1 seems to share slight similarity with the SmKIN3-like group, represented by its branching directly before the SmKIN3-like group (Figure 38).

We showed interaction of SmKIN3 and SmKIN24 with PRO11 in an Y2H system (Figure 39) and interaction of SmKIN3 and PRO11 by means of co-IP (Figure 40). However, successful co-IP results required crosslinking and thus, indicate weak interaction. Since we were not able to overexpress *Smkin24* properly, we assume this to be lethal as previously described for other proteins (Hein *et al.*, 1997, Mahlert *et al.*, 2006). In *N. crassa*, the GCK III NcPRK-9 (SID-1) (homolog of SmKIN3) is part of the fungal SIN, whereas NcSTK-6 (MST-1, homolog of SmKIN24, hereafter NcSTK-6) has a dual role in SIN and the morphogenesis Orb6 network (MOR). Following cytokinesis the morphogenesis network MOR is essential for cell-polarity control and septum formation (Kanai *et al.*, 2005, Verde *et al.*, 1998, Heilig *et al.*, 2013, Heilig *et al.*, 2014). The GCK III NcSID1 (hereafter NcPRK-9) has been shown to phosphorylate DFB-2 and thus trigger its activity during SIN formation (Heilig *et al.*, 2013). The SmKIN24 homolog NcSTK-6 is needed for septal actomyosin ring formation and modulates MOR activity during septum formation in an antagonistic manner (Heilig *et al.*, 2014).

NcPRK-9 and NcSTK-6 both localize to the septa and spindle-pole bodies (SPB) (Heilig *et al.*, 2013, Heilig *et al.*, 2014). In *S. pombe*, SIN components bind to a coiled-coil scaffold SID4 (Morrell *et al.*, 2004). However, a clear homolog of the SIN scaffold SID4 has not been identified in ascomycetes so far (Heilig *et al.*, 2013). Based on interaction studies, STRIPAK PRO11 may serve as scaffold for SmKIN3 and SmKIN24 and thus we hypothesized also

interplay between STRIPAK and SIN in *S. macrospora*. This is supported by findings in fission yeast. SLMAP is a component of the mammalian STRIPAK complex (Goudreault *et al.*, 2009) (1.3.1.7). The fission yeast SLMAP homolog CSC1p was shown to negatively regulate SIN and promotes SIN asymmetry (Singh *et al.*, 2011). In addition, in *D. melanogaster* Ribeiro *et al.* (2010) showed that STRIPAK components negatively regulate HIPPO signaling, which is homologous to the fungal SIN network (Hergovich & Hemmings, 2012). The HIPPO pathway is a central element of tissue-size control in *D. melanogaster* and higher organisms. It consists of an upstream kinase HPO (MST1/2 in mammals), the tumor suppressor mob family protein MATS and respective scaffolding units (Wei *et al.*, 2007, Zhao *et al.*, 2011). Based on interaction of HPO with homologs of MOB3 and Striatin, the *D. melanogaster* STRIPAK complex was identified as the negative regulator of HIPPO signaling and HPO was determined as homolog of mammalian STRIPAK kinases MST4, STK24 and STK25 (Ribeiro *et al.*, 2010). A BLASTP analysis with HPO, MST1 and MST2 protein sequences revealed SmKIN3 and SmKIN24 as orthologs of these kinases in *S. macrospora* (data not shown). However, SmKIN3 and SmKIN24 did not interact with SmMOB3 in a Y2H (Figure 39). Recently, Dettmann *et al.* (2014) identified an interaction between NcSTK-6, the *N. crassa* homolog of SmKIN24, and components of the MAK-2 mitogen-activated protein kinases module (MAPKKK) NRC-1 and (MAPKK) MEK-2, involved in fungal communication between germinating spores (Dettmann *et al.*, 2012, Fleissner *et al.*, 2009). All three kinases of the MAK-2 MAPK module were shown to be weakly associated with STRIPAK components PP2A-A, PP2A-C, Striatin and MOB-3 in *N. crassa* (Dettmann *et al.*, 2014). Thus, STRIPAK components and the SmKIN24 homolog function together in at least one cascade in *N. crassa*. In mammals, CCM3 recruits the GC kinases MST4, STK24 and STK25 but not MINK1 to Striatin (Goudreault *et al.*, 2009, Gordon *et al.*, 2011, Kean *et al.*, 2011). However, a clear homolog of CCM3 has so far not been identified in ascomycetes. Thus, we assume that STRIPAK-associated kinases in *S. macrospora* are not recruited by other proteins to PRO11.

We showed that *Smkin24* is alternatively spliced and has at least 3 isoforms (Figure 35). This is consistent with the mammalian MST4, which also has 3 identified isoforms (Greenman *et al.*, 2007, Ota *et al.*, 2004, Qian *et al.*, 2001). The first three introns of *Smkin24* are localized at the region coding for the kinase domain. These three introns are conserved among ascomycetes (Data not shown). Possibly, expression of different SmKIN24 variants might serve for modified

substrate specificity as shown for other kinases (Wansink *et al.*, 2003) and thus, could help to explain a crosstalk between SIN and STRIPAK. The hypothesized crosstalk between SIN and STRIPAK is shown in Figure 52. However, interaction between PRO11, SmKIN3 and SmKIN24 should be verified by other methods to state these GCK III are clearly STRIPAK-associated kinases.

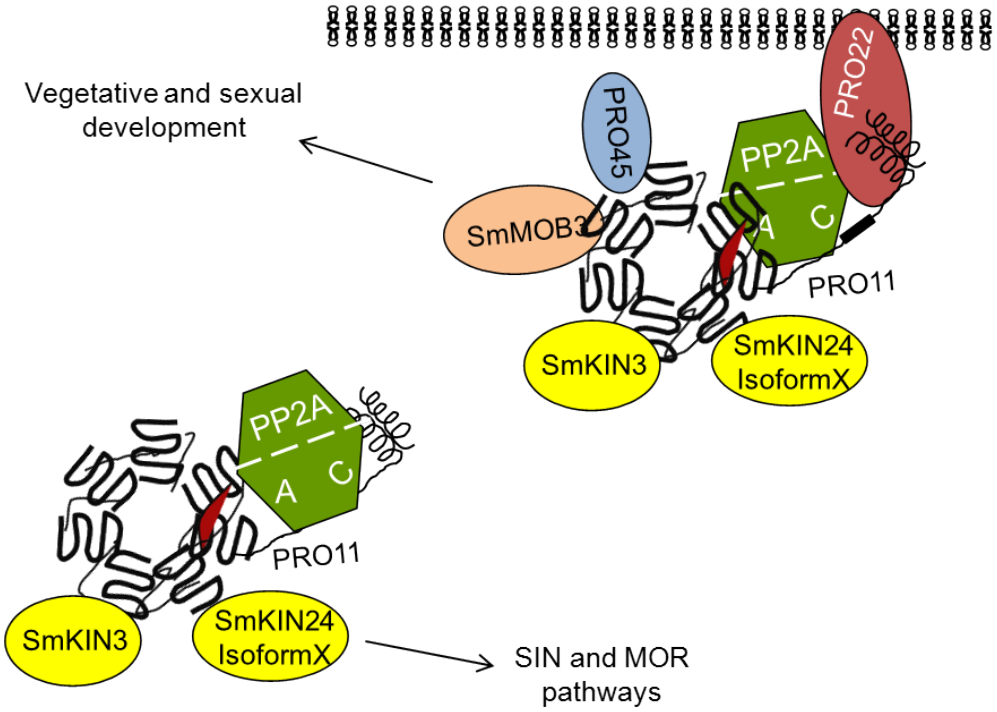

Figure 52. Schematic model for the interplay between STRIPAK and SIN in *S. macrospora*. SmKIN3 and SmKIN24 physically interact with PRO11, which functions as scaffold. Two subcomplexes are assumed, one containing PRO11, SmMOB3, PP2AA and PP2AC, PRO45, PRO22 and one or both kinases SmKIN3 and/or SmKIN24. This complex functions in vegetative and sexual development. The second complex contains PRO11, PP2AA and PP2AC and one or both kinases SmKIN3 and/or SmKIN24. This complex might function in SIN and MOR pathways.

The *N. crassa* homologs of SmKIN3 and SmKIN24 are components implicated in SIN and MOR pathways. Our data suggest an additional role of these GC kinases shown by a possible interaction with *S. macrospora* Striatin homolog PRO11. To close this knowledge gap, the interaction between PRO11 and SmKIN3 or SmKIN24 has to be tested by other *in vivo* methods, e.g. bimolecular-fluorescence complementation coupled with high-resolution microscopy, which could also give more information about the localization of a possible interaction. In addition, interactome studies that are capable to identify also short time interaction partners will help

unravel how the crosstalk between signal pathways and their modulation by complexes is achieved.

4.2.2 SmKIN3 and SmKIN24 affect growth velocity, sexual development and septum formation

Deletion of *Smkin3* does not impair fertility but leads to an increased formation of aerial hyphae and reduced growth velocity. In contrast, the deletion strain ΔSmkin24 is sterile and its lifecycle halted at later protoperithecia development and is also impaired in vegetative growth (Figure 42). A global phenotypic analysis of serine/threonine-protein kinase deletion mutants in *N. crassa* revealed that the *N. crassa Smkin3* homolog *prk-9* has an impact on asexual and sexual development as well as on vegetative growth and aerial hyphae formation (Park *et al.*, 2011). *S. macrospora* undergoes only sexual development, so it is not possible to comment on asexual reproduction. We confirmed the results of Park *et al.* (2011) with respect to the reduced growth rate of the deletion mutant ΔSmkin3 but in contrast to their findings, deletion of *Smkin3* did not impair fruiting-body development and fertility. Heilig *et al.* (2013) reported that *N. crassa* wt x Δprk-9 crosses resulted in no abnormalities during sexual development. Deletion of *stk-6* (homolog of *Smkin24*) in *N. crassa* resulted in reduced aerial hyphae and slightly reduced macroconidia production (Dvash *et al.*, 2010). Similar to the *S. macrospora* ΔSmkin24 mutant which is halted at later protoperithecia development, in *N. crassa* Δstk-6/Δstk-6 crosses resulted in empty perithecia containing no ascospores. In contrast to the *S. macrospora* ΔSmkin24 the mycelial extension rates were not impaired in the *N. crassa* Δstk6 mutant (Heilig *et al.*, 2014). *N. crassa* mutant Δprk-9 and Δstk6 mutants showed hyphal tip swelling, bursting of hyphal tips followed by cytoplasmic leakage (Dvash *et al.*, 2010, Heilig *et al.*, 2013). This phenotype could not be observed in the *S. macrospora* ΔSmkin3 and ΔSmkin24 mutants. Similar to *N. crassa*, deletion of *Smkin3* and *Smkin24* causes defects in septa formation (Heilig *et al.*, 2014, Heilig *et al.*, 2013, Dvash *et al.*, 2010). Consistent to the homologs in *N. crassa*, SmKIN3 and SmKIN24 localize to the septa (Figure 45), but could not be observed at spindle-pole bodies (Heilig *et al.*, 2014, Heilig *et al.*, 2013).

ΔSmkin3 strains exhibited less septa compared to wt and thus, formed elongated hyphal compartments (Figure 46 and Figure 47). This phenotype reverted, most probably due to the accumulation of suppressor mutations, after about 24 h of growth. This is similar to the *N. crassa*

Δprk-9 mutant producing initially aseptate germlings that formed septa at later stages of colony development (Heilig *et al.*, 2013). In addition, germlings derived from ΔSmkin3 protoplasts grow faster than germlings of wt protoplasts (Figure 48). We hypothesized that nutrients, normally provided for septa formation, can be used for initial growth in the deletion strain and thus, may cause the increased initial growth velocity. ΔSmkin24 displays a contrary septation phenotype to ΔSmkin3; it generates more septa, partially gathered in bundle-like structures and abnormal in shape (Figure 46). Septal actomyosin tangel assembly, cortical actomyosin ring (CAR) assembly and CAR constriction are three consecutive stages of septum formation in *N. crassa* (Delgado-Alvarez *et al.*, 2014). The septa observed in ΔSmkin24 resemble unfinished septa at early stages of septum formation, visualized by MYO-2 eGFP localization during SAT and CAR assembly in *N. crassa* (Delgado-Alvarez *et al.*, 2014). Thus, SmKIN24 is required for proper CAR assembly as recently shown by Heilig *et al.* (2014) in *N. crassa*. Despite their contrary phenotypes, SmKIN3 and SmKIN24 function independently in *S. macrospora*. This was shown by the double-deletion mutant ΔSmkin3/ΔSmkin24, which exhibits the phenotypes of both single-deletion strains, however, with respect to septum formation it resembles the ΔSmkin24 mutant (Figure 46 and Figure 47).

4.2.3 The STRIPAK (-like) complex in *S. macrospora*

In filamentous fungi, development of multicellular fruiting bodies requires highly conserved differentiation processes and is essential for sexual reproduction (Pöggeler *et al.*, 2006). For the ascomycete *S. macrospora* Bloemendal *et al.* (2012) recently showed that the STRIPAK complex, a multiprotein complex, functions in this process. The STRIPAK complex in mammals is known to be a major determinant in signaling (Figure 8). Deletion of genes, encoding for the STRIPAK-associated proteins PRO11 (Striatin homolog), PRO22 (STRIP1/2 homolog), PRO45 (SLMAP homolog) and SmMOB3 not only impair sexual development, but also hyphal fusion (Bernhards & Pöggeler, 2011, Bloemendal *et al.*, 2012, Bloemendal *et al.*, 2010, Nordzieke *et al.*, 2014). Thus, it seems that PRO11 in *S. macrospora* functions in developmental processes and serves in signaling concerning fruiting-body development and hyphal fusion. Today, evidence of STRIPAK-associated kinases in ascomycetes is still missing. This led to the name STRIPAK-like complexes, since presence of kinases was eponymous for the supramolecular complex (Frost *et al.*, 2012, Goudreault *et al.*, 2009). Based on interaction studies, we found

indications for GC kinases linked to PRO11, making the STRIPAK-like complex to a full STRIPAK complex (Figure 39 and Figure 40). The following model is based on interaction and localization studies as well as gene characterization and presents todays knowledge combined with our data and indications about the STRIPAK complex in the filamentous fungus *S. macrospora*. Shown are several complexes found at the nuclear envelope, the ER, the Golgi or mitochondria. The displayed functions of the proteins are based on phenotypical analysis after gene deletion or characterized interaction partners, e.g. EPS15, which is implicated in vesicular trafficking.

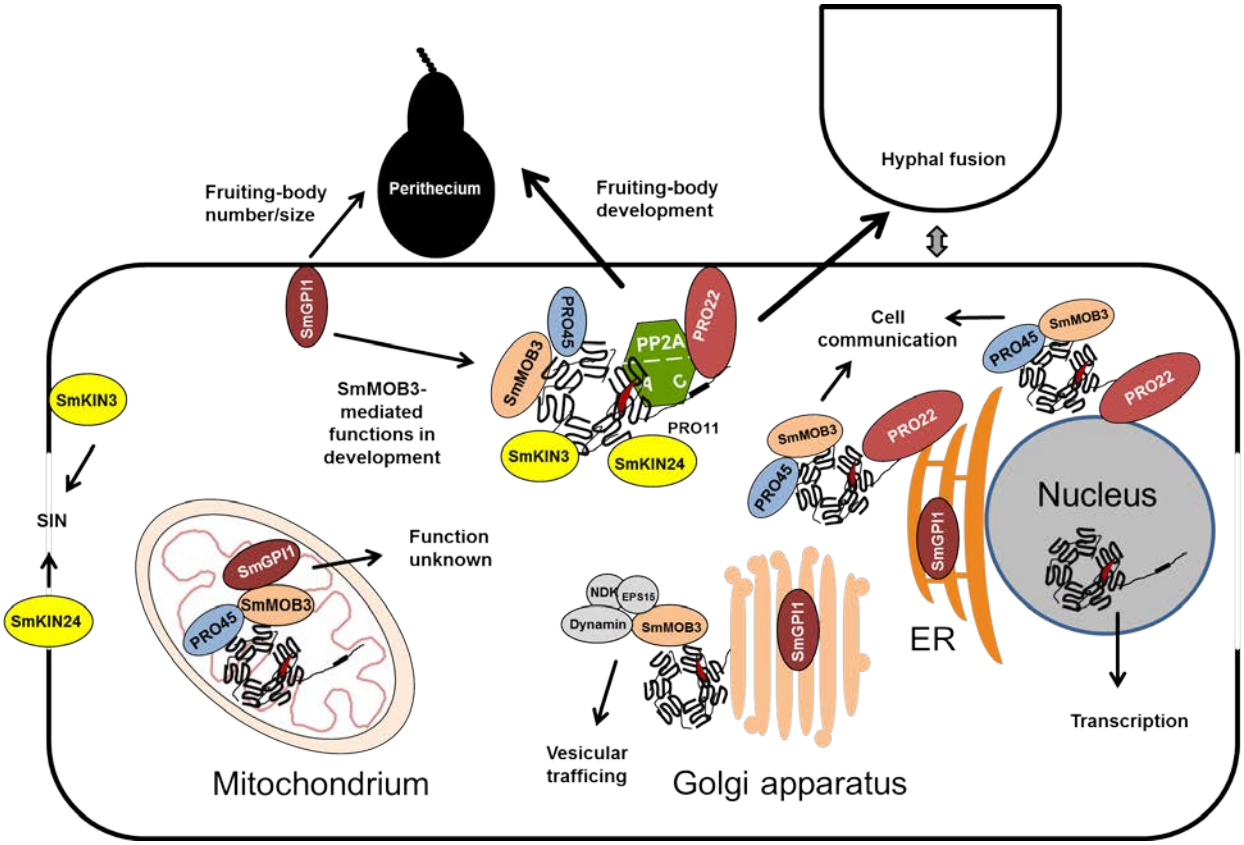

Figure 53. Schematic model of STRIPAK complex in *S. macrospora*. The multi-protein complex functions in hyphal fusion and fruiting-body development. It also might have a function in controlling the number and size of fruiting bodies as well as in vesicular trafficking. This model is based on the results gathered in this study and according to (Bernhards, 2010, Bernhards & Pöggeler, 2011, Bloemendal *et al.*, 2012, Nordzieke *et al.*, 2014, Pöggeler & Kück, 2004).

5. References

Amberg, D., D. Burke & J. Strathern, (2005) Methods in Yeast Genetics: A Cold Spring Harbor Laboratory Course Manual. *Cold Spring Harbor Laboratory Press*.

Andrade, M.A. & P. Bork, (1995) HEAT repeats in the Huntington's disease protein. *Nature genetics* **11**: 115-116.

Ariumi, Y., (2014) Multiple functions of DDX3 RNA helicase in gene regulation, tumorigenesis, and viral infection. *Frontiers in genetics* **5**: 423.

Bai, S.W., M.T. Herrera-Abreu, J.L. Rohn, V. Racine, V. Tajadura, N. Suryavanshi, S. Bechtel, S. Wiemann, B. Baum & A.J. Ridley, (2011) Identification and characterization of a set of conserved and new regulators of cytoskeletal organization, cell morphology and migration. *BMC biology* **9**: 54.

Baillat, G., S. Gaillard, F. Castets & A. Monneron, (2002) Interactions of phocein with nucleoside-diphosphate kinase, Eps15, and Dynamin I. *The Journal of biological chemistry* **277**: 18961-18966.

Baillat, G., A. Moqrich, F. Castets, A. Baude, Y. Bailly, A. Benmerah & A. Monneron, (2001) Molecular cloning and characterization of phocein, a protein found from the Golgi complex to dendritic spines. *Molecular biology of the cell* **12**: 663-673.

Bailly, Y.J. & F. Castets, (2007) Phocein: A potential actor in vesicular trafficking at Purkinje cell dendritic spines. *Cerebellum*: 1-9.

Bartoli, M., A. Monneron & D. Ladant, (1998) Interaction of calmodulin with striatin, a WD-repeat protein present in neuronal dendritic spines. *The Journal of biological chemistry* **273**: 22248-22253.

Bauer, H.C., I.A. Krizbai, H. Bauer & A. Traweger, (2014) "You Shall Not Pass"-tight junctions of the blood brain barrier. *Frontiers in neuroscience* **8**: 392.

Bechtel, S., H. Rosenfelder, A. Duda, C.P. Schmidt, U. Ernst, R. Wellenreuther, A. Mehrle, C. Schuster, A. Bahr, H. Blocker, D. Heubner, A. Hoerlein, G. Michel, H. Wedler, K. Kohrer, B. Ottenwalder, A. Poustka, S. Wiemann & I. Schupp, (2007) The full-ORF clone resource of the German cDNA Consortium. *BMC genomics* **8**: 399.

Becker, D.M. & V. Lundblad, (2001) Introduction of DNA into yeast cells. *Current protocols in molecular biology* **Chapter 13**: Unit13.7.

Ben-Menachem, R., M. Tal, T. Shadur & O. Pines, (2011) A third of the yeast mitochondrial proteome is dual localized: a question of evolution. *PROTEOMICS* **11**: 4468-4476.

Bendixen, C., S. Gangloff & R. Rothstein, (1994) A yeast mating-selection scheme for detection of protein-protein interactions. *Nucleic acids research* **22**: 1778-1779.

Bendtsen, J.D., H. Nielsen, G. von Heijne & S. Brunak, (2004) Improved prediction of signal peptides: SignalP 3.0. *Journal of molecular biology* **340**: 783-795.

Benoist, M., A. Baude, A. Tasmadjian, B. Dargent, J.P. Kessler & F. Castets, (2008) Distribution of zinedin in the rat brain. *Journal of neurochemistry* **106**: 969-977.

Benoist, M., S. Gaillard & F. Castets, (2006) The striatin family: a new signaling platform in dendritic spines. *Journal of physiology, Paris* **99**: 146-153.

Bergametti, F., C. Denier, P. Labauge, M. Arnoult, S. Boetto, M. Clanet, P. Coubes, B. Echenne, R. Ibrahim, B. Irthum, G. Jacquet, M. Lonjon, J.J. Moreau, J.P. Neau, F. Parker, M. Tremoulet, E. Tournier-Lasserve & N. Societe Francaise de, (2005) Mutations within the programmed cell death 10 gene cause cerebral cavernous malformations. *American journal of human genetics* **76**: 42-51.

Bernhards, Y., (2010) Untersuchung der Fruchtkörperentwicklung bei dem Hyphenpilz *Sordaria macrospora*. In: Institute of microbiology and genetic. Georg-August-University Göttingen, pp. 125.

Bernhards, Y. & S. Pöggeler, (2011) The phocein homologue SmMOB3 is essential for vegetative cell fusion and sexual development in the filamentous ascomycete *Sordaria macrospora*. *Current genetics* **57**: 133-149.

Biegert, A., C. Mayer, M. Remmert, J. Soding & A.N. Lupas, (2006) The MPI Bioinformatics Toolkit for protein sequence analysis. *Nucleic acids research* **34**: W335-339.

Birnboim, H.C. & J. Doly, (1979) A rapid alkaline extraction procedure for screening recombinant plasmid DNA. *Nucleic acids research* **7**: 1513-1523.

Blobel, G. & B. Dobberstein, (1975) Transfer of proteins across membranes. I. Presence of proteolytically processed and unprocessed nascent immunoglobulin light chains on membrane-bound ribosomes of murine myeloma. *The Journal of cell biology* **67**: 835-851.

Bloemendal, S., Y. Bernhards, K. Bartho, A. Dettmann, O. Voigt, I. Teichert, S. Seiler, D.A. Wolters, S. Pöggeler & U. Kück, (2012) A homologue of the human STRIPAK complex controls sexual development in fungi. *Molecular microbiology* **84**: 310-323.

Bloemendal, S., K.M. Lord, C. Rech, B. Hoff, I. Engh, N.D. Read & U. Kück, (2010) A mutant defective in sexual development produces aseptate ascogonia. *Eukaryotic cell* **9**: 1856-1866.

Blondeau, C., S. Gaillard, J.P. Ternaux, A. Monneron & A. Baude, (2003) Expression and distribution of phocein and members of the striatin family in neurones of rat peripheral ganglia. *Histochemistry and cell biology* **119**: 131-138.

Bonangelino, C.J., E.M. Chavez & J.S. Bonifacino, (2002) Genomic screen for vacuolar protein sorting genes in *Saccharomyces cerevisiae*. *Molecular biology of the cell* **13**: 2486-2501.

Boyce, K.J. & A. Andrianopoulos, (2011) Ste20-related kinases: effectors of signaling and morphogenesis in fungi. *Trends in Microbiology* **19**: 400-410.

Breitman, M., A. Zilberberg, M. Caspi & R. Rosin-Arbesfeld, (2008) The armadillo repeat domain of the APC tumor suppressor protein interacts with Striatin family members. *Biochimica et biophysica acta* **1783**: 1792-1802.

Bruice, P.Y., (2004) *Organic Chemistry*. Pearson Education Inc.

Burkhard, P., J. Stetefeld & S.V. Strelkov, (2001) Coiled coils: a highly versatile protein folding motif. *Trends in cell biology* **11**: 82-88.

Burkhardt, J.K., D. Schmidt, R. Schoenauer, C. Brokopp, I. Agarkova, O. Bozinov, H. Bertalanffy & S.P. Hoerstrup, (2010) Upregulation of transmembrane endothelial junction proteins in human cerebral cavernous malformations. *Neurosurgical focus* **29**: E3.

Byers, J.T., R.M. Guzzo, M. Salih & B.S. Tuana, (2009) Hydrophobic profiles of the tail anchors in SLMAP dictate subcellular targeting. *BMC cell biology* **10**: 48.

Cardenas, W.B., (2010) Evasion of the interferon-mediated antiviral response by filoviruses. *Viruses* **2**: 262-282.

Caro, L.H., H. Tettelin, J.H. Vossen, A.F. Ram, H. van den Ende & F.M. Klis, (1997) *In silicio* identification of glycosyl-phosphatidylinositol-anchored plasma-membrane and cell wall proteins of *Saccharomyces cerevisiae*. *Yeast* **13**: 1477-1489.

Carroll, A.M., J.A. Sweigard & B. Valent, (1994) Improved vectors for selecting resistance to hygromycin. *Fungal Genet Newslett* **41**: 22.

Castets, F., M. Bartoli, J.V. Barnier, G. Baillat, P. Salin, A. Moqrich, J.P. Bourgeois, F. Denizot, G. Rougon, G. Calothy & A. Monneron, (1996) A novel calmodulin-binding protein, belonging to the WD-repeat family, is localized in dendrites of a subset of CNS neurons. *The Journal of cell biology* **134**: 1051-1062.

Castets, F., T. Rakitina, S. Gaillard, A. Moqrich, M.G. Mattei & A. Monneron, (2000) Zinedin, SG2NA, and striatin are calmodulin-binding, WD repeat proteins principally expressed in the brain. *The Journal of biological chemistry* **275**: 19970-19977.

Chambliss, K.L., I.S. Yuhanna, C. Mineo, P. Liu, Z. German, T.S. Sherman, M.E. Mendelsohn, R.G. Anderson & P.W. Shaul, (2000) Estrogen receptor alpha and endothelial nitric oxide synthase are organized into a functional signaling module in caveolae. *Circulation research* **87**: E44-52.

Chen, H.W., M.J. Marinissen, S.W. Oh, X. Chen, M. Melnick, N. Perrimon, J.S. Gutkind & S.X. Hou, (2002) CKA, a novel multidomain protein, regulates the JUN N-terminal kinase signal transduction pathway in *Drosophila*. *Molecular and cellular biology* **22**: 1792-1803.

Chen, X. & H. Ding, (2011) Increased expression of the tail-anchored membrane protein SLMAP in adipose tissue from type 2 Tally Ho diabetic mice. *Experimental diabetes research* **2011**: 421982.

Chen, Y.K., C.Y. Chen, H.T. Hu & Y.P. Hsueh, (2012) CTTNBP2, but not CTTNBP2NL, regulates dendritic spinogenesis and synaptic distribution of the striatin-PP2A complex. *Molecular biology of the cell* **23**: 4383-4392.

Chen, Y.K. & Y.P. Hsueh, (2012) Cortactin-binding protein 2 modulates the mobility of cortactin and regulates dendritic spine formation and maintenance. *The Journal of neuroscience : the official journal of the Society for Neuroscience* **32**: 1043-1055.

Cheung, J., E. Petek, K. Nakabayashi, L.C. Tsui, J.B. Vincent & S.W. Scherer, (2001) Identification of the human cortactin-binding protein-2 gene from the autism candidate region at 7q31. *Genomics* **78**: 7-11.

Chin, D. & A. Means, (2000) Calmodulin: a prototypical calcium sensor. *Trends in cell biology* **10**: 322-328.

Cho, U.S. & W. Xu, (2007) Crystal structure of a protein phosphatase 2A heterotrimeric holoenzyme. *Nature* **445**: 53-57.

Choudhary, C., C. Kumar, F. Gnad, M.L. Nielsen, M. Rehman, T.C. Walther, J.V. Olsen & M. Mann, (2009) Lysine acetylation targets protein complexes and co-regulates major cellular functions. *Science* **325**: 834-840.

Chow, A., Y. Hao & X. Yang, (2010) Molecular characterization of human homologs of yeast MOB1. *International journal of cancer. Journal international du cancer* **126**: 2079-2089.

Clatterbuck, R.E., C.G. Eberhart, B.J. Crain & D. Rigamonti, (2001) Ultrastructural and immunocytochemical evidence that an incompetent blood-brain barrier is related to the pathophysiology of cavernous malformations. *Journal of neurology, neurosurgery, and psychiatry* **71**: 188-192.

Colot, H.V., G. Park, G.E. Turner, C. Ringelberg, C.M. Crew, L. Litvinkova, R.L. Weiss, K.A. Borkovich & J.C. Dunlap, (2006) A high-throughput gene knockout procedure for *Neurospora* reveals functions for multiple transcription factors. *Proc. Natl. Acad. Sci. U S A* **103**: 10352-10357.

Cosen-Binker, L.I. & A. Kapus, (2006) Cortactin: the gray eminence of the cytoskeleton. *Physiology* **21**: 352-361.

Couet, J., S. Li, T. Okamoto, T. Ikezu & M.P. Lisanti, (1997) Identification of peptide and protein ligands for the caveolin-scaffolding domain. Implications for the interaction of caveolin with caveolae-associated proteins. *The Journal of biological chemistry* **272**: 6525-6533.

Dan, I., S.E. Ong, N.M. Watanabe, B. Blagoev, M.M. Nielsen, E. Kajikawa, T.Z. Kristiansen, M. Mann & A. Pandey, (2002) Cloning of MASK, a novel member of the mammalian germinal center kinase III subfamily, with apoptosis-inducing properties. *The Journal of biological chemistry* **277**: 5929-5939.

Dan, I., N.M. Watanabe, T. Kobayashi, K. Yamashita-Suzuki, Y. Fukagaya, E. Kajikawa, W.K. Kimura, T.M. Nakashima, K. Matsumoto, J. Ninomiya-Tsuji & A. Kusumi, (2000) Molecular cloning of MINK, a

novel member of mammalian GCK family kinases, which is up-regulated during postnatal mouse cerebral development. *FEBS letters* **469**: 19-23.

Dan, I., N.M. Watanabe & A. Kusumi, (2001) The Ste20 group kinases as regulators of MAP kinase cascades. *Trends in cell biology* **11**: 220-230.

De Groot, P.W., K.J. Hellingwerf & F.M. Klis, (2003) Genome-wide identification of fungal GPI proteins. *Yeast* **20**: 781-796.

De Sampaio, G., J.P. Bourdineaud & G.J. Lauquin, (1999) A constitutive role for GPI-anchors in *Saccharomyces cerevisiae*: cell wall targeting. *Molecular microbiology* **34**: 247-256.

Delaval, B. & S.J. Doxsey, (2010) Pericentrin in cellular function and disease. *The Journal of cell biology* **188**: 181-190.

Delgado-Alvarez, D.L., S. Bartnicki-Garcia, S. Seiler & R.R. Mourino-Perez, (2014) Septum development in *Neurospora crassa*: the septal actomyosin tangle. *PloS one* **9**: e96744.

Delpire, E., (2009) The mammalian family of sterile 20p-like protein kinases. *Pflugers Arch - Eur J Physiol* **458**: 953-967.

Delpire, E., (2009) The mammalian family of sterile 20p-like protein kinases. *Pflugers Archiv : European journal of physiology* **458**: 953-967.

Dettmann, A., Y. Heilig, S. Ludwig, K. Schmitt, J. Illgen, A. Fleissner, O. Valerius & S. Seiler, (2013) HAM-2 and HAM-3 are central for the assembly of the Neurospora STRIPAK complex at the nuclear envelope and regulate nuclear accumulation of the MAP kinase MAK-1 in a MAK-2-dependent manner. *Molecular microbiology* **90**: 796-812.

Dettmann, A., Y. Heilig, O. Valerius, S. Ludwig & S. Seiler, (2014) Fungal Communication Requires the MAK-2 Pathway Elements STE-20 and RAS-2, the NRC-1 Adapter STE-50 and the MAP Kinase Scaffold HAM-5. *PLoS genetics* **10**: e1004762.

Dettmann, A., J. Illgen, S. Marz, T. Schurg, A. Fleissner & S. Seiler, (2012) The NDR kinase scaffold HYM1/MO25 is essential for MAK2 map kinase signaling in *Neurospora crassa*. *PLoS genetics* **8**: e1002950.

Dingledine, R., K. Borges, D. Bowie & S.F. Traynelis, (1999) The glutamate receptor ion channels. *Pharmacological reviews* **51**: 7-61.

Dinur-Mills, M., M. Tal & O. Pines, (2008) Dual Targeted Mitochondrial Proteins Are Characterized by Lower MTS Parameters and Total Net Charge. *PloS one* **3**: e2161.

Dirschnabel, D.E., M. Nowrousian, N. Cano-Domínguez, J. Aguirre, I. Teichert & U. Kück, (2014) New insights into the roles of NADPH oxidases in sexual development and ascospore germination in *Sordaria macrospora*. *Genetics* **196**: 729-744.

Djordjevic, J.T., M. Del Poeta, T.C. Sorrell, K.M. Turner & L.C. Wright, (2005) Secretion of cryptococcal phospholipase B1 (PLB1) is regulated by a glycosylphosphatidylinositol (GPI) anchor. *The Biochemical journal* **389**: 803-812.

Dvash, E., G. Kra-Oz, C. Ziv, S. Carmeli & O. Yarden, (2010) The NDR kinase DBF-2 is involved in regulation of mitosis, conidial development, and glycogen metabolism in *Neurospora crassa*. *Eukaryotic cell* **9**: 502-513.

Eisenhaber, B., P. Bork & F. Eisenhaber, (1998) Sequence properties of GPI-anchored proteins near the omega-site: constraints for the polypeptide binding site of the putative transamidase. *Protein Engineering* **11**: 1155-1161.

Eisenhaber, B., P. Bork & F. Eisenhaber, (1999) Prediction of potential GPI-modification sites in proprotein sequences. *Journal of molecular biology* **292**: 741-758.

Eisenhaber, B., P. Bork & F. Eisenhaber, (2001) Post-translational GPI lipid anchor modification of proteins in kingdoms of life: analysis of protein sequence data from complete genomes. *Protein engineering* **14**: 17-25.

Eisenhaber, B., P. Bork, Y. Yuan, G. Loffler & F. Eisenhaber, (2000) Automated annotation of GPI-anchor sites: case study *C. elegans*. *Trends in biochemical sciences* **25**: 340-341.

Elleuche, S. & S. Pöggeler, (2009) Beta-carbonic anhydrases play a role in fruiting-body development and ascospore germination in the filamentous fungus *Sordaria macrospora*. *PloS one* **4**: e5177.

Emanuelsson, O., S. Brunak, G. von Heijne & H. Nielsen, (2007) Locating proteins in the cell using TargetP, SignalP and related tools. *Nature protocols* **2**: 953-971.

Engh, I., M. Nowrousian & U. Kück, (2010) *Sordaria macrospora*, a model organism to study fungal cellular development. *European journal of cell biology* **89**: 864-872.

Engh, I., C. Würtz, K. Witzel-Schlömp, H.Y. Zhang, B. Hoff, M. Nowrousian, H. Rottensteiner & U. Kück, (2007) The WW domain protein PRO40 is required for fungal fertility and associates with Woronin bodies. *Eukaryot. Cell* **6**: 831-843.

Esser, K., (1992) Cryptogams-Cyanaobacteria, Fungi, Algae and Lichens. *Cambridge University Press, London*.

Ewing, R.M., P. Chu, F. Elisma, H. Li, P. Taylor, S. Climie, L. McBroom-Cerajewski, M.D. Robinson, L. O'Connor, M. Li, R. Taylor, M. Dharsee, Y. Ho, A. Heilbut, L. Moore, S. Zhang, O. Ornatsky, Y.V. Bukhman, M. Ethier, Y. Sheng, J. Vasilescu, M. Abu-Farha, J.P. Lambert, H.S. Duewel, Stewart, II, B. Kuehl, K. Hogue, K. Colwill, K. Gladwish, B. Muskat, R. Kinach, S.L. Adams, M.F. Moran, G.B. Morin, T. Topaloglou & D. Figeys, (2007) Large-scale mapping of human protein-protein interactions by mass spectrometry. *Molecular systems biology* **3**: 89.

Fazioli, F., L. Minichiello, B. Matoskova, W.T. Wong & P.P. Di Fiore, (1993) Eps15, a novel tyrosine kinase substrate, exhibits transforming activity. *Molecular and cellular biology* **13**: 5814-5828.

Felsenstein, J., (2013) *PHYLIP (Phylogeny Inference Package) version 3.695.*

Fidalgo, M., A. Guerrero, M. Fraile, C. Iglesias, C.M. Pombo & J. Zalvide, (2012) Adaptor protein cerebral cavernous malformation 3 (CCM3) mediates phosphorylation of the cytoskeletal proteins Ezrin/Radixin/Moesin by mammalian Ste20-4 to protect cells from oxidative stress. *The Journal of biological chemistry* **287**: 11556-11565.

Fleißner, A., A.C. Leeder, M.G. Roca, N.D. Read & N.L. Glass, (2009) Oscillatory recruitment of signaling proteins to cell tips promotes coordinated behavior during cell fusion. *Proceedings of the National Academy of Sciences of the United States of America* **106**: 19387-19392.

Fleißner, A., A. Simonin & N.L. Glass, (2008) Cell Fusion in the Filamentous Fungus, *Neurospora crassa*. In: Cell Fusion. E. Chen (ed). Humana Press, pp. 21-38.

Frieman, M.B. & B.P. Cormack, (2003) The omega-site sequence of glycosylphosphatidylinositol-anchored proteins in *Saccharomyces cerevisiae* can determine distribution between the membrane and the cell wall. *Molecular microbiology* **50**: 883-896.

Frieman, M.B. & B.P. Cormack, (2004) Multiple sequence signals determine the distribution of glycosylphosphatidylinositol proteins between the plasma membrane and cell wall in *Saccharomyces cerevisiae*. *Microbiology* **150**: 3105-3114.

Frost, A., M.G. Elgort, O. Brandman, C. Ives, S.R. Collins, L. Miller-Vedam, J. Weibezahn, M.Y. Hein, I. Poser, M. Mann, A.A. Hyman & J.S. Weissman, (2012) Functional repurposing revealed by comparing *S. pombe* and *S. cerevisiae* genetic interactions. *Cell* **149**: 1339-1352.

Fu, C., P. Iyer, A. Herkal, J. Abdullah, A. Stout & S.J. Free, (2011) Identification and characterization of genes required for cell-to-cell fusion in *Neurospora crassa*. *Eukaryotic cell* **10**: 1100-1109.

Fujita, M. & T. Kinoshita, (2012) GPI-anchor remodeling: potential functions of GPI-anchors in intracellular trafficking and membrane dynamics. *Biochimica et Biophysica Acta (BBA) - Molecular and Cell Biology of Lipids* **1821**: 1050-1058.

Gaillard, S., Y. Bailly, M. Benoist, T. Rakitina, J.P. Kessler, L. Fronzaroli-Molinieres, B. Dargent & F. Castets, (2006) Targeting of proteins of the striatin family to dendritic spines: role of the coiled-coil domain. *Traffic* **7**: 74-84.

Gaillard, S., M. Bartoli, F. Castets & A. Monneron, (2001) Striatin, a calmodulin-dependent scaffolding protein, directly binds caveolin-1. *FEBS letters* **508**: 49-52.

Galian, C., P. Bjorkholm, N. Bulleid & G. von Heijne, (2012) Efficient glycosylphosphatidylinositol (GPI) modification of membrane proteins requires a C-terminal anchoring signal of marginal hydrophobicity. *The Journal of biological chemistry* **287**: 16399-16409.

Gilbert, N.M., L.G. Baker, C.A. Specht & J.K. Lodge, (2012) A glycosylphosphatidylinositol anchor is required for membrane localization but dispensable for cell wall association of chitin deacetylase 2 in *Cryptococcus neoformans*. *mBio* **3**.

Gordon, J., J. Hwang, K. Carrier, C. Jones, Q. Kern, C. Moreno, R. Karas & D. Pallas, (2011) Protein phosphatase 2a (PP2A) binds within the oligomerization domain of striatin and regulates the phosphorylation and activation of the mammalian Ste20-Like kinase Mst3. *BMC biochemistry* **12**: 54.

Goudreault, M., L.M. D'Ambrosio, M.J. Kean, M.J. Mullin, B.G. Larsen, A. Sanchez, S. Chaudhry, G.I. Chen, F. Sicheri, A.I. Nesvizhskii, R. Aebersold, B. Raught & A.C. Gingras, (2009) A PP2A phosphatase high density interaction network identifies a novel striatin-interacting phosphatase and kinase complex linked to the cerebral cavernous malformation 3 (CCM3) protein. *Molecular & cellular proteomics : MCP* **8**: 157-171.

Greenman, C., P. Stephens, R. Smith, G.L. Dalgliesh, C. Hunter, G. Bignell, H. Davies, J. Teague, A. Butler, C. Stevens, S. Edkins, S. O'Meara, I. Vastrik, E.E. Schmidt, T. Avis, S. Barthorpe, G. Bhamra, G. Buck, B. Choudhury, J. Clements, J. Cole, E. Dicks, S. Forbes, K. Gray, K. Halliday, R. Harrison, K. Hills, J. Hinton, A. Jenkinson, D. Jones, A. Menzies, T. Mironenko, J. Perry, K. Raine, D. Richardson, R. Shepherd, A. Small, C. Tofts, J. Varian, T. Webb, S. West, S. Widaa, A. Yates, D.P. Cahill, D.N. Louis, P. Goldstraw, A.G. Nicholson, F. Brasseur, L. Looijenga, B.L. Weber, Y.E. Chiew, A. DeFazio, M.F. Greaves, A.R. Green, P. Campbell, E. Birney, D.F. Easton, G. Chenevix-Trench, M.H. Tan, S.K. Khoo, B.T. Teh, S.T. Yuen, S.Y. Leung, R. Wooster, P.A. Futreal & M.R. Stratton, (2007) Patterns of somatic mutation in human cancer genomes. *Nature* **446**: 153-158.

Guclu, B., A.K. Ozturk, K.L. Pricola, K. Bilguvar, D. Shin, B.J. O'Roak & M. Gunel, (2005) Mutations in apoptosis-related gene, PDCD10, cause cerebral cavernous malformation 3. *Neurosurgery* **57**: 1008-1013.

Guo, Z., (2013) Synthetic Studies of Glycosylphosphatidylinositol (GPI) Anchors and GPI-Anchored Peptides, Glycopeptides, and Proteins. *Current organic synthesis* **10**: 366-383.

Guzzo, R.M., M. Salih, E.D. Moore & B.S. Tuana, (2005) Molecular properties of cardiac tail-anchored membrane protein SLMAP are consistent with structural role in arrangement of excitation-contraction coupling apparatus. *American journal of physiology. Heart and circulatory physiology* **288**: H1810-1819.

Guzzo, R.M., S. Sevinc, M. Salih & B.S. Tuana, (2004) A novel isoform of sarcolemmal membrane-associated protein (SLMAP) is a component of the microtubule organizing centre. *Journal of cell science* **117**: 2271-2281.

Guzzo, R.M., J. Wigle, M. Salih, E.D. Moore & B.S. Tuana, (2004) Regulated expression and temporal induction of the tail-anchored sarcolemmal-membrane-associated protein is critical for myoblast fusion. *The Biochemical journal* **381**: 599-608.

Hamada, K., H. Terashima, M. Arisawa, N. Yabuki & K. Kitada, (1999) Amino acid residues in the omega-minus region participate in cellular localization of yeast glycosylphosphatidylinositol-attached proteins. *Journal of bacteriology* **181**: 3886-3889.

Hanks, S.K. & T. Hunter, (1995) Protein kinases 6. The eukaryotic protein kinase superfamily: kinase (catalytic) domain structure and classification. *FASEB J* **9**: 576-596.

Hao, Q., M. Feng, Z. Shi, C. Li, M. Chen, W. Wang, M. Zhang, S. Jiao & Z. Zhou, (2014) Structural insights into regulatory mechanisms of MO25-mediated kinase activation. *Journal of structural biology* **186**: 224-233.

He, Y., H. Zhang, L. Yu, M. Gunel, T.J. Boggon, H. Chen & W. Min, (2010) Stabilization of VEGFR2 signaling by cerebral cavernous malformation 3 is critical for vascular development. *Science signaling* **3**: ra26.

Heilig, Y., A. Dettmann, R.R. Mourino-Perez, K. Schmitt, O. Valerius & S. Seiler, (2014) Proper actin ring formation and septum constriction requires coordinated regulation of SIN and MOR pathways through the germinal centre kinase MST-1. *PLoS genetics* **10**: e1004306.

Heilig, Y., K. Schmitt & S. Seiler, (2013) Phospho-regulation of the *Neurospora crassa* septation initiation network. *PloS one* **8**: e79464.

Hein, L., M.E. Stevens, G.S. Barsh, R.E. Pratt, B.K. Kobilka & V.J. Dzau, (1997) Overexpression of angiotensin AT1 receptor transgene in the mouse myocardium produces a lethal phenotype associated with myocyte hyperplasia and heart block. *Proceedings of the National Academy of Sciences of the United States of America* **94**: 6391-6396.

Hergovich, A., S.J. Bichsel & B.A. Hemmings, (2005) Human NDR kinases are rapidly activated by MOB proteins through recruitment to the plasma membrane and phosphorylation. *Molecular and cellular biology* **25**: 8259-8272.

Hergovich, A. & B.A. Hemmings, (2012) Hippo signalling in the G2/M cell cycle phase: lessons learned from the yeast MEN and SIN pathways. *Seminars in cell & developmental biology* **23**: 794-802.

Herzog, F., A. Kahraman, D. Boehringer, R. Mak, A. Bracher, T. Walzthoeni, A. Leitner, M. Beck, F.U. Hartl, N. Ban, L. Malmstrom & R. Aebersold, (2012) Structural probing of a protein phosphatase 2A network by chemical cross-linking and mass spectrometry. *Science* **337**: 1348-1352.

Hoffman, C.S. & F. Winston, (1987) A ten-minute DNA preparation from yeast efficiently releases autonomous plasmids for transformation of *Escherichia coli*. *Gene* **57**: 267-272.

Hofmann, K. & P. Bucher, (1995) The FHA domain: a putative nuclear signalling domain found in protein kinases and transcription factors. *Trends in biochemical sciences* **20**: 347-349.

Holmes, K., O.L. Roberts, A.M. Thomas & M.J. Cross, (2007) Vascular endothelial growth factor receptor-2: structure, function, intracellular signalling and therapeutic inhibition. *Cellular signalling* **19**: 2003-2012.

Hu, Y., C. Leo, S. Yu, B.C. Huang, H. Wang, M. Shen, Y. Luo, S. Daniel-Issakani, D.G. Payan & X. Xu, (2004) Identification and functional characterization of a novel human misshapen/Nck interacting kinase-related kinase, hMINK beta. *The Journal of biological chemistry* **279**: 54387-54397.

Huang, C.Y., Y.M. Wu, C.Y. Hsu, W.S. Lee, M.D. Lai, T.J. Lu, C.L. Huang, T.H. Leu, H.M. Shih, H.I. Fang, D.R. Robinson, H.J. Kung & C.J. Yuan, (2002) Caspase activation of mammalian sterile 20-like kinase 3 (Mst3). Nuclear translocation and induction of apoptosis. *The Journal of biological chemistry* **277**: 34367-34374.

Huang, J., T. Liu, L.G. Xu, D. Chen, Z. Zhai & H.B. Shu, (2005) SIKE is an IKK epsilon/TBK1-associated suppressor of TLR3- and virus-triggered IRF-3 activation pathways. *The EMBO journal* **24**: 4018-4028.

Hwang, J. & D.C. Pallas, (2014) STRIPAK complexes: structure, biological function, and involvement in human diseases. *The international journal of biochemistry & cell biology* **47**: 118-148.

Hyodo, T., S. Ito, H. Hasegawa, E. Asano, M. Maeda, T. Urano, M. Takahashi, M. Hamaguchi & T. Senga, (2012) Misshapen-like kinase 1 (MINK1) is a novel component of striatin-interacting phosphatase and kinase (STRIPAK) and is required for the completion of cytokinesis. *The Journal of biological chemistry* **287**: 25019-25029.

Ilangumaran, S., H.T. He & D.C. Hoessli, (2000) Microdomains in lymphocyte signalling: beyond GPI-anchored proteins. *Immunology today* **21**: 2-7.

Ip, Y.T. & R.J. Davis, (1998) Signal transduction by the c-Jun N-terminal kinase (JNK)--from inflammation to development. *Current opinion in cell biology* **10**: 205-219.

Jacobsen, S., M. Wittig & S. Pöggeler, (2002) Interaction between mating-type proteins from the homothallic fungus *Sordaria macrospora*. *Current genetics* **41**: 150-158.

Jones, D.R. & I. Varela-Nieto, (1998) The role of glycosyl-phosphatidylinositol in signal transduction. *The international journal of biochemistry & cell biology* **30**: 313-326.

Kanai, M., K. Kume, K. Miyahara, K. Sakai, K. Nakamura, K. Leonhard, D.J. Wiley, F. Verde, T. Toda & D. Hirata, (2005) Fission yeast MO25 protein is localized at SPB and septum and is essential for cell morphogenesis. *The EMBO journal* **24**: 3012-3025.

Kaneko, S., X. Chen, P. Lu, X. Yao, T.G. Wright, M. Rajurkar, K. Kariya, J. Mao, Y.T. Ip & L. Xu, (2011) Smad inhibition by the Ste20 kinase Misshapen. *Proceedings of the National Academy of Sciences of the United States of America* **108**: 11127-11132.

Kawabata, T. & H. Inoue, (2007) Detection of physical interactions by immunoprecipitation of FLAG- and HA-tagged proteins expressed at the *his-3* locus in *Neurospora crassa*. *Fungal Genetics Newsletter*.

Kean, M.J., D.F. Ceccarelli, M. Goudreault, M. Sanches, S. Tate, B. Larsen, L.C. Gibson, W.B. Derry, I.C. Scott, L. Pelletier, G.S. Baillie, F. Sicheri & A.C. Gingras, (2011) Structure-function analysis of core STRIPAK Proteins: a signaling complex implicated in Golgi polarization. *The Journal of biological chemistry* **286**: 25065-25075.

Kinoshita, T., (2014) Enzymatic mechanism of GPI-anchor attachment clarified. *Cell Cycle* **13**: 1838-1839.

Klix, V., M. Nowrousian, C. Ringelberg, J.J. Loros, J.C. Dunlap & S. Pöggeler, (2010) Functional characterization of MAT1-1-specific mating-type genes in the homothallic ascomycete *Sordaria macrospora* provides new insights into essential and nonessential sexual regulators. *Eukaryotic cell* **9**: 894-905.

Koch, M.R. & L. Pillus, (2009) The glucanosyltransferase Gas1 functions in transcriptional silencing. *Proceedings of the National Academy of Sciences* **106**: 11224-11229.

Kosugi, S., M. Hasebe, M. Tomita & H. Yanagawa, (2009) Systematic identification of cell cycle-dependent yeast nucleocytoplasmic shuttling proteins by prediction of composite motifs. *Proceedings of the National Academy of Sciences* **106**: 10171-10176.

Krapp, A. & V. Simanis, (2008) An overview of the fission yeast septation initiation network (SIN). *Biochemical Society transactions* **36**: 411-415.

Krishnan, K.S., R. Rikhy, S. Rao, M. Shivalkar, M. Mosko, R. Narayanan, P. Etter, P.S. Estes & M. Ramaswami, (2001) Nucleoside diphosphate kinase, a source of GTP, is required for dynamin-dependent synaptic vesicle recycling. *Neuron* **30**: 197-210.

Kück, U., S. Pöggeler, M. Nowrousian, N. Nolting & I. Engh, (2009) *Sordaria macrospora, a model system for fungal development.,* p. 17-39. Springer Verlag, Heidelberg, New York.

Kulkarni, R.D., H.S. Kelkar & R.A. Dean, (2003) An eight-cysteine-containing CFEM domain unique to a group of fungal membrane proteins. *Trends in biochemical sciences* **28**: 118-121.

la Cour, T., L. Kiemer, A. Mølgaard, R. Gupta, K. Skriver & S. Brunak, (2004) Analysis and prediction of leucine-rich nuclear export signals. *Protein Eng. Des. Sel.* **17**: 527-536.

Laemmli, U.K., (1970) Cleavage of structural proteins during the assembly of the head of bacteriophage T4. *Nature* **227**: 680-685.

Lalli, E. & P. Sassone-Corsi, (1994) Signal transduction and gene regulation: the nuclear response to cAMP. *The Journal of biological chemistry* **269**: 17359-17362.

Lankes, W., A. Griesmacher, J. Grunwald, R. Schwartz-Albiez & R. Keller, (1988) A heparin-binding protein involved in inhibition of smooth-muscle cell proliferation. *The Biochemical journal* **251**: 831-842.

Larkin, M.A., G. Blackshields, N.P. Brown, R. Chenna, P.A. McGettigan, H. McWilliam, F. Valentin, I.M. Wallace, A. Wilm, R. Lopez, J.D. Thompson, T.J. Gibson & D.G. Higgins, (2007) Clustal W and Clustal X version 2.0. *Bioinformatics* **23**: 2947-2948.

Lecellier, G. & P. Silar, (1994) Rapid methods for nucleic acids extraction from Petri dish-grown mycelia. *Current genetics* **25**: 122-123.

Lechward, K., O.S. Awotunde, W. Swiatek & G. Muszynska, (2001) Protein phosphatase 2A: variety of forms and diversity of functions. *Acta biochimica Polonica* **48**: 921-933.

Lee, W.S., C.Y. Hsu, P.L. Wang, C.Y. Huang, C.H. Chang & C.J. Yuan, (2004) Identification and characterization of the nuclear import and export signals of the mammalian Ste20-like protein kinase 3. *FEBS Lett.* **572**: 41-45.

Li, D. & R. Roberts, (2001) WD-repeat proteins: structure characteristics, biological function, and their involvement in human diseases. *Cellular and molecular life sciences : CMLS* **58**: 2085-2097.

Li, E. & K. Hristova, (2006) Role of receptor tyrosine kinase transmembrane domains in cell signaling and human pathologies. *Biochemistry* **45**: 6241-6251.

Li, S., J. Couet & M.P. Lisanti, (1996) Src tyrosine kinases, Galpha subunits, and H-Ras share a common membrane-anchored scaffolding protein, caveolin. Caveolin binding negatively regulates the auto-activation of Src tyrosine kinases. *The Journal of biological chemistry* **271**: 29182-29190.

Li, X., R. Zhang, H. Zhang, Y. He, W. Ji, W. Min & T.J. Boggon, (2010) Crystal structure of CCM3, a cerebral cavernous malformation protein critical for vascular integrity. *The Journal of biological chemistry* **285**: 24099-24107.

Lieber, T., S. Kidd, E. Alcamo, V. Corbin & M.W. Young, (1993) Antineurogenic phenotypes induced by truncated Notch proteins indicate a role in signal transduction and may point to a novel function for Notch in nuclei. *Genes & development* **7**: 1949-1965.

Lin, A., A. Hokugo, J. Choi & I. Nishimura, (2010) Small cytoskeleton-associated molecule, fibroblast growth factor receptor 1 oncogene partner 2/wound inducible transcript-3.0 (FGFR1OP2/wit3.0), facilitates fibroblast-driven wound closure. *The American journal of pathology* **176**: 108-121.

Lin, J.L., H.C. Chen, H.I. Fang, D. Robinson, H.J. Kung & H.M. Shih, (2001) MST4, a new Ste20-related kinase that mediates cell growth and transformation via modulating ERK pathway. *Oncogene* **20**: 6559-6569.

Linding, R., R.B. Russell, V. Neduva & T.J. Gibson, (2003) GlobPlot: Exploring protein sequences for globularity and disorder. *Nucleic acids research* **31**: 3701-3708.

Lisa-Santamaria, P., A. Jimenez & J.L. Revuelta, (2012) The protein factor-arrest 11 (Far11) is essential for the toxicity of human caspase-10 in yeast and participates in the regulation of autophagy and the DNA damage signaling. *The Journal of biological chemistry* **287**: 29636-29647.

Liu, J., Q. Zheng, Y. Deng, C.S. Cheng, N.R. Kallenbach & M. Lu, (2006) A seven-helix coiled coil. *Proceedings of the National Academy of Sciences of the United States of America* **103**: 15457-15462.

Lorber, B., M.L. Howe, L.I. Benowitz & N. Irwin, (2009) Mst3b, an Ste20-like kinase, regulates axon regeneration in mature CNS and PNS pathways. *Nature neuroscience* **12**: 1407-1414.

Lord, K.M. & N.D. Read, (2011) Perithecium morphogenesis in *Sordaria macrospora*. *Fungal Genetics and Biology* **48**: 388-399.

Low, M.G., (1989) Glycosyl-phosphatidylinositol: a versatile anchor for cell surface proteins. *FASEB J* **3**: 1600-1608.

Lu, Q., D.C. Pallas, H.K. Surks, W.E. Baur, M.E. Mendelsohn & R.H. Karas, (2004) Striatin assembles a membrane signaling complex necessary for rapid, nongenomic activation of endothelial NO synthase by estrogen receptor alpha. *Proceedings of the National Academy of Sciences of the United States of America* **101**: 17126-17131.

Lu, T.J., W.Y. Lai, C.Y. Huang, W.J. Hsieh, J.S. Yu, Y.J. Hsieh, W.T. Chang, T.H. Leu, W.C. Chang, W.J. Chuang, M.J. Tang, T.Y. Chen, T.L. Lu & M.D. Lai, (2006) Inhibition of cell migration by autophosphorylated mammalian sterile 20-like kinase 3 (MST3) involves paxillin and protein-tyrosine phosphatase-PEST. *The Journal of biological chemistry* **281**: 38405-38417.

Luca, F.C., M. Mody, C. Kurischko, D.M. Roof, T.H. Giddings & M. Winey, (2001) *Saccharomyces cerevisiae* Mob1p is required for cytokinesis and mitotic exit. *Molecular and cellular biology* **21**: 6972-6983.

Ma, H.L., Y.L. Peng, L. Gong, W.B. Liu, S. Sun, J. Liu, C.B. Zheng, H. Fu, D. Yuan, J. Zhao, P.C. Chen, S.S. Xie, X.M. Zeng, Y.M. Xiao, Y. Liu & D.W. Li, (2009) The goldfish SG2NA gene encodes two alpha-type regulatory subunits for PP2A and displays distinct developmental expression pattern. *Gene regulation and systems biology* **3**: 115-129.

Ma, X., H. Zhao, J. Shan, F. Long, Y. Chen, Y. Zhang, X. Han & D. Ma, (2007) PDCD10 interacts with Ste20-related kinase MST4 to promote cell growth and transformation via modulation of the ERK pathway. *Molecular biology of the cell* **18**: 1965-1978.

Maddi, A., A. Dettman, C. Fu, S. Seiler & S.J. Free, (2012) WSC-1 and HAM-7 Are MAK-1 MAP Kinase Pathway Sensors Required for Cell Wall Integrity and Hyphal Fusion in *Neurospora crassa*. *PloS one* **7**: e42374.

Maerz, S., A. Dettmann, C. Ziv, Y. Liu, O. Valerius, O. Yarden & S. Seiler, (2009) Two NDR kinase-MOB complexes function as distinct modules during septum formation and tip extension in *Neurospora crassa*. *Molecular microbiology* **74**: 707-723.

Mahlert, M., L. Leveleki, A. Hlubek, B. Sandrock & M. Bolker, (2006) Rac1 and Cdc42 regulate hyphal growth and cytokinesis in the dimorphic fungus *Ustilago maydis*. *Molecular microbiology* **59**: 567-578.

Maller, J.L., (2003) Signal transduction. Fishing at the cell surface. *Science* **300**: 594-595.

Marchler-Bauer, A., S. Lu, J.B. Anderson, F. Chitsaz, M.K. Derbyshire, C. DeWeese-Scott, J.H. Fong, L.Y. Geer, R.C. Geer, N.R. Gonzales, M. Gwadz, D.I. Hurwitz, J.D. Jackson, Z. Ke, C.J. Lanczycki, F. Lu, G.H. Marchler, M. Mullokandov, M.V. Omelchenko, C.L. Robertson, J.S. Song, N. Thanki, R.A. Yamashita, D. Zhang, N. Zhang, C. Zheng & S.H. Bryant, (2011) CDD: a Conserved Domain Database for the functional annotation of proteins. *Nucleic acids research* **39**: D225-D229.

Martindale, J.L. & N.J. Holbrook, (2002) Cellular response to oxidative stress: signaling for suicide and survival. *Journal of cellular physiology* **192**: 1-15.

Masloff, S., S. Pöggeler & U. Kück, (1999) The *pro1*(+) gene from *Sordaria macrospora* encodes a C6 zinc finger transcription factor required for fruiting body development. *Genetics* **152**: 191-199.

Mason, J.M. & K.M. Arndt, (2004) Coiled coil domains: stability, specificity, and biological implications. *Chembiochem : a European journal of chemical biology* **5**: 170-176.

Matsuki, T., J. Chen & B.W. Howell, (2013) Acute inactivation of the serine-threonine kinase Stk25 disrupts neuronal migration. *Neural development* **8**: 21.

Mayor, S. & H. Riezman, (2004) Sorting GPI-anchored proteins. *Nature Reviews Molecular Cell Biology*: 110-120.

Mendoza, M., S. Redemann & D. Brunner, (2005) The fission yeast MO25 protein functions in polar growth and cell separation. *European journal of cell biology* **84**: 915-926.

Moqrich, A., M.G. Mattei, M. Bartoli, T. Rakitina, G. Baillat, A. Monneron & F. Castets, (1998) Cloning of human striatin cDNA (STRN), gene mapping to 2p22-p21, and preferential expression in brain. *Genomics* **51**: 136-139.

Moreno, C.S., W.S. Lane & D.C. Pallas, (2001) A mammalian homolog of yeast MOB1 is both a member and a putative substrate of striatin family-protein phosphatase 2A complexes. *The Journal of biological chemistry* **276**: 24253-24260.

Moreno, C.S., S. Park, K. Nelson, D. Ashby, F. Hubalek, W.S. Lane & D.C. Pallas, (2000) WD40 repeat proteins striatin and S/G(2) nuclear autoantigen are members of a novel family of calmodulin-binding proteins that associate with protein phosphatase 2A. *The Journal of biological chemistry* **275**: 5257-5263.

Morrell, J.L., G.C. Tomlin, S. Rajagopalan, S. Venkatram, A.S. Feoktistova, J.J. Tasto, S. Mehta, J.L. Jennings, A. Link, M.K. Balasubramanian & K.L. Gould, (2004) Sid4p-Cdc11p assembles the septation initiation network and its regulators at the *S. pombe* SPB. *Cur. Biol.* **14**: 579-584.

Mosavi, L.K., T.J. Cammett, D.C. Desrosiers & Z.Y. Peng, (2004) The ankyrin repeat as molecular architecture for protein recognition. *Protein science : a publication of the Protein Society* **13**: 1435-1448.

Muro, Y., E.K. Chan, G. Landberg & E.M. Tan, (1995) A cell-cycle nuclear autoantigen containing WD-40 motifs expressed mainly in S and G2 phase cells. *Biochemical and biophysical research communications* **207**: 1029-1037.

Neer, E.J., C.J. Schmidt, R. Nambudripad & T.F. Smith, (1994) The ancient regulatory-protein family of WD-repeat proteins. *Nature* **371**: 297-300.

Nicholas, K.B., H.B. Nicholas & D.W. Deerfield, (1997) GeneDoc: Analysis and Visualization of Genetic Variation. *EMBNEWnews 4*.

Nogueira, E., M. Fidalgo, A. Molnar, J. Kyriakis, T. Force, J. Zalvide & C.M. Pombo, (2008) SOK1 translocates from the Golgi to the nucleus upon chemical anoxia and induces apoptotic cell death. *The Journal of biological chemistry* **283**: 16248-16258.

Nonaka, H., K. Takei, M. Umikawa, M. Oshiro, K. Kuninaka, M. Bayarjargal, T. Asato, Y. Yamashiro, Y. Uechi, S. Endo, T. Suzuki & K. Kariya, (2008) MINK is a Rap2 effector for phosphorylation of the postsynaptic scaffold protein TANC1. *Biochemical and biophysical research communications* **377**: 573-578.

Nordzieke, S., T. Zobel, B. Franzel, D.A. Wolters, U. Kück & I. Teichert, (2014) A fungal SLMAP homolog plays a fundamental role in development and localizes to the nuclear envelope, ER, and mitochondria. *Eukaryotic cell*.

Nowrousian, M., (2010) Next-generation sequencing techniques for eukaryotic microorganisms: sequencing-based solutions to biological problems. *Eukaryot. Cell* **9**: 1300-1310.

Nowrousian, M. & P. Cebula, (2005) The gene for a lectin-like protein is transcriptionally activated during sexual development, but is not essential for fruiting-body formation in the filamentous fungus Sordaria macrospora. *BMC microbiology* **5**: 64.

Nowrousian, M., S. Frank, S. Koers, P. Strauch, T. Weitner, C. Ringelberg, J.C. Dunlap, J.J. Loros & U. Kück, (2007) The novel ER membrane protein PRO41 is essential for sexual development in the filamentous fungus *Sordaria macrospora*. *Mol. Microbiol.* **64**: 923-937.

Nowrousian, M., S. Masloff, S. Pöggeler & U. Kück, (1999) Cell differentiation during sexual development of the fungus *Sordaria macrospora* requires ATP citrate lyase activity. *Molecular and cellular biology* **19**: 450-460.

Nowrousian, M., C. Ringelberg, J.C. Dunlap, J.J. Loros & U. Kück, (2005) Cross-species microarray hybridization to identify developmentally regulated genes in the filamentous fungus *Sordaria macrospora*. *Mol. Genet. Genomics* **273**: 137-149.

Nowrousian, M., J.E. Stajich, M. Chu, I. Engh, E. Espagne, K. Halliday, J. Kamerewerd, F. Kempken, B. Knab, H.C. Kuo, H.D. Osiewacz, S. Pöggeler, N.D. Read, S. Seiler, K.M. Smith, D. Zickler, U. Kück & M. Freitag, (2010) De novo assembly of a 40 Mb eukaryotic genome from short sequence reads: *Sordaria macrospora*, a model organism for fungal morphogenesis. *PLoS genetics* **6**: e1000891.

Nowrousian, M., I. Teichert, S. Masloff & U. Kuck, (2012) Whole-Genome Sequencing of *Sordaria macrospora* Mutants Identifies Developmental Genes. *G3 (Bethesda)* **2**: 261-270.

Nowrousian, M., C. Würtz, S. Pöggeler & U. Kück, (2004) Comparative sequence analysis of *Sordaria macrospora* and *Neurospora crassa* as a means to improve genome annotation. *Fungal Genet. Biol.* **41**: 285-292.

O'Lone, R., M.C. Frith, E.K. Karlsson & U. Hansen, (2004) Genomic targets of nuclear estrogen receptors. *Molecular endocrinology* **18**: 1859-1875.

Olsen, J.V., B. Blagoev, F. Gnad, B. Macek, C. Kumar, P. Mortensen & M. Mann, (2006) Global, *in vivo*, and site-specific phosphorylation dynamics in signaling networks. *Cell* **127**: 635-648.

Orlean, P. & A.K. Menon, (2007) Thematic review series: lipid posttranslational modifications. GPI-anchoring of protein in yeast and mammalian cells, or: how we learned to stop worrying and love glycophospholipids. *Journal of lipid research* **48**: 993-1011.

Ota, T., Y. Suzuki, T. Nishikawa, T. Otsuki, T. Sugiyama, R. Irie, A. Wakamatsu, K. Hayashi, H. Sato, K. Nagai, K. Kimura, H. Makita, M. Sekine, M. Obayashi, T. Nishi, T. Shibahara, T. Tanaka, S. Ishii, J. Yamamoto, K. Saito, Y. Kawai, Y. Isono, Y. Nakamura, K. Nagahari, K. Murakami, T. Yasuda, T. Iwayanagi, M. Wagatsuma, A. Shiratori, H. Sudo, T. Hosoiri, Y. Kaku, H. Kodaira, H. Kondo, M. Sugawara, M. Takahashi, K. Kanda, T. Yokoi, T. Furuya, E. Kikkawa, Y. Omura, K. Abe, K. Kamihara, N. Katsuta, K. Sato, M. Tanikawa, M. Yamazaki, K. Ninomiya, T. Ishibashi, H. Yamashita, K. Murakawa, K. Fujimori, H. Tanai, M. Kimata, M. Watanabe, S. Hiraoka, Y. Chiba, S. Ishida, Y. Ono, S. Takiguchi, S. Watanabe, M. Yosida, T. Hotuta, J. Kusano, K. Kanehori, A. Takahashi-Fujii, H. Hara, T.O. Tanase, Y. Nomura, S. Togiya, F. Komai, R. Hara, K. Takeuchi, M. Arita, N. Imose, K. Musashino, H. Yuuki, A. Oshima, N. Sasaki, S. Aotsuka, Y. Yoshikawa, H. Matsunawa, T. Ichihara, N. Shiohata, S. Sano, S. Moriya, H. Momiyama, N. Satoh, S. Takami, Y. Terashima, O. Suzuki, S. Nakagawa, A. Senoh, H. Mizoguchi, Y. Goto, F. Shimizu, H. Wakebe, H. Hishigaki, T. Watanabe, A. Sugiyama*, et al.*, (2004) Complete sequencing and characterization of 21,243 full-length human cDNAs. *Nature genetics* **36**: 40-45.

Otten, P., G.P. Pizzolato, B. Rilliet & J. Berney, (1989) [131 cases of cavernous angioma (cavernomas) of the CNS, discovered by retrospective analysis of 24,535 autopsies]. *Neuro-Chirurgie* **35**: 82-83, 128-131.

Ouyang, H., X. Chen, Y. Lu, I.B. Wilson, G. Tang, A. Wang & C. Jin, (2013) One single basic amino acid at the omega-1 or omega-2 site is a signal that retains glycosylphosphatidylinositol-anchored protein in the plasma membrane of *Aspergillus fumigatus*. *Eukaryotic cell* **12**: 889-899.

Page, R.D.M., (1996) Tree View: An application to display phylogenetic trees on personal computers. *Computer applications in the biosciences : CABIOS* **12**: 357-358.

Paladino, S., S. Lebreton, S. Tivodar, V. Campana, R. Tempre & C. Zurzolo, (2008) Different GPI-attachment signals affect the oligomerisation of GPI-anchored proteins and their apical sorting. *Journal of cell science* **121**: 4001-4007.

Park, G., J.A. Servin, G.E. Turner, L. Altamirano, H.V. Colot, P. Collopy, L. Litvinkova, L. Li, C.A. Jones, F.G. Diala, J.C. Dunlap & K.A. Borkovich, (2011) Global analysis of serine-threonine protein kinase genes in *Neurospora crassa*. *Eukaryotic cell* **10**: 1553-1564.

Parton, R.G. & K. Simons, (2007) The multiple faces of caveolae. *Nature reviews. Molecular cell biology* **8**: 185-194.

Paulick, M.G. & C.R. Bertozzi, (2008) The glycosylphosphatidylinositol anchor: a complex membrane-anchoring structure for proteins. *Biochemistry* **47**: 6991-7000.

Pelham, H.R., (1990) The retention signal for soluble proteins of the endoplasmic reticulum. *Trends in biochemical sciences* **15**: 483-486.

Petersen, T.N., S. Brunak, G. von Heijne & H. Nielsen, (2011) SignalP 4.0: discriminating signal peptides from transmembrane regions. *Nature methods* **8**: 785-786.

Pfeiffer, N.V., D. Dirndorfer, S. Lang, U.K. Resenberger, L.M. Restelli, C. Hemion, M. Miesbauer, S. Frank, A. Neutzner, R. Zimmermann, K.F. Winklhofer & J. Tatzelt, (2013) Structural features within the

nascent chain regulate alternative targeting of secretory proteins to mitochondria. *The EMBO journal* **32**: 1036-1051.

Pichlmair, A., O. Schulz, C.P. Tan, T.I. Naslund, P. Liljestrom, F. Weber & C. Reis e Sousa, (2006) RIG-I-mediated antiviral responses to single-stranded RNA bearing 5'-phosphates. *Science* **314**: 997-1001.

Pierleoni, A., P. Martelli & R. Casadio, (2008) PredGPI: a GPI-anchor predictor. *BMC bioinformatics* **9**: 392.

Pittet, M. & A. Conzelmann, (2007) Biosynthesis and function of GPI proteins in the yeast *Saccharomyces cerevisiae*. *Biochimica et biophysica acta* **1771**: 405-420.

Pöggeler, S. & U. Kück, (2004) A WD40 repeat protein regulates fungal cell differentiation and can be replaced functionally by the mammalian homologue striatin. *Eukaryotic cell* **3**: 232-240.

Pöggeler, S. & U. Kück, (2006) Highly efficient generation of signal transduction knockout mutants using a fungal strain deficient in the mammalian ku70 ortholog. *Gene* **378**: 1-10.

Pöggeler, S., S. Masloff, B. Hoff, S. Mayrhofer & U. Kück, (2003) Versatile EGFP reporter plasmids for cellular localization of recombinant gene products in filamentous fungi. *Current genetics* **43**: 54-61.

Pöggeler, S., M. Nowrousian, S. Jacobsen & U. Kück, (1997) An efficient procedure to isolate fungal genes from an indexed cosmid library. *J Microbiol Meth* **29**: 49-61.

Pöggeler, S., M. Nowrousian & U. Kück, (2006) Fruiting-body development in ascomycetes. In: The Mycota I. K. Esser (ed). Berlin, Heidelberg, New York: Springer, pp. 325-355.

Pöggeler, S., M. Nowrousian, C. Ringelberg, J.J. Loros, J.C. Dunlap & U. Kück, (2006) Microarray and real time PCR analyses reveal mating type-dependent gene expression in a homothallic fungus. *Mol. Genet. Genomics* **275**: 492-503.

Pöggeler, S., S. Risch, U. Kück & H.D. Osiewacz, (1997) Mating-type genes from the homothallic fungus *Sordaria macrospora* are functionally expressed in a heterothallic ascomycete. *Genetics* **147**: 567-580.

Pombo, C.M., J.V. Bonventre, A. Molnar, J. Kyriakis & T. Force, (1996) Activation of a human Ste20-like kinase by oxidant stress defines a novel stress response pathway. *The EMBO journal* **15**: 4537-4546.

Pombo, C.M., T. Force, J. Kyriakis, E. Nogueira, M. Fidalgo & J. Zalvide, (2007) The GCK II and III subfamilies of the STE20 group kinases. *Frontiers in bioscience : a journal and virtual library* **12**: 850-859.

Ponchon, L., C. Dumas, A.V. Kajava, D. Fesquet & A. Padilla, (2004) NMR solution structure of Mob1, a mitotic exit network protein and its interaction with an NDR kinase peptide. *Journal of molecular biology* **337**: 167-182.

Preisinger, C., B. Short, V. De Corte, E. Bruyneel, A. Haas, R. Kopajtich, J. Gettemans & F.A. Barr, (2004) YSK1 is activated by the Golgi matrix protein GM130 and plays a role in cell migration through its substrate 14-3-3zeta. *The Journal of cell biology* **164**: 1009-1020.

Qian, Z., C. Lin, R. Espinosa, M. LeBeau & M.R. Rosner, (2001) Cloning and characterization of MST4, a novel Ste20-like kinase. *The Journal of biological chemistry* **276**: 22439-22445.

Rapoport, T.A., (2007) Protein translocation across the eukaryotic endoplasmic reticulum and bacterial plasma membranes. *Nature* **450**: 663-669.

Raz, L., M.M. Khan, V.B. Mahesh, R.K. Vadlamudi & D.W. Brann, (2008) Rapid estrogen signaling in the brain. *Neuro-Signals* **16**: 140-153.

Raza, H., (2011) Dual localization of glutathione S-transferase in the cytosol and mitochondria: implications in oxidative stress, toxicity and disease. *FEBS Journal* **278**: 4243-4251.

Read, N.D., A. Fleißner & N.L. Glass, (2010) *Hyphal Fusion*. ASM Press, Washington.

Rech, C., I. Engh & U. Kuck, (2007) Detection of hyphal fusion in filamentous fungi using differently fluorescence-labeled histones. *Current genetics* **52**: 259-266.

Record, C.J., A. Chaikuad, P. Rellos, S. Das, A.C. Pike, O. Fedorov, B.D. Marsden, S. Knapp & W.H. Lee, (2010) Structural comparison of human mammalian ste20-like kinases. *PloS one* **5**: e11905.

Ribeiro, P.S., F. Josué, A. Wepf, M.C. Wehr, O. Rinner, G. Kelly, N. Tapon & M. Gstaiger, (2010) Combined functional genomic and proteomic approaches identify a PP2A complex as a negative regulator of Hippo signaling. *Molecular and cellular biology* **39**: 521-534.

Robinson, P.J., (1997) Signal transduction via GPI-anchored membrane proteins. *Advances in experimental medicine and biology* **419**: 365-370.

Roca, M.G., J. Arlt, C.E. Jeffree & N.D. Read, (2005) Cell biology of conidial anastomosis tubes in *Neurospora crassa*. *Eukaryotic cell* **4**: 911-919.

Salcini, A.E., M.A. Hilliard, A. Croce, S. Arbucci, P. Luzzi, C. Tacchetti, L. Daniell, P. De Camilli, P.G. Pelicci, P.P. Di Fiore & P. Bazzicalupo, (2001) The Eps15 *C. elegans* homologue EHS-1 is implicated in synaptic vesicle recycling. *Nature cell biology* **3**: 755-760.

Sambrook, J. & D.W. Russell, (2001) *Molecular cloning : a laboratory manual*. Cold Spring Harbor Laboratory, Cold Spring Harbor, N.Y.

Schindler, D. & M. Nowrousian, (2014) The polyketide synthase gene *pks4* is essential for sexual development and regulates fruiting body morphology in *Sordaria macrospora*. *Fungal Genetics and Biology* **68**: 48-59.

Schinkmann, K. & J. Blenis, (1997) Cloning and characterization of a human STE20-like protein kinase with unusual cofactor requirements. *The Journal of biological chemistry* **272**: 28695-28703.

Schneider, H., M. Errede, N.H. Ulrich, D. Virgintino, K. Frei & H. Bertalanffy, (2011) Impairment of tight junctions and glucose transport in endothelial cells of human cerebral cavernous malformations. *Journal of neuropathology and experimental neurology* **70**: 417-429.

Schulte, J., K.J. Sepp, R.A. Jorquera, C. Wu, Y. Song, P. Hong & J.T. Littleton, (2010) DMob4/Phocein regulates synapse formation, axonal transport, and microtubule organization. *The Journal of neuroscience : the official journal of the Society for Neuroscience* **30**: 5189-5203.

Sepp, K.J., P. Hong, S.B. Lizarraga, J.S. Liu, L.A. Mejia, C.A. Walsh & N. Perrimon, (2008) Identification of neural outgrowth genes using genome-wide RNAi. *PLoS genetics* **4**: e1000111.

Sestak, S., I. Hagen, W. Tanner & S. Strahl, (2004) Scw10p, a cell-wall glucanase/transglucosidase important for cell-wall stability in *Saccharomyces cerevisiae*. *Microbiology* **150**: 3197-3208.

Shim, W.B., U.S. Sagaram, Y.E. Choi, J. So, H.H. Wilkinson & Y.W. Lee, (2006) FSR1 is essential for virulence and female fertility in *Fusarium verticillioides* and *F. graminearum*. *Molecular plant-microbe interactions : MPMI* **19**: 725-733.

Siegel, A.M., H. Bertalanffy, J.J. Dichgans, C.E. Elger, H. Hopf, N. Hopf, M. Keidel, A. Kleider, G. Nowak, R.A. Pfeiffer, J. Schramm, S. Spuck, H. Stefan, U. Sure, C.R. Baumann, G.A. Rouleau, D.J. Verlaan, E. Andermann & F. Andermann, (2005) Familial cavernous malformations of the central nervous system. A clinical and genetic study of 15 German families. *Der Nervenarzt* **76**: 175-180.

Simonin, A.R., C.G. Rasmussen, M. Yang & N.L. Glass, (2010) Genes encoding a striatin-like protein (ham-3) and a forkhead associated protein (ham-4) are required for hyphal fusion in *Neurospora crassa*. *Fungal genetics and biology : FG & B* **47**: 855-868.

Simons, K. & D. Toomre, (2000) Lipid rafts and signal transduction. *Nature reviews. Molecular cell biology* **1**: 31-39.

Singh, N.S., N. Shao, J.R. McLean, M. Sevugan, L. Ren, T.G. Chew, A. Bimbo, R. Sharma, X. Tang, K.L. Gould & M.K. Balasubramanian, (2011) SIN-inhibitory phosphatase complex promotes Cdc11p dephosphorylation and propagates SIN asymmetry in fission yeast. *Current biology : CB* **21**: 1968-1978.

Smith, T.F., C. Gaitatzes, K. Saxena & E.J. Neer, (1999) The WD repeat: a common architecture for diverse functions. *Trends in biochemical sciences* **24**: 181-185.

Stavridi, E.S., K.G. Harris, Y. Huyen, J. Bothos, P.M. Verwoerd, S.E. Stayrook, N.P. Pavletich, P.D. Jeffrey & F.C. Luca, (2003) Crystal structure of a human Mob1 protein: toward understanding Mob-regulated cell cycle pathways. *Structure* **11**: 1163-1170.

Stefanova, I., V. Horejsi, I.J. Ansotegui, W. Knapp & H. Stockinger, (1991) GPI-anchored cell-surface molecules complexed to protein tyrosine kinases. *Science* **254**: 1016-1019.

Stevens, F.C., (1983) Calmodulin: an introduction. *Canadian journal of biochemistry and cell biology* **61**: 906-910.

Su, Y.C., C. Maurel-Zaffran, J.E. Treisman & E.Y. Skolnik, (2000) The Ste20 kinase misshapen regulates both photoreceptor axon targeting and dorsal closure, acting downstream of distinct signals. *Molecular and cellular biology* **20**: 4736-4744.

Sugden, P.H., L.J. McGuffin & A. Clerk, (2013) SOcK, MiSTs, MASK and STicKs: the GCKIII (germinal centre kinase III) kinases and their heterologous protein–protein interactions. *Biochemical Journal* **454**: 13-30.

Sukotjo, C., A.A. Abanmy, T. Ogawa & I. Nishimura, (2002) Molecular cloning of wound inducible transcript (wit 3.0) differentially expressed in edentulous oral mucosa undergoing tooth extraction wound-healing. *Journal of dental research* **81**: 229-235.

Sunyaev, S.R., F. Eisenhaber, I.V. Rodchenkov, B. Eisenhaber, V.G. Tumanyan & E.N. Kuznetsov, (1999) PSIC: profile extraction from sequence alignments with position-specific counts of independent observations. *Protein engineering* **12**: 387-394.

Sunyaev, S.R., Eisenhaber F., Rodchenkov I.V., Eisenhaber B., Tumanyan V.G. & K. E.N., (1999) Prediction of potential GPI-modification sites in proprotein sequences. *Protein engineering* **12**: 387-394.

Tan, B., X. Long, H. Nakshatri, K.P. Nephew & R.M. Bigsby, (2008) Striatin-3 gamma inhibits estrogen receptor activity by recruiting a protein phosphatase. *Journal of molecular endocrinology* **40**: 199-210.

Tanabe, O., D. Hirata, H. Usui, Y. Nishito, T. Miyakawa, K. Igarashi & M. Takeda, (2001) Fission yeast homologues of the B' subunit of protein phosphatase 2A: multiple roles in mitotic cell division and functional interaction with calcineurin. *Genes to cells : devoted to molecular & cellular mechanisms* **6**: 455-473.

Tanti, G.K. & S.K. Goswami, (2014) SG2NA recruits DJ-1 and Akt into the mitochondria and membrane to protect cells from oxidative damage. *Free Radical Biology and Medicine* **75**: 1-13.

Tanti, G.K., N. Singarapu, R. Muthuswami & S.K. Goswami, (2014) Among the three striatin family members, SG2NA was first to arise during evolution. *Front Biosci (Schol Ed)* **6**: 1-15.

Teichert, I., M. Nowrousian, S. Pöggeler & U. Kück, (2014) The filamentous fungus *Sordaria macrospora* as a genetic model to study fruiting-body development. *Adv Genet* **87**: 201-246.

Teichert, I., G. Wolff, U. Kück & M. Nowrousian, (2012) Combining laser microdissection and RNA-seq to chart the transcriptional landscape of fungal development. *BMC genomics* **13**: 511.

Thomas, J.R., R.A. Dwek & T.W. Rademacher, (1990) Structure, biosynthesis, and function of glycosylphosphatidylinositols. *Biochemistry* **29**: 5413-5422.

Towbin, H., T. Staehelin & J. Gordon, (1979) Electrophoretic transfer of proteins from polyacrylamide gels to nitrocellulose sheets: procedure and some applications. *Proceedings of the National Academy of Sciences of the United States of America* **76**: 4350-4354.

Trammell, M.A., N.M. Mahoney, D.A. Agard & R.D. Vale, (2008) Mob4 plays a role in spindle focusing in Drosophila S2 cells. *Journal of cell science* **121**: 1284-1292.

Tran, H., D. Bustos, R. Yeh, B. Rubinfeld, C. Lam, S. Shriver, I. Zilberleyb, M.W. Lee, L. Phu, A.A. Sarkar, I.E. Zohn, I.E. Wertz, D.S. Kirkpatrick & P. Polakis, (2013) HectD1 E3 ligase modifies adenomatous

polyposis coli (APC) with polyubiquitin to promote the APC-axin interaction. *The Journal of biological chemistry* **288**: 3753-3767.

Tsukita, S., S. Yonemura & S. Tsukita, (1997) ERM proteins: head-to-tail regulation of actin-plasma membrane interaction. *Trends in biochemical sciences* **22**: 53-58.

Tucker, C.L., L.A. Peteya, A.M. Pittman & J. Zhong, (2009) A genetic test for yeast two-hybrid bait competency using RanBPM. *Genetics* **182**: 1377-1379.

Vaknin, Y., Y. Shadkchan, E. Levdansky, M. Morozov, J. Romano & N. Osherov, (2014) The three *Aspergillus fumigatus* CFEM-domain GPI-anchored proteins (CfmA-C) affect cell-wall stability but do not play a role in fungal virulence. *Fungal genetics and biology : FG & B* **63**: 55-64.

van der Voorn, L. & H.L. Ploegh, (1992) The WD-40 repeat. *FEBS letters* **307**: 131-134.

Varsano, T., M.Q. Dong, I. Niesman, H. Gacula, X. Lou, T. Ma, J.R. Testa, J.R. Yates, 3rd & M.G. Farquhar, (2006) GIPC is recruited by APPL to peripheral TrkA endosomes and regulates TrkA trafficking and signaling. *Molecular and cellular biology* **26**: 8942-8952.

Verde, F., D.J. Wiley & P. Nurse, (1998) Fission yeast orb6, a ser/thr protein kinase related to mammalian rho kinase and myotonic dystrophy kinase, is required for maintenance of cell polarity and coordinates cell morphogenesis with the cell cycle. *Proceedings of the National Academy of Sciences of the United States of America* **95**: 7526-7531.

Verlaan, D.J., J. Roussel, S.B. Laurent, C.E. Elger, A.M. Siegel & G.A. Rouleau, (2005) CCM3 mutations are uncommon in cerebral cavernous malformations. *Neurology* **65**: 1982-1983.

Vitulo, N., A. Vezzi, G. Galla, S. Citterio, G. Marino, B. Ruperti, M. Zermiani, E. Albertini, G. Valle & G. Barcaccia, (2007) Characterization and evolution of the cell cycle-associated mob domain-containing proteins in eukaryotes. *Evolutionary bioinformatics online* **3**: 121-158.

Voigt, O. & S. Pöggeler, (2013) Autophagy genes *Smatg8* and *Smatg4* are required for fruiting-body development, vegetative growth and ascospore germination in the filamentous ascomycete *Sordaria macrospora*. *Autophagy* **9**: 33-49.

Voss, K., S. Stahl, E. Schleider, S. Ullrich, J. Nickel, T.D. Mueller & U. Felbor, (2007) CCM3 interacts with CCM2 indicating common pathogenesis for cerebral cavernous malformations. *Neurogenetics* **8**: 249-256.

Wang, C.L., W.B. Shim & B.D. Shaw, (2010) *Aspergillus nidulans* striatin (StrA) mediates sexual development and localizes to the endoplasmic reticulum. *Fungal genetics and biology : FG & B* **47**: 789-799.

Wang, M., S.U. Amano, R.J. Flach, A. Chawla, M. Aouadi & M.P. Czech, (2013) Identification of Map4k4 as a novel suppressor of skeletal muscle differentiation. *Molecular and cellular biology* **33**: 678-687.

Wansink, D.G., R.E. van Herpen, M.M. Coerwinkel-Driessen, P.J. Groenen, B.A. Hemmings & B. Wieringa, (2003) Alternative splicing controls myotonic dystrophy protein kinase structure, enzymatic activity, and subcellular localization. *Molecular and cellular biology* **23**: 5489-5501.

Wei, X., T. Shimizu & Z.C. Lai, (2007) Mob as tumor suppressor is activated by Hippo kinase for growth inhibition in Drosophila. *The EMBO journal* **26**: 1772-1781.

Wielowieyski, P.A., S. Sevinc, R. Guzzo, M. Salih, J.T. Wigle & B.S. Tuana, (2000) Alternative splicing, expression, and genomic structure of the 3' region of the gene encoding the sarcolemmal-associated proteins (SLAPs) defines a novel class of coiled-coil tail-anchored membrane proteins. *The Journal of biological chemistry* **275**: 38474-38481.

Wu, W.K., C.H. Cho, C.W. Lee, D. Fan, K. Wu, J. Yu & J.J. Sung, (2010) Dysregulation of cellular signaling in gastric cancer. *Cancer letters* **295**: 144-153.

Xiang, Q., C. Rasmussen & N.L. Glass, (2002) The *ham-2* locus, encoding a putative transmembrane protein, is required for hyphal fusion in *Neurospora crassa*. *Genetics* **160**: 169-180.

Xu, Y., Y. Xing, Y. Chen, Y. Chao, Z. Lin, E. Fan, J.W. Yu, S. Strack, P.D. Jeffrey & Y. Shi, (2006) Structure of the protein phosphatase 2A holoenzyme. *Cell* **127**: 1239-1251.

Yla-Herttuala, S., T.T. Rissanen, I. Vajanto & J. Hartikainen, (2007) Vascular endothelial growth factors: biology and current status of clinical applications in cardiovascular medicine. *Journal of the American College of Cardiology* **49**: 1015-1026.

Yogev, O., A. Naamati & O. Pines, (2011) Fumarase: a paradigm of dual targeting and dual localized functions. *The FEBS journal* **278**: 4230-4242.

Young, N. & J. Moss, (2000) *PNH and the GPI-Linked Proteins*. Academic press.

Yu, X.X., X. Du, C.S. Moreno, R.E. Green, E. Ogris, Q. Feng, L. Chou, M.J. McQuoid & D.C. Pallas, (2001) Methylation of the protein phosphatase 2A catalytic subunit is essential for association of Balpha regulatory subunit but not SG2NA, striatin, or polyomavirus middle tumor antigen. *Molecular biology of the cell* **12**: 185-199.

Zhang, M., L. Dong, Z. Shi, S. Jiao, Z. Zhang, W. Zhang, G. Liu, C. Chen, M. Feng, Q. Hao, W. Wang, M. Yin, Y. Zhao, L. Zhang & Z. Zhou, (2013) Structural mechanism of CCM3 heterodimerization with GCK III kinases. *Structure* **21**: 680-688.

Zhao, B., K. Tumaneng & K.-L. Guan, (2011) The Hippo pathway in organ size control, tissue regeneration and stem cell self-renewal. *Nature cell biology* **13**: 877-883.

Zheng, X., C. Xu, A. Di Lorenzo, B. Kleaveland, Z. Zou, C. Seiler, M. Chen, L. Cheng, J. Xiao, J. He, M.A. Pack, W.C. Sessa & M.L. Kahn, (2010) CCM3 signaling through sterile 20-like kinases plays an essential role during zebrafish cardiovascular development and cerebral cavernous malformations. *The Journal of clinical investigation* **120**: 2795-2804.

Zhou, T.H., K. Ling, J. Guo, H. Zhou, Y.L. Wu, Q. Jing, L. Ma & G. Pei, (2000) Identification of a human brain-specific isoform of mammalian STE20-like kinase 3 that is regulated by cAMP-dependent protein kinase. *The Journal of biological chemistry* **275**: 2513-2519.

Zhu, W., E.K. Chan, J. Li, P. Hemmerich & E.M. Tan, (2001) Transcription activating property of autoantigen SG2NA and modulating effect of WD-40 repeats. *Experimental cell research* **269**: 31